


# Mobile measurement system for clinical diagnosis

*A Transepidermal Water Loss Probe*

By

**Hellema Anaelle Laura Ibrahim**

 0000-0002-2909-08340



London South Bank University

School of Engineering

A dissertation submitted in partial fulfilment of the requirements  
for the degree of Doctor of Philosophy in the School of Engineering

May 2019

# Abstract

Transepidermal water loss (TEWL) is commonly used as a surrogate marker for skin barrier function. Although current devices enable TEWL to be measured with ease and precision under controlled laboratory conditions, they do not yield reliable readings in an uncontrolled environment. This project aimed to develop a new TEWL device that is mobile, i.e. that would fit in the pocket and measure TEWL anywhere. For this, the prototype had to be portable, wireless and to have good autonomy. In addition the prototype performances were evaluated in terms of repeatability and sensitivity. The primary design is based on a closed-chamber to limit the effect of the environment. Moreover, the use of a fan to remove surface water and homogenise the micro-climate in the chamber was introduced. Mathematical modelling and measurements of water vapour and heat flux in closed TEWL chambers of a range of geometries was investigated to establish ideal sensors locations and blower flow rates. It was found that the fan decreased repeatability but increased sensitivity. In addition, it decreased coefficient of variation of measurements on moist skin, contrary to other TEWL chamber methods. Furthermore, lower fan speed yielded better precision. Finally, the gradient calculation is the crucial part of a TEWL measurement and Least Square Fitting was used to stabilise the readings and improve repeatability at the expense of computational speed. The work suggests that it should be possible to develop a viable new design that can generate measurements in the field that are easy to make and reliable but further work is needed to establish accuracy evaluation from a calibration with a fixed quantity of water and to develop a full commercial product.

# Dedication

To my husband for his guidance and help for reflection.  
To my colleagues (now friends) for their advice and help.  
To my family and friends for their moral support.

# Declaration

I, Hellema Ibrahim, declare that the thesis entitled, "Mobile measurement system for clinical diagnosis" and the work presented in it are my own. All sources are cited and can be found in the references section.



# Acknowledgements

I would like to thank London South Bank University and Biox Systems Limited for sponsoring the joint PhD studentship. I would also like to thank Dr Perry Xiao, Professor Mohammad Ghavammi and Dr Elliott Berg for their supervision. I would like to thank my colleagues and friends Dr Lori Ciortea, Dr Hassan Zabihi, Dr Zaneta Muranko, Dr Ousmane Abdoulaye Oumar, Mr Peter Labib for their support and guidance. I also would like to thank John Harper, Peter Adams, Silvio Lavandeira, Mehdi Zahir and Ken Unadkat for their help and advices.

# Nomenclature

$\alpha$	Thermal diffusivity of the air ( $m^2/s$ )
$\Delta$	Time difference (s)
$\Delta m$	Mass difference (kg)
$\rho$	Medium density ( $kg/m^3$ )
$A$	Area ( $m^2$ )
$AH$	Absolute humidity ( $kg/m^3$ )
$AVD$	Actual vapour density ( $kg/m^3$ )
$C$	Water concentration ( $kg/m^3$ )
$C_p$	Specific heat of the air ( $J/kg^\circ C$ )
$D'$	Diffusivity constant ( $0.670 \times 10^{-3} m.h/P$ )
$D_w$	Mass diffusivity of water in the air ( $m^2/s$ )
$k$	Rate of change of humidity during measurement
$k_a$	Thermal conductivity of air ( $W/m^\circ C$ )
$K_m$	Concentration membrane ratio
$L$	Length (m)
$M$	Molar mass of water (18 g/mol)
$m$	Mass (kg)
$o$	Thickness of the stratum corneum (m)
$P$	Vapour pressure (Pa)
$P_s$	Saturation vapour pressure (Pa)

$P_{SC/w}$	Permeability coefficient ( $\text{mol}/\text{cm}^2\cdot\text{s}$ )
$Q$	Heat flux density ( $\text{W}/\text{m}^3$ )
$R$	Universal gas constant ( $8.314\text{J}/\text{mol}^\circ\text{C}$ )
$Re$	Diffusion resistance ( $\text{s}/\text{m}$ )
$RH$	Relative humidity (%)
$SVD$	Saturation vapour density ( $\text{kg}/\text{m}^3$ )
$T$	Temperature ( $^\circ\text{C}$ )
$t$	Time (s)
$T_o$	Initial temperature ( $^\circ\text{C}$ )
$T_{amb}$	Ambient temperature ( $^\circ\text{C}$ )
$u$	Equation solution
$y$	Space coordinate (m)

# Contents

<b>1</b>	<b>Introduction</b>	<b>23</b>
1.1	e-Health . . . . .	24
1.2	Transepidermal Water Loss Measurement . . . . .	25
1.2.1	Rational . . . . .	26
1.2.2	Research question . . . . .	26
1.2.3	Hypotheses . . . . .	26
1.2.4	Research Goals . . . . .	27
1.2.5	Research objectives . . . . .	27
1.3	Summary . . . . .	29
<b>2</b>	<b>Theoretical background and literature review</b>	<b>30</b>
2.1	Introduction . . . . .	30
2.2	Skin histology . . . . .	31
2.3	Non invasive measurements of the skin are important . . . . .	31
2.4	Other instruments and techniques not related to TEWL or hydration measurement . . . . .	32
2.5	Review of methods for measuring skin hydration . . . . .	33
2.5.0.1	Applications . . . . .	33
2.5.0.2	Parameters influencing hydration measurement . . . . .	34
2.5.0.3	Instruments to measure water content . . . . .	34
2.6	TEWL <sup>1</sup> as a measure of skin barrier function . . . . .	39
2.6.0.1	Definition . . . . .	39
2.6.0.2	Applications . . . . .	39
2.7	Theoretical background to TEWL measurement devices . . . . .	40
2.7.1	Fick's Law . . . . .	40
2.7.2	TEWL definition and skin . . . . .	41
2.7.3	Measurement principle . . . . .	42
2.7.4	Link between hydration and TEWL . . . . .	44
2.8	Currently available devices for measuring TEWL . . . . .	45

---

<sup>1</sup>Transepidermal Water Loss

2.8.1	Different approaches . . . . .	45
2.8.2	Portable methods . . . . .	46
2.8.3	Open chamber devices . . . . .	47
2.8.4	Closed unventilated chamber devices . . . . .	48
2.8.5	Condenser chamber: Aquaflux . . . . .	48
2.9	Generic issues relating to TEWL measurement . . . . .	51
2.9.0.1	Definitions . . . . .	51
2.9.0.2	Difficulty of obtaining reliable measurements . . . . .	51
2.9.1	Factors that influence TEWL . . . . .	52
2.9.2	Calibration . . . . .	53
2.9.2.1	Importance of calibration . . . . .	53
2.9.2.2	How to calibrate a closed chamber instrument . . . . .	53
2.9.3	Ideal measurement conditions . . . . .	54
2.9.3.1	Stabilisation time and measurement time . . . . .	55
2.9.3.2	Measurement procedure . . . . .	56
2.9.3.3	Clean skin . . . . .	57
2.9.3.4	Skin site . . . . .	57
2.9.3.5	Probe temperature . . . . .	58
2.9.3.6	Flow turbulence . . . . .	58
2.9.3.7	Sweating and acclimatisation . . . . .	58
2.9.3.8	Pressure on the skin . . . . .	59
2.9.3.9	Geometry . . . . .	59
2.9.3.10	Angle of measurement from vertical . . . . .	59
2.9.3.11	Conclusion on the measurement conditions . . . . .	59
2.10	Review of the strengths and limitations of currently available devices	60
2.10.1	Comparison between systems . . . . .	60
2.10.2	Conclusion on the comparison between instruments . . . . .	61
2.10.3	Conclusion on the three methods to measure TEWL . . . . .	62
2.10.4	Literature gap: as a group, what current instruments are missing	63
2.11	Research project definition . . . . .	63
2.11.1	Research question . . . . .	63
2.11.2	Aim . . . . .	64
2.11.3	Research objectives . . . . .	64
2.11.4	Functional design specification . . . . .	64
2.11.4.1	Precision . . . . .	64
2.11.4.2	Sensitivity . . . . .	64
2.11.4.3	Mobile . . . . .	64
2.11.5	Discussion of the functional specification . . . . .	65
2.11.6	Outline design specification . . . . .	65

2.12	Strategy for the project . . . . .	66
2.12.1	Outline design specification . . . . .	66
2.12.2	Use of a fan to remove the SSWL . . . . .	66
2.12.3	Simulations . . . . .	67
2.12.4	Gradient calculation process . . . . .	67
2.12.4.1	Variation of gradient with time variation $\Delta$ . . . . .	67
2.12.4.2	Timing of the gradient computation . . . . .	68
2.12.5	Measurement procedure . . . . .	69
2.12.5.1	Rest . . . . .	69
2.12.5.2	Total duration . . . . .	69
2.12.5.3	Signal processing . . . . .	70
2.12.6	Calibration . . . . .	70
2.12.6.1	Current calibration methods . . . . .	71
2.12.6.2	RHT sensor calibration . . . . .	71
2.12.6.3	Calibration against another instrument . . . . .	71
2.12.6.4	Calibration with a fixed quantity of water . . . . .	72
2.12.7	Conclusion on the strategy . . . . .	73
2.13	Development Project Definition . . . . .	74
2.13.1	Hypothesis . . . . .	74
2.13.2	Deliverables . . . . .	74
2.13.3	Contributions to knowledge . . . . .	74
2.14	Thesis outline . . . . .	75
2.15	Summary . . . . .	75
<b>3</b>	<b>Mathematical Modelling and Simulations</b>	<b>77</b>
3.1	Introduction . . . . .	77
3.2	Aim . . . . .	77
3.3	Parameters found in the literature . . . . .	78
3.3.1	Assumptions . . . . .	82
3.4	Mathematical model of a closed chamber instrument . . . . .	83
3.4.1	Mass diffusion . . . . .	83
3.4.2	Heat transfer . . . . .	84
3.5	Numerical solution . . . . .	84
3.6	Discussion . . . . .	86
3.7	Summary . . . . .	90
<b>4</b>	<b>Experimental Work</b>	<b>91</b>
4.1	Introduction . . . . .	91
4.2	Methodology for prototype design, manufacture and testing . . . . .	91
4.2.1	Development . . . . .	91

4.2.1.1	Software . . . . .	92
4.2.1.2	Physical . . . . .	92
4.2.1.3	Hardware . . . . .	92
4.2.2	Experiments . . . . .	93
4.2.2.1	Strategy . . . . .	93
4.2.2.2	Duration of experiments . . . . .	93
4.2.2.3	Environmental variations . . . . .	93
4.2.2.4	Time of the day . . . . .	94
4.2.2.5	Calibration with the Aquaflux . . . . .	94
4.2.2.6	Simulations . . . . .	94
4.3	Requirements . . . . .	94
4.3.1	TEWL measurement . . . . .	94
4.3.2	Quick measurement . . . . .	95
4.3.3	Temperature control . . . . .	95
4.3.4	Chamber geometry . . . . .	95
4.3.5	Printed circuit board (PCB) . . . . .	96
4.3.6	Position of the sensor . . . . .	97
4.3.7	Portability . . . . .	97
4.3.8	Connectivity . . . . .	98
4.3.8.1	Requirements . . . . .	98
4.3.8.2	Protocols and standards . . . . .	98
4.3.8.3	Summary of protocols . . . . .	100
4.3.8.4	Comparison and solution chosen . . . . .	101
4.3.9	Blowers and Fans . . . . .	102
4.3.9.1	Blower or fan . . . . .	102
4.3.9.2	MagLev . . . . .	104
4.3.9.3	Speed and flow . . . . .	104
4.3.9.4	Position of the blowers . . . . .	104
4.3.9.5	Summary . . . . .	104
4.3.10	Proportional-Integral-Derivative(PID) . . . . .	105
4.3.10.1	Tuning . . . . .	105
4.3.10.2	Final choice . . . . .	106
4.3.11	Screen . . . . .	106
4.3.11.1	Requirements . . . . .	106
4.3.11.2	Capacitive . . . . .	107
4.3.11.3	Resistive . . . . .	107
4.3.11.4	Comparison . . . . .	107
4.3.11.5	Solution chosen . . . . .	108
4.3.12	Battery . . . . .	108

4.3.13	Non Volatile Memory . . . . .	108
4.3.13.1	Solution chosen . . . . .	110
4.3.14	Relative humidity and temperature sensor . . . . .	110
4.3.15	Development boards . . . . .	110
4.3.15.1	Central Processing Unit . . . . .	111
4.3.15.2	Connectivity . . . . .	111
4.3.15.3	Inertial measurement unit . . . . .	111
4.3.15.4	Summary of the Arduino 101 . . . . .	111
4.3.15.5	Later versions of prototypes . . . . .	112
4.3.16	Touchscreen and SD card . . . . .	112
4.3.17	Threading . . . . .	114
4.3.18	Ergonomic probe design . . . . .	114
4.4	3D printing . . . . .	116
4.4.1	Fixed parameters for the printing . . . . .	116
4.4.2	Part orientation . . . . .	116
4.4.3	Layer thickness . . . . .	117
4.4.4	Temperature . . . . .	117
4.4.5	Infill . . . . .	118
4.4.6	Speed . . . . .	118
4.4.7	Flow rate . . . . .	118
4.4.8	Deposition speed . . . . .	118
4.4.9	The first layer . . . . .	118
4.4.10	Retraction . . . . .	119
4.4.11	Casing shell . . . . .	119
4.4.12	Tuning of the stepper drivers of the x,y and z axis . . . . .	119
4.4.13	Minimum layer time . . . . .	119
4.4.14	Conclusion on 3D printing . . . . .	120
4.5	Diurnal variations . . . . .	120
4.5.1	Introduction . . . . .	120
4.5.2	Materials and methods . . . . .	121
4.5.3	Data collection . . . . .	121
4.5.4	Results . . . . .	122
4.5.5	Discussion . . . . .	122
4.5.6	Conclusion . . . . .	124
4.6	Prototype 1 . . . . .	125
4.6.1	Rationale . . . . .	125
4.6.2	Materials and Methods . . . . .	125
4.6.2.1	Description of the equipment . . . . .	125
4.6.2.2	Methodology . . . . .	126



4.6.2.3	Data collection . . . . .	126
4.6.2.4	Specific methodology . . . . .	126
4.6.3	Results . . . . .	129
4.6.3.1	Methods to improve repeatability . . . . .	129
4.6.3.2	General skin measurements: . . . . .	130
4.6.3.3	Calibration: . . . . .	130
4.6.3.4	Simulation: . . . . .	132
4.6.4	Discussion . . . . .	132
4.6.5	Conclusion . . . . .	133
4.7	Prototype 3 . . . . .	134
4.7.1	Description . . . . .	134
4.7.2	Rational . . . . .	135
4.7.3	Testing . . . . .	136
4.7.4	Results . . . . .	136
4.7.4.1	Gradient calculation: . . . . .	136
4.7.4.2	Experimental results with 9 mm fan: . . . . .	136
4.7.4.3	Results with 12 mm fan: . . . . .	137
4.7.4.4	Calibration: . . . . .	142
4.7.4.5	Simulation: . . . . .	143
4.7.5	Discussion . . . . .	158
4.7.6	Conclusion . . . . .	159
4.8	Prototype 4 . . . . .	160
4.8.1	Description . . . . .	160
4.8.2	Rationale . . . . .	160
4.8.3	Testing . . . . .	162
4.8.4	Results . . . . .	163
4.8.4.1	Gradient calculation method: . . . . .	163
4.8.4.2	Results: . . . . .	163
4.8.4.3	Impact of air conditioning: . . . . .	168
4.8.4.4	Calibration: . . . . .	169
4.8.5	Discussion . . . . .	169
4.8.6	Conclusion . . . . .	171
4.9	Prototype 5.1 . . . . .	172
4.9.1	Description . . . . .	172
4.9.1.1	Chamber . . . . .	172
4.9.1.2	PCB . . . . .	172
4.9.1.3	Casing . . . . .	172
4.9.2	Rationale . . . . .	174
4.9.3	Testing . . . . .	175

4.9.4	Results . . . . .	175
4.9.4.1	Gradient computation method: . . . . .	175
4.9.4.2	Results: . . . . .	175
4.9.4.3	Calibration: . . . . .	176
4.9.4.4	Simulation: . . . . .	176
4.9.5	Discussion . . . . .	177
4.9.6	Conclusion . . . . .	178
4.10	Prototype 7.1 . . . . .	178
4.10.1	Description . . . . .	178
4.10.1.1	Overview . . . . .	178
4.10.1.2	Geometry . . . . .	178
4.10.1.3	PCB . . . . .	178
4.10.2	Gradient calculation . . . . .	181
4.10.3	Rationale . . . . .	181
4.10.4	Testing . . . . .	182
4.10.5	Results . . . . .	182
4.10.5.1	Gradient computation method: . . . . .	182
4.10.5.2	Results without the fan: . . . . .	182
4.10.5.3	Comparison with and without the fan: . . . . .	183
4.10.5.4	Results with different $\Delta$ and start time: . . . . .	185
4.10.5.5	Calibration: . . . . .	185
4.10.5.6	Simulation: . . . . .	187
4.10.5.7	Battery life: . . . . .	187
4.10.6	Discussion . . . . .	187
4.10.7	Conclusion . . . . .	191
4.11	Prototype 9 . . . . .	191
4.11.1	Description . . . . .	191
4.11.1.1	New gradient calculation method . . . . .	191
4.11.1.2	Implementation on C# . . . . .	194
4.11.2	Rationale . . . . .	197
4.11.3	Testing . . . . .	198
4.11.4	Results . . . . .	199
4.11.4.1	Gradient calculation tentatives . . . . .	199
4.11.4.2	Results: . . . . .	199
4.11.4.3	Calibration: . . . . .	200
4.11.4.4	Simulation: . . . . .	200
4.11.5	Chamber 9 with the final method for gradient computation . . . . .	203
4.11.5.1	Least squared fitting tuning: . . . . .	203
4.11.5.2	Results: . . . . .	206

4.11.5.3	Calibration: . . . . .	209
4.11.5.4	Quick summary of the results to date . . . . .	209
4.11.5.5	Extended measurement session with the optimal configuration . . . . .	213
4.11.5.6	Skin surface water loss: . . . . .	214
4.11.6	Discussion . . . . .	218
4.11.6.1	Basic gradient calculation method . . . . .	218
4.11.6.2	Least Square Fitting gradient calculation method . . . . .	219
4.11.6.3	Optimal configuration . . . . .	220
4.11.6.4	Surface Water . . . . .	221
4.11.7	Conclusion . . . . .	222
4.12	Comparison of prototypes . . . . .	222
4.12.1	Error rate below 5% and ranking Top 4: . . . . .	223
4.12.2	Accuracy . . . . .	223
4.12.3	Sensitivity . . . . .	224
4.12.4	Autonomy . . . . .	224
4.12.5	Mobility and portability . . . . .	224
4.12.6	Outside a laboratory . . . . .	224
4.13	Summary of prototypes . . . . .	224
4.13.1	Sensor position . . . . .	225
4.13.2	Fan Speed and SSWL <sup>2</sup> . . . . .	225
4.13.3	Cap and anatomical site . . . . .	226
4.13.4	Calculation timing . . . . .	226
4.13.5	Calculation method . . . . .	226
4.14	Conclusion . . . . .	226
<b>5</b>	<b>Conclusions and Future Work</b>	<b>228</b>
5.1	Introduction . . . . .	228
5.2	Conclusions on research questions . . . . .	228
5.3	Future work recommendations . . . . .	230
5.3.1	Technique development for the next version of prototype . . . . .	230
5.3.1.1	Device management . . . . .	230
5.3.1.2	Full integration . . . . .	231
5.3.1.3	Electronics . . . . .	231
5.3.1.4	Computational fluid dynamics . . . . .	231
5.3.1.5	Mechanical design . . . . .	231
5.3.2	Skin measurements . . . . .	231
5.3.2.1	The use of different caps . . . . .	232

---

<sup>2</sup>Skin Surface Water Loss

5.3.2.2	Gravity study . . . . .	232
5.3.2.3	Contact pressure . . . . .	232
5.3.2.4	Calibration . . . . .	232
5.3.2.5	Observers and subjects . . . . .	232
5.4	Summary . . . . .	233
<b>A</b>	<b>Probe Configuration Performances Comparison</b>	<b>234</b>
A.1	Repeatability Ranking . . . . .	234
A.2	Sensitivity with the Aquaflex . . . . .	238

# List of Figures

2.1	Skin Anatomy (adapted from (HumanAnatomyLibrary 2018)) . . . . .	31
2.2	Open chamber instrument . . . . .	47
2.3	H4300, an example of closed chamber instrument . . . . .	49
2.4	Vapometer, an example of closed chamber instrument . . . . .	50
2.5	Condenser chamber instrument . . . . .	50
3.1	Schematic diagram of heat transfer in a closed chamber . . . . .	85
3.2	Temperature profile as a function of spatial coordinate and time . . . . .	87
3.3	Humidity profile as a function of spatial coordinate and time . . . . .	88
4.1	GATT profile hierarchy - from the specification (Bluetooth SIG (Bluetooth Special Interest Group): Kirkland Washington USA 2014) . . . . .	103
4.2	Auto tuning of the PID . . . . .	106
4.3	Touchscreen . . . . .	113
4.4	Flow diagram of the chamber tasks . . . . .	115
4.5	Diurnal Variations measured on the volar forearm measured during a week . . . . .	123
4.6	Chamber 1 . . . . .	125
4.7	Chamber 1 . . . . .	131
4.8	Chamber 1 simulation . . . . .	132
4.9	Chamber 3 . . . . .	134
4.10	Android application to gather measurements data . . . . .	135
4.11	15 measurements on the VF <sup>3</sup> : RH <sup>4</sup> and temperature variations with Chamber 3 . . . . .	137
4.12	Chamber 3: The gradient was noisy and running average helps to clean the signal . . . . .	138
4.13	Sliding average methods applied to the gradient of humidity . . . . .	140
4.14	Comparison smoothing filters: rectangular, triangular, pseudo gaussian and Savitzky-Golay . . . . .	140

---

<sup>3</sup>Volar Forearm

<sup>4</sup>Relative Humidity

4.15	Chamber 3 with a 12 mm blower measuring RH, AH, temperature and water flux on moist skin (six applications of 30 seconds on the VF)	142
4.16	Correlation between Aquaflux and Chamber 3 using running average method: results presented here . . . . .	143
4.17	Correlation between Aquaflux and Chamber 3 using different TEWL computations methods . . . . .	144
4.18	ANSYS simulations of temperature profile for a 2D model of Chamber 3 without the fan . . . . .	146
4.18	ANSYS simulations of temperature profile for a 2D model of Chamber 3 without the fan . . . . .	147
4.19	ANSYS simulations of humidity profile for a 2D model of Chamber 3 without the fan . . . . .	148
4.19	ANSYS simulations of humidity profile for a 2D model of Chamber 3 without the fan . . . . .	149
4.20	ANSYS simulations of temperature profile for a 2D model of Chamber 3 with 9 mm fan . . . . .	150
4.20	ANSYS simulations of temperature profile for a 2D model of Chamber 3 with 9 mm fan . . . . .	151
4.21	ANSYS simulations of humidity profile for a 2D model of Chamber 3 with 9 mm fan . . . . .	152
4.21	ANSYS simulations of humidity profile for a 2D model of Chamber 3 with 9 mm fan . . . . .	153
4.22	ANSYS Simulations of Velocity Vectors for a 2D model of Chamber 3 with 9 mm fan . . . . .	154
4.22	ANSYS Simulations of Velocity Vectors for a 2D model of Chamber 3 with 9 mm fan . . . . .	155
4.23	ANSYS simulations of water vapour concentration for a 2D model of Chamber 3 with 9 mm fan . . . . .	156
4.23	ANSYS simulations of water vapour concentration for a 2D model of Chamber 3 with 9mm fan . . . . .	157
4.24	Heat profile of the dissipation . . . . .	158
4.25	Chamber 4 . . . . .	161
4.26	Chamber 4 cross section and identification of sensors . . . . .	161
4.27	Probe 4 PCB . . . . .	162
4.28	Measurements of a long duration with Chamber 4 . . . . .	165
4.29	Comparison of gradient measured with 3 positions of sensor . . . . .	166
4.30	Evolution of error rate with the voltage (and therefore the fan speed) in chamber 4 with a 9mm blower . . . . .	167

4.31	Back to back 9mm blowers speed varying with metal plate thickness and grounding . . . . .	168
4.32	Observation of the effect of the blowers in the microclimate . . . . .	169
4.33	Correlation between the Aquaflux and the Chamber 4 with one 9mm blower, for 3 sensor positions . . . . .	170
4.34	Chamber 5.1 . . . . .	172
4.35	Chamber 5.1 PCB and schematic . . . . .	173
4.36	Chamber 5.1 casing design . . . . .	174
4.37	Casing closing design detail . . . . .	174
4.38	Humidity and gradient for Chamber 5.1 without blowers . . . . .	176
4.39	Calibration curve with Chamber 5.1 equipped with two 15mm blowers	177
4.40	Chamber 7.1 PCB and schematic . . . . .	179
4.41	Chamber 7.1 casing design . . . . .	180
4.42	Chamber 7.1 case closure . . . . .	180
4.43	Chamber 7.1 cap closure . . . . .	180
4.44	Chamber 7.1 casing and use . . . . .	181
4.45	Performances of sensitivity and repeatability in function of the type of blowers (CFM=Cubic Feet per Minute) . . . . .	184
4.46	Variation of delta and start time on the error rate . . . . .	185
4.47	Correlation curve between Chamber 7.1 and the Aquaflux . . . . .	186
4.48	Calibration curve between probe 7.1 (with one or two fans) and the Aquaflux . . . . .	187
4.49	Correlation curve between Chamber 7.1 and the Aquaflux for various values of $\Delta$ time . . . . .	188
4.50	Chamber 9 cross section and sensor positions . . . . .	192
4.51	Chamber 9 casing in CAD . . . . .	192
4.52	First version of Chamber 9 casing 3D printed . . . . .	192
4.53	Second version of the casing for Chamber 9 . . . . .	193
4.54	Least Square Fitting Software Flow Diagram . . . . .	196
4.55	Screenshot of C# software to monitor the measurement data and perform least square fitting . . . . .	198
4.56	Correlation curves between chamber 9 and the Aquaflux . . . . .	201
4.57	Chamber 9 Simulation results in Fluent at 30s: Temperature, RH distributions and velocity vectors at t = 30 seconds . . . . .	202
4.58	Real and simulated 30s measurement on the VF with fan at maximum speed . . . . .	204
4.59	Typical curve of $\chi^2$ variation with time during a measurement . . . . .	205
4.60	Coarse tweaking results . . . . .	207
4.61	Fine tweaking results . . . . .	208

---

4.62	Correlation curve with different caps using Least Square Fitting . . .	210
4.63	Correlation curve with sensor 1 and sensor 3 . . . . .	211
4.64	Correlation Curve with minimum and maximum speed, on the VF, cheek and palm . . . . .	212
4.65	7 skin sites of the arm . . . . .	213
4.66	Calibration of the last probe with the best configuration . . . . .	215
4.67	Droplet evaporation. Gradient measured at different times: 3 min, 2 min, 1 min before, immediately after, 1 min, 2 min, 6 min, 7 min and 8 min after the droplet application with chamber 9 at maximum speed with sensor 3 and the small cap. . . . .	216
4.68	Evolution of the absolute humidity measured three times consecu- tively on the volar forearm with a droplet of water at different fan speeds. . . . .	217
4.69	Evolution of TEWL with time on skin with forced surface water. This was measured at maximum fan speed with sensor 3 and the small cap.	218



# Acronyms

<b>AC</b> Air Conditionning.....	94
<b>AES</b> Advanced Encryption Standard.....	99
<b>AH</b> Absolute Humidity.....	43
<b>BC</b> Boundary Conditions.....	86
<b>BLE</b> Bluetooth Low Energy.....	99
<b>BVP</b> Boundary Value Problem	
<b>CF</b> Calibration Factor.....	53
<b>CFD</b> Computational Fluid Dynamics.....	92
<b>CPU</b> Central Processing Unit.....	111
<b>FDM</b> Fused Deposition Modeling.....	116
<b>IC</b> Initial Conditions	
<b>I2C</b> Inter IC (Integrated Circuit).....	95

<b>IMU</b> Inertial measurement unit .....	111
<b>IoT</b> Internet of Things .....	98
<b>LED</b> Light Emitting Diode.....	108
<b>MagLev</b> Magnetic Levitation .....	139
<b>LiPo</b> Lithium-ion Polymer .....	187
<b>LSF</b> Least Square Fitting .....	209
<b>PCB</b> Printed Circuit Board .....	24
<b>PID</b> Proportional Integral Derivative.....	227
<b>PLA</b> Poly Lactic Acid.....	117
<b>PWM</b> Pulse Width Modulation .....	106
<b>OS</b> Operating System .....	113
<b>PDE</b> Partial Derivative Equations.....	78
<b>RAM</b> Random Access Memory .....	109
<b>RH</b> Relative Humidity .....	16
<b>RHT</b> Relative Humidity and Temperature couple.....	43

<b>SC</b> Stratum Corneum .....	31
<b>SCH</b> Stratum Corneum Hydration .....	34
<b>SD</b> Secure Digital .....	110
<b>SPI</b> Serial Peripheral Interface .....	110
<b>SSWL</b> Skin Surface Water Loss .....	14
<b>TEWL</b> Transepidermal Water Loss .....	7
<b>UART</b> Universal Asynchronous Receiver Transmitter .....	101
<b>VF</b> Volar Forearm .....	16
<b>WiFi</b> Wireless Fidelity .....	25
<b>MQTT</b> Message Queuing Telemetry Transport .....	100

# Chapter 1

## Introduction

The appearance of new information and telecommunications technologies has a widespread impact and can affect almost all industries. The Internet of Things (IoT) has developed in an abundant variety of disciplines including video surveillance and drones, healthcare, energy production, manufacturing, agriculture, retail, transportation and aviation to name a few (Gilchrist 2016). IoT has emerged partly as a result of the decreasing cost of internet-capable devices. The incorporation of electronics and electronic devices into all aspects of modern life mean that IoT has already been applied to a vast array of products. A few examples of existing smart connected products or assets are (Behmann & Wu 2015):

- Smart homes and buildings
- Smart energy
- Smart factories
- Smart cities
- Smart vehicles
- Smart watches

IoT has benefits for both the end user and companies. Customers benefit from better control over aspects of their lives using IoT products that provide improved functionality over non-IoT products (e.g. energy smart meters improve home energy usage leading to lower utility bills). IoT also permits better visibility for companies on their own operations. For example, companies can collect data for audit purposes that allow for improved services, assets management, and improved business processes using lean methodologies such as Six Sigma.

The purpose of this project was to develop an IoT medical device, which falls within the category of e-health.

## 1.1 e-Health

E-health is a branch of IoT that makes use of devices used in healthcare settings to monitor the patient state using sensors and smart healthcare applications (Khalil 2017). An early example of e-health for patient benefit was the development of telepresence robots. These remote-controlled audiovisual robots allow healthcare professionals to interact with patients who live in remote locations and/or are unable to attend a nearby hospital. Giraff was one of the first devices that allowed remote communication between carers and patients and has been used successfully for people with dementia (González-Jiménez et al. 2012). Remote monitoring of patients' homes using Giraff can facilitate independent living as it can provide important information related to healthcare-related aspects of patient behaviour that would not otherwise be apparent in an outpatient consultation. For example, surveillance of mealtimes could confirm that patients had eaten their food and taken their medication, and be prompted by the carer remotely if they had forgotten.

With the emergence of flexible Printed Circuit Boards PCB<sup>1</sup> there has been an emergence of wearables, especially for fitness and self-monitoring of diseases (Bush et al. 2018). Sensors on wearable devices can measure and evaluate vital signs such as:

- Blood pressure
- Heart rate
- Capillary blood glucose

This information can be sent to a medical service that can analyse the data or inform a medical professional. The remote monitoring of patients with chronic diseases such as diabetes is particularly handy for medical prevention, therapy and rehabilitation over long periods of time (Li et al. 2018).

A recent publication studied the different types of smartphone applications for improving psychological health by enabling skills training on aspects such as focus, attention, and coping with life difficulties (Bush et al. 2018). It observed that applications were used for illness management, supporting care, and passive symptom tracking (looking for patterns in physical activity levels and social interactions). It also distinguished five different types of data collected from these applications:

- Self-reported data
- Performance data
- Phone-based sensor data

---

<sup>1</sup>Printed Circuit Board

- Wearable sensor data
- Data from social media

Smartphone applications have been used to benefit a diverse range of patient groups in the home setting, such as palliative care patients (Dhiliwal & Salins 2015), elderly people suffering from social isolation, (González-Jiménez et al. 2012) and patients with chronic diseases in remote locations (Li et al. 2018). All these applications promote patient autonomy and prevent unnecessary travel to healthcare facilities for baseline assessments.

Another interesting research project is the Huggeable, a therapeutic robot for paediatric patients. It is a soft teddy bear able to actively interact with a person (Goris et al. 2008). Sensors throughout its skin react to touch from the user. It also has a visual and auditory system with cameras, temperature and electrical field sensors to detect humans. This information is processed in an embedded processor with WiFi<sup>2</sup> connectivity.

The number of available apps can provide a crude estimate of the scale of interest in IoT e-health. In 2017, it was estimated that major app stores were supporting over 259,000 different e-health applications (Paglialonga et al. 2017)

To conclude, in e-health, there are three types of applications (Pereir et al. 2018):

- Self-monitoring
- Home-monitoring
- Hospital systems

The aim of this project is to develop a mobile IoT e-health device for measuring skin barrier function that can be used for remote monitoring and in hospital clinics.

## 1.2 Transepidermal Water Loss Measurement

Skin is the largest human organ and the measure of its health is difficult. One of the measurements performed on the skin is transepidermal water loss (TEWL). Many instruments on the market measure TEWL and this project aims to develop an upgrade to the Aquaflux to make it portable. In order to be portable, the instrument has to be light and wireless. Measurements on the skin follow guidelines. In order to perform measurements on the skin, the environment has to be controlled. Unfortunately, there are no instrument working outside controlled laboratory conditions not even the Aquaflux.

---

<sup>2</sup>Wireless Fidelity

### 1.2.1 Rational

Although there are several TEWL measurement techniques on the market, most techniques, such as AquaFlux, are limited to controlled laboratory environments. There are TEWL measurement techniques that are portable, but their performances have left a lot to be desired. As illustrated by Imhof et al. (2014), even with Vapometer, one of the top end portable techniques, still has a variability of more than 10%. There is a genuine need for an accurate, reliable, and portable TEWL measurement method.

To address this gap, this project aims to develop a portable TEWL measurement technique that is accurate and reliable. Such technique could be hugely beneficial. People who suffer from skin diseases will be grateful to have a method to evaluate their condition. There are over 13 million people living with skin diseases in the UK (Schofield et al. 2009). Healthcare professionals would find a reliable way to diagnostic the effect of medication on the skin disease. More importantly, it can also be used to evaluate cosmetics which market represents billions. Potential customers are huge as not everyone has a laboratory at their disposal. Rational is highlighted after the literature and provided in section 2.10.4.

### 1.2.2 Research question

To develop such technique, a novel approach is needed. As explained in 2.11 the research question is: is it possible to develop a novel approach for accurate TEWL measurements that can work outside of a laboratory and what factors influence this performance?

### 1.2.3 Hypotheses

This research builds on existing AquaFlux technology. The sensor and chamber design are based on AquaFlux, but with the cold plate condenser. Definitions to describe a good experiment and instrument are given in section 2.9.0.1. A good measurement has to be valid, repeatable, accurate. The research question comprises three hypothesis for this project.

H1: A closed-chambered design improves TEWL measurement by portability. AquaFlux requires mains power supply, and a dedicated computer to run a dedicated complex software, which often requires one day of on-site training. AquaFlux is therefore mainly limited to laboratory use and only by trained operators. The proposed device will be handheld, battery powered, and all the calculations will be done on the device, no dedicated computer is needed. It can therefore be used outside the laboratory. In this way, it is simpler and easier to use than AquaFlux,

and hence more efficient. The closed-chambered design, without the condenser, should still conduct a good measurement, in the terms of accuracy, repeatability, and precision. It should be comparable to that of AquaFlux, and better than other TEWL devices such as Tewameter, Vapometer etc.

H2: A Fan-chambered design speeds up the measurement. By using a fan can make the vapour distribution within the measurement chamber reaches equilibrium state quicker and hence speed up the measurements. This also makes it more efficient than AquaFlux.

H3: A Fan-chambered design reduces the effect of the skin surface water on the TEWL measurements. By setting fan at different speed, we would be able to differentiate the skin surface water from TEWL, as the skin surface evaporation changes as fan speed changes, while TEWL does not.

#### 1.2.4 Research Goals

The research goals outline the strategy for the research to confirm or reject the hypotheses. It followed the steps:

- To test prototypes and find their flaws to improve and build another prototype.
- Analyse the effect of a fan on TEWL measurements.
- The test of prototypes in laboratory conditions will be done on a volunteer. The performances will be compared with another instrument, tested on the same volunteer. The instrument used for comparison is the Aquaflux, as the project is sponsored by Biox Systems Limited to develop a novel TEWL instrument.
- Then a test outside of laboratory conditions will be performed. The performances will be evaluated.

A TEWL measurement technique to work outside a laboratory to be tested using different:

- chamber designs in terms of geometry
- sensors positions
- calculations of TEWL

#### 1.2.5 Research objectives

In order to develop a prototype and test the hypothesis, the project relies on these activities:



- Conducting a literature review
- Developing new mathematical models
- Designing and building different chambers
- Designing software architecture and implementation (embedded software for control, IoT monitoring, data analysis, USB graphical interface)
- Designing algorithms and methods to calculate and approximate what we would like to measure

Conducting a literature review can provide a good background overview of the project, this helps to test all three hypothesis. Developing new mathematical models provides a better understanding of the physics behind the measurements, which also help to test all three hypothesis. Designing and building different chambers help to test hypothesis H1 and H2. Designing software architecture and implementation involves both developing software for embedded systems as well as for Windows, this is crucial for testing all three hypothesis. Finally, designing algorithms and methods to calculate what we would like to measure is also important, which help to test hypothesis H1 and H3.

The second hypothesis is to improve the Aquaflex design by making it portable. For this, the design chapter will go through the requirement of portability. It will also describe the different elements required for the instrument to be portable. Achieving the build and integration of these elements is another objective of the project. Finally the third hypothesis is about the fan reducing the effect of the skin on the measurements. For testing this hypothesis, a comparison between measurements with fan and without will be conducted for each prototype. For the last two hypothesis, there is a need to construct a physical object capable to measure TEWL. In order to construct this object, we need to understand what needs to be measured and what are the elements required in a instrument. The mathematical modelling helps to understand what is measured. Mathematical modelling helps to formulate a method, technique or algorithm to measure TEWL. Mathematical modelling can also recommend design choices. The design part of the project helps to identify and understand the components of the instrument. By designing an instrument some questions arised, in terms of parameters of the measurement, such as the best position of elements. These questions could be answered with simulations or by direct measurements if the design allows the test of the parameter. Performing measurements in vivo helps to understand the practicalities of a measurement. This knowledge would have an influence on the experimental method but also the design, and could be taken into account for the next iteration. Testing prototypes also aims to approve or reject design choices or hypotheses.

The design of the algorithm for calculating and improving the measurements includes understanding of the physical phenomenon and its approximation (it is an approximation because this provides numerical solutions) by mathematical techniques. The algorithm as described here is a high level algorithm. Then a software will be designed and developed corresponding to this high level algorithm. Software design comprises on different tasks such as, conceptualisation of a system, definition of an architecture in order to perform the functions of an instrument as per requirements established further in the thesis on one hand, but also the inherent functions at a lower level in the second hand. Functions required by the IoT instrument changed during the development, by adding new or removing features to the prototype. Software design also includes framing the software, i.e. scoping what is going to be implemented. In addition, software design comprises the consideration, test and selection of technologies to achieve the aims defined by the requirements. Furthermore, software design covers implementation of the design. The implementation of the design lead to software development and testing of basic features, necessary to run the algorithm discussed above. Software implementation covers detailed questions and choices related to common algorithms and data structures problems. Project lasted three years and the codebase needed maintenance, therefore repeating software engineering activities were necessary.

### **1.3 Summary**

Skin barrier function can be measured using TEWL, a precise but challenging method of assessment. Measurements must follow rigorous procedures in a laboratory, which has hindered the development of mobile TEWL measurement devices that can be used in non-laboratory settings. This has severely limited the wider use of such devices, as potential customers such as dermatologists need to be able to use TEWL measurement devices in non-laboratory setting (e.g. outpatient clinics). This thesis focuses on developing a portable TEWL instrument that performs well in uncontrolled environments, using the Aquaflux AF200 as the benchmark.

# Chapter 2

## Theoretical background and literature review

### 2.1 Introduction

This thesis aims to build a measurement system for clinical diagnosis of dermatological diseases by assessing the integrity of the skin barrier. Transepidermal Water Loss (TEWL) has been chosen as the estimate of skin barrier function for this study. This chapter explores the theoretical background of TEWL measurement and the methods used by instruments specialising in the measurement of TEWL. It will cover the following areas specific to this project:

- The physiology of the skin as it relates to hydration and TEWL
- Why it is important to be able to measure skin hydration and TEWL
- Description and critical review of methods for measuring skin hydration
- Theoretical background to TEWL measurement devices
- Currently available devices for measuring TEWL
- Generic issues relating to TEWL measurement
- Review and comparison of current instruments
- Functional specification and discussion
- Strategy for the project
- A guide to the rest of the thesis

## 2.2 Skin histology

The skin is a complex multiphase and multiscale medium (Wang et al. 2006). It is constituted of three layers; the epidermis, dermis and hypodermis. The upper part of the skin is the Stratum Corneum (SC<sup>1</sup>) also known as the horny layer (Fig. 2.1).

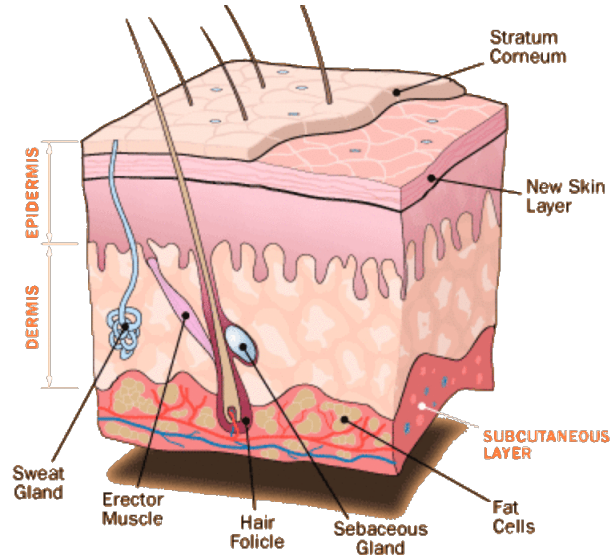


Figure 2.1: Skin Anatomy (adapted from (HumanAnatomyLibrary 2018))

The skin evolves in response to many circumstantial conditions such as the atmosphere, mechanical and chemical forces and intrinsic changes like ageing. It is a sensory organ with nerves to feel heat and pressure. The skin is essential for protecting the body from environmental contamination and for maintaining thermoregulation and homeostasis. Importantly, it is also responsible for body fluid retention.

## 2.3 Non invasive measurements of the skin are important

As the skin is essential for safeguarding life, it is important to have non invasive methods for its examination. Whilst it is possible to use invasive methods to analyse the skin (e.g. punch biopsies for histology to assess skin architecture), this is not justifiable to assess the efficacy of e.g. cosmetics creams. In addition, invasive procedures have an increased risk compared to non invasive methods (e.g. bleeding, infection), which may affect patients with chronic skin conditions requiring serial measurements of skin function over long periods of time.

<sup>1</sup>Stratum Corneum

However, non-invasive measurement of the SC and skin function is difficult. There are different types of instruments measuring different aspects of the skin; some focus on analysing skin structure and geometry whilst others aim to assess skin barrier function. The scope of this research falls within the latter of these two categories.

## 2.4 Other instruments and techniques not related to TEWL or hydration measurement

Instruments to measure skin usually rely on hydration or TEWL measurement. The description of such instruments can be found later in this chapter. There are other skin characterisation instruments on the market. Apart from hydration and TEWL, other biophysical analysis techniques for the skin include (van Erp et al. 2018):

- Greasiness (skin surface lipids)
- Erythematous (red) skin colour, using:
  - Reflectance spectro-photometry
  - Tristimulus colorimetry
  - Diffused reflectance spectroscopy
- Skin morphology with reflectance confocal microscopy

There are many components other than water that can be measured, such as salt or sebum content. The sebumeter is a small probe with an attached test strip pressed against the skin for 30 seconds. The skin surface lipid sticks onto the opaque test strip surface, which becomes increasingly transparent with increasing quantity of lipids. The sebum content can be deduced from the transparency of the test strip, measured with an optical system. Other bio markers have been used, for example to monitor chronic renal failure pathogenesis (Portugal-Cohen et al. 2011). The skin pH can be measured with a flat glass electrode or tape stripping (Darlenski et al. 2009). Additionally, other SC compounds can be analysed using tape harvesting, cyanoacrylate strip and solvent extraction (Darlenski et al. 2009).

There are several non-invasive imaging techniques (for example, optical coherence tomography is a laser-based method that provides a cross-sectional image of the skin to a depth of up to 2mm (Olsen et al. 2018)). Magnetic resonance imaging, generated by the alignment of protons within the water molecules of the human body, is well-suited for skin water content measurement (Leveque & Querleux 2003). However, the equipment remains expensive and is not amenable to being developed into a mobile device at present.

Finally, skin elasticity can be measured with the Cutometer MPA580 (Courage & Kazaka, Germany)(Nakatani et al. 2013) or the elasticity probe of the multidetector from Courage & Khazaka (Hua et al. 2017).

## 2.5 Review of methods for measuring skin hydration

Hydration in this context refers specifically to stratum corneum hydration, or SCH. Hydration is the water capacity of the moisture content of the horny layer. SCH is considered an important factor in cosmetics and is a sign of healthy skin. Hydration levels are expressed in % relative to mass ratio (see Eq. 2.2) or more commonly to volume ratio (see Eq 2.1). The corneocytes, cells in the epidermis, provide the mechanical strength to the skin barrier as well as its hygroscopic, moisturising and elastic properties (Darlenski et al. 2009). The degree of skin hydration depends on the molecular mobility in the SC lipid and protein components (Pham et al. 2016). The lipids contained in the corneocytes help to maintain water content levels (Leveque et al. 1977).

$$\text{Hydration level as volume ratio} = \frac{\text{volume of water}}{\text{volume of water} + \text{volume of dry skin}} \quad (2.1)$$

$$\text{Hydration level as mass ratio} = \frac{\text{mass of water}}{\text{mass of water} + \text{mass of dry skin}} \quad (2.2)$$

Hydration can also be seen as a process in opposition to dehydration. Water transport through the skin is related to both diffusion and convection phenomena (Li et al. 2015). Li et al. studied the dynamics of water transport in the SC in the context of non-inflammatory skin swelling (Li et al. 2015). Swellings can be explained by the hydration of the SC when exposed to liquid water or high relative humidity RH. Water content has a significant impact on skin permeability (Li et al. 2015). However, its impact on the permeability constant is not as important as the impact of changes in temperature (Blank et al. 1967).

### 2.5.0.1 Applications

Hydration can also be used as a measure of skin barrier function. Like TEWL, it can be used to assess skin conditions and evaluate the effects of topical products, with applications in cosmetics, the pharmaceutical industry and dermatology. Although

the applications are the same for TEWL and hydration, the effects of medical conditions and medications on them are inversely related (Berardesca et al. 2018). For example, the hydrating properties of a cosmetic product are achieved by preventing TEWL via occlusion of the skin (Pham et al. 2016).

### 2.5.0.2 Parameters influencing hydration measurement

SCH<sup>2</sup> tends to be relatively stable during the measurement time (Imhof et al. 2009). Contrary to TEWL, the SCH does not show circadian variation (time of the day dependant rhythms) (Yosipovitch et al. 1998). However, hydration measurement is significantly affected by the microclimate, including the environmental temperature. (Rogiers 2001). Some instruments measure electrical properties and any substance between the skin and the electrodes impact the measurement. Furthermore they can be affected by temperature change and skin gland activity thus skin and room temperature have to be controlled (Berardesca et al. 1997).

Guidelines have been published with the aim to standardise the measurement of skin hydration content (Rogiers 2001), (Berardesca et al. 1997).

### 2.5.0.3 Instruments to measure water content

The methods employed to measure hydration levels can be divided into three categories (Darlenski et al. 2009):

1. Microwave methods
2. Electrical methods
3. Spectroscopic methods

The microwave technique is the least commonly used. It can be used to evaluate skin moisturisation and hydration (Darlenski et al. 2009). Jacques demonstrated the measurement of water content variations in human skin using a probe operating at 1 GigaHertz (Jacques 1979). The probe was pressed onto the skin and the microwave circuit measured the dielectric constant and therefore the variations of hydration levels in the horny layer. Its relative obscurity is probably because its principle is closely related to the more common electrical methods.

Electrical methods can be based on one of two principles (Berardesca et al. 1997):

1. Measurement of capacitance and conductance; or
2. Measurement of dielectric constants and depth profile.

---

<sup>2</sup>Stratum Corneum Hydration

### Measurement by capacitance and conductance:

**Overview of methods:** This category of electrical techniques includes the evaluation of (Sotoodian & Maibach 2012) :

- Capacitance C in Farad [F]
- Conductance G in Siemens [S]
- Impedance Z in Ohm [ $\Omega$ ]
- Resistance R in Ohm [ $\Omega$ ]
- Phase angle  $\phi$  in radians

One can see that conductance, impedance, resistance and phase angle are closely related. Resistance R is the impedance Z with a phase  $\phi$  of 0 (Eq. 2.3).

$$|Z| = R \text{ and } \arg(Z) = \phi \quad (2.3)$$

The conductance G is the inverse of impedance Z (Eq. 2.4)

$$Z = \frac{U}{I} = \frac{1}{G} \quad (2.4)$$

where the tension U and the intensity I have sinusoidal forms.

Thus there are two families of methods here, conductance and capacitance. Capacitance of a conductive object is the sum of the electrical charges of the object divided by the potential of the conductive object (Eq. 2.5):

$$C = \frac{Q}{U} \quad (2.5)$$

Where C is the capacitance (Farads F), Q the charge (Coulombs C) and U the difference of electrical potential between two points (Volts V).

**Principles:** These systems use probes to measure the electrical properties of the horny layer, which depend on the water content. Capacitance-based tools apply an oscillating electric field to measure the capacitance of the skin surface, which rely upon the high dielectric constant of water content relative to other skin elements (Yosipovitch et al. 1998). Capacitance is a widely used technique to assess the water content of the SC (Le Fur et al. 2001). In contrast, conductance-based tools apply an electric current to measure the conductance of the skin (van Erp et al. 2018). Similarly, an electrical impedance tool measures the resistance of the SC to an alternating current. Impedance is widely used to evaluate the hydration levels



(Byrne 2010). Historically, the first technique to appear was conductance with two dried electrodes (Tagami et al. 1980). The probes can have a concentric or cross lamellar geometry that can be applied with different pressures (Leveque & Querleux 2003).

**Commercial instruments:** Dermalab (Cortex Technology, Hadsund, Denmark) has two hydration probes, one using the conductance method and the other using the capacitance method. The Corneometer (Courage and Khazaka, GmbH, Cologne, Germany) is based on capacitance measurement. The latter is the most widely used instrument for skin hydration because of its consistent reproducibility (Byrne 2010) and the fact that it has been on the market for a long time.

### Measurement of dielectric constants and hydration depth profile:

**Principle:** Developments in these techniques have allowed for the assessment of water content at different depths in the skin. Capacitance and conductance-based instruments work at low, medium or high frequencies (Leveque & Querleux 2003). They use multiple frequencies in order to assess the dielectric constants at different depths of the skin. This allows for measurement of hydration of both the SC and the epidermis below (Mayrovitz et al. 2013), (Berardesca et al. 1997). By measuring the tissue dielectric constant they allow the user to understand the body composition. There is a negative correlation between these constants and the total body fat percentage, confirming the observation that fat percentage increases with depth (Berardesca et al. 1997).

**Depth:** The maximum depth reached with the variation of frequency is (van Erp et al. 2018), (Clarys et al. 2012):

- 45  $\mu\text{m}$  for capacitance based instrument determined from the capability of the digital probe of the Corneometer CM 825<sup>®</sup>;
- 15  $\mu\text{m}$  for conductance(or impedance) based instrument determined from the capability of the Skicon-200 EX<sup>®</sup>.

However older publications (Berardesca et al. 1997) provide a larger depth for the capacitance instrument (Corneometer CM820-825) up to 60-100  $\mu\text{m}$ . Current brochure claims a small depth of 10-20  $\mu\text{m}$  for the CM 825 (Courage+Khazaka electronic GmbH 2019). Epsilon from Biox Systems Limited measure the near-surface dielectric permittivity and can be linked to capacitance. Its penetration is 20  $\mu\text{m}$  according

the manufacturer's brochure from 2018 (Biox Systems Ltd 2018) although the website claims  $5\mu\text{m}$ . Unfortunately, there are no independent penetration testing in the literature.

The measurement of tissue dielectric constant of human skin can be done at 1.23 Mhz for the horny layer and 300 Mhz for depths of 0.5, 1.5, and 2.5 mm (Mayrovitz et al. 2013). In their experiment, an open ended coaxial probe was used because it is sensitive to free and bounded water contained in the skin (Mayrovitz et al. 2013). In addition, this method permits the assessment of oedema and lymphoedema anywhere on the body. Other techniques are only validated for use on the limbs (Mayrovitz et al. 2009).

Finally, the last generation of capacitance instruments now permits 2D mapping.

### **2D mapping by electrical capacitance:**

**Description:** These instruments can produce a 2D map using a multisensor probe (Berardesca et al. 2018). SkinChip is the patented technology behind capacitive imaging. It uses a fingerprint sensor to create a 2D map. It is described as safe, simple and effective (Leveque & Querleux 2003). In addition to skin hydration imaging, it permits (Ou et al. 2014):

- Skin texture analysis
- Skin 3D surface profile
- Skin micro relief measurements

**Limitations:** Hydration is usually measured with capacitance (Le Fur et al. 2001), especially since the appearance of SkinChip that allows for 2D imaging of the horny layer. However, there are a few limitations. The micro reliefs of the skin, such as pores and skin lines, have an impact on the measurements (Leveque & Querleux 2003). The electrodes are relatively large and can be too big to detect local hydration variations (Batisse et al. 2006). Moreover, it is impossible to evaluate with precision the depth in the SC where the information comes from (van Erp et al. 2018); depending of shape of the electrodes and the instrument frequency (low, medium or high) the water level measured corresponds to a different depth within the epidermis (Batisse et al. 2006). Furthermore, flat electrodes have difficulty maintaining consistent contact with round surfaces and the probes tend to lose full contact with the skin (Batisse et al. 2006). Finally, all electrical methods rely on the measurement of the electrical property of the SC rather than the true water content (van Erp et al. 2018). These instruments are best applied to the evaluation

of variations in water content rather than the quantitative assessment of the water per volume of horny layer (Batisse et al. 2006) (Leveque & Querleux 2003) .

A solution to the measurement of absolute rather than relative hydration can be found in spectroscopic methods.

**Spectroscopic method:** Confocal Raman spectroscopy permits the direct measurement of the water content of the SC (van Erp et al. 2018).

**Principle:** Raman spectroscopy is a laser-based method in which a laser is projected onto an object of interest, producing a spectrum from the monochromatic light source. This is done in order to evaluate vibrational, rotational, and other low-frequency modes (Byrne 2010). In the context of skin measurement, a small quantity of energy from the laser reaches the molecules of the skin, causing excitation of the electrons of these molecules. Electrons have several vibrational energy states, and the energy needed for the electron to have a higher energy state relies on its situation (Caspers et al. 2001). Factors affecting this include:

- Molecular structure
- Molecular interactions
- Chemical environment

**Instruments:** The first commercial instrument for in-vivo measurements based on confocal Raman spectroscopy was manufactured by River Diagnostics. It can precisely measure both the water concentration and depth profile (Byrne 2010).

**Applications:** This method has been used a number of applications. For example, it can be used to calculate the water to protein ratio in the horny layer, as it allows for the measurement of different component's reactions to the laser (Egawa et al. 2007). It can also evaluate the skin permeability to water depending on the depth. This last application constitutes a non-invasive *in vivo* method for the evaluation of skin barrier integrity (van Logtestijn et al. 2015).

As the spectroscopic technique measures absolute water concentration, possible applications include (Darlenski et al. 2009):

- The objective assessment of skin disease severity (using skin barrier integrity as a surrogate marker);
- Measuring the water gradient in the horny layer; and
- Objective support for the claims of topical skin products on improved skin hydration (cosmetic or healthcare).

**Conclusion on measurement of hydration** Hydration can be measured with electrical methods, microwave methods or confocal Raman spectroscopy. The first type of instruments discussed are convenient but only allow for the measurement of hydration-induced electrical properties. They have several limitations and are better at measuring variations of water content rather than absolute values. Whilst Raman spectroscopy is capable of producing a direct measurement of water content, the device itself is bulky and the spectra generated difficult to interpret without training (van Erp et al. 2018).

## 2.6 TEWL as a measure of skin barrier function

Trans-Epidermal Water Loss (TEWL) measurement is a well-established non invasive method to characterise the water barrier function of the skin in physiological and pathological conditions (Miteva et al. 2006). It is used to predict the irritancy and evaluate the efficacy of a therapy. Serial TEWL measurements during infancy have also been shown to predict the development of atopic dermatitis in later life (Horimukai et al. 2016)

### 2.6.0.1 Definition

Skin barrier function can be evaluated by measuring the rate of insensible perspiration. One definition of insensible perspiration is the diffusion of water through the skin without taking into account the secretory processes (e.g. sweating) (Nilsson 1977). The rate of diffusion depends on the keratinisation of the epidermis and the removal of water vapour by the environment. Insensible perspiration is now more commonly referred to as TEWL: trans-epidermal water loss. TEWL can be described as water diffusion and evaporation from the skin. A more physical definition of TEWL would be flux density, i.e. a quantity of water per unit area per unit time (Imhof et al. 2009).

### 2.6.0.2 Applications

The applications for TEWL measurement are primarily cosmetic and clinical (Rogiers 2001), (Leveque 1989), (Fluhr 2005).

Within cosmetics, TEWL measurement can be used to measure skin hydration before and after the application of moisturisers to assess their effectiveness (Leveque 1989). Rogiers, Houben and DePaepe indicate that TEWL measurement can assist with (Fluhr 2005):

- Supporting the claims made for cosmetic products: suitability for sensitive skin, skin compatibility of cleansing products, modulation of the barrier func-

tion by deposition of lipids, increasing skin hydration and the moisturising properties of skin care products, positive effects on the shaving process, protective effects against ultraviolet damage

- Development of innovative cosmetic ingredients and finished products
- Use of non-invasive methodology in safety testing of existing cosmetics on human skin

In dermatology, TEWL measurement can be used in (Rogiers 2001), (Fluhr 2005):

- The study of irritancy of chemicals
- The susceptibility of patients to skin irritation and irritant contact dermatitis
- Assessment of effect of dermatological sensitising agents in occupational settings
- The early detection of signs of skin injury following trauma
- The monitoring of skin pathologies such as disorders of keratinisation and atopic dermatitis

In particular, TEWL measurement can play a pivotal role in assessing the efficacy of existing and in-development treatments for a number of dermatological conditions. Examples include the effect of corticosteroid therapy for acute radiation dermatitis and phototherapy for neonatal jaundice (Fluhr 2005).

## 2.7 Theoretical background to TEWL measurement devices

### 2.7.1 Fick's Law

Regardless of chamber type, all TEWL measurement devices using chambers measure the vapour concentration gradient from the skin. It is based on Fick's first law, also known as the law of diffusion: the propagation of molecules in a fluid (including gaz) vary linearly with the gradient of concentration. The gradient is a vector with  $x$  dimensions but to simplify the explanation, the description that follows would be done in one dimension. The rate of diffusion across a plane perpendicular to this dimension, is proportional to the concentration difference between the two side of the plane. Similarly, the rate of diffusion across a membrane (in this scenario, skin)

is directly proportional to the concentration gradient of the substance (here, water) on the two sides of the membrane and inversely related to the thickness of the membrane. Therefore, the flux of water goes from regions of high concentration (the skin and body) to regions of low concentration (the environment). It is inversely proportional to the spatial gradient of concentration:

$$J = -D_w \frac{\partial C}{\partial y} \quad (2.6)$$

Where:

- J is the diffusion flow rate, expressed in mol or kg per unit of area ( $m^{-2}$ ) over time ( $s^{-1}$ );
- $D_w$  is the diffusivity constant, expressed in  $m^2s^{-1}$  is a function of water concentration;
- C is the mass or molar concentration; and
- y is the distance in the direction of diffusion, expressed in metres.

It assumes a steady state.

### 2.7.2 TEWL definition and skin

TEWL, also known as insensible water loss, is the diffusion of water from the body through the epidermis and into the atmosphere (Youngson 2005). Although insensible water loss could also include diffusion and evaporation of water from other parts of the body (e.g. the lungs), TEWL specifically refers to water loss through the epidermis (Farlex 2012). It is denoted by the letter J because it is a flux of water through a surface (J is often used in physics to denote flux).

The SC is a physical barrier. By applying Fick's law to a simple membrane, Leveque stated that in the case of the membrane being the skin (Leveque 1989):

$$J = \frac{K_m \cdot D_w \cdot C_s}{o} \quad (2.7)$$

Where:

- J is the diffusion flow rate per unit of area (i.e. flux);
- $K_m$  is the concentration sorbed in the membrane / the concentration in solution (a partition coefficient);
- $D_w$  is the diffusivity constant for water, in  $m^2s^{-1}$ ;

- $C_s$  is the concentration gradient of water between the two sides of the membrane (SC); and
- $o$  is the thickness of the membrane.

The SC is able to create a strong barrier to the dermis. This is due to its unique structure comprising of 6 - 20 layers of interleaved corneocytes (Ya-Xian et al. 1999).

TEWL values are related to water concentration gradients within the SC (Sothodan & Maibach 2012), (Blank et al. 1984). The flux  $J$  depends on the permeability coefficient  $P_{SC/w}$  and the concentration differences between the superficial and deep layers of the epidermis (Wang et al. 2006):

$$J = P_{SC/w} \cdot (C_{w/1} - C_{w/2})$$

The skin is hygroscopic, meaning that it attracts and holds the humidity of the air. (Tagami et al. 1980). Diffusivity is directly linked to the water content and the degree of skin swelling (Li et al. 2016).

According to Blank et al., TEWL should be constant in an environment which has a relative humidity (RH) between 20 and 80% (i.e. for an individual in a temperate climate) (Blank et al. 1984). It means TEWL should remain the same if humidity changes within the range. Similar results have been found by Li et al. (Li et al. 2016). However, the TEWL measurement guidelines stress the importance of a controlled environment - in other words, it is better to keep RH and temperature constant during a measurement, rather than letting it fluctuate. Therefore, this is these guidelines that would be followed in this project because hygroscopic properties of skin could vary with RH. Therefore the skin swelling or drying of the skin would be better accounted for in such controlled circumstances.

So far, I have been discussing steady state TEWL once acclimatisation of the subject has occurred. There is also dynamic TEWL that occurs prior to acclimatisation of the subject. This occurs when the measurement is done straight after the subject exposes the site for measurement, i.e. when an occlusive cover such as a shirt sleeve is removed from the skin. The water trapped inside the skin escapes quickly (Cohen et al. 2009). Because dynamic TEWL can be harder to predict and will be affected by the type of skin occlusion (e.g. light shirt vs. heavy jacket), the EEMCO guidelines recommend the measurement of (steady state) TEWL after 30 minutes of acclimatisation (Rogiers 2001).

### 2.7.3 Measurement principle

The measurement of TEWL can be performed with an open chamber, a closed unventilated chamber or a condenser chamber. They are all based on the same

principle; the principle of measurement is based on the water vapour concentration gradient, which in turn is based on Fick's law of diffusion.

Without convection, there is a boundary layer about 1 cm thickness where a gradient of humidity can be observed (Wheldon & Monteith 1980), (Leveque 1989), (Miteva et al. 2006). Leveque adapted Fick's law for the measurement of TEWL (Leveque 1989):

$$J = D' \times \frac{\partial P}{\partial y} \quad (2.8)$$

Where:

- P is the vapour pressure in Pascals (Pa);
- y is the axis orthogonal (perpendicular) to the skin;
- $\frac{\partial P}{\partial y}$  is the vapour pressure spatial gradient in Pa/m; and
- D' is the diffusivity constant,  $D' = 0.670 \times 10^{-3}$  in  $m.h.P^{-1}$ .

Nilsson (Nilsson 1977) provided one of the first definitions of TEWL: the continuous water exchange through the human skin. In addition, he provided D' as a function of temperature and atmospheric pressure. Similarly, Imhof et al. described the two mathematical definitions of TEWL above (see Eq. 2.8 and Eq. 2.7) but used the concentration of water in air (i.e. humidity) rather than the vapour pressure in Pa (Imhof et al. 2009). This gives information regarding the type of sensor to be used (humidity sensor rather than a pressure sensor). In practice, chamber sensors usually measure the RH rather than absolute humidity (AH) and the temperature. In this work, the two physical values of RH and temperature that are captured simultaneously by the sensor will be denoted as RHT<sup>3</sup>. Lowe compared various methods (Lowe 1977) to convert RH to AH<sup>4</sup>. Lowe's polynomial see Eq. 2.9 can be used to calculate saturation (a.k.a. equilibrium) vapour pressure (Pa) from the temperature T expressed in °C. It is a polynomial so it is quick to calculate.

---

<sup>3</sup>Relative Humidity and Temperature couple

<sup>4</sup>Absolute Humidity



$$\begin{aligned}
SVP = & (6.10889961 + \\
& T * (0.04436518521 + \\
& T * (0.01428945805 + \\
& T * (0.0002650648471 + \\
& T * (0.000003031240396 + \\
& T * (0.00000002034080948 + \\
& 6.136820929E - 11 * T)))))) \quad (2.9)
\end{aligned}$$

The partial vapour pressure can be deduced from the definition of RH, which is the ratio between the partial vapour pressure and the saturation vapour pressure:

$$RH = \frac{P_w}{SVP} \quad (2.10)$$

The absolute humidity (AH) can be deduced from the ideal gas law ( $PV=nRT$ ) and molar mass definition  $M = \frac{m}{n}$ :

$$AH = \frac{m}{V} = \frac{P_w \cdot M}{R \cdot T} \quad (2.11)$$

Where:

- AH is the concentration in  $kg \cdot m^{-3}$ ;
- M is the molar mass of  $H_2O = 18.01528 g \cdot mol^{-1}$ ;
- $P_w$  is the vapour pressure in Pascal;
- R is the gas constant =  $8.3145 J \cdot mol^{-1} \cdot K^{-1}$ ; and
- T is the temperature in Kelvin.

This RH to AH transformation can be used not only for the closed chamber but any type of evaporimeter.

#### 2.7.4 Link between hydration and TEWL

Oil-based moisturisers and emollients exert their action by occluding the skin, leading to water retention in the SC and subsequent increase in the skin hydration level (van Logtestijn et al. 2015), (Stamatas et al. 2008). Through this, skin care products aim to improve SC barrier function and decrease the rate of TEWL.

According to the model created by Li et al, diffusivity and hydration are related. Water content is correlated with the water diffusion coefficient in the SC (Li et al. 2016).

Hydration is closely linked to TEWL. Studies have shown a correlation between (Nonato & Lund 2001):

- TEWL and capacitance (and therefore hydration);
- Impedance spectroscopy and TEWL; and
- Permeability to blanching and TEWL.

## 2.8 Currently available devices for measuring TEWL

In this first part, the variety of the different techniques to measure TEWL will be described: systems, operating principles, source of errors and methods.

### 2.8.1 Different approaches

There are 3 main methods to measure TEWL: open, closed and condenser chamber (Alexander et al. 2018), (van Erp et al. 2018), (Imhof & McFeat 2014), (Elkeeb et al. 2010), (Barel et al. 2017), (Plessis et al. 2013). To these 3 methods can be added the ventilated or vented closed chamber (Fluhr & Darlenski 2014) (Qassem & Kyriacou 2019) (Freire & Lopes 2019) and the semi-open chamber (Berardesca et al. 2018). Barel et al. provided an overview of the methods to measure TEWL but actually reference the book of Leveque (Leveque 1989) for a more complete list. To the best of the author knowledge, this is the most exhaustive list in the literature. The techniques and instruments available to measure/estimate TEWL can be separated by measurement coverage:

- Measurements of whole body insensible losses (incubator-based, primarily for infants)
  - Body weight
  - Urine osmolarity
  - Weight of hygroscopic substance following exposure to effluent incubator air
- Small site skin measurement
  - Closed chamber using the weight of a hygroscopic substance
  - Ventilated chamber

- Electro hygrometer
- Dew point hygrometer
- Thermal conductivity cell
- Infra-red water vapour analyser
- Electrolytic water vapour analyser
- Dielectric permittivity device
- Electromagnetic probe

Of note, in the literature the terms 'unventilated chamber' and 'closed chamber' are used to describe the same chamber type; closed chamber is preferred. A full description of open and closed chambers will be provided in chapter two.

Many of these instruments are large and not capable of being transformed into a mobile device. As this study is designed to develop a mobile device for TEWL measurement, the ongoing focus will be on portable devices.

## 2.8.2 Portable methods

The ideal instrument for TEWL measurement should have the following characteristics (Leveque 1989):

1. The device should not change the physical and chemical properties of the stratum corneum;
2. The measurement area should be of an intermediate size: small enough for good sensitivity or to measure a specific body part, large enough to minimise skin variability;
3. The measurement should allow the recording of minute variations in function of time and space; and
4. Measurement time should not exceed two or three minutes to avoid sweat caused by stressing the subject.

All these requirements are justified. For example, devices that alter skin properties during use (e.g. electrical methods) may have an inadvertent effect on TEWL. Large measurement areas can be impractical for use; e.g. the electro hygrometer discussed by Leveque was 25 cm<sup>2</sup> in surface area. When compared to these specifications, Leveque concluded that the Evaporimeter was the best commercially available instrument in 1989 - an open chamber based on the measurement of an evaporation gradient (Leveque 1989). Ventilated chambers were deemed suboptimal as they falsely elevated TEWL by passing affluent air over the skin (Leveque 1989).

There have been recent studies with new open and closed chambers have been developed since the publication by Leveque (Imhof et al. 2009), (Shah et al. 2005), (Barel & Clarys 2006). In order to broaden our design inspiration and possibilities, the methods approached in this literature review focus on closed and open chamber designs.

### 2.8.3 Open chamber devices

Open chambers calculate the gradient of humidity between two sensors (see Figure 2.2a) using Fick's law, from RH measurements. Using Fick's law assumes water vapour transport by diffusion only. The Figure 2.2b shows an example of an open-chamber instrument: the Evaporimeter from Servomed (Stockholm, Sweden). Open chambers rely on Fick's first law of diffusion (see Eq. 2.8). The main limitation of open chambers is their sensitivity to the environment. Indeed, their measurements can be disrupted by room air currents such as the opening of a door, window or someone breathing (Miteva et al. 2006).

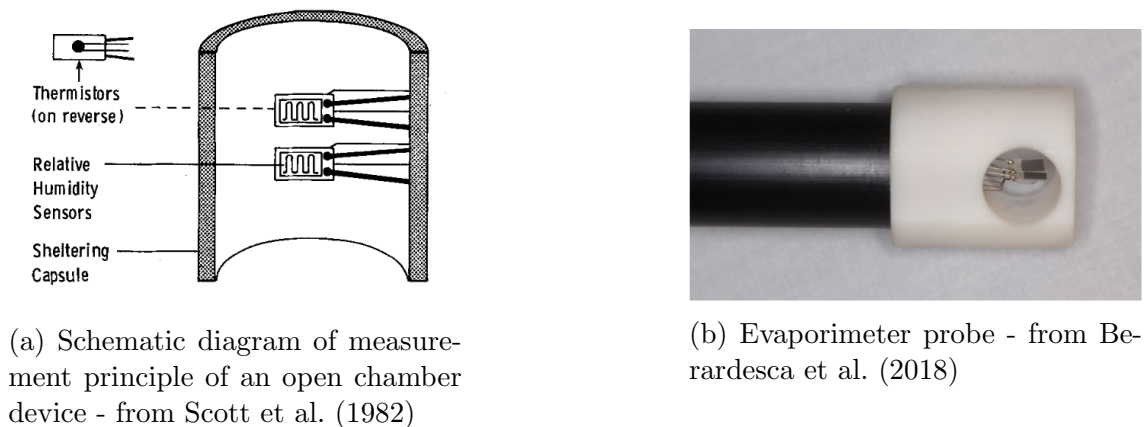


Figure 2.2: Open chamber instrument

### 2.8.4 Closed unventilated chamber devices

Closed chamber devices calculate  $\frac{\partial C}{\partial t}$  the gradient of humidity between two time points, with a single combined RH and temperature sensor. The figures shows examples of closed chambers; the H4300 (Nikkiso-Ysi Co, Tokyo, Japan) in Figure 2.3 and the Vapometer (Delphin Technologies Ltd, Kuopio, Finland) in Figure 2.4. This gradient is assumed linear for a short period of time (Nuutinen et al. 2003):

$$RH(t) = RH_{ambient} + kt$$

$RH_{ambient}$  being equivalent to  $RH_{t=0}$ .

Logically, the concentration of water in air is also the mass in the volume of the chamber prior to measurement, initially with a concentration  $C_{ini}$  :

$$C_w = C_{ini} + kt \quad (2.12)$$

Where:

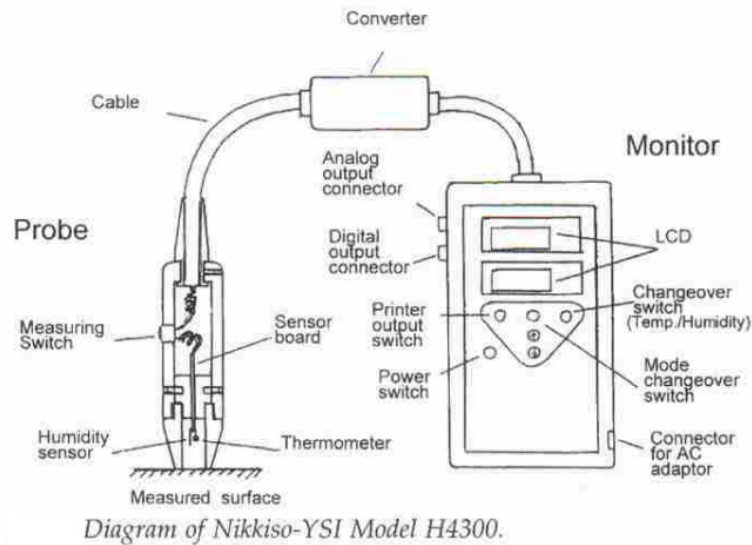
- t is time;
- k is the slope of the rising humidity with regards to time, during measurement; and
- $C_w$  is the concentration of water in air (i.e. humidity).

k is proportional to the TEWL and depends on measurement conditions such as skin surface water loss (SSWL), the ambient temperature and humidity.

RH only varies linearly with time within a certain range. Limitations of this linearisation are the ability of the air to accept the water diffusion from the skin if the air is not saturated, and only being able to work within the operating conditions of the sensor. For example, if the instrument is applied until saturation, RH would reach an asymptote.

### 2.8.5 Condenser chamber: Aquaflux

Imhof et al. assert that the AquaFlux condenser chamber also measures the diffusion gradient like an open chamber, but from the rate the humidity increase (Imhof et al. 2009), like a closed unventilated chamber. The principle of measurement finds its grounds in the phenomenon of diffusion of water evaporated from the stratum corneum to the air (see Figure 2.5). Imhof et al. provided Fick's law using variation as a difference between two quantities instead of a gradient or partial derivatives, to



(a) Diagram of closed chamber instrument - from Tagami et al. (2002)



(b) H4300 probe - from (Tagami et al. 2002)

Figure 2.3: H4300, an example of closed chamber instrument

describe this process of diffusion ( see Eq. 2.13), :

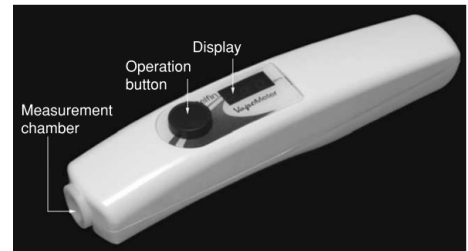
$$J = D \cdot \frac{\Delta c}{\Delta z} \quad (2.13)$$

where  $\Delta c$  is a positive concentration difference across the membrane (expressed in  $kg/m^3$ ) and  $\Delta z$  is the distance orthogonal to the skin, membrane or layer thickness expressed in metres.

In the condenser chamber method, a condenser is a peltier-cooled surface at the



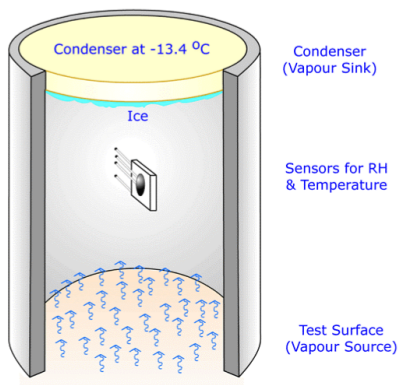
(a) Inside the Vapometer - from Berardesca et al. (2018)



(b) Vapometer probe - from Nuutinen et al. (2003)

Figure 2.4: Vapometer, an example of closed chamber instrument

far end of the chamber that removes water vapour by freezing it. This approach has the benefit to control the micro-climate inside the chamber. A mathematical modelling of this chamber can be found in Cui et al. (2007). It assumes that the diffusivity for the diffusion and heat transfer within the chamber are constant over time.



(a) Schematic diagram of the measurement principle of a condenser chamber - from Imhof et al. (2005)



(b) Aquaflux Instrument - from Biox (2019)

Figure 2.5: Condenser chamber instrument

## 2.9 Generic issues relating to TEWL measurement

### 2.9.0.1 Definitions

In statistics, an experiment can be qualified with respect to:

- Repeatability: A measurement yield the same value after being repeated with the same setup
- Reproducibility: A experiment yield the same value after being repeated by another person, with another instrument
- Reliability: Consistency of a experiment result over time
- Statistical stability: resistance of the study to random errors and how it copes against small sample size for example
- Relative Precision: is the ratio between the absolute precision (the error on the value measured) and the value measured. A coefficient of variation is a measure of relative precision.

An instrument's performances can be evaluated with regards to:

- Precision: if the readings are similar, the experiment is repeatable and the instrument has good repeatability;
- Accuracy: if the measurements are close to the reference value. There is no official gold standard for TEWL instrument but in this project the aim is to provide measurements close to the Aquaflux;
- Stability: Resistance to degradation, ageing and harsh environment;
- Sensitivity: is the capability of an instrument to measure a small change;
- Resolution: the smallest change detected by the instrument

### 2.9.0.2 Difficulty of obtaining reliable measurements

Instruments are calibrated, against an artificial subject, for example salts with known evaporation value, to make sure that the measurements are valid. However, in vivo, TEWL is a small quantity, that can be affected by many factors discussed in section 2.9.1. Therefore it is difficult to obtain reliable measurements. Instruments have different range of operation. Furthermore there is a large number of instruments available on the market. Because of their numbers, their repeatability and



their eclectic range, it is difficult to compare instruments between each others, because they would need to be compared all together, in exactly the same conditions, on the same subject with different observers. Thus there are no gold standard to measure TEWL.

In this field there have been many debates centred on the best method for obtaining reliable measurements. Unsurprisingly, there has been no consensus around a particular technique. Most publications have focused on comparative studies and procedures: comparing the performances of different tools (Wheldon & Monteith 1980), comparing new tools with their predecessor as the benchmark (Fluhr 2005), (Shah et al. 2005) (Barel & Clarys 2006)(Tagami et al. 2002), the establishment of standard methodologies (Leveque 1989), and the establishment of guidelines (Pinnagoda et al. 1990), (Rogiers 1995).

Further discussion on TEWL and skin measurement guidelines can be found in 2.9.1.

### 2.9.1 Factors that influence TEWL

According to Pinnagoda et al. and Rogiers, the factors that influence TEWL can be sorted in three broad categories (Pinnagoda et al. 1990), (Rogiers 2001), (Rogiers 1995):

- Subject-dependent factors: Age, sex, race, sweating, vascular effects, skin effect temperature diurnal variation, anatomical sites
- Environmental factors: Air convection (requiring the use of shielding box), ambient air temperature and humidity that can be influenced by direct light, seasonal variation and geography.
- Instrument factors: zero drift due to humidity change and temperature change (use of insulated gloves), surface plane (to avoid chimney effect and maintain good contact pressure), contact pressure (change of distance between skin and sensor)

It is important to try and control for as many of these factors as possible to allow for more consistent readings. For example, TEWL measurement is usually conducted in laboratory conditions by trained personnel with controlled ambient temperature, lighting, and so forth. To control for anatomical site variation, the same sites are usually measured to allow for comparison of readings over time and between devices. According to Rogiers, the sites of measurement are usually the forearm, the palm of the hand, the fold of the arm and the forehead (Rogiers 1995). To control for instrument factors, calibration of the device is essential.

## 2.9.2 Calibration

### 2.9.2.1 Importance of calibration

It is important to note that there is no absolute measure of TEWL. Barel and Clarys suggested that measurements from an instrument should ideally be compared with the weight of the amount of water that evaporates from the skin surface (Barel & Clarys 2006). Another study proposed to express results as relative values rather than absolute values for TEWL (Fluhr 2005). In addition, it has been observed that calibration depends on boundary layer thickness (the microenvironment immediately adjacent to the skin that potentially has a higher humidity than the wider environment) as well as diffusivity of water through the skin (Wheldon & Monteith 1980).

### 2.9.2.2 How to calibrate a closed chamber instrument

There are various methods to calibrate a closed chamber:

- Nilsson presented a calibration box with different salt solutions. In this method, several salt solutions of varying known evaporation rates were used to calibrate an instrument. (Nilsson 1977).
- Nuutinen et al. studied a closed chamber device (Vapometer) and outlined the 'wet cup' method of calibration. This consisted of a Petri dish with a semipermeable membrane cover and a known quantity of water inside. The device was placed against the membrane and the Petri dish periodically weighed over time (to associate a reading with a particular volume of water loss that had evaporated) so that the rate of water loss could be calculated and compared with device readings (Nuutinen et al. 2003). A Calibration Factor (CF) can be derived (Nuutinen et al. 2003):

$$J = CF \times k \quad (2.14)$$

CF<sup>5</sup> takes into account the volume of the chamber, the contact area on the skin, the conversion from RH to AH and the response time of the humidity sensor.

- Imhof et al. proposed an inverted wet cup flux source method (Imhof et al. 2009). In this version of the wet cup method, the Petri dish is filled with water and a semipermeable membrane attached at the top that allows water vapour (but not condensed water) through. The Petri dish is then inverted and placed

---

<sup>5</sup>Calibration Factor

on top of a TEWL device/sensor and the rate of water loss measured. The advantage of the inverted wet cup method over the wet cup method is that it eliminates the air gap between the water surface and the membrane.

However, this method has been showed to be flawed because of the uncertainty of the diffusion resistance ( $R_e$ ) of the membrane (which is inversely proportional to the diffusivity, see equation 2.15) (Imhof 2007):

$$R_e = \frac{Length}{D_w} \quad (2.15)$$

- The same publication by Imhof also discussed a new droplet method that can be used for TEWL devices that have the ability to record time series (Imhof et al. 2009). In this method, a known small volume of water (droplet-sized) is placed inside the chamber and the water flux measured over time until the droplet has fully evaporated. However, this method is less-suited to closed chambers unless the total volume of water is less than the volume needed to fully saturate the air within the closed chamber, otherwise the water will not fully evaporate (Shah et al. 2005).

Some improvements to current calibration methods have been suggested (Miteva et al. 2006). These include:

- Gravimetric determination of evaporation rates;
- Repeatability checks by measuring with the same probe on really close sites, and check the repeatability at different anatomical sites;
- Checking the influence of air movement on measurements with and without protection around the probe;
- Comparing the measurements with a heated and non heated probe; and
- Conducting measurements using a skin model made from a semi-permeable membrane on top of a bottle to imitate diffusion from the skin.

In summary, calibration is necessary to yield values and to obtain consistent, reliable results . Similarly, the measurement process is also crucial to compare the results of measurements between different instruments.

### 2.9.3 Ideal measurement conditions

Barel et al. highlighted that measurement conditions are central to consistent measurement and described how to secure ideal measurements using the Evaporimeter (Barel & Clarys 2006). However, these factors can be applied to other open and closed chambers.

### 2.9.3.1 Stabilisation time and measurement time

**Measurement time:** A longer measurement time is preferred for open chambers because otherwise it would be more sensitive to variations from skin movement, shivering or SSWL (De Paepe et al. 2005). This principle also applies to closed or any other type of chamber. However, the measurement time in unventilated closed chambers is typically quite short (< 10 seconds) (Plessis et al. 2013), (Fluhr et al. 2006). A 20 seconds application time is likely to be too long at high evaporation rates because the humidity sensor can saturate (Nuutinen et al. 2003). This can affect the readings and the determination of the gradient of RH over time. A  $\Delta$  calculated over too long a time could therefore underestimate TEWL as the rate would reach saturation before the end time point (Nuutinen et al. 2003).

**Stabilisation time:** Grove et al. have previously conducted research trying to identify the ideal start time using an open chamber device (Grove et al. 1999). They started the TEWL measurement 40 seconds after application of the device and measured for 10, 15 and 20 seconds to calculate the mean, the standard deviation and the water loss rate, without smoothing filters. For an open chamber, the order of magnitude of "start time" is given by  $(\text{diffusion length})^2 / \text{diffusion coefficient}$  (Gioia & Celleno 2002):

$$\frac{L^2}{D_w} \leq t \quad (2.16)$$

Where:

- L is the length of the chamber; and
- $D_w$  is the diffusion coefficient of water vapour in air.

According to the same author, the first 30 seconds of a measurement are usually of no use as the steady state will not yet have been reached. Guidelines recommend a stabilisation time of 30-45 seconds (Pinnagoda et al. 1990).

For a closed chamber, the start time needs to be much lower because the microclimate will see its humidity saturate quicker. A variety of start times have been proposed to obtain good measurements; 4 seconds (Nuutinen et al. 2003), 5 seconds (Mündlein et al. 2008) and 10 seconds (Cohen et al. 2009), (Plessis et al. 2013). Through mathematical modelling, some have argued that closed chambers cannot provide accurate measurements because they don't take into account the first 30 seconds (Raynor et al. 2004). However, this view is not generally accepted.

**Total application duration:** For their closed chamber device (H4300), Tagami et al. found that the determination of the gradient started 4 seconds after the

application of the chamber on the skin. The linear part of the slope depends on the evaporation rate and lasts from 3 to 5 seconds. The total time of application was not long enough to block the normal evaporation of water from the skin. During this measurement the temperature increased by  $0.5^{\circ}\text{C}$  (Tagami et al. 2002).

Similarly, Pinnagoda advised that for open chambers the measurement time should be as short as possible (Pinnagoda et al. 1990). They found that stabilisation requires 30 to 45 seconds, consistent with another study (Fluhr 2005). Reading time could be increased for damaged skin.

Nuutinen et al. (Nuutinen et al. 2003) recommended a maximum application time of 20 seconds for closed chambers as longer measurement times would prevent further TEWL measurements due to saturation of the air within the chamber. A long registration of the slope may lead to low TEWL because of this saturation (the curve before linear reaches an asymptote). The closed-chamber H4300 was found to provide much lower values for high TEWL than the conventional open-chamber Dermalab (Tagami et al. 2002).

The challenge of TEWL measurement lies in the precise determination of the slope of RH vs time. Furthermore, they postulated that the smaller the evaporation rate is the longer the time needed to determine the slope and vice versa. The same article concluded that for an open chamber, a long measurement time is required due to a long stabilization of the instrument's readings.

**Duration of a measurement session:** Lastly, Barel et al. found that with the Evaporimeter and Tewameter, the thermal equilibrium of the probe is reached after 10 to 15 minutes when the temperature is equal to skin temperature (around  $30^{\circ}\text{C}$ ). The impact of this on TEWL measurement is that TEWL will continuously increase until after 10 to 15 minutes, and then the TEWL reaches a constant level (Barel & Clarys 2006).

Thus, measurement time is important for both closed chambers and open chambers. Alongside measurement time, there are a number of other recognised parameters to take in consideration for the measurement of skin barrier function.

### 2.9.3.2 Measurement procedure

**Rest** For a closed chamber, a rest period of 20 seconds between measurements is required for the skin to return to room RHT (Kikuchi et al. 2017), (Tagami et al. 2002), De Paepe et al. (2005). For an open chamber this is less of an issue because the air in the chamber moves more freely and return to initial conditions quicker. However, at least 5 seconds between sequential measurements is recommended (Plessis et al. 2013).

**Total duration** The measurement session should not exceed 17 minutes, as this is the minimum time needed by the skin to react to a change in RH (Imhof et al. 2009).

### Signal processing

**Sampling** The number of sensor readings per second is four for the Dermalab open chamber (Grove et al. 1999). Custom-made instruments in other investigations can provide up to five recordings per second (Nuutinen et al. 2003), (Mündlein et al. 2008). As stated above, the Aquaflux obtains two readings per second (Imhof et al. 2014).

**Filters** Signal processing filters are removed for open chambers so the operator can follow up all of the fluctuations (Grove et al. 1999).

#### 2.9.3.3 Clean skin

Maibach et al. recommend to clean the skin before measurement (Leveque 1989) because creams and other products can release water and false the readings. The measurement also cannot be taken straight after the topical application of a cosmetic product. Such products can release water giving a falsely elevated TEWL measurement, and can also prevent TEWL by acting as a barrier to TEWL through the stratum corneum (Rogiers 2001).

Of note, Barel et al. observed high rates of TEWL on damaged skin. Instruments tend to underestimate the TEWL in these circumstances due to the high flux (Barel & Clarys 2006).

#### 2.9.3.4 Skin site

A few studies state that measurements can vary significantly between different anatomical sites varies (Rogiers 2001), (Pinnagoda et al. 1990), (Rogiers 1995). Barel & Clarys (2006) stated that the regions of the forehead and the palms of the hand should be avoided because they yield data with high coefficient of variation (CV) from 30 to 50%, giving misleading results. Rogiers et al. established the following ranking of anatomical sites with decreasing coefficients of variation (Rogiers 2001):

- Palm of the hand
- Sole of the foot
- Forehead, postauricular skin, nail, dorsum of the hand

- Forearm, upper arm, thigh, chest, abdomen, back

Thus, the anatomical sites listed in the last group are best suited for TEWL measurement, i.e. provides repeatable measurements.

### **2.9.3.5 Probe temperature**

As discussed above, the TEWL can increase until the temperature of the probe has reached thermal equilibrium with the skin temperature (30°C), normally achieved after 10 to 15 minutes. Therefore, measurements should not commence until the probe has been warmed up for 15 minutes. Rogiers (Rogiers 1995) and Barel (Barel & Clarys 2006) suggest that this can be achieved by warming the probe on an area of skin that is not going to be used for measurement.

### **2.9.3.6 Flow turbulence**

It is essential to avoid turbulence in the room where measurements are being taken (Rogiers 2001) and to measure only convection flow (Imhof et al. 2009). To minimise the air currents, it is recommended to use protection cover or shielding box with an open top around the instrument (Rogiers 2001), (Barel & Clarys 2006), (Pinnagoda et al. 1990). However, another study (Pinnagoda et al. 1990) highlighted the importance of understanding the impact of using a cover: it suppresses the convection currents, and the TEWL values will be lower than without a cover.

### **2.9.3.7 Sweating and acclimatisation**

The measurement of TEWL relies on the hypothesis the subject doesn't sweat during the measurement. It is fundamental to avoid stress and exercise before or during the measurement session; the person being tested should not eat or consume any excitants like coffee or tobacco prior to measurement (Rogiers 2001), (Fluhr 2005).

Pinnagoda et al. suggest to avoid sweat with the help of acclimatisation: the subject would wait in the room for their skin to adapt to the environmental changes for 15-30 minutes before the study, with the skin being measured uncovered (Pinnagoda et al. 1990). They recommend this because the skin temperature is so important to TEWL. The skin temperature will be affected by the temperature of the environment, so the room temperature needs to be maintained between 20-22°C. Above this threshold, the TEWL can increase significantly (Fluhr 2005), (Tagami et al. 2002). The measurement site should be uncovered to be acclimatised (Fluhr 2005). Barel et al. highlighted the need to control the temperature and relative humidity RH. They also propose acclimatisation of the test person and affirm that due to Fick's law, TEWL decreases with increased external RH (Barel & Clarys 2006). Another

interesting observation is the 'chimney effect'; a standing person with skin warmer or cooler than the ambient air temperature can cause an increased convection of air near the surface of their skin (Pinnagoda et al. 1990) (Rogiers 2001). Taking into account these factors, guidelines recommend that for TEWL measurement, the room temperature should be 22°C and RH<60% (Rogiers 2001), (Fluhr 2005) .

#### **2.9.3.8 Pressure on the skin**

Barel et al. also alluded to the important work of Nilsson (Nilsson 1977), Pinnagoda (Pinnagoda et al. 1990), and Rogiers (Rogiers 1995) that showed the influence of the instrument pressure on the skin (Barel & Clarys 2006). Nilsson reported that TEWL readings increase by 10% per 100 g of load and recommended a contact force of maximum 40 grams by not actively pressing the probe against the skin (Nilsson 1977).

Imhof et al. (Imhof et al. 2009) stated that open chambers are more susceptible to pressure effects than closed chamber instruments due to the proximity of sensors to the skin surface in open chambers (risking direct skin contact) and because of the weaker structure of open chamber probes.

#### **2.9.3.9 Geometry**

Nilsson asserted that the chamber geometry can have a significant impact on the TEWL measurement (Nilsson 1977). Factors including the chamber diameter and the proximity of sensor to skin will affect the probe's measurements.

#### **2.9.3.10 Angle of measurement from vertical**

Imhof et al. (Imhof et al. 2009) discovered that TEWL varied depending on the angle of measurement, i.e. the way probe is handled. For the Aquaflux, when the sensors are below the chamber's cylinder axis, the measurement error can increase to 6 %. Conversely, when the sensors are above the chamber axis, the measurement error stays within  $\pm 1\%$ . Cohen et al. also observed differences with the angle of measurement (Cohen et al. 2009). According to the studies by Pinnagoda et al. (Pinnagoda et al. 1990) and Rogiers (Rogiers 2001), measurements should be taken on a plane surface. Indeed, it is easier to maintain a steady probe position and pressure against the skin on a horizontal plane in order to seal the perimeter of chamber.

#### **2.9.3.11 Conclusion on the measurement conditions**

Guidelines propose a rigid protocol to address some of the multiple potential sources of measurement errors: contact time, probe temperature, flow turbulence, subject



acclimatisation, cleanliness of the skin, choice of anatomical site, diurnal variation, angle of measurement, and pressure on the skin (Pinnagoda et al. 1990), (Rogiers 2001). The more recently revised version of the EMMCO guidance (Berardesca et al. 2018), although providing a review of different instruments, does not provide protocols for skin measurement.

## 2.10 Review of the strengths and limitations of currently available devices

Current available instruments are listed in table 2.1.

Table 2.1: List of portable TEWL instruments available on the market

Device Name	Make	Design
Evaporimeter	Servomed (Stockhom, Sweden)	Open chamber
Dermalab	Cortex Technology (Hadsund, Denmark)	Open chamber
Tewameter	Courage and Kazaka(Koln, Germany)	Open chamber
H4x00	Nikkiso Ysi Co (Tokyo, Japan)	Closed chamber
Vapometer	Delphin (Kuopio, Finland)	Closed chamber
Aquaflux	Biox Systems Ltd (London, UK)	Condenser chamber

### 2.10.1 Comparison between systems

The first comprehensive assessment of the performance of a mobile TEWL device was published by Wheldon and Monteith (Wheldon & Monteith 1980). To the best of the author’s knowledge, it’s the first performance review in the literature that included errors, calibration process and accuracy. However, it compared these performance parameters to theoretical results rather than the performance of another instrument.

A more recent comparison between two open-chambers and one closed-chamber was conducted by Shah (Shah et al. 2005): the (open-chamber) Tewameter and Evaporimeter devices were compared to the closed chamber Vapometer instrument. This study claimed that all three instruments had good repeatability and small standard deviations, suggesting good precision. They also highlighted some of the major advantages of the closed chamber: Because it creates an enclosed micro-environment for measurement, it limits the effect of external and body-induced air currents within and around the chamber, facilitating shorter measurement times and allowing for local and frequent measurement on different anatomical sites (Shah et al. 2005).

Another article comparing the closed chamber H3400 and the open chamber Dermalab found the two devices to have similar sensitivity (ability to measure varia-

tions), reproducibility (ability to reproduce the experiment with different observers, instruments, environment) and variability (the range of variation compare to the average) (Tagami et al. 2002). However, due to the different methodologies employed in providing an estimate of TEWL, the values generated were not directly comparable.

It has been argued that the amount of pressure on the skin has a greater impact on TEWL measurement using open chamber instruments than closed chamber instruments (Imhof et al. 2009). This phenomenon is explained by the position of the sensors on open chambers that are closer to the skin surface and may then touch the skin during measurement. In addition, open probes are less structurally robust and are prone to distortion.

Previous publications have compared the three methodologies. Elkeeb et al. (Elkeeb et al. 2010) found the Aquaflux condenser chamber to be significantly more sensitive than the Tewameter TM210 open chamber or the Vapometer closed chamber. The same observation was noted by Farahmand et al. (Farahmand et al. 2009), that the condenser chamber was more sensitive than the open chamber Tewameter TM210 or closed chamber Vapometer, as well as being able to demonstrate the tape stripping effect (the increase in TEWL observed after having adhesive tape quickly removed from the skin surface). According to Farahmand (Farahmand et al. 2009), the Aquaflux condenser chamber showed a strong correlation with the open chamber Tewameter TM210 and the closed chamber Vapometer SWL-2. The difference in absolute measurement values was likely due to varying calibration methods.

## 2.10.2 Conclusion on the comparison between instruments

All instruments provide different results because of their design, a few characteristics of them can be found on table 2.2. Different design leads to different results and their comparison can be found in table 2.3. The technical characteristics have been found in the brochures of each manufacturer, for this reason, only the last version of the instrument was taken into account: for example, the TM300 instead of the TM210 for the Tewameter, or the H4500 instead of the H4300. Furthermore the performances haven't been assessed by an independent organisation. Performances and information about the various instruments in the tables can be found:

- Evaporimeter by Barel & Clarys (1995) and Blichmann & Serup (1987)
- Dermalab by Cortex (2016) and Cortex (2020)
- Tewameter by Barel & Clarys (1995)
- H4500 by Tagami et al. (2002), Kikuchi et al. (2017) and Salvo et al. (2014)

Table 2.2: Comparison of few designs characteristics between TEWL instruments

Device	Wireless (Yes / No)	Chamber Diameter(mm)	Chamber Height(mm)
Evaporimeter	No	12	15
Dermalab	No	10	10
Tewameter	Yes	10	20
H4500	Yes	8	18
Vapometer	Yes	11	-
Aquaflux	No	5	10

Table 2.3: Comparison of performances between TEWL instruments. These values can be found in the references indicated in the text.

Device	Range(g/m <sup>2</sup> /h)	Resolution(g/m <sup>2</sup> /h)	Error (% or g/m <sup>2</sup> /h)
Evaporimeter	0-300	0.1	15%
Dermalab	0-250	0.1	0.3%
Tewameter	0-70	0.1	$\pm 0.5 \text{ g/h/m}^2$
H4500	0-300	-	-
Vapometer	3-200	1	0.05%
Aquaflux	0-250	0.07	0.05%

- Vapometer by Delphin (2020)
- Aquaflux by Biox (2019)

### 2.10.3 Conclusion on the three methods to measure TEWL

In conclusion, whilst TEWL can be measured with precision using both open and closed chambers, closed chambers have a number of advantages:

- Improved control of the micro-environment by preventing environmental air flow;
- Precise measurement with a small CV scatter;
- Resistance to the effects of increased probe pressure on the skin during measurement; and
- Robust structural design resisting distortion.

All instruments have pros and cons. Their comparison as a family of instruments can be found in 2.4. According to the literature, the Aquaflux has the highest sensitivity than any other instrument. Moreover there is no need to pause between measurements (until at least a few days or weeks). In addition, it is sensitive to tape stripping. It is marked as an advantage because some users want to measure

Table 2.4: Comparison between TEWL measurement methods

Method	Device	Advantages	Limitations
Open	Evaporimeter Tewameter Dermalab	- First to appear, has been considered the de facto standard - No purge time required	- Subject to environment air flows - Longer measurement time
Closed unventilated	Vapometer H4x00	- Short measurement time - Good sensitivity	- Accumulation of vapour affects microclimate - Purge time required - Continuous measurement impossible
Condenser	Aquaflux	- Highest sensitivity than any other method - No rest time required - Tape stripping sensitive	- Longer measurement time

the effect of tape stripping. Therefore it is better to have the functionality than not having it. Having the feature gives more options for the customer.

#### 2.10.4 Literature gap: as a group, what current instruments are missing

There are many factors that influence measurement of the skin barrier function, including choice of instrument, the subject and anatomical site for measurement, the method of calibration employed and the environmental conditions during the measurement. At the time of writing, there is no TEWL device that has been validated for use outside of the strict controlled conditions of a laboratory setting. This thesis will investigate the design of a new portable TEWL measurement device that is less vulnerable to the effects of external conditions in non-laboratory settings.

## 2.11 Research project definition

This research project can be defined with the research question, aim and the objectives.

### 2.11.1 Research question

The literature review identified a gap. There are no instrument working outside of a laboratory. Is it possible to make a portable TEWL instrument that performs well in uncontrolled environments, and what factors influence this performance?

### 2.11.2 Aim

To develop a portable TEWL instrument for use in non-laboratory settings.

### 2.11.3 Research objectives

1. To develop a portable instrument that does not need to be physically connected to a computer during measurement (wireless, data logging, evaluation, display and input) that also has low energy consumption and autonomy.
2. To develop a new instrument design for TEWL measurement in an uncontrolled environment that respects the four requirements of Leveque (Leveque 1989) presented in section 2.8.2.

Performance parameters such as precision (repeatability), sensitivity and accuracy compared to Aquaflux was evaluated. To measure the repeatability, the coefficient of variation (also named the error) was calculated. To measure the sensitivity and the accuracy compared to Aquaflux, the slope of the calibration curve between the two instrument was calculated.

### 2.11.4 Functional design specification

#### 2.11.4.1 Precision

The new device has to measure TEWL with precision. The Aquaflux has a repeatability error of 5% : i.e. the coefficient of variation on repeat measurements is of the order of 5%. This is the target of this project.

#### 2.11.4.2 Sensitivity

In addition, the instrument has to be as sensitive as the Aquaflux, i.e. that a plot of new device readings (y-axis) against Aquaflux readings (x-axis) should have a gradient of at least one. It has been compared with the Aquaflux. There is no quantitative target to be expressed, the comparison is done on a graph.

#### 2.11.4.3 Mobile

The instrument has to be mobile. We will know if we succeed the project if the tests return True for the following expressions:

- An antenna for telecommunications : the rate has to be sufficient
- Autonomy : the instrument has to run for a certain amount of time before the need to be recharged

Table 2.5: Technologies answering to high level requirements

Requirement	Existing technology
Precision	Closed chamber
Sensitivity	Condenser-chamber
Mobile	Integration of existing solution
Autonomy	Integration of existing solution
Performing outside laboratory	Tests to be performed

- Able to measure outside a laboratory setting

These are the raw requirements. Connectivity is a vast feature that need to be scoped. Connectivity will be expressed in more details in the detailed design requirements in section 4.3.

### 2.11.5 Discussion of the functional specification

This section is a discussion of each of the items in the functional specification, indicating for each: firstly, if it can be met with existing technology and, if so, how the best of the available options is to be identified; and secondly where significant work will be required to define needs more clearly or develop new solutions For some of the requirements above, the technology to achieve them already exist and has been implemented, see table 2.5. The first column shows the requirement in question, the broad requirement from the previous section. The second column provide the name of the method, solution or technology that would fill the high level requirement. For example, for precision the solution retained is using a closed chamber. For the requirements of mobility and autonomy, the project relied on the integration of existing solution. However for last item, more significant work has been required to develop a new solution.

In conclusion, the performance of existing devices suggests that it should be possible to meet the specification for the new device by using a closed chamber design but that mobility, portability and autonomy will need to be addressed, which precision and sensitivity will likely to be difficult and above all maintaining performance outside laboratory would be the most challenging.

### 2.11.6 Outline design specification

First, the aim is to achieve comparable performances than another commercialised instrument, with regards to precision and sensitivity. Secondly, the prototype has to be mobile. In order to be portable it needs connectivity. Finally, the instrument has to function well outside of a laboratory. Outside a laboratory, there are air currents, so the chamber will be closed. Outside a laboratory, the environmental conditions

are not as well controlled and the subject can sweat. When a instrument include sweat in the measurement of TEWL, the reading will be wrong, too high and not repeatable. In the next part is suggested a solution to avoid taking into account sweat during the measurement of TEWL.

## 2.12 Strategy for the project

This section presents novel features and calculation considerations for a new portable TEWL measurement device. They are different approaches in order to get consistant and valid measurements. In the first subsection, we give an outline design specification and in the following subsections, different approaches to address the different problems of the 'specification'. All these subsections are part of the strategy of the project. More details are provided in the design section, with testing strategy and instrument requirements, with detailed specification in section 4.3.

### 2.12.1 Outline design specification

First, the aim is to achieve comparable performances than another commercialised instrument, with regards to precision and sensitivity. Secondly, the prototype has to be mobile. In order to be portable it needs connectivity. Finally, the instrument has to function well outside of a laboratory. Outside a laboratory, there are air currents, so the chamber will be closed. Outside a laboratory, the environmental conditions are not as well controlled and the subject can sweat. When a instrument include sweat in the measurement of TEWL, the reading will be wrong, too high and not repeatable. In the next part is suggested a solution to avoid taking into account sweat during the measurement of TEWL. This is part of the strategy for attempting to meet the functional design specification given in table 2.5. The elements precision and sensitivity from the requirements table are going to be addressed with the combination of a few methods described after. The element 'mobile' from the design specification is going to be addressed with an antenna. The element 'autonomy' from the design specification is going to be addressed by a battery. The element 'performing outside a laboratory' from the design specification is going to be addressed using a fan. This is the strategy that is going to be exposed below.

### 2.12.2 Use of a fan to remove the SSWL

Skin surface water loss (SSWL) is a possible cause behind the variability seen during TEWL measurements. Whilst the Aquaflux AF200 addresses this using a condenser, this takes some time to remove the SSWL as it freezes on the condenser. This project will investigate using a fan as an alternative to the condenser to remove the SSWL in

a more timely fashion. The electronics for fan-based SSWL removal are also smaller and simpler than a condenser, making it more suited to developing a mobile device. This measurement technique is novel and has not been explored in the literature to date.

This is part of the strategy for attempting to meet the functional design specification given in the requirements table above. The element 'performing outside a laboratory' from the design specification is going to be addressed using a fan. This is the best approach because the principal problem of measuring TEWL is distinguishing it from sweat. By removing surface water, we remove the problem.

### 2.12.3 Simulations

Simulation is used to try designs without the need of prototyping. Use of a mathematical model has helped to understand the micro-climate. This is part of the strategy for attempting to meet the functional design specification given in the requirements table above. Simulations don't answer to a specific requirements but support all of them, i.e. prevision, sensitivity, performance outside a laboratory. Simulations could also be performed in networking and autonomy but this is not the point here. This is the best approach because it is what is usually what is done in a development project.

### 2.12.4 Gradient calculation process

This section presents considerations for humidity gradient calculation. These reflections have been produced by this project work and are not coming from the literature review. There is no similar published article. This is part of the strategy of the project.

To determine TEWL, the gradient of humidity over time must be calculated. This is expressed by the ratio of the concentration difference over the time difference. However, the elapsed time between the start and end of the measurement (denoted as  $\Delta$ ) can be experimentally altered in order to increase performances like repeatability. Measurements can be shorter or longer and can start with a delay after application of the device (i.e. time  $\neq 0$ ) to wait for a steady state. More details are provided in the following parts.

#### 2.12.4.1 Variation of gradient with time variation $\Delta$

A longer measurement time is preferred because otherwise it would be more sensitive to variations from skin movement, shivering or SSWL. However, the measurement time in unventilated closed chambers is typically quite short ( $< 10$  seconds). This



can affect the readings and the determination of the gradient of RH over time. A  $\Delta$  calculated over too long a time could therefore underestimate TEWL as the rate would reach saturation before the end time point. To determine the ideal measurement time, this project will calculate and compare measurements made with  $\Delta$  over several different durations; 1, 5, 10 and 20 seconds. This is part of the strategy for attempting to meet the functional design specification given in the requirements table above. The 'elements' precision and sensitivity from the requirements table are going to be addressed with an adapted gradient calculation process. Here we are playing with the variation of gradient with time variation. This is difficult to say if it's the best approach to attain our objectives. Please refer to the literature review for comparison of measurement time. However it's going to be used in conjunction with other methods to improve repeatability and sensitivity.

#### 2.12.4.2 Timing of the gradient computation

Fick's first law can be applied only during the steady state of the system, otherwise Fick's second law can be applied for unsteady state. For a steady state, the diffusion rate is constant, whereas for an unsteady state, the diffusion is a function of time. It's because the incoming flux of water in the microclimate can vary with time, i.e. the concentration at the surface of the orifice of the chamber doesn't attain its equilibrium instantaneously upon a change of conditions. In other words, there are a few turbulences in the microclimate after application of the chamber on the skin: caused by the movement of the instrument towards the skin, then the impact of the chamber on the skin. The timing is therefore important. This time when measurement start just after device application on the skin will be referred to as "start time" or "stabilisation time".

The Aquaflux AF200 measures the TEWL twice per second from a start time of 30 seconds. The Aquaflux controls its microclimate that cannot saturate. So the longer it waits to provide a TEWL value, the more precise will be the measurement. The measurement can last up to 90 seconds, until the standard deviation is  $\leq 0.075$ . In this work, the total application time on the skin should ideally last less than 30 seconds. Therefore, start time +  $\delta$  shall not exceed this total duration. A trade-off has to be found between precision and accuracy: saturation of the chamber has to be avoided or the TEWL calculated will be lower than expected. In addition. Thus the different timings will be compared to find an optimal technique.

We presented a table with requirements (see table 2.5). These requirements defined a basic functional design specification. In this section we determine a strategy for attempting to meet this simple specification. The elements precision and sensitivity from the requirements table are going to be addressed with the timing or start time for the gradient calculation. Please refer to the literature review for com-

parison of stabilisation time. This was the best approach because it is logical the application of a instrument on the skin will create perturbation on the microclimate. In addition, it is usually what is done during the study of a TEWL instrument.

### **2.12.5 Measurement procedure**

In order to meet the requirements outlined in the 'specification', a strategy to obtain good repeatability and sensitivity is to develop and adapt and measurement procedure that would yield good results. For this, a few methods are going to be employed: the rest between measurements, the total duration of the session and some signal processing techniques. This is difficult to say if it's the best approach but this is a tentative to obtain good results.

#### **2.12.5.1 Rest**

To determine the ideal rest duration for the TEWL chamber between measurements, this project will test and compare measurements made with several different durations : 30, 60, 120, 240, 360 seconds. This is part of the strategy for attempting to meet the functional design specification given in the requirements table above. The elements precision and sensitivity from the requirements table are going to be addressed with an adapted measurement procedure. Here we are playing with the duration of the rest between applications. This is difficult to say if it's the best approach. Please refer to the literature review for comparison of resting time. However it's going to be used in conjunction with other methods to improve repeatability and sensitivity.

#### **2.12.5.2 Total duration**

The measurement session should not exceed 17 minutes. This is important to allow for correlation between instruments. It is expected that up to five measurements can be obtained in this time frame. In order to meet the requirements outlined in the 'specification', a strategy to obtain good repeatability and sensitivity is to develop and adapt and measurement procedure that would yield good results. For this, the total duration of the session has to be taken into account. This is a good approach to have satisfying results in terms of repeatability and sensitivity because this is constraint. A constraint is a rule that has to be taken into account in order to obtain valid and repeatable results. This has an impact on the strategy to meet the functional design specification.

### 2.12.5.3 Signal processing

**Sampling:** As stated above, the Aquaflex obtains two readings per second (Imhof et al. 2014). This would be the minimum to achieve in this project. Different sampling were tested and compared in order to get good prototype performances.

This is part of the strategy for attempting to meet the functional design specification given in the requirements table above. The elements precision and sensitivity from the requirements table are going to be addressed with an adapted signal processing. Here we are playing with the sampling. It's the best approach because it's a straightforward method to remove variation and smooth the signal. It is the best method because it's a simple tool from signal processing which is a mandatory activity when handling signals. There are signals transmissions in every communication and control systems. Please refer to the literature for comparison of sampling. In addition it's going to be used in conjunction with other methods to improve repeatability and sensitivity.

**Filters:** As explained in the literature review, signal processing filters are removed for open chambers so the operator can follow up all of the fluctuations. This is justified for low frequencies (4 measurements per seconds) but not for high frequencies. During this work a short sampling rate ( 0.02 seconds) provided a quick shift from positive to negative flux. Thus the need for smoothing was evident. This project used difference sampling rate for different prototypes. This is part of the strategy for attempting to meet the functional design specification given in the requirements table above. The elements precision and sensitivity from the requirements table are going to be addressed with an adapted signal processing. Here we are talking about filters, that are reversely linked to sampling. It's the best approach because signal processing is important in electronics. However it has to be studied. Please refer to the literature for comparison of sampling. In addition it's going to be used in conjunction with other methods to improve repeatability and sensitivity.

### 2.12.6 Calibration

The importance of calibration has been discussed in 2.9.2, and the procedures delineated. In this section, more details and the approach taken in this study will be discussed.

This is part of the strategy for attempting to meet the functional design specification given in the requirements table above. The elements precision and sensitivity from the requirements table are going to be addressed with an adapted calibration. However it has to be studied. Please refer to the literature for more details on the calibration. In there the reader will find a justification of the calibration. Finally,

every instrument have to be calibrated before being delivered to the customers.

#### 2.12.6.1 Current calibration methods

Calibration is the experimental determination of the transfer function of a device. The sensitivity describes the slope of the transfer function.

Calibration methods of TEWL instruments consist of calibration of the sensors and then TEWL gravimetric calibration. It is usually done by the manufacturer. At the end user's side, the calibration can be tweaked with a zero flux calibration for the Aquaflux.

#### 2.12.6.2 RHT sensor calibration

The calibration of the sensors is usually not necessary because they are supplied with a NIST (National Institute of Standards and Technology) traceable calibration certificate.

#### 2.12.6.3 Calibration against another instrument

Calibration using another instrument has to be done in the same conditions, because the TEWL varies with humidity. According to Fick's law, the quantity of water by diffusion depends of the concentration on the other side of the membrane, i.e. in the skin during a TEWL measurement. To establish the calibration, the measurements from the chamber prototypes were calibrated against the Aquaflux.

**Outputs:** By comparing prototypes with the Aquaflux, a few quantities as defined in 2.9.0.1 can be established:

- Precision, or repeatability, if the points are close together or sparse;
- Accuracy, which is the difference from a true value ( in this case using the Aquaflux as our reference); and
- Sensitivity, or the smallest amount of change detectable. This is the slope of the transfer function, i.e. the calibration curve.

These three outputs are the criterias to choose the best configurations of parameters that constitute the instrument studied in this endeavour. This selection method use the Aquaflux for reference. Therefore it is different from what has been previously discussed in the literature where only the correlation between instruments and sensitivity is calculated (see 2.10). Indeed there no gold standard in TEWL measurement so the accuracy cannot be measured.

**Method:** The total volume of water evaporating from the skin during measurement is a very small quantity. Therefore, the TEWL measurement device must be precise and sensitive. To overcome this problem, the calibration will be done on a minimum and a maximum TEWL anatomical site (volar forearm vs. palm). A benefit of this method is that it also demonstrates the greatest possible range of values.

TEWL measurements are often performed on the volar forearm (VF) because it produces repeatable measurements and is easy to access without exposing the subject. It also provides a low value for TEWL. The VF is therefore well suited to determine the minimum range of the calibration curve.

The maximum of the calibration curve can be calibrated using the palm. However, the palm can give an erroneously high reading as it is a skin area with many sweat glands. The error rate can be decreased by measuring at the edge of the palm. When the results during calibration had a higher error rate on the palm than predicted, measurements were taken on the wrist. The cheek was used as a middle value to confirm the line between the two extremes of the VF and the palm.

Measurements were performed in triplicate, quadruplicate or quintuplicate and a calibration measurement was performed before each run with the Aquaflux. Unfortunately, not all the configurations have been tested at the same time. They have been tested against the Aquaflux each time, the Aquaflux was used as a reference. A study of optimal rest between each repeats was also conducted.

This is part of the strategy for attempting to meet the functional design specification given in the requirements table above. The elements precision and sensitivity from the requirements table are going to be addressed with an adapted calibration. Here is the description of calibration method with another instrument. It is a good approach because it is quick to do. Please refer to the literature for more details on the calibration. In addition it's going to be used in conjunction with other methods of calibration.

#### 2.12.6.4 Calibration with a fixed quantity of water

Two gravimetric calibration techniques are presented here: the wet cup and the droplet, followed by two calculation methods.

**Wet cup:** This method is the most widespread method for calibration. As discussed in the literature review, it uses a semi-permeable membrane with water in a container beneath.

**Droplet:** The droplet method consists of the observation of the evaporation of a droplet of a known volume ( $5\mu g$ ) to dryness.

This is part of the strategy for attempting to meet the functional design specification given in the requirements table above. The elements precision and sensitivity from the requirements table are going to be addressed with an adapted calibration. This section is about the technique used for calibration with a fixed quantity of water. This is the best approach because the accuracy of the instrument can be directly measured with a fixed quantity of water. However it has to be studied in terms of determination of the quantity of water from the measurements. These is being described just below.

**By correlation:** Taking the wet cup example, the chamber is placed on the membrane and the slope  $k$  of  $RH(t)$  curve is recorded. A CF as described in the literature review takes into account the volume of the chamber, the contact area on the skin, the conversion from RH to AH and the response time of the humidity sensor. This relies on the assumption that the RH changes is linear over time.

**By integration:** The definition of mass flux is:

$$J = \frac{\Delta m}{A \cdot \Delta t} \quad (2.17)$$

Where  $m$  is the mass of water and  $A$  is the area.

To calculate the flux  $J$ , we need to integrate the area below the curve of TEWL to find the measured quantity of water:

$$m = A \times \int_0^{\infty} J dt \quad (2.18)$$

This is part of the strategy for attempting to meet the functional design specification given in the requirements table above. The elements precision and sensitivity from the requirements table are going to be addressed with an adapted calibration. This section focused on the calculation for the calibration with a fixed quantity of water. They are good approaches to experiment with because they are possible to set up. Please refer to the literature review for comparison of calibration methods. Finally, these methods are going to be used in conjunction with other methods to improve repeatability and sensitivity.

### 2.12.7 Conclusion on the strategy

The biggest challenges expected are the behaviour of the fan with the skin microclimate because this is new. It also create a turbulent flow, complicated to predict. The effect of the fan has to be studied precisely, within the chamber. The effect of

the fan on TEWL has to be analysed. Because it is new, it is a critical aspect to address with the highest priority.

## **2.13 Development Project Definition**

This development project can be defined with the hypothesis tested, deliverables and the contribution to knowledge.

### **2.13.1 Hypothesis**

The aim is to develop a TEWL instrument for use in non-laboratory settings. The research question includes the factors that influence the performance of the instrument. This research focus using a fan to reduce the effect of the skin and to homogenise quickly the chamber of measurement. The use of a fan to blow surface water would permit the measurement of TEWL outside a laboratory. The new design will provide a more precise and accurate measurement.

### **2.13.2 Deliverables**

- Literature review
- Mathematical models
- Hardware prototypes: circuit, Printed Circuit Boards (PCBs)
- Software for the microcontroller and computer
- Chamber prototypes
- Probe casing design and manufacture

### **2.13.3 Contributions to knowledge**

This thesis provides original contributions to knowledge in the following areas:

- Theoretical investigation of the measurement technologies
- Theoretical investigation of the mobile technologies
- Mathematical modelling of temperature and humidity in a closed chamber
- Design of a new measurement chamber
- Design of a new electronic circuit for a closed chamber

- Microcontroller software development
- Prototype system integration and testing
- Prototype calibration
- Evaluation of performances and benchmarking
- TEWL computation methods

## 2.14 Thesis outline

In order to design a portable instrument less susceptible to external conditions, the relevant parameters have to be defined and their effect on TEWL measurement need to be discussed in more depth.

Chapter 3 delineates the core operation of the instrument and delves into the mathematical and numerical modelling.

Chapter 4 presents the development of the prototypes: for each version, the design and the experimental results are presented. Chapter 5 summarises the results, draws conclusions on the research and stipulates recommendations for future work.

## 2.15 Summary

In this chapter, a comprehensive description of TEWL and hydration measurements methods was given. TEWL was defined using Fick's law, describing the physical phenomenon of diffusion. The human skin diffusion processes were also characterised.

Following this, the main instruments relying on the measurement of TEWL were reviewed and compared, individually and as group. The main instrument families for TEWL measurement i.e. the open chamber, the closed chamber and finally the Aquaflux condenser chamber were compared.

Lastly, the strategy for this development project was outlined. First, the use of a fan to remove the surface water was presented. Then, the humidity gradient calculation was depicted. Two parameters  $\Delta$  and start time, corresponding to the timing of the measurement, were introduced. Furthermore, the data acquisition procedure was detailed, including the recommended rest time between measurements, the total duration and the signal processing. Calibration methods were expressed: first the calibration process with another instrument and then with a fixed quantity of water.

The next chapter explores the mathematical modelling behind TEWL measurement. In order to understand fully the way the instruments obtain and process data,



it is beneficial to model the chamber to guide the design process and adapt potential prototypes to more accurately measure TEWL.

# Chapter 3

## Mathematical Modelling and Simulations

### 3.1 Introduction

TEWL is a natural phenomenon that can be observed with humidity sensors. In order to fully understand the diffusion phenomenon and its behaviour in a measurement chamber, it is critical to make a model of this process. In engineering project management, an important early step is to build a digital representation of a system and to perform simulations. It helps to try different systems designs to find the best working theoretical model, without the costs of manufacturing multiple physical systems. Two pieces of software have been chosen for this project: Matlab and ANSYS. Matlab is a tool for numerical calculation in Engineering, and ANSYS is a leader in numerical calculations and its solver Fluent is a well recognised software used in Computational Fluid Dynamics (CFD).

### 3.2 Aim

Simulations is used to try different designs without manufacturing it. The aim of the mathematical modelling is, for example, to try different size and check where it would be better to place the sensor. In the design specification laid out in the previous chapter, a solution to avoid taking into account sweat during the measurement of TEWL was presented: the use of a fan. In order to understand the effect of the fan on the micro-climate the modelling of the interior of the chamber is useful. The idea here is to identify regions where the mixing is less important. However, the effect of the fan on the skin is out of scope, because of the simplifications made in the model. The instrument performances will be evaluated on the repeatability, the sensitivity and the accuracy compared to the Aquaflux. With the simulation

models, the design can be tweaked in order to obtain the best repeatability and sensitivity. The goal is to maximize the flux for a given TEWL input. By having a maximum flux measured, the sensitivity is higher. In addition, avoiding turbulent flow would help to have a higher repeatability. For every given chamber geometry and design, doing a simulation will help to identify the regions where to place the sensors in order to maximise the flux amplitude but also minimise the turbulences.

### 3.3 Parameters found in the literature

This section reviews factors that have previously been discussed in the literature as relevant to the modelling of TEWL measurement in a closed chamber.

The first fundamental part consists of articulating the problem. The three equations of conservation, continuity, momentum and energy, are the base to build a mathematical model of the natural processes of heat transfer and diffusion (Rohsenow et al. 1998), (Luikov 1968). The two processes obey the heat Partial Derivative Equation (PDE<sup>1</sup>) and will be described in more detail in 3.4.

**Boundary layer:** The expected results of the simulations should show a gradient. According to Fick's law, (see Eq. 2.6 in Chapter 2), the water vapour concentration follows a gradient from the skin surface as it emanates into the atmosphere; this zone is known as the boundary layer. It's width is a constant, evaluated as 7-10mm from the skin surface (Fluhr 2005), (Nilsson 1977), (Wheldon & Monteith 1980). More recent publications have called into question the existence of the boundary layer on uncovered skin, but this has not been experimentally proven (Imhof et al. 2009). The value of 10mm will be used for the analysis of the simulation results. This boundary layer affects the humidity gradient. Conversely, the temperature gradient in this area is very small (Nilsson 1977). In the absence of convection, the gradient expands infinitely until it meets a surface like a wall.

**Mass diffusion:** The inputs for a model of the mass transport diffusion phenomenon are:

- The diffusivity of water vapour in air at a specific temperature;
- The skin releasing a flux  $J$  towards the chamber ( $J \neq 0$ ) so the skin is a Neumann <sup>2</sup> condition; and
- The chamber sides that are insulated with a flux = 0.

---

<sup>1</sup>Partial Derivative Equations

<sup>2</sup>

Previous observations of diffusivity have shown that it is not constant and increases with hydration (Wu 1983) (Blank et al. 1984). The coefficient of diffusion depends on the humidity gradient between the two sides of the SC (see Eq. 2.7). Changes in ambient humidity modify the concentration of water on each side of the SC. For example, a reduction in ambient humidity increases the gradient and the flow  $J$ . This dehydration would lead to a reduction in the coefficient of diffusion (Leveque 1989), (Blank et al. 1984).

The diffusion coefficient can be approximated with 8% error using the Chapman–Enskog method (Cussler 2009) from kinetic theory. Chapman-Enskog method is used to simplify and solve the non linear Boltzmann equation, to determine the speeds before and after collisions of particuls (Kremer 2011) using approximations. Kinetic theory of gas is linked to collision theory where: for low concentration of matter there are few collision and for high concentration, there are more collisions. Diffusion coefficient can be expressed with the temperature (see Eq. 3.1). The mass diffusivity  $D_w$  is therefore strongly correlated with temperature: because it is expressed with  $T$  and two of its parameters depends on  $T$ .

$$D_{ij} = \frac{A}{8} \left( \frac{N}{2\pi} \left( \frac{1}{M_i} + \frac{1}{M_j} \right) \right)^{1/2} \frac{(kT)^{3/2}}{p\sigma_{12}^2 \Omega_{ij}^*} \quad (3.1)$$

Where:

- $T$  is the absolute temperature;
- $\sigma_{ij}$  is the average collision diameter  $\sigma_{ij}$  is calculated as the arithmetic average of the individual  $\sigma$ s
- $\sigma$  is the cross section: the probability of interaction of a particle for a specific reaction, here, the diffusion, the cross section is also a function of the temperature of nucleus;
- 1 and 2 are indices for the air and the water vapour;
- $N$  is the Avogadro number;
- $M$  are the molar mass;
- $p$  is the pression;
- $k$  is the Boltzmann constant; and
- $\Omega_{ij}^*$  is the collision integral in the Boltzmann equation ((Lieberman & Lichtenberg 2005)). It related to the collision of particuls  $i, j$  approximated by solid spheres. The collision integral is a value used in the Boltzmann equation. The

differential angular range of the scattered particle is  $\partial\Omega$  and the differential size of the cross section is  $\partial\sigma$ . The ratio  $\frac{\partial\Omega}{\partial\sigma}$  is integrated in the Boltzmann equation in order to find the probability distribution of velocity of a particle, as a function of time. It is a function of the temperature and can be calculated with Lennard-Jones potential.

A number of diffusivity values can be found in the literature. Nilsson used a diffusivity constant of  $D_w = 0.0929 \text{ m}^{-2} \cdot \text{h}^{-1}$  (Nilsson 1977) for a water vapour mixture with air at a temperature of 300K and an atmospheric pressure of 101 kPa. Wheldon used a molecular diffusion coefficient of water vapour in air at 25°C,  $D_w = 2.49 \times 10^{-5} \text{ m}^{-2} \cdot \text{s}^{-1}$ , noting that it increases by 0.7% per degree temperature rise (Wheldon & Monteith 1980). More recent published values are  $0.242 \text{ cm}^2 \cdot \text{s}^{-1}$  from Engineering ToolBox (2018a) or  $0.282 \text{ cm}^2 \cdot \text{s}^{-1}$  at 25 °C (Cussler 2009). These numerous values of  $D_w$  enumerated above have been tested and did not provide observable differences on the simulations. The last value given here was used in the Matlab models displayed later in this chapter:

$$D_w = 2.82 \times 10^{-5} \text{ m}^2 \cdot \text{s}^{-1} \text{ (SI)} \quad (3.2)$$

According to Imhof et al., a normal volar forearm TEWL is  $10 \text{ g} \cdot \text{m}^{-2} \cdot \text{h}^{-1}$  (Imhof et al. 2009). This value is an appropriate value to use for calculating the flux  $J$  coming out of the skin and was used for the simulations with Matlab:

$$J = 2.78 \cdot 10^{-6} \text{ kg} \cdot \text{m}^2 \cdot \text{s}^{-1} \text{ (SI)} \quad (3.3)$$

The humidity of the skin  $RH_{skin}$  has been studied, but no recent publications have provided as exhaustive results as Mole (Mole 1948). In this project the experimental conditions kept RH between 40 and 60%. According to Mole, this corresponds to  $RH_{skin}$  between 25 and 30%. As these values were derived many decades ago, new values used for  $RH_{skin}$  in these models were derived experimentally.

**Thermal diffusion:** Similarly, the heat model has three inputs:

- The thermal diffusivity of the air;
- The skin temperature; and
- The walls of the chamber (It is assumed that inside the cylinder, walls are insulated and no heat transfer from inside the chamber to the material of the cylinder is possible)

The thermal diffusivity  $\alpha$  is expressed as :

$$\alpha = \frac{k_a}{\rho \times C_p} \quad (3.4)$$

Where:

- $k$  is thermal conductivity;
- $C_p$  is specific heat; and
- $\rho$  is the density of the medium (the air).

Thermal diffusivity depends on the humidity as increasing humidity will increase the density of the air. For simplification of the models, it is common in the literature to consider the thermal and mass diffusivity constant (Cui et al. 2007). The mass diffusivity expressed in Eq. 3.1 is depending on the temperature according to kinetic theory. To simplify the mathematical models and their numerical solutions on MATLAB, the diffusivity is assumed constant. The thermal diffusivity depends on the pressure and the temperature but the range of operation of a closed chamber during a TEWL measurements would not have much thermal diffusivity variations (Engineering ToolBox 2018b). The specific heat used for water vapour is  $1.996 \text{ kJ} \cdot \text{kg}^{-1} \cdot \text{K}^{-1}$  (Engineering ToolBox 2003).

Because the thermal conductivity of water vapour is only available at high temperatures when water is in gas form, it is difficult to calculate the thermal diffusivity from Eq. 3.4 for the range of operation of a TEWL instrument. The thermal diffusivity of water at 400K is  $2.338 \times 10^{-5}$  (Eckert & Drake Jr 1959). However, the thermal diffusivity of water in liquid form is much lower. Thermal diffusivity of water vapour in air at 20 °C is  $0.215 \text{ cm}^2 \cdot \text{s}^{-1}$  (Montgomery 1947), which is quite close to the thermal diffusivity of dry air ( $0.22059 \text{ cm}^2 \cdot \text{s}^{-1}$ ). Therefore these Montgomery values will be used for 293K or dry air diffusivity for other temperatures:

$$\alpha = 2.15 \cdot 10^{-4} \text{ m}^2 \cdot \text{s}^{-1} \text{ (SI)} \quad (3.5)$$

For the heat equation, the boundary condition for the skin is going to be approximated to a Dirichlet<sup>3</sup> condition with a constant value. Mole established formulas and charts for the temperature and RH of the skin and presumed the upper limit of  $T_{skin}$  to be 35.6 °C (Mole 1948). Whilst Mole did not determine the ambient temperature  $T_{amb}$  at which no sweating occurred, they did determine that at temperatures above 32 °C the sweating becomes so profuse so as to make the measurement of RH

<sup>3</sup>In mathematics, a Dirichlet condition is a boundary condition imposed on a differential equation or partial differential equation where the value of the solutions at this boundary has to verify to solve the equation. In the case of Dirichlet, it has to be a constant value over time.

too complex. More recent papers have stated that the ambient temperature has to be maintained at 22 °C to avoid sweat (Rogiers 1995). According to Rogiers, the skin temperature is  $30.9 \pm 1.0$  °C. Yosipovitch et al measured a skin temperature between 31 °C and 33 °C (Yosipovitch et al. 1998). Grice et al. measured a temperature between 25 °C and 39 °C (Grice et al. 1971). Some research expresses the temperature of the skin as a function of the ambient temperature  $T_{amb}$  (Saltin et al. 1972)(Eq.3.6).

$$T_{skin} = 27 + 0.22 \cdot T_{amb} \quad (3.6)$$

Another paper expressed  $T_{skin}$  with the environmental conditions of temperature and RH (Cravello & Ferri 2008)(Eq.3.7). This model has a  $R^2$  coefficient of 0.7 which constitutes a good regression:

$$T_{skin} = 32.6187 + 0.3017 \cdot (T_{amb} - 25) + 0.00608 \cdot (RH_{amb} - 65) \quad (3.7)$$

More recent research has shown an average of 34 °C on the arm (Munir et al. 2009). This is the latter case used for modelling in this project: the skin as a Dirichlet condition fixed at 34 °C:

$$T_{skin} = 307 \text{ K (SI)} \quad (3.8)$$

### 3.3.1 Assumptions

The phenomenon of TEWL is too complex to be fully described mathematically. Some assumptions are needed to simplify the problem in order to build a computational description. This simplification facilitates the abstraction of the phenomenon and its understanding. The models are evaluated with the following assumptions:

- The process can be regarded as isothermal;
- There is no hysteresis effect of sorption and desorption;
- The process can be modelled in one dimension: the area of the chamber is large compare to chamber length, following the direction of the diffusion process;
- Water vapour is an ideal gas;
- Diffusion coefficients are constant values that have been provided in the sections above; and
- Vapour partial pressure is the only driving force.

## 3.4 Mathematical model of a closed chamber instrument

This section mathematically describes the Boundary Value Problem BVP of a closed chamber.

There are two PDEs to resolve: one for the vapour diffusion or mass transfer and one for the heat transfer.

### 3.4.1 Mass diffusion

Vapour diffusion is an equalisation process. If there are equal amounts of vapour on each side of a plane, there is no diffusion of molecules across that plane as there is already an equilibrium of particles of water. If there are more molecules on one side of the plane, there would be transport in the direction of the highest to the lowest concentration.

Vapour diffusion is driven by the difference in vapour concentration, i.e. the difference in humidity by volume.

**Fick's First Law of Diffusion:** As stated in 2.8, Fick's first law is:

$$J = -D_w \times \frac{\partial C_w}{\partial y} \quad (3.9)$$

Where  $D_w$  is the coefficient of diffusion in the medium.

**Fick's second law of diffusion:**

$$\frac{\partial C_w}{\partial t} = \frac{\partial^2 C_w}{\partial y^2} \quad (3.10)$$

**Boundary conditions:** At  $y = 0$  (touching the skin):

$$\frac{\partial C_w}{\partial y} \Big|_{y=0} = J \quad (3.11)$$

At  $y = L$  (the length of the chamber):

$$\frac{\partial C_w}{\partial y} \Big|_{y=L} = 0 \quad (3.12)$$

because it is a wall with flux = 0 (Neumann <sup>4</sup> condition).

---

<sup>4</sup>In mathematics, a Neumann condition is a boundary condition imposed on a differential equation or partial differential equation that solutions in order to solve the equation has to verify at this boundary. In the case of Neumann, the derivative has to be a constant value over time



### 3.4.2 Heat transfer

Under normal conditions, there is heat transfer from the skin to the air. This is also true when taking measurements with a closed chamber (Fig. 3.1). Heat is transferred from areas of high temperature to low temperature. Fourier's law of heat conduction expresses the rate of heat transfer  $q$  proportional to negative temperature  $u$  gradient:

$$\vec{q} = -\alpha \cdot \nabla u$$

If we ignore the heat exchange into the cylindrical walls, the temperature distribution can be calculated in one dimension:

$$Q = -k_a \cdot \frac{\partial u}{\partial y} \quad (3.13)$$

where  $Q$  is the heat flux density and  $k_a$  is the thermal conductivity of the air.

The law of conservation of energy states that the energy variation in a segment during  $\Delta t$  is equal to the heat coming inside minus the heat going outside.

The conservation of energy within the axis  $y$  and Fourier's law (Eq. 3.13 leads to the heat equation 3.14:

$$\frac{\partial}{\partial t} u(t, y) = \alpha \cdot \frac{\partial^2}{\partial y^2} u(t, y), \quad y \in (0, L) \quad (3.14)$$

For a simplified model, the skin is a condition of the first kind with a fixed temperature of  $34^\circ\text{C}$ . The body uses thermoregulation to keep the temperature stable, so a Dirichlet condition is set. In this skin measurement problem, the boundary conditions are:

$$u(t, 0) = u_{skin} \quad \text{and} \quad \frac{\partial u(t, L)}{\partial y} = 0 \quad (3.15)$$

and the initial conditions are:

$$u(0, y) = f(y) = u_{ini} \quad (3.16)$$

Where  $u_{ini}$  is the initial constant value.

The principle of measurements and the mathematical models associated with it have been described. The next topic of discussion is the implementation of these principles in MATLAB.

## 3.5 Numerical solution

The models were run with the boundary conditions (BC) and initial conditions (IC):

- $T_{skin} = 34^\circ\text{C}$

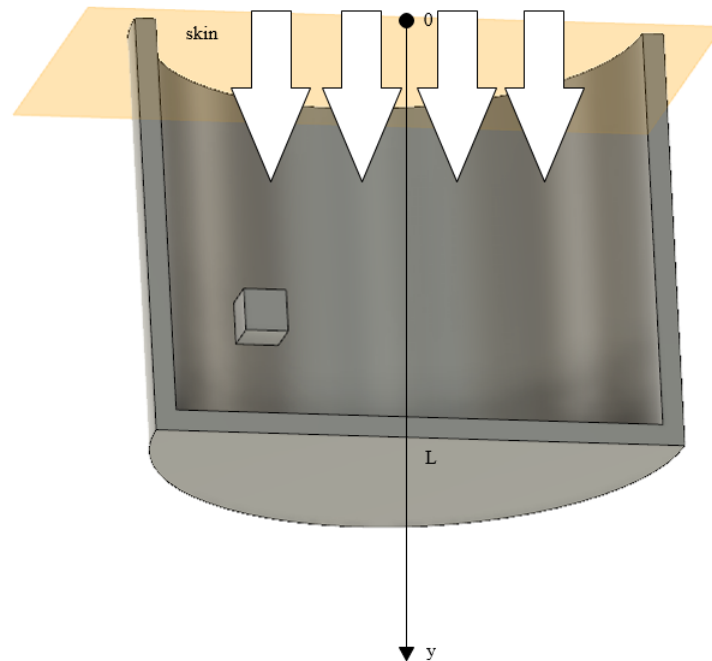


Figure 3.1: Schematic diagram of heat transfer in a closed chamber

- $J = 10g \cdot m^{-1} \cdot h^{-1}$
- $RH_{ini} = 50\%$
- $T_{ini} = 25^{\circ}C$

MATLAB provides the function `pdepe` to solve problems for systems of parabolic PDEs in the one space variable ( $x$ ) and time ( $t$ ) with an initial value and specific boundary value. The PDE has the form :

$$c(x, t, u, \frac{\partial u}{\partial x}) \frac{\partial u}{\partial t} = x^{-m} \frac{\partial}{\partial x} (x^m f(x, t, u, \frac{\partial u}{\partial x})) + s(x, t, u, \frac{\partial u}{\partial x})$$

For all  $t$  and for  $x$  left or right boundary conditions, the solution must satisfy a boundary condition  $u_l$  and  $u_r$  of the form :

$$p(x, t, u) + q(x, t) f(x, t, u, \frac{\partial u}{\partial x}) = 0$$

The parameters used for the heat transfer PDE were:

- $s = 0$
- $c = \frac{1}{\alpha}$  with  $\alpha$  being the thermal diffusivity discussed in section 3.3

- $b = DuDx$

The parameters used for the BC<sup>5</sup> were:

- $pl = ul - T_{skin}$  with  $T_{skin} = 34^\circ \text{C}$
- $ql = 0$
- $pr = 0$
- $qr = 1$

The initial condition was set to  $u_0 = 25^\circ \text{C}$ .

The same parameters were used for the mass diffusion process, except for these parameters:

- $D_w$  (water vapour mass diffusivity) =  $0.282 \times 10^{-4} m^2 \cdot s^{-1}$
- $ql = 1$
- $pl = J/D$  with  $J = 2.78 \cdot 10^{-6} kg \cdot m^2 \cdot s^{-1}$
- $pr = 0$
- $qr = 1$
- $u_0 = 50 \%$

The function pdepe doesn't permit the calculation of the steady state so the microclimate at 300 seconds was calculated. After a few experiments with a similar chamber, it can be assumed that equilibrium is found before a few minutes of the application. In addition, the simulations were run with larger numbers and no differences of simulations results were observed. The temperature and humidity profile can be seen on Fig. 3.2 and Fig. 3.3 respectively.

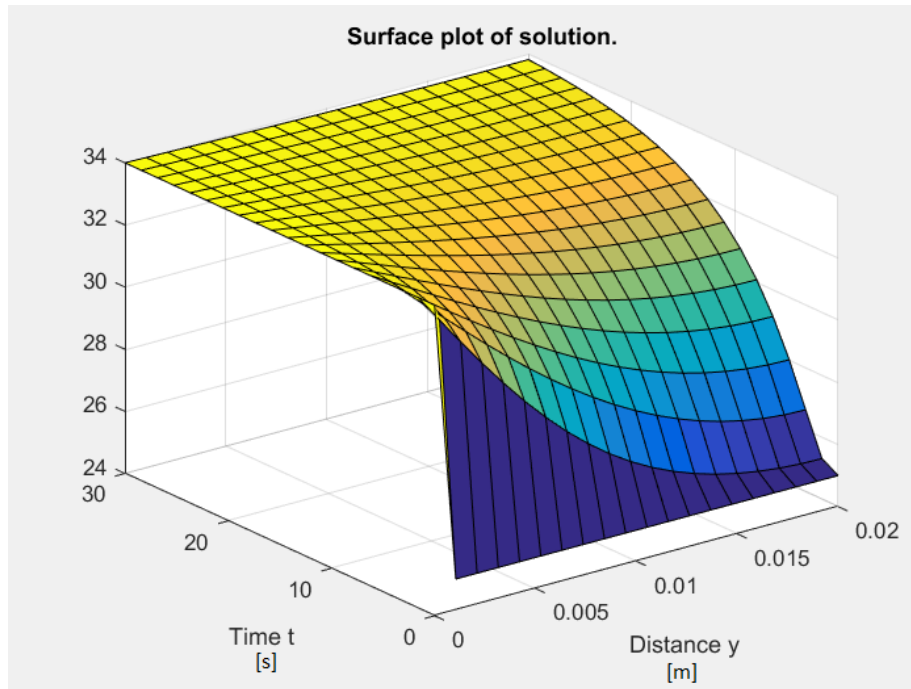
Unfortunately, the measurement of TEWL within a chamber of 2cm diameter and height is not a one dimensional problem. The walls are not infinitely far from the axis. Thus the problem has to be modelled taking into account more than one dimension.

## 3.6 Discussion

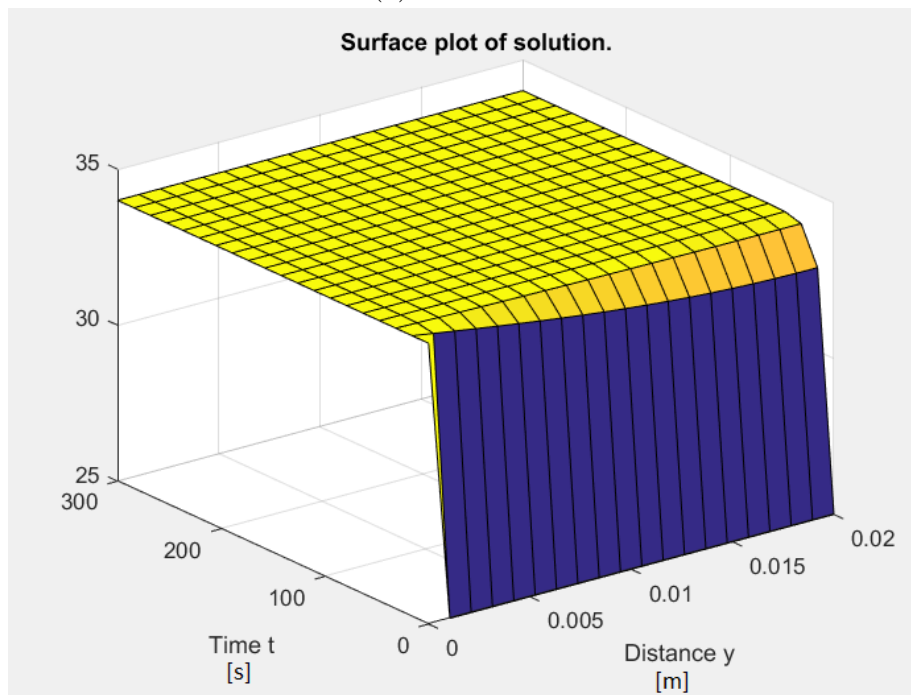
In this section the humidity and temperature are discussed in order to have a better understanding of the processes occurring in a closed chamber during a measurement on the skin. The water vapour concentration depends on the initial and boundary

---

<sup>5</sup>Boundary Conditions

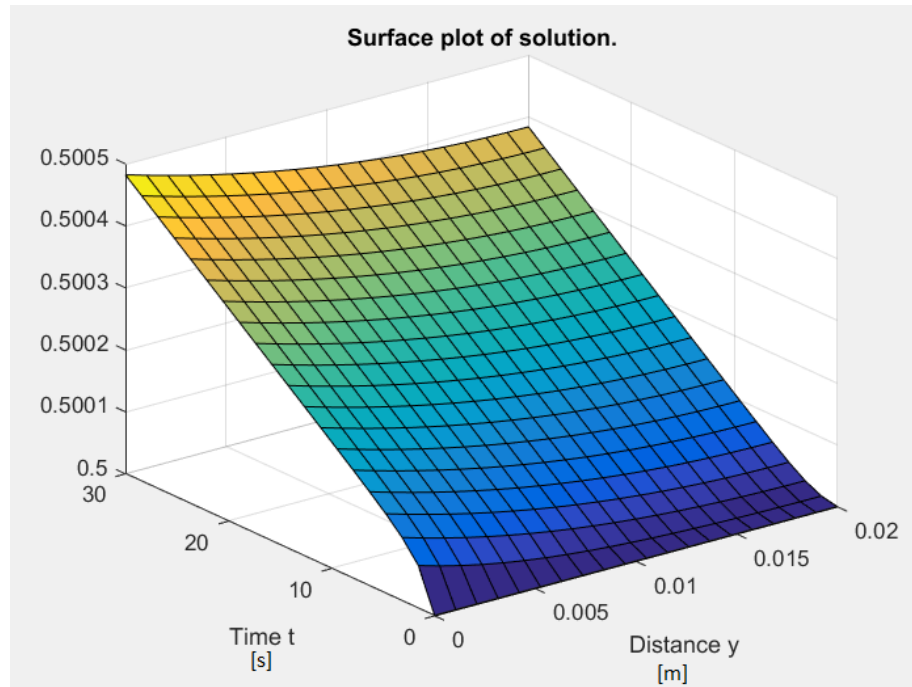


(a) 30 seconds

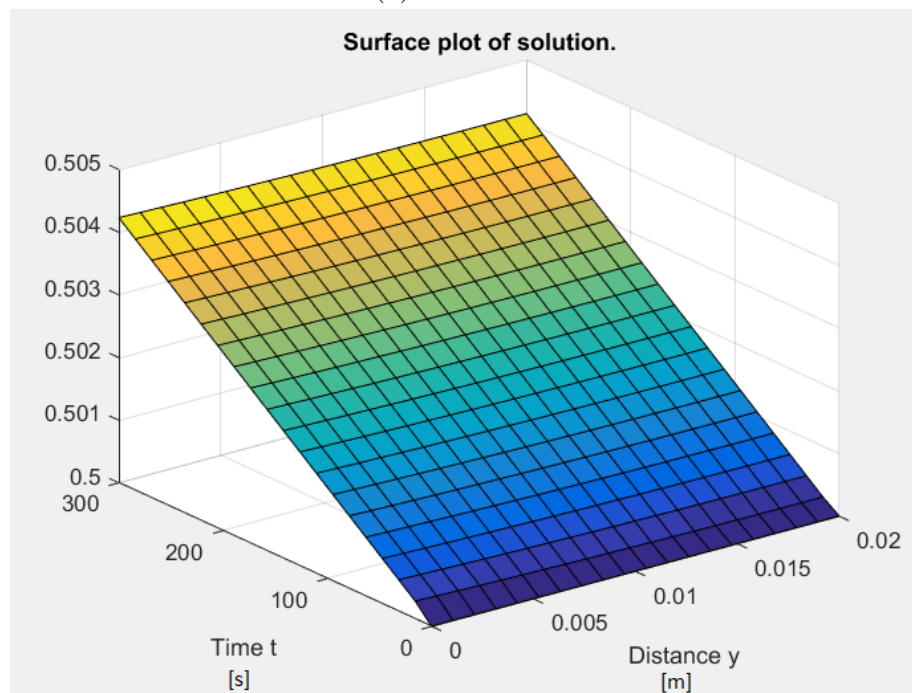


(b) 300 seconds

Figure 3.2: Temperature profile as a function of spatial coordinate and time



(a) 30 seconds



(b) 300 seconds

Figure 3.3: Humidity profile as a function of spatial coordinate and time

conditions. The phenomenon of diffusion is a equalisation process. Thermal and mass transport diffusion are driven by differences in temperature and concentration respectively. The flux  $J$  depends on the spatial vapour concentration distribution. The vapour density gradient is inversely proportional to the flux: a negative vapour concentration gradient along the  $\vec{y}$  axis gives a positive flux, and a positive humidity gradient, negative flux. If there is mass transport from the skin to the measurement chamber, there is a positive flux  $J$ . In the absence of sweating, this flux is TEWL, the object of measurement in this study. In the MATLAB model in 1D, it seems the temperature profile reach the equilibrium before 30 seconds. The gradient is small in term of space, compare to the gradient of humidity.

The aim of simulations and how it relates to the project was to identify the suitable regions of the chamber to :

- maximise the flux to have an optimal sensitivity
- minimise the turbulence to have the best repeatability.

Unfortunately the flux couldn't be maximised with different heights or widths of the cylinder. No difference was found between models when varying these two parameters. Regarding the maximisation of the flux, it would be higher in the region closer to the skin, so it would be preferable to place the sensor near the skin. However, it makes it vulnerable to the environment (as it would not be protected by the walls of the chamber) and water (from the skin, like sweat). However if the blower is directed towards the skin, as it is intended to, in order to remove the SSWL, it means the sensor near the skin will be subjected to a lot of turbulence. A trade off has to be found between sensitivity and repeatability. Because there is no direct formula between sensitivity and flux amplitude, and turbulence and repeatability, it is a trade off difficult to evaluate with models. Thus, building prototypes may help to study this trade-off.

Furthermore, the 3D modelling of the blower with ANSYS couldn't be completed and it was decided to build some prototypes instead of pursuing the simulations to understand the effect of blowers and compare designs.

In the next chapter, various chamber designs are presented. There are three main designs: circular, ellipsoidal, and half cylindrical. Because the modelling has been only done in 2D, the ellipsoidal and circular cylindrical have the same cross section and would lead to the same models. There are two designs family left and their simulation, with the comparison to the experimental results, is in the next chapter.

### 3.7 Summary

In summary, during a measurement with a closed chamber, the humidity and temperature keeps increasing until it reaches a steady state. The water concentration and temperature distribution are not homogeneous at the beginning, due to perturbations of the chamber movement. They will gradually stabilise as they reach a steady state. At the steady state, the water vapour density is linearly distributed along the axis of the chamber. The modelling hasn't been achieved in 3D and the need to build a physical prototype to compare the configurations was therefore necessary.

# Chapter 4

## Experimental Work

### 4.1 Introduction

The aim of the project is to develop a TEWL instrument that has good repeatability, sensitivity and accuracy. For this the instrument is compared to the Aquaflux. The simulations haven't provided a clear vision of where should be located the RHT sensor: a trade-off had to be found between repeatability and sensitivity. In addition the models are not in 3D and some have assumptions. It is ideal to build a prototype and changes the parameters in the software if possible, to evaluate what is the best configuration.

Development of hardware and software follows a waterfall model: First, the definition of the requirements, then the design phase, and then the implementation and the verification that the prototype answers the requirements. There is also an underlying iterative process: after a prototype is designed, built and evaluated, a new prototype is then conceptualised with a higher clarity of the requirements and feedback from the previous versions. The evaluation of the prototype was performed by a battery of tests, explored further in section 4.2.

### 4.2 Methodology for prototype design, manufacture and testing

#### 4.2.1 Development

These are the engineering methodologies: they establish requirements that yield a design, an implementation that is finally tested and deployed. The requirements and the engineering solutions are in 4.3.



#### 4.2.1.1 Software

The development was modular. First the individual drivers were developed or adapted from existing libraries. Then a code using these drivers was developed. Finally, these were exported to C++ libraries whose methods were invoked from the `main()`. The `main()` is the first function called when a program is run in C or C++ (and other languages like Java and Python) it is the entry point to a program.

#### 4.2.1.2 Physical

For the construction of the casing, a V model was used:

- First the design with CAD;
- Then the manufacture of parts;
- Checking if the parts have been correctly printed; and
- Checking the integration, that they fit well and if the final product is usable.

In addition, the CADs of the probes were used for the CFD<sup>1</sup> simulations. The setup for 3D printing is described in 4.4.

#### 4.2.1.3 Hardware

The development was iterative. First, a simple circuit was produced and evolved to a more complicated product. Like the software, the development was modular. Hardware was tested for these features:

- Touchscreen: touch, pressure calibration by trying different values in the firmware and see what was responsive
- SD card: how many measurements can be copied at each access to the memory
- Connectivity: performance evaluation with a sniffer. Network assessment is usually performed with Wireshark, was previously called Ethereal, it is the world's most widely-used network protocol analyzer. It is free and open-source.

Ideally, the configurations of the fans, sensor position, gradient calculations, connectivity solution and chamber geometry should be compared. However, due to time constraints, this was not a full 2k factorial study where every combinations was tested.

---

<sup>1</sup>Computational Fluid Dynamics

## 4.2.2 Experiments

### 4.2.2.1 Strategy

The evaluation of the prototypes were performed by using a variety of tests that fit into the following three categories:

- Checking that the prototype meets the requirements
- Assessing the capacity and functionality of the hardware and software
- Assessing the quality of TEWL measurement results

Performances like repeatability were evaluated, e.g. by measuring the coefficient of variations as per (Imhof et al. 2009). In this exercise, the error rate (standard deviation divided by the mean, i.e. coefficient of variation) was compared. Since the errors of measurement had two potential sources (instrument and skin), the measurements were performed 3-5 times. This allowed for an assessment of repeatability by calculating the coefficient of variations between these measurements. To counteract the skin variability, measurements were performed at different anatomical sites. Other statistics tools such as box plots were used to observe the distributions of the results. Plots outside of the box were considered outliers, and the bigger the box the more variation, suggesting lower precision.

Skin barrier function measurements results are usually presented with TEWL value and standard deviation of this value. In this thesis, the error rates or coefficient of variation was provided instead. It has the advantage of taking less space, describing one value instead of two. Also, with TEWL not being an absolute value, it is advantageous to normalise it. The coefficient of variation is normalised to the mean, it is important to use a normalised measure of repeatability to allow for comparison of the performance of different instruments (Imhof et al. 2009).

### 4.2.2.2 Duration of experiments

Prior experiments on chamber 1 shown no improvements with longer experiment. Measurements last 30 seconds, with a rest of 30 seconds in between measurements. The measurement session should not exceed 17 minutes. This is important to allow for correlation between instruments. It is expected that up to five measurements can be obtained in this time frame.

### 4.2.2.3 Environmental variations

The environment was controlled with one or two air-con. A temperature around 22°C was maintained in order to avoid sweat.

#### 4.2.2.4 Time of the day

Measurements were usually performed in the middle of the day. This is because some time was needed to get the AC<sup>2</sup> to cool down the room at the right temperature. This time was usually achieved around lunch time. The measurements were performed in parallel on the Aquaflux and the tested prototype.

#### 4.2.2.5 Calibration with the Aquaflux

Measurements are performed with the prototype tested as well as the Aquaflux. This is to draw the calibration curve to deduce the sensitivity of the instrument compare to the Aquaflux.

#### 4.2.2.6 Simulations

TEWL measured by the Aquaflux was used as an input for the 3D modelling. Simulations were performed to compare RH temperature and gradient of humidity measured in the prototype chamber.

### 4.3 Requirements

#### 4.3.1 TEWL measurement

As mentioned in 2.8.2, Leveque stated the specifications for a good TEWL instrument (Leveque 1989):

1. The device should not change the physical and chemical properties of the stratum corneum;
2. The measurement area should be of an intermediate size : small enough for good sensitivity or to measure a specific body part, large enough to minimise skin variability ;
3. The measurement should allow the recording of minute variations in function of time and space; and
4. Measurement should not exceed two or three minutes to avoid sweat caused by stressing the subject.

In addition, this project was aiming to develop an improved instrument, compare to the existing ones, in particular the Aquaflux. The instrument had to provide work outside of a laboratory setting. Furthermore, it aimed to have repeatable results

---

<sup>2</sup>Air Conditioning

and have good sensitivity compared to the Aquaflux. Thus, the target performances are the one of the Aquaflux. It has for repeatability 0.05 %. And the sensitivity of the Aquaflux is  $0.07 \text{ g} \cdot \text{m}^{-2} \cdot \text{h}^{-1}$ .

### 4.3.2 Quick measurement

It is preferable to perform quick measurements for three reasons:

- It minimises the risk of environmental influence on the measurement (e.g. varying pressure and chamber position during TEWL measurement);
- It allows for more measurements to be repeated during the 17 minute window in which skin will not have yet reacted significantly to any changes in RH; and
- The readings are more precise because the smaller the gradient is, the bigger the range of precision (Imhof & McFeat 2014).

Guidelines for TEWL measurement in a non-controlled environment (e.g. an office) suggest a measurement time of less than 10 seconds (Plessis et al. 2013).

The measurements were performed using a SHT31 sensor from Sensiron. It uses I2C<sup>3</sup> protocol and can communicate with a speed up to 1 MegaHertz. The sensor is set up for high repeatability: 0.10% RH and 0.06 °C. The accuracy is  $\pm 2\%$  for RH and  $\pm 0.3$  °C for temperature. With these parameters for accuracy and repeatability, the measurement time is usually 12.5-15 milliseconds. In drivers implemented in this project, the measurement time used was 12.5 milliseconds. All measurements were successful using this configuration : the sensor had enough time to measure and return a positive result without error code.

### 4.3.3 Temperature control

Various strategies have been put in place to keep the temperature constant during measurement, such as avoiding dissipation blowers and using a well-controlled environment. After a while, and when measurements are performed continuously in a row, the system gets warmer. This is problematic because the air of the microclimate must be kept constant and not rise too much. Guidelines have asserted that between 22 and 30°C, TEWL can double (Pinnagoda et al. 1990). This project aims to control the temperature to maintain it constant.

### 4.3.4 Chamber geometry

The shape of the chamber is a geometrical aspect that can affect TEWL measurement.

---

<sup>3</sup>Inter IC (Integrated Circuit)

A cylindrical design for the measuring head minimizes the influence of turbulence inside the probe for the Tewameter according to (Miteva et al. 2006). Most measurement chambers on the market have this shape.

Using a small chamber would be beneficial to measure the gradient quickly as the flux would reach the sensor more quickly. In terms of geometry for the future instrument, a smaller chamber is preferred. In a similar manner, the flow increases in a conical tube, in the direction of the larger to the smaller diameter. This is known as the venturi effect and can be explained by the Bernoulli equation (Eq. 4.1), where 1 and 2 are the indices of two points on the cone axis:

$$p_2 - p_1 = \frac{\rho}{2} \cdot (v_2^2 - v_1^2) \quad (4.1)$$

Where  $p_1$  and  $p_2$  are the pressure at points 1 and 2,  $\rho$  the density of the fluid, and  $v_1$  and  $v_2$  the velocity at two points. Ideally, the chamber would be conic but for easy manufacture, the cylinder has been chosen in this project.

Regarding the size of the input flux, i.e. the skin surface in contact, the smaller the flux, the bigger is the measurement range (Imhof & McFeat 2014). Better precision can be achieved with a cap that has a smaller orifice. The final prototype had a few caps to test different orifice sizes.

### 4.3.5 Printed circuit board (PCB)

The instrument needs to contain:

- A microcontroller
- A component for connectivity such as Bluetooth or WiFi to communicate with a computer or other device
- An LCD screen for displaying results in real time
- A user input interface
- A memory such as an SD card to store the results and display previous results
- The RH and temperature (RHT) sensor to measure the gradient of humidity
- The blowers to homogenise the chamber interior
- A potentiometer to control the speed of the fans
- A battery capable to support all of the above components

It is necessary to read the measurements but also to interact with the instrument. Touchscreens are very affordable because of the high demand in the smartphone industry. For simplicity, the solution chosen was a touchscreen with SD card reader, the ILI9341 from Adafruit.

Therefore, the PCB file under Eagle consists of a schematic and a board layout. They will contain the components above and the additional pull up resistor or capacitor necessary for smooth operation.

### 4.3.6 Position of the sensor

Theoretically, a short chamber would be advantageous as it would facilitate quick measurement and the sensor would be close to the skin. As discussed previously, there is an insulating layer of air around the skin (the boundary layer) that has a gradient of humidity and temperature. In the absence of temperature changes, air convection and draughts, the boundary layer has been determined to be 7-10 mm above the skin surface (Wheldon & Monteith 1980), (Miteva et al. 2006). Generally speaking, the faster the flow of air around the body, the thinner the boundary layer is (de Dear et al. 1997). The air in the boundary layer is more stable after a measurement period, regardless of whether or not the chamber is open or closed. Viscosity losses within the boundary layer adjacent to the inner cylindrical wall of the chamber also act to suppress air circulation by natural convection (Imhof et al. 2009).

Open chamber instruments are more vulnerable to pressure effects than closed-chamber instruments because (Imhof et al. 2009):

- The sensors are placed close to the skin surface and may come into contact with the skin at moderate contact pressure; and
- The probe construction is less robust and can distort with contact pressure.

For this project, a few positions of the sensor have been tested. However, in general, the sensor was positioned further away from the skin. Whilst the above are general considerations relevant to the development of any TEWL measurement system, there are some other considerations that are more specific to this project

### 4.3.7 Portability

The instrument has to be portable. Whilst there are many solutions and architectures available, the minimum requirement is for the device to be comfortably held in one hand by the person taking the measurement. Size of the probe has to be reasonable. The weight of the future instrument has to be as light as possible, but

also robust. Ideally, the prototype has to be easy to use and to carry, so there is some ergonomics questions to be addressed when designing the casing.

### 4.3.8 Connectivity

In order to have a truly mobile system that is not reliant on a desktop computer at the time of measurement, options for connectivity need to be explored.

#### 4.3.8.1 Requirements

This project aims to build a portable instrument:

- That won't be connected to a computer for the following user needs:
  - Wireless transfer data
  - Data logging
  - Evaluation
  - Display
  - Human interaction/user input
- and provides low energy consumption and autonomy, i.e. the device can be used for several hours without being recharged. A smartphone (Samsung S7) with a new 3600 mAh battery can last 12 hours, depending on its usage. By deactivating smart functionalities and running the bare the minimum this battery charge can extend to 24 hours.

Ideally, the prototype had to reach this target of 12 hours. End-users would be disappointed if they had to recharge the battery during the day. It had to cope with a full day of usage. Since the explosion of computer technologies in the seventies, many technologies have been developed for device connectivity. With the advent of IoT<sup>4</sup>, there have also been a number of new developments in low energy technologies. Thus, the choice of components for this instrument are broad.

#### 4.3.8.2 Protocols and standards

The solutions available for the PHY layer are infrared, radio, optical, satellite and mobile link.

---

<sup>4</sup>Internet of Things

**Wireless radio solution** There are two main families of wireless standards for radio link:

- 802.15.4
- 802.11

**IEEE 802.15.4 standard:** This standard describes Low-Rate Wireless Personal Area Networks (LR-WPAN) (802 2015). It covers a short range (10-30 metres) and low data rate (20-40 kilobits/second) on the frequency band 800 MegaHertz. It allows star and peer-to-peer topologies. It is the basis for ZigBee, Bluetooth, and WirelessHART technologies (Khalil 2017).

**Bluetooth:** This standard uses the 2.4 to 2.485 Gigahertz frequency band. The latest version of the technology is version 5 (Bluetooth SIG (Bluetooth Special Interest Group): Kirkland Washington USA 2016). However, at the time of this project only components answering to 4.2 specification (Bluetooth SIG (Bluetooth Special Interest Group): Kirkland Washington USA 2014) were available. Version 5 allows for a higher bit rate, so a quicker transfer is possible if the range or the data rate is reduced. Bluetooth 4.2 introduces features for the IoT such as:

- Low energy secure connection;
- Link layer privacy; and
- Internet Protocol Support Profile (IPSP) version 6 for devices to support smart homes.

Bluetooth Low Energy (BLE<sup>5</sup>) was previously called Wibree and then Bluetooth Smart. It is based on Bluetooth with the same data rate but consumes much less energy. BLE applies the following security on the bluetooth link (Sandhya & Devi 2012):

- Elliptic curves Diffie Hellman key exchange; and
- Advanced Encryption Standard AES<sup>6</sup> in Counter with Cipher Block Chaining Message Authentication Code (CBC-MAC) Mode, otherwise known as CCM mode.

---

<sup>5</sup>Bluetooth Low Energy

<sup>6</sup>Advanced Encryption Standard



**802.11 Wi-Fi:** WiFi is part of the IEEE 802.11 family and is short for Wireless Fidelity (Aime et al. 2007). They regulate the wireless local area networks that first appeared in 1997. The rate of WiFi depends on the channel frequency used, the number of antennae and geographical regions. For example, there are 11 channels for the USA and 13 channels in Europe in the 2.4 Gigahertz range. The data rate transfer is 11 Megabits/second and the range is between 40-90 metres indoors and 300 metres outdoors (Khalil 2017). However, these are the values of an enhanced protocol and higher throughput is reached at 100 Megabits/second (802 2009). There are three options for WiFi security: Wired Equivalent Privacy (WEP), WiFi Protected Access (WPA) and WPA2. To the author's knowledge, WPA2 is the method usually used for authentication and encryption. It uses on the wireless link (Hassinen 2006):

- AES in CCM mode;
- Temporal Key Integrity Protocol (TKIP); and
- Message integrity checks.

#### 4.3.8.3 Summary of protocols

The standard convergence is approaching as it is not only computer networks but also many fields that rely on such protocols (health, aerospace, energy, etc.). There are many Industrial IoT protocols to choose from and the most commonly deployed are MQTT<sup>7</sup>, Extensible Messaging and Presence Protocol (XMPP), Advanced Message Queuing Protocol (AMQP) and Data Distribution Service(DDS) (Gilchrist 2016). Several initiatives are working to align standards on various topics such as:

- Disease management, e.g. management of a chronic disease outside of a clinical setting
- Ageing independently using technology and services to live longer at home
- Health and fitness

The principal initiatives are:

- Continua Health Alliance ([www.pchalliance.org](http://www.pchalliance.org))
- Personal Connected Health Alliance (PCHA)

The main standards for e-Health are Li et al. (2018) :

- ISO / IEEE 11073 PHD

---

<sup>7</sup>Message Queuing Telemetry Transport

- one Machine to Machine (oneM2M, onem2m.org)
- OMA LwM2M (Lightweight Machine to Machine from Open Machine Alliance)

However, some of these have limitations. ISO/IEEE 11073 doesn't have IP for transport layer. This is a problem because the Internet uses IP. oneM2M cannot be used with wearable devices using Zigbee or Bluetooth. These technologies all use a gateway, that bridges the device to the server in the cloud. However, alternatives to gateways for E-health applications are being explored (Pereir et al. 2018). The specification of the prototype has been decided after comparison in the part below.

#### 4.3.8.4 Comparison and solution chosen

The 2 PHY layer wireless technologies chosen were BLE and WiFi because of the availability of the components. The protocol above this depends on the sublayer.

**Bluetooth Low Energy for PHY layer** The Arduino 101 microprocessor has an integrated BLE chip nRF51822 that made the first developments quick and easy. The nRF51822 from Nordic supports Bluetooth version 4.2.

The project was migrated to a more powerful microcontroller used by a previous version of a Biox instrument, the ATSAME70. This development board doesn't have integrated Bluetooth or WiFi. In this project, other components supporting BLE (ZS040 and RN4678) were used.

**Wi-Fi for PHY layer** WiFi reach longer distances and has better security. ESP8266 is widely used and ATWINC1500 was easy to implement because it has drivers available for ATSAME70.

**Session layer:** MQTT is the application layer service chosen for this project. One significant reason for this is the publisher/subscriber pattern, which is also used during the implementation of the Android applications (see section 4.7.1). MQTT can also be easily implemented on WiFi. There are a few examples on the manufacturer's websites (Atmel n.d.), (Adafruit 2016) using ATWINC1500 or ESP8266 microchips to access to the MQTT broker, as well as other publications outlining the use of ESP8266 as a MQTT gateway that can then be paired with a Bluetooth Low Energy (BLE) device. However the ESP8266 and the RN4678 are also accessed with serial command. Transmitting via UART<sup>8</sup> is not very efficient, **USART!**<sup>9</sup> is better synchronised and can reach more bauds. It is also possible to use

---

<sup>8</sup>Universal Asynchronous Receiver Transmitter

<sup>9</sup>**USART!**

a smartphone for the MQTT/BLE Gateway. MQTT can also be implemented over BLE using MQTT for Sensor Networks (MQTT-SN). This protocol also supports the BLE UART Service from Nordic. However, there are no libraries available for the Arduino electronics platform. This project attempted to implement a network and transport layer for MQTT Paho from Eclipse. It has a library for Ethernet/IP, but not for BLE. Unfortunately due to a lack of time and appropriate Wi-Fi components, it was not possible to pursue this further in this project.

### Application layer

**Over Wi-Fi:** HTTP was used by Arduino with ESP8266 to access the host with URL and port 80. HTTP has GET and POST methods, to receive data and send information respectively. However, HTTP is pull only; the data is sent only when there is a request. In this project, it is beneficial to have a publisher subscriber pattern like MQTT. There are a few MQTT brokers available online that can display a dashboard on a browser. In this project Jumpway and Adafruit were used. They work in the same way; an account is set up with private keys. The feeds corresponding to the sensors are set up in the online dashboard and the devices are registered.

**Over Bluetooth:** Nordic BLE Services have a library for Arduino (as they are integrated) and Android, and so it was easy to connect the two. It was also possible to add the MQTT gateway component to the project using Jumpway and Samsung Artik. The BLE standard is based on GATT, an acronym for the Generic Attribute Profile. It defines how services and characteristics are discovered and transfer data. The profile defines the use case and the functions needed. The profile consists of several services that contain characteristics. This hierarchy can be seen in Figure 4.1.

### 4.3.9 Blowers and Fans

In this thesis, the aim is to develop a portable instrument. After studying the mobility in terms of telecommunications, one other aspect is to achieve the resistance to the environment impact. In addition to a closed-chamber design, a solution suggested here is a air flow blowing towards the skin to remove skin surface water, homogenise the chamber and measure TEWL. This section covered fans.

#### 4.3.9.1 Blower or fan

There are two types of air moving devices, either axial fans or centrifugal blowers.

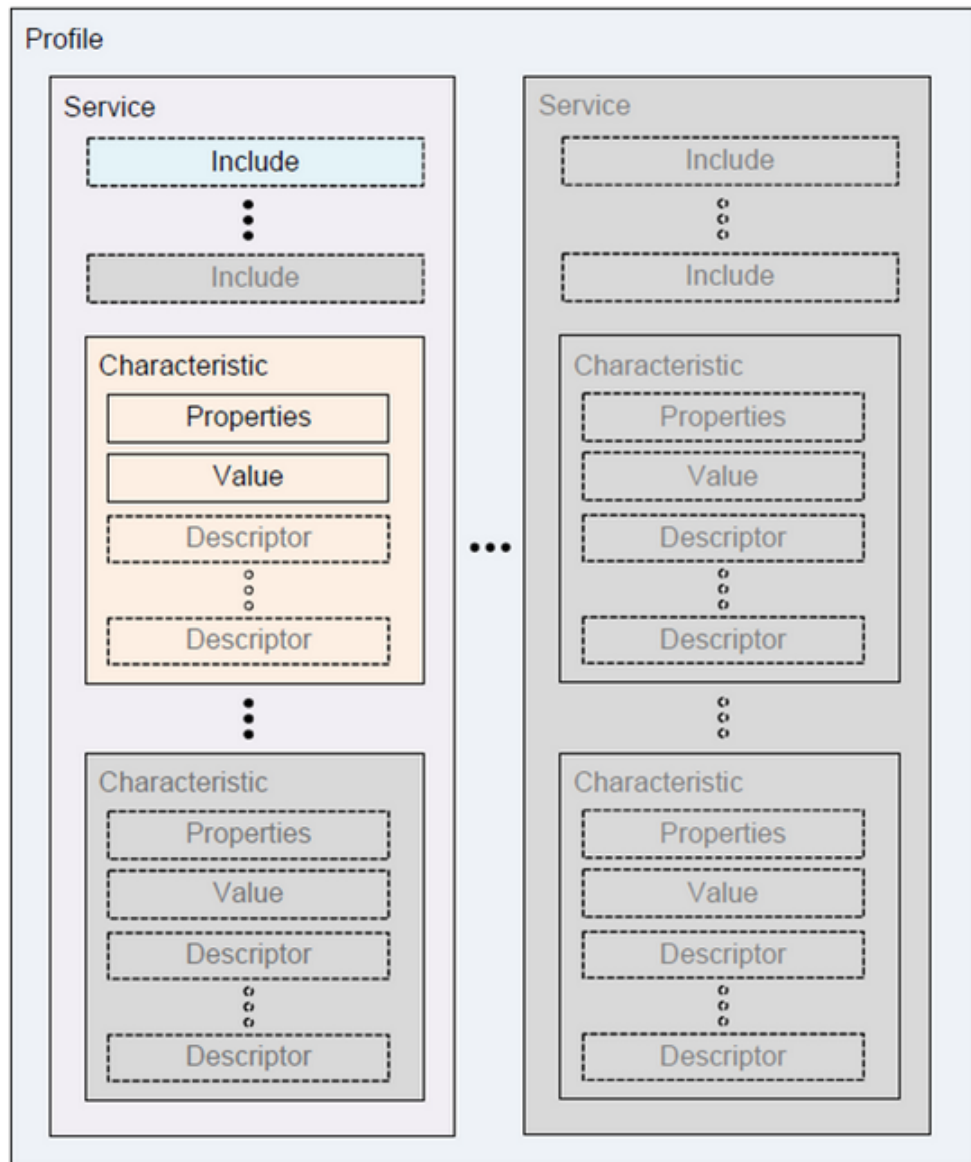


Figure 4.1: GATT profile hierarchy - from the specification (Bluetooth SIG (Bluetooth Special Interest Group): Kirkland Washington USA 2014)

#### 4.3.9.2 MagLev

MagLev means Magnetic Levitation and they function with magnetic bearings. They are described as one of the most innovative developments in turbomachinery (Ji et al. 2008). They use either Lorentz force or reluctance to keep a rotor at stable levitation (Amrhein et al. 2016). There is no contact between the rotor and the stator as it uses magnetic forces. Therefore, there is no need for a lubrication system because of the negligible friction. Moreover, low friction means low noise. They also have the advantage of active control because the magnetic fields are controlled electrically (Le & Wang 2016). In addition, this technology is sturdy because it does not suffer from mechanical wear (Pesch et al. 2015) and has better reliability, low energy consumption and small maintenance costs (Amrhein et al. 2016). The magnetic bearings can work in harsh environments such as low or high temperatures and vacuums (Ji et al. 2008), as well as in the presence of corrosive, toxic or abrasive fluids (Amrhein et al. 2016). They are used in industrial compressors, blowers, turbo molecular pumps and flywheel storage systems (Fan et al. 2010).

**Impeller shape** A larger base of the impeller does not increase the efficiency of the fan (Chunxi et al. 2011).

#### 4.3.9.3 Speed and flow

The higher the rotation speed, the smaller the volume and the higher the power density (Fan et al. 2010). The higher the speed, the higher the flow. The purpose of the blower is to reduce the air barrier thickness at the skin surface.

#### 4.3.9.4 Position of the blowers

Several blowers can be added to increase the airflow of the drying process. They can be positioned back to back in order to not use too much space in the chamber. Fans are said to be in parallel. The blowers are positioned in a symmetrical manner, as far as possible from the skin to allow a good mixing of the chamber air.

#### 4.3.9.5 Summary

Sunon products were chosen because of the advantages of using a levitating rotor with less friction. Blowers were preferred over fans because blowers offer better air velocity. Fans cope better with back pressure.

### 4.3.10 Proportional-Integral-Derivative(PID)

A PID controller or regulator is a control system that increases the performance of a servo control. It is a closed loop system and is widely used in industry to correct various signals. It is popular due to its simple implementation, robust design and low maintenance requirements (Jaen-Cuellar et al. 2013). A PID regulator can be software or hardware-based. In this project, a software PID was set up. In both cases, it follows an algorithm that:

1. Calculates the error (differences between the input and the desired value)
2. Adjusts a signal in function of the target value and the error it tries to minimise

As the name suggests, PID controllers acts on three aspects:

- Proportional: The error is multiplied by a gain factor  $G$
- Integral: The error is integrated over time and divided by a gain factor  $T_i$
- Derivative: the error is derived and multiplied by a gain factor  $T_d$

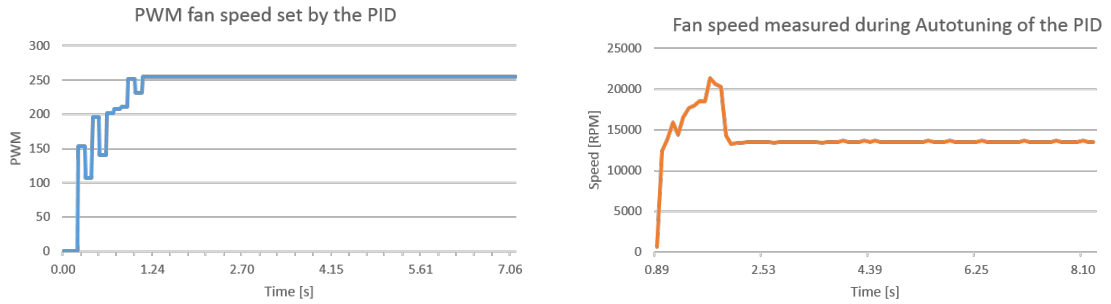
A PID controller was developed to control the speed of the blowers.

The variation of speed is 1% during a session of measurements (for eight measurements total: four measurements on the volar forearm and four measurements on the palm). The variation during one application of 30 seconds ranges from 0.0-1.2%. The measurement of the speed uses interrupts. It could be possible to improve the measurements of the speed of the fan by increasing the resolution factor, however this would take more time. By adding a software PID to the programme, the processing time is already increased.

#### 4.3.10.1 Tuning

Tuning the PID controller can be challenging. To achieve this, there are several approaches:

- Empirical methods: Ziegler-Nichols (open and closed loop), Nyquist inverse and Cohen-Coon;
- Analytical methods: Root locus and frequency response analysis (Jaen-Cuellar et al. 2013);
- Genetic algorithms (Krohling et al. 1997), (Krohling & Rey 2001), (Aly 2011); and
- Neural networks (Zribi et al. 2018), (Annisa et al. 2018), (Rivas-Echeverria et al. 2001).



(a) Pulse Width Modulation (PWM) sent to the fan when auto tuning the PID      (b) Speed of the fan measured when auto tuning the PID

Figure 4.2: Auto tuning of the PID

#### 4.3.10.2 Final choice

For simplicity reasons, the PID and Auto Tuning library from Arduino were chosen. The Auto Tuning program set the initial tuning parameters  $G$ ,  $C_i$  and  $C_t$  described above. If the error is large then the programme uses large tuning parameters. If the error is small, the measured speed is close to the desired speed and more conservative tuning parameters are used. The auto-tuning can be seen in Fig. 4.2. On Fig. 4.2a the target speed is sent to the fan in PWM<sup>10</sup> to adjust the speed measured by the micro controller on Fig. 4.2b.

### 4.3.11 Screen

A screen is a convenient way to convey information to the user.

#### 4.3.11.1 Requirements

It must display three distinct screens:

- A menu to:
  - Start a measurement with different configurations;
  - Display previous measurements;
  - Browse storage content; and
  - Allow bluetooth pairing to a smartphone or a WiFi connection.
- Measurement: time series of relative humidity and temperature.
- Lists: of measurements or files.

<sup>10</sup>Pulse Width Modulation

There are at least two physical values to display so a colour screen is preferred for clarity. It has to be large enough to read text easily but small enough to be on a handheld device. It would be beneficial to have a touchscreen so the user can select directly a function on the menu. Using a touchscreen also takes up less physical space on the device, otherwise some kind of keyboard, joystick or buttons would be necessary. There are four types of technology available for touchscreens: (Holzinger 2002):

- Capacitive
- Resistive
- Surface Acoustic Wave (SAW)
- Optical or infra-red

#### **4.3.11.2 Capacitive**

A capacitive touchscreen has a layer with a capacitive component, i.e. that has the capacity to store electricity. When the touchscreen is touched, a small amount of charges is attracted to the point of contact. Electrodes located at each side of the panels measure the voltage across them and send the information to a microcontroller unit. Capacitive touchscreen can be used with a finger but not a stylus. This technology provides good clarity and longevity due the absence of moving parts. They are not affected by liquids like water or grease (Bhalla & Bhalla 2010).

#### **4.3.11.3 Resistive**

Resistive touchscreens are made of two conductive parallel panels. If no pressure is applied, the two panels are not electrically connected. When a mechanical pressure is applied, the impedance between the two layers is lowered at the point of contact. A system of sensors measures the distance between the point of pressure and the electrodes and then computes the X-Y coordinates of this point (Aguilar & Meijer 2002). Resistive touch screens can be used by any solid object, such as a gloved finger or a pencil (Holzinger 2002).

#### **4.3.11.4 Comparison**

One study set their subject to test resistive and capacitive touchscreens through a list of tasks and recorded the systems errors and mistakes (Burnett et al. 2013). They rated the capacitive technology to be of higher quality in terms of sensitivity, speed and recognition of actions. However, this study is only applicable to the two specific screens tested. More comprehensive studies are available (Holzinger 2002).



An extensive comparison of the technologies can be found in the literature (Bhalla & Bhalla 2010). In this thesis, the important elements to consider are the resolution, the response time, the calibration, the cost and the activation (i.e. the recognition of usage that triggers an action). A comparison of the various touchscreen technologies can be found in Table 4.1.

Table 4.1: Comparison of touchscreen technologies (Bhalla & Bhalla 2010)

Touch	Resolution	Response Time	Calibration	Activation	Cost
Resistive	Medium	<15 ms	Once	Anything	Low
Capacitive	Medium	20 ms	Regular	Conductive	High
Acoustic	High	>10 ms	Once	Finger/Pen	Moderate
Infra red	Medium	>20 ms	No drift	Finger/Pen	High

#### 4.3.11.5 Solution chosen

Like any project, a trade off had to be found between cost and quality. It is preferable to have a good response time, good resolution, one calibration and low cost. The choice inclined towards resistive technology. The screen ILI9341 from Adafruit was selected. Adafruit provides drivers with free GNU license online so it's only fair to support them. ILI9341 works with a 4 wire technology. It is a color LCD touchscreen with a TFT display measuring 6 cm in diagonal. It has a bright backlight with four white LED<sup>11</sup>s. The resolution is 240 x 320 pixels and it weighs 30.5g.

#### 4.3.12 Battery

Lithium-ion polymer batteries (LiPo) can provide portable devices with a low weight energy source with high energy density (Kramer & Geraldly 2006). They are small and light. For this project, a LiPo battery was ideal because it could add autonomous and stable power supply to a mobile device. It has also shown good results (i.e. long duration at maximum performance) in various studies (Kos & Kramberger 2017). They can be also be combined (Olivo et al. 2012). The batteries purchased from MikroElektronika provide a voltage of 3.7V and a capacity of 2000 mAh. It was also chosen because it is compatible with the charger MIKROE-1198 VOLT USB Power Management for MCP73832. They measure 63 mm x 43.5 mm x 7 mm and weigh 45g. It can be fully charged in 6 hours and has a life cycle of 300 charges.

#### 4.3.13 Non Volatile Memory

There are four different families of non volatile memory:

---

<sup>11</sup>Light Emitting Diode

- ROM: Read Only Memory;
- NVRAM: Non Volatile Random Access Memory (RAM<sup>12</sup>);
- Magnetic; and
- Optical.

Within ROM, the options are (Ibrahim 2010):

- ROM that is programmed at the factory and cannot be changed by the user.
- PROM Programmable Read Only Memory - memories can be programmed with a controller.
- EPROM Erasable Programmable Read Only Memory - memories can be programmed with a suitable controller and erased with an ultra violet light projected through a small clear glass window.
- EEPROM: Electrically Erasable Programmable Read Only Memory - memories can be erased and reprogrammed using a programming device. Some microcontrollers have built-in EEPROMs.
- Flash EEPROM - This is a quicker version of the EEPROM. It is based on MOSFET, Metal Oxide Semiconductor Field Effect Transistors.

Regarding this project, the Arduino 101 has a Intel Curie with 384 kiloBytes Flash, while ARM Cortex M7 SAME70 has 2048 kiloBytes of embedded flash.

Within NVRAM, there are the following solutions (Freitas et al. 2008):

- FeRAM: Ferroelectric RAM
- MRAM: Magneto Resistive RAM
- ReRAM: Resistive RAM
- PC-RAM: Phase Change RAM
- Solid Electrolyte

Magnetic memories are magnetic tape (popular in the 1980s and 1990s, e.g. hard disk drives). Optical memory are, as the name suggests, optical (CD, DVD, BlueRay, etc.).

The mainstream solution for non volatile memory is the Flash EEPROM based the floating gate technology. The gate can be either NAND (Not AND) or NOR (Not OR). Flash represents nearly 100% of the market (Xue et al. 2011).

---

<sup>12</sup>Random Access Memory

#### 4.3.13.1 Solution chosen

The solution chosen was Flash, in particular an SD<sup>13</sup> card because of:

1. Drivers availability;
2. Convenient transfer for debugging on a computer; and
3. Easy integration with a touchscreen.

An SD card has nine pins and a switch to enable and disable write access on the card. There are two modes of operation: SD bus and SPI<sup>14</sup> bus. In this project the mode SPI was used because of the integration with the touchscreen.

#### 4.3.14 Relative humidity and temperature sensor

The sensor for humidity and temperature selected was the Sensirion SHT31 (Sensirion AG, Stäfa, Switzerland). This make and model were chosen for:

- Their accuracy: as mentioned earlier, for RH readings  $\pm 2\%$  for RH between 0-100% RH and for temperature readings:  $\pm 0.2$  °C for a range between 0 and 90°C
- Their use in other high technology (Rianjanu et al. 2018)
- Their reliability in harsh environments (Buchberger et al. 2018)

In addition, the Aquaflux uses the same sensors, allowing for convenient comparison.

The SHT31 data line (SDA) and clock line (SCL) have to be connected to pull up resistors. For this the pull up was done at the level of the microcontroller by programming the pin mode in the software. The SHT31 supports I2C fast mode and frequencies of up to 1 MegaHertz. Commands and data are encoded with 16 bits and are protected with a cyclic redundancy check (CRC). The 16 bits command includes a 3 bit CRC checksum, whereas 16 bits data sent by the sensor is succeeded by an 8 bit CRC checksum. The commands can specify the repeatability of the measurement: low, medium and high.

#### 4.3.15 Development boards

The Arduino 101 was initially used for the prototypes. Its specifications are reviewed below.

---

<sup>13</sup>Secure Digital

<sup>14</sup>Serial Peripheral Interface

#### 4.3.15.1 Central Processing Unit

The Arduino CPU<sup>15</sup> has two cores:

- ARC (Argonaut RISC (Reduced Instruction Set Computer) Core): an embedded 32-bit processor
- Intel x86 System on Chip Quark: a 32 bit microcontroller for low power consumption

The Intel Curie is also equipped with the Intel Enhanced privacy ID (EPID) Signature. It is an enhancement of the Direct Anonymous Attestation algorithm used for digital signatures (Brickell & Li 2007). It is also used to implement device management protocols for IoT.

#### 4.3.15.2 Connectivity

From chamber 2 onwards the connectivity technology used was Bluetooth, integrated on the Curie module. It has Nordic nRF51822 with a 32 bit CPU with 256 kiloBytes of flash and 16 kiloBytes of RAM. The 2.4 GigaHertz transceiver transmits at +4 dBm and supports Bluetooth Low Energy and Nordic Gazell protocol stacks. The Cortex M0 (from the Nordic) communicates with the Quark Core of the Curie via UART with Request To Send / Clear To Send. Finally, it has AES encryption capabilities.

#### 4.3.15.3 Inertial measurement unit

The orientation of the probe is important, and this can be recorded using an inertial measurement unit (IMU<sup>16</sup>). It has been shown that TEWL readings can be affected by the way in which the device is handled during measurement. A comprehensive study was done comparing TEWL measurement results with the angle of the Aquaflex probe (Imhof et al. 2009). Fortunately, there is an IMU on the Intel Curie module; a six axis accelerometer and gyroscope from Bosh. The BMI160 is connected to the ARC processor via SPI. It provides 16 bits measurement data. This sensor is activated only if necessary, thereby reducing the power consumption.

#### 4.3.15.4 Summary of the Arduino 101

Arduino is a well-established vendor of prototyping platforms. The Arduino 101 model was chosen for three reasons:

1. It has a integrated Bluetooth, ideal for quick prototyping;

---

<sup>15</sup>Central Processing Unit

<sup>16</sup>Inertial measurement unit

2. It has an integrated IMU. This allows for the collection of data from the gyroscope to know how well the instrument is being held. This could allow for gradient calculations adjustments based on the angle of measurement.
3. It was the latest version available at the time of deciding on a development board. The CPU is an Intel Curie module running at 32 MegaHertz with two cores, an x86 (Quark) and a 32-bit ARC architecture core, both clocked at 32 MegaHertz. Along with its 196 kiloBytes flash memory, these high specifications are important for the size of the programmes needed for the prototypes.

#### 4.3.15.5 Later versions of prototypes

Later in the project, the Arduino 101 was replaced by the tinyTILE, a smaller version of the 101, in order to have a smaller probe and the SAME70, in order to have more features running at the same time. The ATSAME70 has an ARM Cortex M7 with 32 bits running 300 MegaHertz. In addition, it has 2048 kiloBytes of flash memory and a Float Processing Unit. A more powerful core was required to perform all the tasks. The full code for the Arduino 101 did not fit on the 384 kiloBytes of flash memory, even after optimisation. Optimisation can be done by the compiler but also manually. Optimisation options and techniques include:

- Choice of the best data type - the one that is sufficient and takes the least space
- Avoid type conversion
- Pass data by reference
- Good return value
- Loop unrolling (remove the loop)
- Loop-invariant code motion (also called loop hoisting or scalar promotion)

In practice, features had to be deactivated and used with parsimony. Moreover, the Arduino 101 and tinyTILE do not have enough timers available for setting and measuring the fan speed whilst simultaneously maintaining a connection via serial bus.

#### 4.3.16 Touchscreen and SD card

From prototype 2, the prototypes had an LCD screen with an integrated SD card. It displays a menu of actions for the user to choose from (see Fig. 4.3a). It also displays



(a) At the startup of the device: menu

(b) Beginning measurement or: new grid

Figure 4.3: Touchscreen

measurements and renews the screen when the measurement is longer than the width of the screen (see Fig. 4.3b). The orientation of the screen during measurement is vertical for better RHT values precision reading. The humidity range is 20-100 % and the temperature range is 10-40°C.

The Adafruit ILS9341 was chosen for three reasons:

- It is small enough to fit on a instrument that can be easily held in the hand.
- It is big enough to display a graph with RH&T variations in real time.
- It has an Arduino library provided by Adafruit.

A datalogger was developed to record the time, relative humidity and temperature in a text file.

There are many tasks already required by the micro controller:

- Recording of Relative Humidity and Temperature sensors
- Providing Wireless connectivity: accepting connection
- Data logging on the SD card
- Blower speed management
- Measuring Probe orientation
- Sending the data by serial bus for further analysis: mishandling detection and other errors.

With this many tasks, an operating system (OS<sup>17</sup>) is needed. The OS tested was Zephyr and FreeRTOS.

<sup>17</sup>Operating System

### 4.3.17 Threading

A CPU alternates between different tasks using the priority based round robin scheduling algorithm, i.e. it alternates between tasks by taking into account the priority of the tasks.

**Routines:** Figure 4.4 shows the routines taken care of by the microcontroller:

- Battery management: checking the status of the battery, alerting if there is a problem
- Wireless connection: sending new data to publish
- Blower control: reading the fan speed
- Measurements from the RHT sensor
- Display and File management: menu, display measurements and write measurements on the card
- Sending data to a computer for further analysis (UART)
- The probe orientation from the IMU

**Scheduling:** RTOS uses pre-emptive scheduling, i.e. the scheduler can switch context to start a higher priority task. The routines all have the same priority. Threads have several statuses: not started, waiting, suspended, terminated in Zephyr and ready, suspended, and blocked in RTOS. While for Zephyr, the scheduler divides the time into slices measured in system clock ticks. Regarding memory allocation, the scheduler uses the first fit algorithm; each item is run in the heap bin where it first fit. The heap size is configurable. Timer Counter using interrupts is used for counting the speed. Interrupts are considered like a task.

**Shared resources:** Instead of using shared resources, lock mutex and semaphores, the choice was to use messages to send between two tasks with the functions Queue-Handle and xQueueCreate.

Having reviewed the different components needed, the PCB needed to support all the components described above.

### 4.3.18 Ergonomic probe design

The probe casing design has the following requirements:

- The instrument is easy to take in the hand

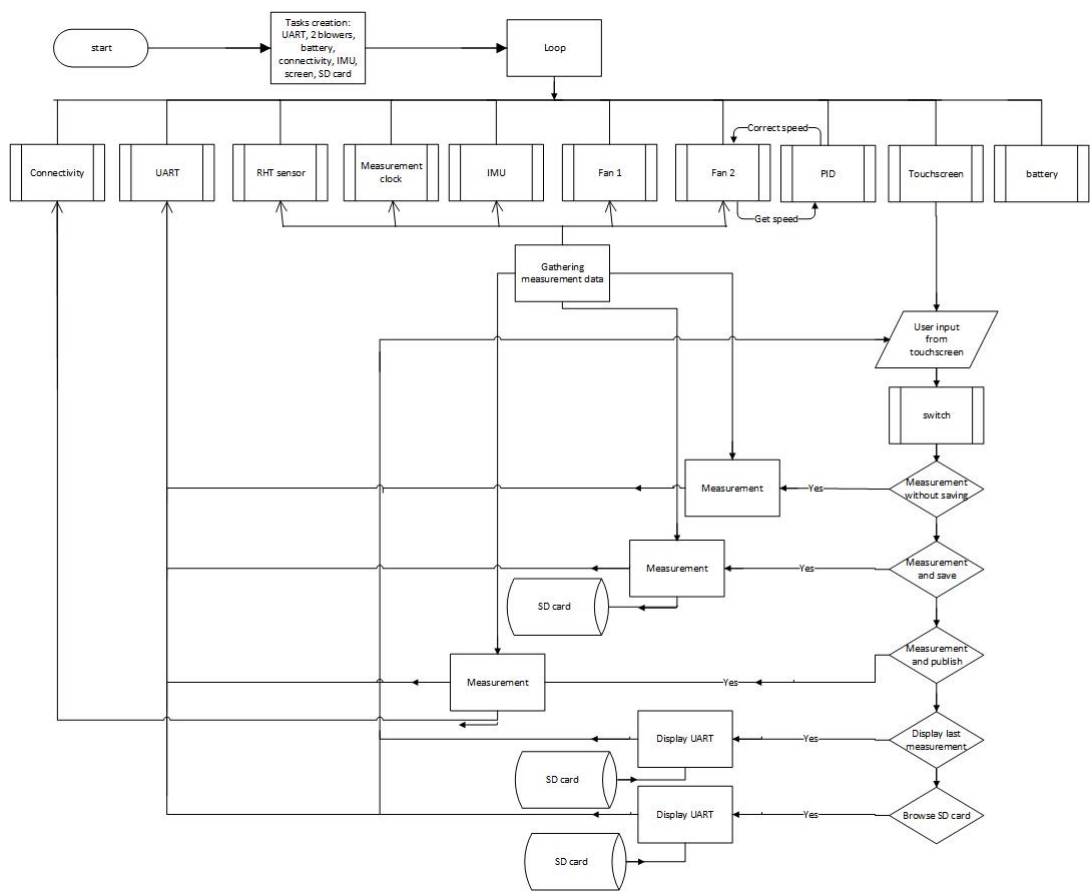


Figure 4.4: Flow diagram of the chamber tasks



- It is possible to read the screen and see the results whilst holding the instrument
- It is possible to change the speed of the blowers, so it needs a hole for the potentiometer
- The case is easy to open to change components

And the following constraints:

- Cheap to produce, using 3D printing for prototyping
- Within the maximum tolerances of the 3D printer
- Inherited constraints from the PCB manufacture

Many designs were made and a few prototypes printed. They were ergonomically suitable in the views of the author. However, a study on several people or customers to see how they find the handling of the instrument would be beneficial.

## 4.4 3D printing

Multiple challenges were met during the manufacturing process using FDM<sup>18</sup>. The Anet A8 is a budget version of the Prusa I3 MK3. The slicer software used was Cura v14 and the configuration file was imported and adapted from another printer model. The volume of the printer was set at 220x220x240mm. It is important to check this volume to have a understanding of the render before printing.

### 4.4.1 Fixed parameters for the printing

In the tests carried out, there were fixed parameters such as diameter of the filament fixed at 1.75mm, and the nozzle size fixed at 400 $\mu$ m.

### 4.4.2 Part orientation

The part orientation is crucial in 3D printing. It has an influence on the build time, the part sturdiness and the surface finish (Redwood 2019). The part will be slightly more solid in the XY direction than the Z direction for various polymers (Lee et al. 2007), (Cruz et al. 2015), (Bagsik et al. 2010).

---

<sup>18</sup>Fused Deposition Modeling

### 4.4.3 Layer thickness

The common recommendation is  $100\mu\text{m}$  if there are no predominant conic surfaces (Lanzotti, Del Giudice, Lepore, Staiano & Martorelli 2015). The layer height depends on the nozzle diameter. Layer height should not exceed 80% of the nozzle diameter (Zuza 2018). In our case the maximal layer height was  $320\mu\text{m}$ . If the layer height is too high, the layers won't stick well to the previous layer resulting in a low rigidity and poor surface texture of the object.

A smaller layer thickness results in better quality of the print, higher resolution and possibly encloses gaps better (Salinas 2014). Too low a layer height can cause the plastic to be pushed back into the nozzle, leading to the extruder wheel struggling to push the filament through. This behaviour will manifest itself with clicking noises and grinding of the filament. In the worst case, the plastic can expand and change state inside the hot end (Rambaud 2016). The minimum layer height is therefore set at  $1/4$  of the nozzle diameter. In our case, the minimum layer was  $100\mu\text{m}$ .

The typical layer height is between  $50$  and  $400\mu\text{m}$ . If one wants to print an object with curves or holes, more accurate results will be obtained using a lower layer (Brooks et al. 2011). However, if one wants to focus on the strength of the object, is better to have taller layers. Parts printed in PLA<sup>19</sup> at a  $300\mu\text{m}$  layer height have approximately 20% higher robustness than parts printed at  $100\mu\text{m}$  (Cain 2019). The choice of the layer height also depends on the the bed position, so calibration is fundamental (Lanzotti, Martorelli & Staiano 2015).

A trade off was found with a layer thickness of  $200\mu\text{m}$ .

### 4.4.4 Temperature

Temperature of the extrusion is one of the most important factors for 3D printing (Salinas 2014). This variable affects the surface quality of the object. Too high a temperature creates more strings between the separate parts of the print. The temperature also changes with the filament (Salinas 2014).

Regarding the temperature of the hot end of the nozzle, PLA optimal temperature is  $200^\circ\text{C}$ . However, the hot end had some issues to reach this temperature. The printer systematically attained a few degrees below the target temperature. One workaround was to start the print and manually decrease the threshold to force the printer to start the process, then re-increase the temperature to the target. An other workaround was to cover the fans with insulating tape, to keep the air hot.

Regarding the temperature of the bed,  $50^\circ\text{C}$  is the default parameter. However,  $55^\circ\text{C}$  was found to be better at keeping the object attached on the hot bed.

---

<sup>19</sup>Poly Lactic Acid

In the end, the hot end/hot bed temperature ratio 195°C/55°C was finally used. The temperature is closely linked to the fan speed . It is important for the fan to cool the hot end adequately to avoid warping.

#### 4.4.5 Infill

The quality of the print can be improved by increasing the infill (Salinas 2014). It was set at 20%.

#### 4.4.6 Speed

On the specifications, 120mm/s is the stated maximum. However, this can only be reached by the highest tuned versions of the A8. It can usually print between 40-60 mm/s. For this work, 30mm/s did not provide adequate results, as under-extrusion phenomenon was observed. Therefore the maximum print speed used was 25 mm/s.

#### 4.4.7 Flow rate

By default, flow rate on Cura is 100%. The common recommendation is 110% if there are no predominant conic surfaces (Lanzotti, Del Giudice, Lepore, Staiano & Martorelli 2015). This setting produced good results.

#### 4.4.8 Deposition speed

The default extrusion speed is 95 mm/s. When the printer produced an under-extruded part, the extrusion speed was increased from 95mm/s to 97mm/s. This was done on the printer directly because the software was being run on the printer. Lower deposition speeds are preferable (Lanzotti, Martorelli & Staiano 2015).

#### 4.4.9 The first layer

The first layer is the most strategic thing to get right. The first layer needs to stick on the hot bed, otherwise the object can bend slightly during printing (warping). In the worse case scenario, the printer can be found in the middle of a sea of filament.

the success of the first layer also depends on the layer speed, nozzle height and width, and fan speed. The parameters used for the first layer were:

- Minimum speed: 20 mm/s
- Initial layer thickness: 0.3 mm
- Fan speed: 30%, gradual increase to 50% at 0.5mm

Bed levelling is also crucial and was performed before each test.

The use of supports can assist to obtain a positive first layer. These are the parameters in Cura:

- Support type: None, touching, buildplate or everywhere
- Platform adhesion type: None, brim or raft

One skirt of 3 mm of minimum 150 mm length was added to all prints, just to prepare the nozzle for printing the first layer effectively.

It is also possible to use other physical means to support: glass, glue, hairspray, blue painter tape, etc. The latter option was preferred.

#### **4.4.10 Retraction**

The retraction speed is an important variable to avoid plastic drips. It was set to 40 mm/s (default is 45 mm/s). The minimum distance was set to 4.5 mm (default is 4mm). This was used to avoid frequent retractions.

#### **4.4.11 Casing shell**

The casing shell has to be a multiple of the nozzle diameter. The shell or wall thickness was set to 1.2 mm (default was 1.6 mm). The strength of the object can be increased by having a higher value, which also decreases the chances of filament leaks. However, this has an associated cost in time and materials.

#### **4.4.12 Tuning of the stepper drivers of the x,y and z axis**

The stepper drivers of the x, y, z axis consist off checking the voltage of the input of the step motor. The stepper motor is a NEMA 17 SL42STH40-1684A and should be 2.8V.

#### **4.4.13 Minimum layer time**

For smaller areas, the printer nozzle often deforms the printed part as the plastic gets caught by the nozzle. Several tests were performed to adapt the cool down after each pass of the nozzle. There are several solutions to cooling; increasing the fan speed, decreasing the temperature and increasing the minimum layer time. The temperature was already low, so the solution was to increase the fan speed after 0.5mm and the minimum layer time to 30 seconds.

#### 4.4.14 Conclusion on 3D printing

A trade off was achieved between temperature, fan speed, layer thickness and extrusion speed.

Adaptation of the design on CAD was necessary because the slicer parameters were not working:

- 3mm wall thickness
- 1.5mm constraints

To conclude, a balance was needed between the CAD design and the capability of the 3D printer.

### 4.5 Diurnal variations

Diurnal variations are relevant in this work because of the need to take measurements at the same time of the day so results can be compared with each other.

#### 4.5.1 Introduction

In skin measurements guidelines (Pinnagoda et al. 1990) and a TEWL meta-analysis (Kottner et al. 2013), seasonal rhythms in TEWL have been described. Variation as part of the circadian rhythm has been mentioned in the EEMCO guidelines (Rogiers 2001) and (Berardesca et al. 2018), but without a definitive description of the exact circadian pattern.

Diurnal variations of TEWL have been observed with the Tewameter TM 300 (Firooz et al. 2016), (Yosipovitch et al. 1998), Tewameter TM210C (Le Fur et al. 2001) and the Servomed Evaporimeter (Chilcott & Farrar 2000), (Spruit 1971). Of note, all these studies were related to open chambers devices and used the same established protocol. Despite this, the results are inconsistent. These studies have respectively found the following peak times for TEWL (where TEWL is the highest):

- Single peak: 09:00, 12:00, 16:00, 18:00.
- Two peaks: 08:00 and 16:00.

As these results are vastly different, it can only be concluded that studies have shown a diurnal variation but have not established a consistent pattern for when peak TEWL occurs. The human body demonstrates circadian rhythm on a variety of biological parameters like cortisol. However whilst some authors have suggested circadian variations, no pattern have been identified. Reasons for this are factors

provided in 2.9.1: variations on the laboratory settings, divergence of methodologies, difference of instruments, variations between subjects...

Diurnal variation has not been investigated with the Aquaflux, the micro-climate controlled closed chamber. Moreover, the condenser chamber has mathematically higher intrinsic sensitivity than other TEWL measurement devices because of the number of sensors (Imhof et al. 2002). Also a study shown than Aquaflux has higher repeatability and better accuracy (through calibration) than the Delfin Vapometer (Imhof et al. 2009). However these studies are not independant.

### 4.5.2 Materials and methods

In this experiment, all measurements were performed on a 35 years old healthy Caucasian female volunteer. Before the measurements, the participant was acclimatised for 30 minutes in an air conditioned room with a temperature of 20.5°C and RH = 49.3%. The volunteer refrained from using soap and cream for 12 hours before assessment. The measurement was done on an anatomical site easy to obtain repeat measurements: the middle of the volar forearm (VF), far from the wrist or the elbow to avoid areas with more sweat glands. In addition, to make sure the measurement was performed exactly on the same location day after day, for a week, a natural distinctive point was chosen - a point 11 cm proximal from the wrist crease, and 1 cm medial from the wrist flexor tendons. The environmental conditions were kept within the ranges recommended in the EEMCO Guidelines (Rogiers 2001). Air conditioning was used to keep the room temperature at 21°C. The AC settings were cold air and a low velocity fan to not disrupt the micro-climate near the skin. The first day, measurements were performed at 11am, 3pm, 5pm and 7pm to compare to the three time point analysis (8am, 12pm, 4pm) of Firooz et al. (2016). The results were different from the ones expressed in the literature . From the second day, a 12 hour study was conducted from 7:30 am to 7:30pm. Below are the environmental conditions of the room during the week of tests (Table 4.2). The investigation was conducted over a week to validate the events of two consecutive time spans as per the recommendation from Reinberg et al. (1998) to measure during a continuous period of at least 48 hours.

### 4.5.3 Data collection

The Aquaflux software was used in TEWL mode. It was easy and quick to perform several measurements consecutively without the need to rest in between. The measurements were done in triplicate and the average TEWL value on the right and the left VF calculated at every hour. So the measurements were done hourly from 7:30 to 19:30 on each of the five days over a week long period. The subject didn't con-

Table 4.2: Ambient temperature and RH on four consecutive days

RH (%)	Temperature (°C)
39.8	21.4
43.5	20.8
49.9	20.0
47.5	21.5

sumed any caffeinated drinks between the hourly measurements. The subject was free to leave the room but re-acclimatisation was done between each measurement sessions.

#### 4.5.4 Results

The mean and standard deviation of TEWL was calculated throughout the day on the right and left volar forearms (Figure 4.5). Similar variations for TEWL were observed on left and right arm, with a slightly higher value for the left arm ( $\approx 0.86\%$ ), see Table 4.3. This level of difference is about what would be expected from the instrument error. The average TEWL value for the left and right is 13.36 and 14.23  $g \cdot m^{-2} \cdot h^{-1}$ . Although statistically significant (student t-test  $p = 0.0053$ ) the difference falls in the instrument precision of 0.05%

Date	Daily Average Right	Daily Average Left
18/04/2018	16.39	18.71
19/04/2018	16.65	18.30
20/04/2018	15.49	17.03
23/04/2018	13.58	13.89
24/04/2018	14.24	14.94
weekly average	15.27	16.57

Table 4.3: Daily mean TEWL measured on the volar forearm, right and left.

TEWL was highest at the beginning of the day, and then stabilised to 15-16  $g \cdot m^{-2} \cdot h^{-1}$  after the subject was in the air-conditioned room for a while. It sometimes increases slightly towards the end of the day.

#### 4.5.5 Discussion

Chilcott et al. used the Evaporimeter and found a high TEWL at the beginning of the day, slowly decreasing until the end of the measurement session finishing at 17:00 (Chilcott & Farrar 2000). Other research reported a TEWL higher in the evening and at night compared to the morning (Elsner et al. 2004), (Sotoodian &

### Diurnal Variation of Transepidermal Water Loss (TEWL) from the Volar Aspect of the Forearm in One Participant

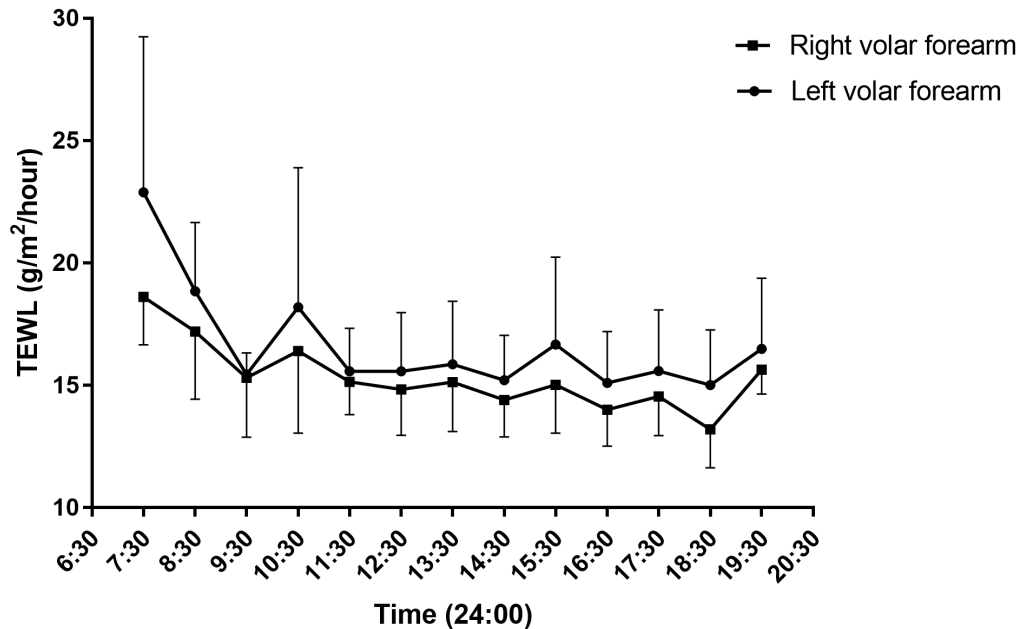


Figure 4.5: Diurnal Variations measured on the volar forearm measured during a week

Maibach 2012). Firooz et al. measured TEWL at three time points and found it to be higher at 12:00 than at 16:00, and lowest at 08:00 (Firooz et al. 2016).

According to Yosipovitch et al., TEWL of the VF is lowest at 06:00 and highest at 18:00 (Yosipovitch et al. 1998). Le Fur et al. reported a complete analysis over 24 hours, with 2 maximum peaks seen at 08:00 and 16:00 and a minimum at 18:00 onwards (Le Fur et al. 2001). Rogiers et al. stated the TEWL is said to be higher in the afternoon than the morning (Rogiers 2001). Some investigations suggest that TEWL diurnal variation is linked to ambient temperature (Yosipovitch et al. 1998), (Pinnagoda et al. 1990), (Spruit 1971). However, Denda et al. showed that cutaneous barrier repair was independent of changes in skin temperature and cortisol level whilst observing TEWL variations after tape stripping (Denda & Tsuchiya 2000).

In this experiment, TEWL values of  $16\text{--}20\text{ g} \cdot \text{m}^{-2} \cdot \text{h}^{-1}$  have been observed, which are much lower than the  $42\text{--}74\text{ g} \cdot \text{m}^{-2} \cdot \text{h}^{-1}$  seen in the study by Firooz et al. (2016). This may be due to the type of TEWL measurement device being used (Aquaflux vs. Tewameter) or the difference in ethnicity of the test subject(s) (Caucasian vs. Middle Eastern). Despite this, they also observed higher TEWL values in the morning than in the evening. The same results were found by Chilcott



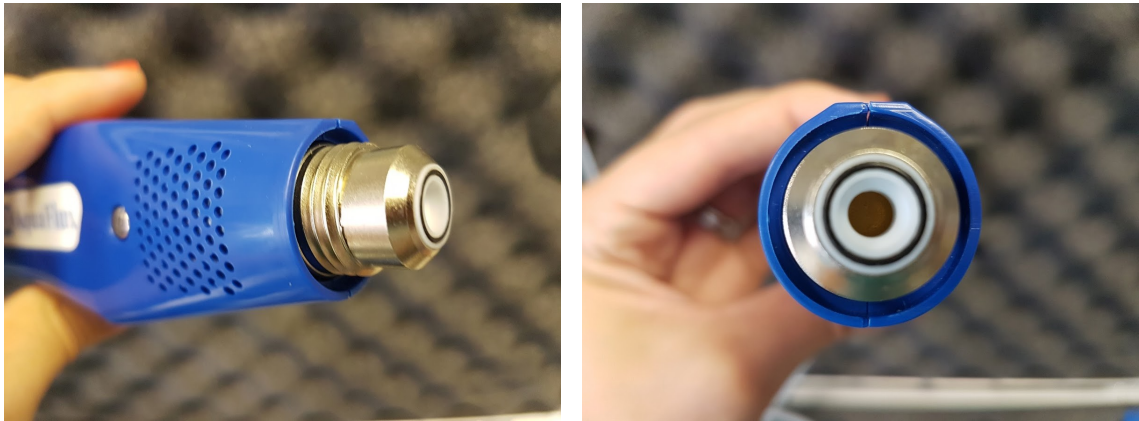
& Farrar (2000); a maximum TEWL at the beginning of the day at 09:00 that slowly decreases until the end of the day, reaching a nadir at 17:00.

In this study, TEWL was high at the start of the experiment and then decreased and stabilised by mid-morning. The subject had been cycling for 10 minutes prior to the experiment, on each of the five days. Despite having one hour from the end of exercise to acclimatise to the air-conditioned room, it appears that the exercise may still have been having an influence on the earlier TEWL measurements. From the third measurement (09:30 am), the TEWL reached a stable average value. This suggests that a minimum of 4 hours is required to get a true measurement post-exercise, which is much more than the 15-30 minutes suggested in most of the guidelines (Rogiers 2001), (Elsner et al. 2004). The variations during the day are quite small compared to the descending slope at the beginning. The commuting impact could be due to physical (e.g. sweating, increased body heat) or hormonal (e.g. exercise-induced cortisol release) mechanisms. Physical exercise and caffeine consumption should be kept to a minimum (Rogiers 2001) (Sotoodian & Maibach 2012), because the extra stimulation could increase TEWL. If so, acclimatisation needs to be longer than the guidelines suggest (Le Fur et al. 2001), (Rogiers 2001) as recovery after a ten minute cycle appears to take up to 2h 30min. Further controlled studies on these stimulants (e.g. prescribed cycling sessions on an exercise bike, consumption of known volumes of caffeine) and their effect on TEWL should to be conducted on more subjects.

#### 4.5.6 Conclusion

This is the first report of the Aquaflex being used to measure diurnal variations of TEWL. Many investigations have been conducted without recognising a single pattern of circadian rhythm. This study confirms the results of Chilcott & Farrar (2000) using an open chamber. In both studies TEWL is higher during the morning than the afternoon. A confounding factor may be the short exercise session taken one hour prior to the first measurement. Future studies should investigate circadian rhythm in a larger number of subjects, as well as the effect of season and geographical location, as well as the effect of other possible confounding factors such as exercise and caffeine.

In the rest of this chapter only probe 1, 3, 4, 5.1, 7.1 and 9 are presented. Chamber 2 had large diameter of 41 mm and small height 10 mm. Another chamber not presented here was transparent to observe gradient with a thermal camera. Moreover, the gradient calculations are omitted; they will be discussed and compared in the experimental results section.



(a) Side chamber 1

(b) Front chamber 1

Figure 4.6: Chamber 1

## 4.6 Prototype 1

### 4.6.1 Rationale

One of the main strategies for achieving portability in a new device was to avoid the use of a condenser in the chamber. Condenser is the main reason that AquaFlux needs mains power supply. Therefore, to make a handheld device powered by battery, we have to remove the condenser. But condenser is the main innovative approach that makes AquaFlux more accurate, more repeatable, and more precise. So the challenge of the project is to develop a closed-chamber TEWL measurement device without using the condenser, and can still maintain reasonable accuracy, repeatability and precision. A natural place to start, therefore, was to characterise the performance of the existing Aquaflux chamber with its condenser switched off. This was used (i) to develop a standard methodology for evaluating and characterising subsequent experimental prototype designs; (ii) to provide a baseline against which to measure improvements in subsequent prototypes; and (iii) to provide a convenient test bed for initial investigations into the impact on measurements of such factors as rest period between measurements.

### 4.6.2 Materials and Methods

#### 4.6.2.1 Description of the equipment

Prototype 1 chamber is a cylinder of 5 mm diameter and 10 mm depth, as shown in Figure 4.6. The bottom of the cylinder is sealed and the top is open to skin surface. The temperature and humidity sensor is at the middle of the cylinder. The AquaFlux software on PC logs the relative humidity and temperature of the sensor twice every second.

#### 4.6.2.2 Methodology

In this part we will see what experimental procedures were conducted. This chamber aims to establish the methodology that can be found in section 4.2. All measurements were performed on one participant. The gradient were calculated for each measurements. In addition the precision via the coefficient of variation, and the sensitivity via the calibration slope were evaluated.

#### 4.6.2.3 Data collection

Probe 1 was the Aquaflux in idle mode without the condenser turned on. The chamber provided RH and temperature information. It was sent through USB and saved by the Aquaflux software. The post processing was done on spreadsheets and on MATLAB. In the previous chapter, the designs were described. In this chapter, the post-processed results are depicted. These consist of:

- Concentration - Absolute Humidity calculation
- Gradient calculation
- Display of the results
- Further computations for analysis of the results (errors, comparisons, fitting etc.)

RH is not stable during measurements and varies with temperature. The concentration of water is therefore a more accurate measure than RH. In addition, the concentration is easily connected to the mass of water and the TEWL, a flux of water quantity through a surface area.

The RH and temperature gives the absolute humidity (AH) with the polynomial formula 2.9 seen in section 2.7.3. The gradient calculation for this chamber is:

$$\text{Humidity Gradient} = \frac{\partial C}{\partial t} = \frac{\Delta AH}{\Delta t} \quad (4.2)$$

The Aquaflux software in time series records one measurement per second in a text file.

#### 4.6.2.4 Specific methodology

The generic methodology has been developed with this chamber. The aim was to define: the duration of measurements, the rest between measurements, different ideas to purge the closed chamber. It was an exploratory phase. Measurement were done on one participant using chamber 1.

The following variations to the measurement protocol were tested to see their effect on the coefficient of variation:

- Increasing measurement time : 30 seconds to 60 seconds
- Longer rest phases between applications of the chamber on the skin: 30s, 60s, 120s, 240s, and 360s
- Wafting the probe in between measurements to empty it
- Using a cooling fan to blow near and into the probe
- Using an Air conditioning (AC) unit to keep the temperature constant in the room
- Isolating the probe handle to avoid heat transfer from the hand to the measurement chamber
- Measuring TEWL at other anatomical sites like the calf

The last six tests aimed to keep the temperature stable or to bring it back to initial value. In each of these experiments, what was varied is the variable after the description of the variable. The participant, and all the variables of the others bullet points except the one in question were kept constant. What was measured is RH and temperature, as mentioned above, and also, in more details, in the next section called 'Data Collection'. The measurement were performed under constant environmental conditions as much as possible. As mentioned in the general methodology and in the description above, there were three repeat measurements. The justification for the answers to these questions is: it is a discovery phase in order to define the methodology.

**Impact of measurement time on repeatability of TEWL measurements:**

The purpose of this block of work was to investigate the impact of measurement time on the repeatability of TEWL measurements. Five repeat measurements were made on the volunteer's mid-volar forearm using each of two measurement times (30s and 60s) and the coefficients of variation for each of the two sets of measurements compared. Furthermore, the repeatability can be compared with the others methods presented in the list above.

**Impact of rest time between applications of the chamber on the skin on repeatability:**

The purpose of this block of work was to investigate the impact of measurement time on the repeatability of TEWL measurements. Five repeat measurements were made on the volunteer's mid-volar forearm using each of two

measurement times (30s, 60s, 120s, 240s, and 360s) and the coefficients of variation for each of these sets of measurements compared. Furthermore, the repeatability can be compared with the others methods presented in the list above.

**Impact of purging the chamber of water vapour between measurements on repeatability:** The purpose of this block of work was to see if purging the chamber of water vapour between measurements would improve measurement repeatability. Five repeat TEWL measurements were made on the mid-volar forearm. The chamber was vigorously shaken in the air for 30s or 60s to actively purge it of water vapour. The coefficient of variation for each of the sets can be compared with the other methods to improve repeatability.

**Impact of a fan to blow near and into the probe between measurements on repeatability:** The purpose of this block of work was to see if purging using a fan the chamber of water vapour between measurements would improve measurement repeatability. Five repeat TEWL measurements were made on the mid-volar forearm. Then the fan blow into the chamber for 30s to actively purge it of water vapour. The repeatability can be compared with the rest of the methods presented in the list above.

**Impact of using the AC during measurements on repeatability:** The purpose of this block of work was to see if purging the chamber of water vapour between measurements would improve measurement repeatability. Eight repeat TEWL measurements were made on the mid-volar forearm. Then the chamber was left to rest for 30s while the AC was on with the fan mode. The coefficient of variation for each of the sets can be compared with the other methods to improve repeatability.

**Impact of isolating probe on repeatability:** The purpose of this block of work was to see if purging the chamber of water vapour between measurements would improve measurement repeatability. Five repeat TEWL measurements were made on the mid-volar forearm with isolation of the probe. The hand would not transfer heat to the probe it was holding. The coefficient of variation for each of the sets can be compared with the other methods to improve repeatability.

**Impact on the skin site on repeatability:** The purpose of this block of work was to investigate the impact of skin site on the repeatability of TEWL measurements. Five repeat measurements were made on the volunteer's mid-volar forearm using each of two sites (calf and arm) and the coefficients of variation for each of the two sets of measurements compared.

**General TEWL measurements:** In order to compare with the other prototypes, some additional measurements were performed. The methodology will be the same for the rest of the prototypes, as described in the general methodology section at the beginning of this chapter. Measurements were performed with the prototype and the Aquaflux. This is to draw the calibration curve. In addition, the TEWL measured by the Aquaflux was used as an input for the 3D modelling. Simulations were performed and the RH and temperature distribution presented in the results. We performed measurements of RH and temperature for an application of 30 seconds and a rest of 30 seconds between measurements, on three location sites of the volar forearm: three sites on the axis of the arm, with 6 cm space in between. Measurements were performed on the wrist, the elbow and the VF. In this experiment, the skin site was varied and the participant, the duration of the measurement, the environmental conditions and the instrument were kept constant. What was measured is RH and temperature, as mentioned above. The measurement were performed under constant environmental conditions as much as possible. As mentioned in the general methodology above, there were three repeat measurements. The justification for the answers to these questions is: the values appears like an acceptable average to use as a baseline to be compared with other chambers.

### 4.6.3 Results

In this part is presented the results, using tables and graphs to display them clearly.

#### 4.6.3.1 Methods to improve repeatability

The following variations to the measurement protocol were tested to see their effect on the error.

##### **Impact of measurement time on repeatability of TEWL measurements:**

It was observed 52% error for 30 seconds application vs. 34% error for 60s application.

##### **Impact of rest time between applications of the chamber on the skin on**

**repeatability:** It was observed 36%, 39%, 39%, 37%, 51% error for rest periods of 30s, 60s, 120s, 240s and 360s respectively.

##### **Impact of purging the chamber of water vapour between measurements**

**on repeatability:** It was observed 30.8% error for 60s shake and 113% error for 30s shake.

**Impact of a fan to blow near and into the probe between measurements on repeatability:** It was observed 36% error

**Impact of using the AC during measurements on repeatability:** It was observed 47% error.

**Impact of isolating probe on repeatability:** It was observed 46% error.

**Impact on the skin site on repeatability:** It was observed 36% error for the VF and 53% error for the calf.

The errors were still quite high and could come from the gradient calculation. Therefore in the next part of this work, what is considered as a good result is the repeatability of the measurement. In conclusion, measuring for longer periods gave more repeatable results. However, shaking the probe, using a cooling fan or air conditioning units provoked additional flow and did not improve the error.

#### 4.6.3.2 General skin measurements:

It is expected that the flux gradually reduces during the measurement. According to Fick's law 2.8, the diffusion flux is proportional to the negative gradient of concentrations. Therefore, the flux will decrease gradually as the humidity increases within the chamber.

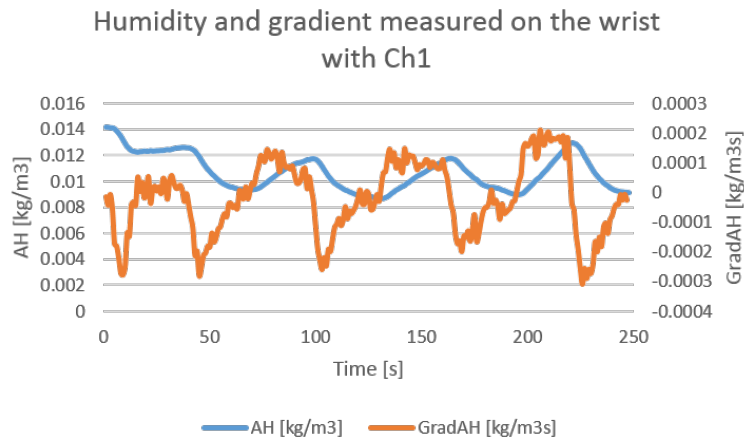
We performed measurements of RH and temperature for an application of 30 seconds and a rest of 30 seconds between measurements, on three location sites of the volar forearm (Fig. 4.7): three sites on the axis of the arm, with 6 cm space in between.

As expected, the gradient was more pronounced at the wrist than the middle VF because of the presence of more sweat glands.

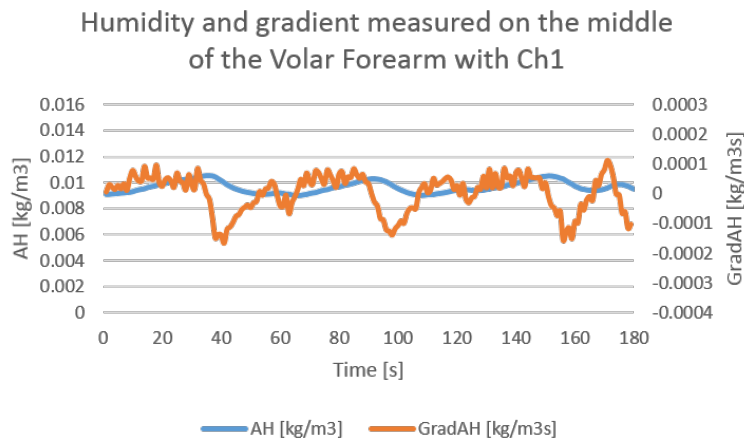
The error or coefficient of variation was roughly the same for the wrist (52%), the elbow (53 %) and the middle of the VF (47%). This is quite high, in comparison with the Aquaflux under normal circumstance (with the condenser turn on) that has a 5% error. The error could be reduced with the calculation method (sampling, duration and timing of the computation of the gradient). The error could also be minimised by altering elements of the experimental protocol. The methods to improve repeatability were presented above, they consist in lengthening the measurement time and to reduce the temperature variations in the chamber.

#### 4.6.3.3 Calibration:

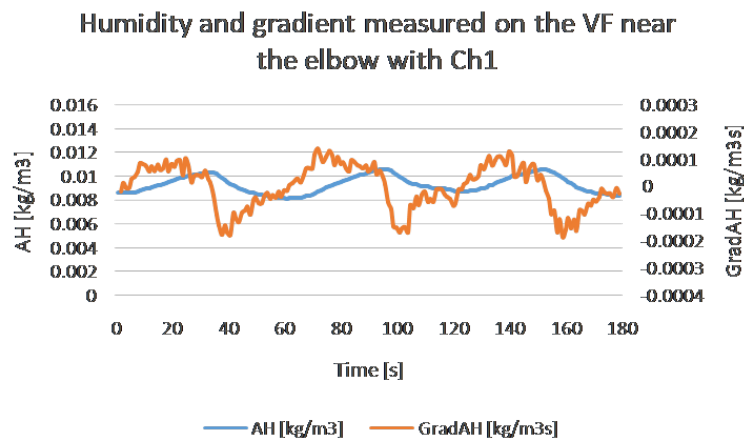
Calibration is usually based on the gravimetric method. In this thesis, the method used was correlation with the Aquaflux. The Aquaflux was the first instrument from



(a) Four measurements on the VF near the wrist for 30s followed by 30s rest



(b) Three measurements in the middle of the VF for 30s followed by 30s rest



(c) Three measurements on the VF near the elbow for 30s followed by 30s rest

Figure 4.7: Chamber 1



Biox Systems Limited. The error seen in Chamber 1 (Aquaflux with the condenser off) is large, especially when compared to the Aquaflux (with the condenser on) that has a 5% error. Correlation between the two instruments can be shown by plotting the calculated gradient measured by Chamber 1 against the Aquaflux values for a small and a large TEWL. The results are not shown here because the values were quite sparse and the error rate was high. Possible solutions to improve the correlation could be stricter environmental control and improved gradient calculation. New methods to control the environment were explored from Chamber 2. Some improvements on the calculation method were made from Chamber 3.

#### 4.6.3.4 Simulation:

The ANSYS simulation was run for 30 seconds with 1 second time intervals. For better precision, the simulation was run with double precision and fine meshing and was not simplified to a 2D model. The results can be seen in Fig. 4.8.

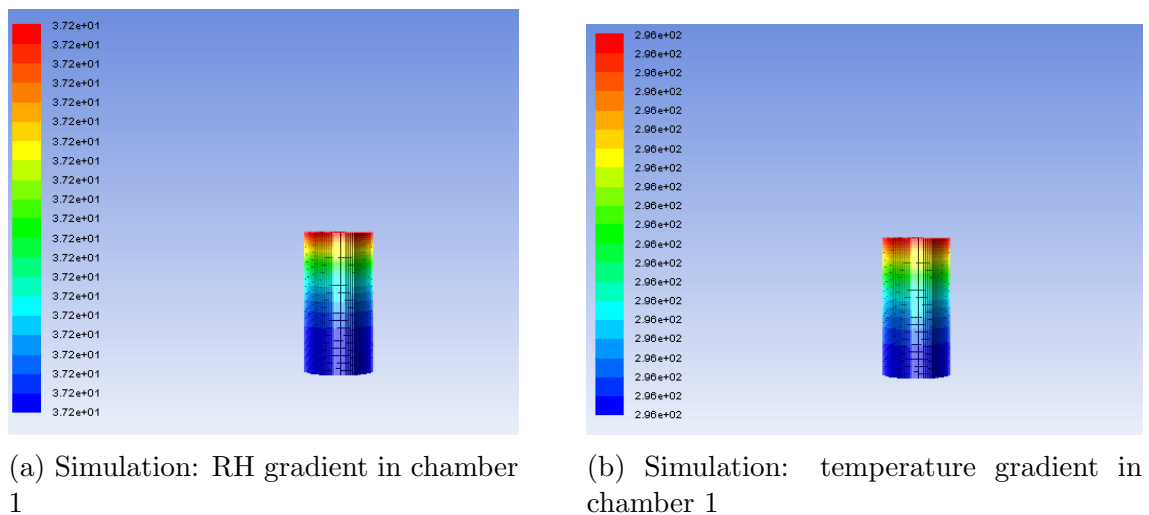


Figure 4.8: Chamber 1 simulation

#### 4.6.4 Discussion

In this part we will discuss the results of what we discovered and giving the impact on chamber performance of the variables with which we experimented. While using probe 1, the gradient is larger on the wrist or the palm rather than the volar forearm. These extreme values have therefore been used as the limit of the range for the calibration function. Furthermore, to get the best repeatability, it is preferable to measure TEWL on the volar forearm. This conclusion is consistent with other published work (for example Rogiers (1995)).

Regarding the operating protocol for the thesis, it has been found that the later the gradient is calculated, the better is repeatability. The impact on chamber

performance was better repeatability and the variable that was experimented with was the length of application (60s vs 30s). There is no published work to confirm or not these results.

However, it would be nice to have a quick measurement. So an objective of this project would be to minimise the duration. In addition, the rest duration doesn't have to be longer, 30 seconds is sufficient. The impact on chamber performance was better repeatability and the variable that was experimented with was the length of rest between applications (30s, 60s, 120s, 240s, 360s). There is no published work to compare these results with.

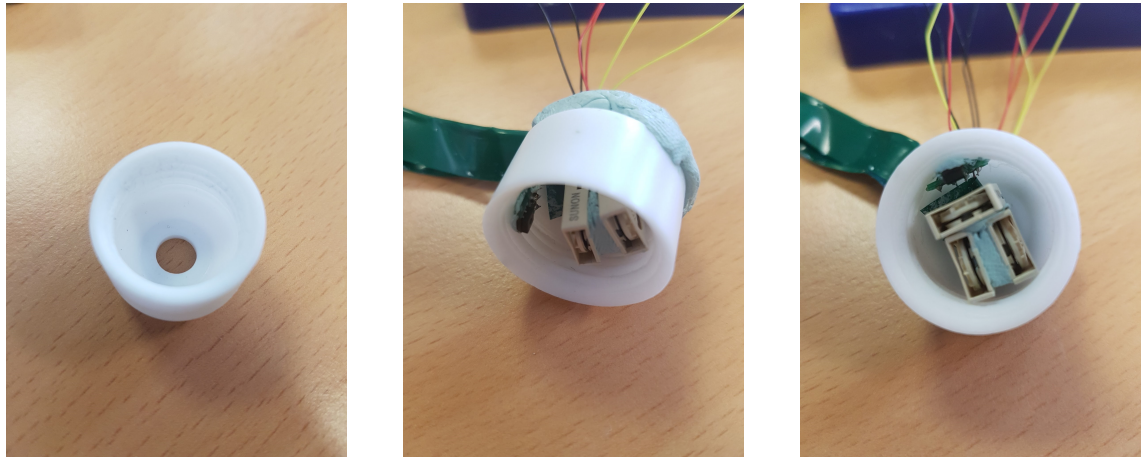
Moreover, various methods to purge the closed chamber have been tested, wafting the probe was better than using a fan to blow in it, in terms of coefficient of variation. The impact on chamber performance was better repeatability and the variable that was experimented with was the method to purge the chamber. There is no published work to discuss these results.

Finally, two methods to reduce the impact of the environment, using an isolation of the probe handle and using air-con but one is not better than the other. The impact on chamber performance was better repeatability and the variable that was experimented with was the method to isolate the measurement. There is no published work to confirm these results.

We discussed the results. Referring back to the aims for this module (to define a experimental method), we were able to achieve the aims in full, although the development method was agile and experimental method was fluid. More specifically, we learn that rest duration doesn't impact the repeatability for example. But there are other items that were useful and informative in terms of the overall aims of the project. In regards to the experimental method, the rest between application were 30 seconds; wafting the probe, use of the AC and isolation were recommended. For the duration of the application, ideally it has be minimal to not strain user patience, but it has to provide good enough results. The Aquaflux provides results usually in 30 to 45 seconds (by default, but depending on the precision) so the aim is to obtain a measurement in 30 seconds. This last paragraph contains notes from the result from this module which helped us to plan subsequent work modules.

#### 4.6.5 Conclusion

Prototype 1 results show that it is possible to conduct reliable TEWL measurements using a closed chamber without a condenser. The results show that it takes about 30 seconds to conduct a TEWL measurement. This is already much faster than a standard AquaFlux measurement, which typically takes about one minute. The results also show that the temperature inside the chamber increases during the



(a) Without RHT sensor and blowers

(b) With RHT sensor and 2x9mm blowers

(c) With RHT sensor and 3x9mm blowers

Figure 4.9: Chamber 3

measurements and decreases after the measurements. Air conditioning can also affect the measurements. The next step is to introduce a fan into the measurement chamber, this can further speed up the measurements and eliminating the effect of skin surface water. Several prototypes have been developed, but only a few selected will be presented here.

## 4.7 Prototype 3

### 4.7.1 Description

Chamber 3 is 18 mm height with a 20 mm diameter. It has a small design for two reasons; firstly for better contact to the skin and also for more precise measurements as per (Imhof & McFeat 2014). In the interest of planet resources saving, Chamber 3 has been made from a cap of the Aquaflux, see 4.9a. It is big enough to contain up to three 9 mm blowers or two 12 mm blowers, see 4.9b and 4.9c. Using one, two or three blowers enables different flow rates. The larger the blower is, the bigger the flow rate: 17 mm blower flow rates are stronger than those of 9 mm blowers. The speed of the blowers is controlled by Pulse Width Modulation (PWM).

Bluetooth Low Energy (BLE) is integrated on the Arduino 101 and an Android application has been developed to communicate with the microcontroller (see Fig. 4.10). The Android application scans and displays the devices available. The user can then select to display the measurement data and device information. The Android application used the following two libraries:

- BluetoothLeGatt: for the BLE Gatt service. The chamber is a Gatt server and the smartphone is a client. The chamber sends Gatt characteristics to

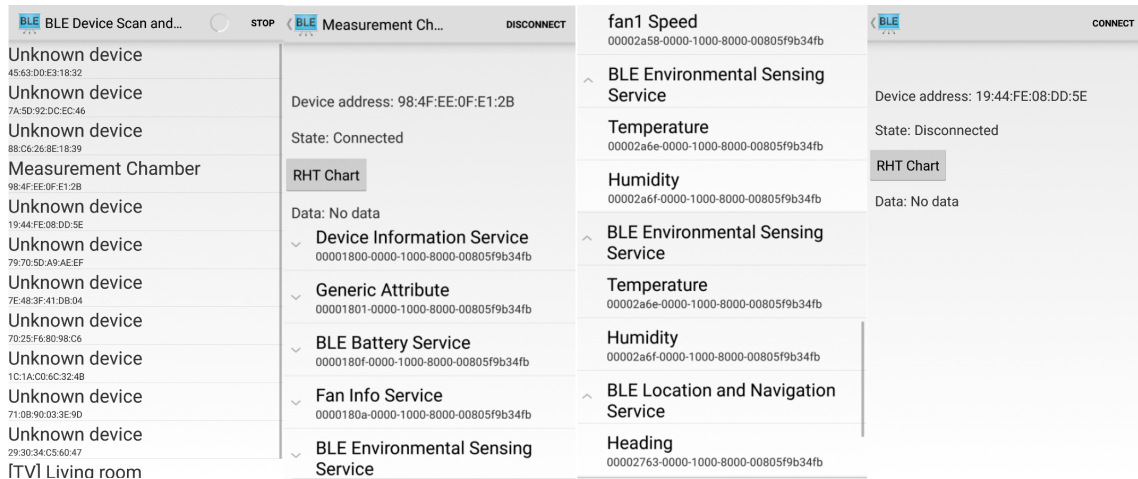


Figure 4.10: Android application to gather measurements data

its subscribers. Characteristics implemented are RH, temperature in double precision data type, the battery level, the gyroscope information (heading, pitch and roll) and the blowers speed.

- MPAndroidChart: to display the charts for RH and temperature in real time.

The communication between the smartphone and the instrument can be monitored with a sniffer: Texas Instrument CC2240. This comes in the form of a dongle that is plugged into a PC. It has an antenna listening on a specific part of the spectrum to capture the data transmitted. The data is then displayed on the PC with Wireshark, the most widely used network protocol analyser. It allows for the observation of the packets at different layers. This process is completely transparent to the users.

## 4.7.2 Rational

The aim of the project is to develop an instrument that can measure TEWL outside of a controlled environment. In order to minimise the environment effect, a closed chamber design was chosen. The first chamber was testing measurements with a closed chamber in order to come up with an operational method, while the second one was the first try of closed chamber with a fan. However it used a large fan, the chamber was big and tall its diameter was still too large chamber 3 was designed. Chamber 3 is a cylinder, smallest as possible, but large enough to accommodate different fan sizes. Chamber 3 allowed for different fan configurations, with one to three 9 mm and one to two 12 mm fans possible. It was possible to increase or decrease the speed of blowers using PWM. However the study was limited to vary the models and numbers of blowers in order to change the air flow. Moreover, it was possible to lengthen the duration of measurement to get a stable gradient after

excluding the SSWL.

### 4.7.3 Testing

With chamber 1 an operating protocol has been established: the measurements are performed by application of 30 seconds and rest of 30 seconds. The location sites are the palm and volar forearm on one participant. All measurements are done in a controlled environment. They are first performed on the prototype, then with the Aquaflux in order to have a reference for calibration. Measurements are at least done in triplicate. The general methodology can be found in section 4.2. For this chamber, measurements have been done with and without the fan. In addition, an objective was to create different air flow by combining several fans and using different fans size. Also, the use of the fan aim to remove surface water. Therefore water drops were applied on the skin to simulate sweat. The impact on the TEWL measurement was studied. Finally, signal processing have been investigated with this chamber by trying out different gradient calculations and smoothing filters. Signal processing was used to refine and get the best output from the inputs: this constitutes refinement of calculation method.

### 4.7.4 Results

Measurements were taken on the volar forearm, see below for more details.

#### 4.7.4.1 Gradient calculation:

In order to compare all of the configurations above, a new algorithm for gradient calculation was used. Afterwards, different methods were tried. The vapour concentration was calculated with Lowe polynomial (see Eq. 2.9). Then a running average was performed for a duration of 1 second to smooth the gradient. Then an average of the flux was calculated for the first 10 seconds. Ten seconds was chosen to allow for quick results. This method will be referred to as 'Average Smooth 10'.

#### 4.7.4.2 Experimental results with 9 mm fan:

**Results without the fan:** Fifteen consecutive measurements of relative humidity and temperature were performed on the volar forearm (Fig. 4.11).

The gradient of humidity was calculated from the relative humidity and temperature information and compared to the relative humidity (Fig. 4.12a). As the gradient was very noisy, a running average of 1, 2 and 3 seconds was calculated to show the effect of the smoothing (Fig. 4.12b).

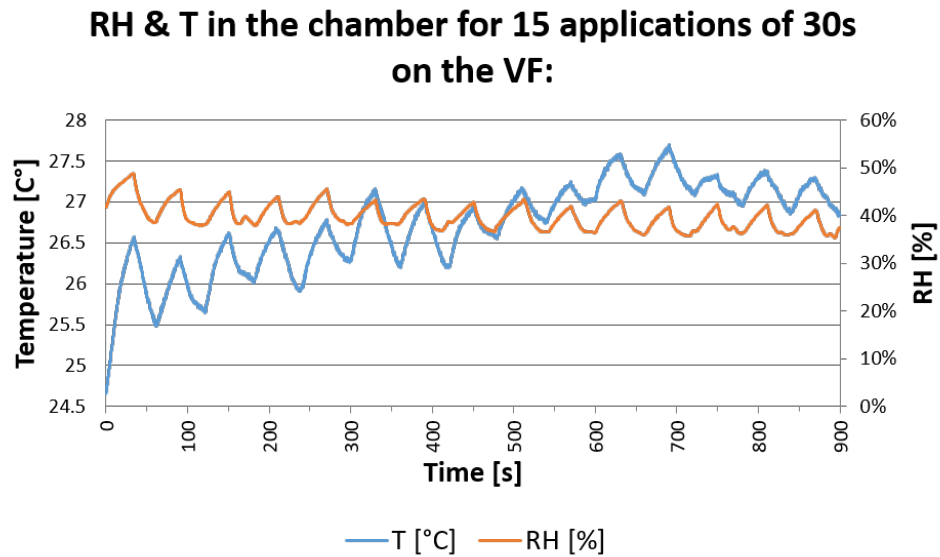


Figure 4.11: 15 measurements on the VF: RH and temperature variations with Chamber 3

During a measurement session with application and rest times of 30 seconds, the coefficient of variation was 32.8% without the fan.

**Results with 9 mm fan:** During a session with application and rest time of 30 seconds, the error was 49.5% with one 9 mm fan.

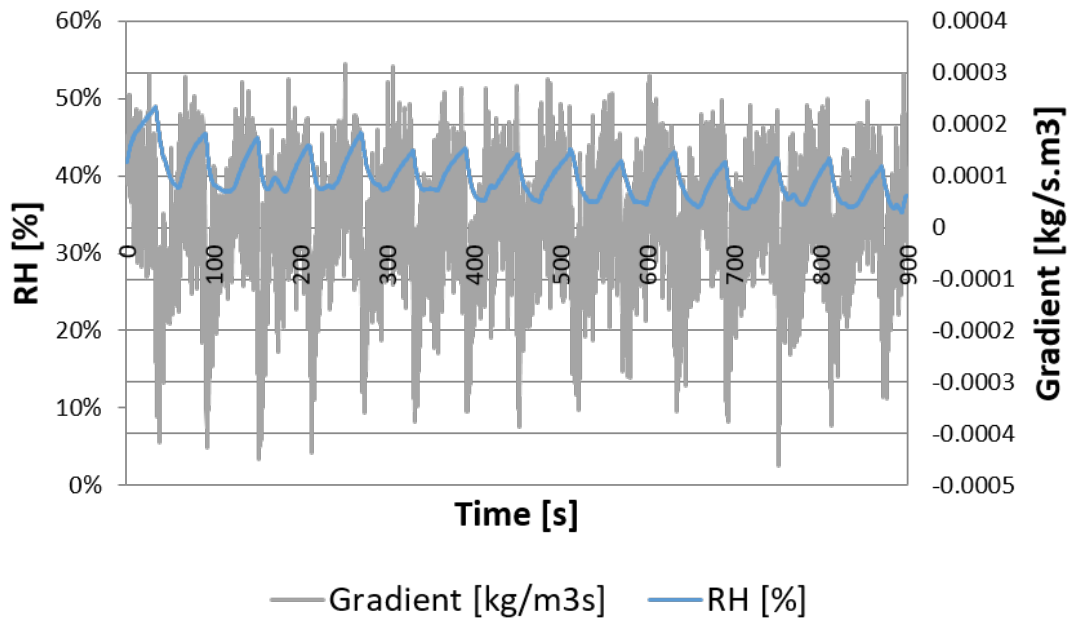
**Comparison case with and without the 9 mm fan:** With the internal fan on, RH had a lot of outliers at time = 0. The temperature was also variable. Similarly at 10s of measurement with the internal fan on, RH had a lot of outliers and the temperature was also still variable. At  $t = 20$  seconds and 30 seconds, RH had less outliers than previously but RH and temperature varied more when using a fan than without.

#### 4.7.4.3 Results with 12 mm fan:

During a measurement session with application and rest times of 30 seconds, the coefficient of variation was 55.6% with a 12 mm fan.

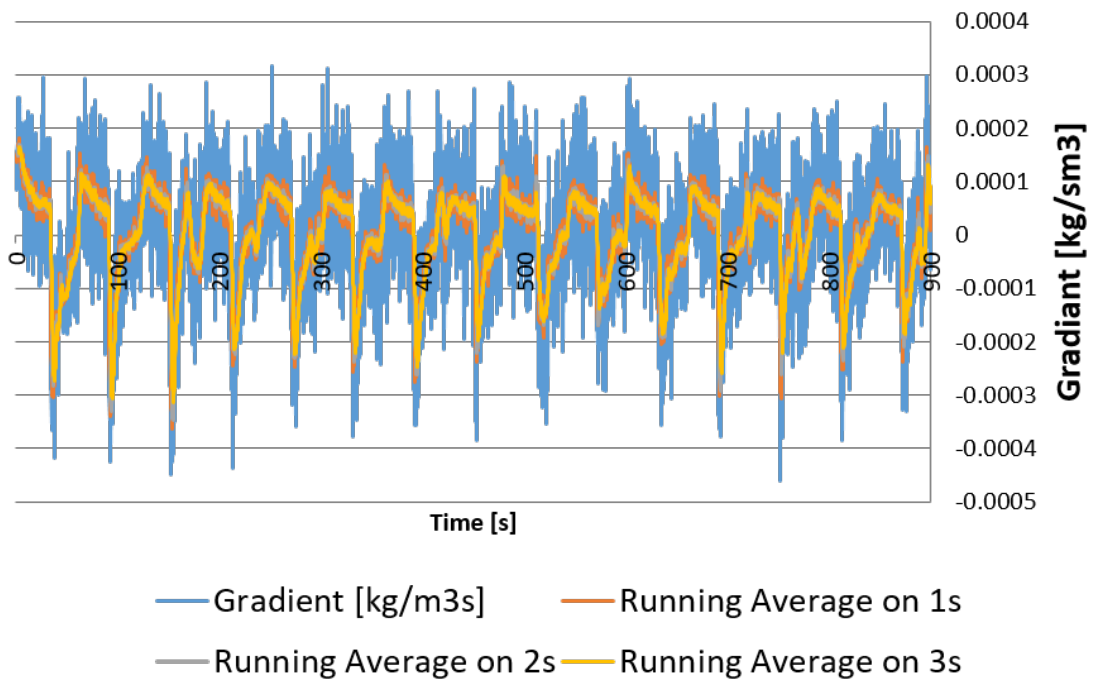
**Comparison of 9 mm and 12 mm fan:** The amplitude of the humidity curve was much greater for the 12 mm blower; therefore, the variability was less with the 9 mm blower. With the 12 mm blower, the flux was also higher. This resulted in a shorter time for the flux to become constant. The pressure in output of one, two, three 9 mm, one and two 12 mm blowers have been measured with a pressure sensor

### RH & its gradient in the chamber for 15 applications of 30s on the VF:



(a) Gradient of Humidity compared with RH

### Variation of the window of the running average for 15 applications of 30s on the VF:



(b) Gradient of Humidity and its running average

Figure 4.12: Chamber 3: The gradient was noisy and running average helps to clean the signal

but the precision of this pressure instrument wasn't good enough to measure the variations between these configurations.

**Results with two 9 mm fans:** During a session with application and rest times of 30 seconds, the error was 41.1% with 2 x 9 mm fans in parallel. For a longer application and rest time of one minute, the error was similar (38.1%).

**Results with three 9 mm fans:** During a session with application and rest times of 30 seconds, the error was slightly smaller; 33.5% with 3 x 9 mm fans in parallel. For a longer application and rest time of one minute, the error increased to 39,7 %.

**Results with two 12 mm fans:** During a session with application and rest times of 30 seconds, the error was 37.3% with 2 x 12 mm fans in parallel. For a longer application and rest time of one minute, the error increased to 43.8%.

**Conclusion on the different configurations:** There is no real benefit from increasing the number of fans in the various configurations. Lengthening the duration of application and rest time from 30 seconds to 60 seconds did not provide better results using the same method of gradient calculation. The error rate was smallest when not using a fan.

**Magnetic Levitation impact on fan speed:** With two 9 mm fans in parallel, a high frequency sound was heard. The distance required between the fans to avoid MagLev<sup>20</sup> interference with aluminium plate (grounded or not) was studied see 4.8.4.2. The fans did not stop working even with no gap in between. The speed of the fans was measured and was not affected by the distance between the fans.

**Smoothing filters:** In this thesis, three types of smoothing filters were compared for the same frame window ( $\Delta = 1$  second)(Fig. 4.13):

- Rectangular or boxcar (one sliding average);
- Triangular Window (two passes of sliding average); and
- Pseudo Gaussian (three passes of sliding average with weight).

Savitzky-Golay was modelled using the function `sgolay` from the MATLAB Signal Processing Toolbox, with order 3 and frame length of 1 second. Pseudo Gaussian provided the best results for this set of measurements (Fig. 4.14).

---

<sup>20</sup>Magnetic Levitation



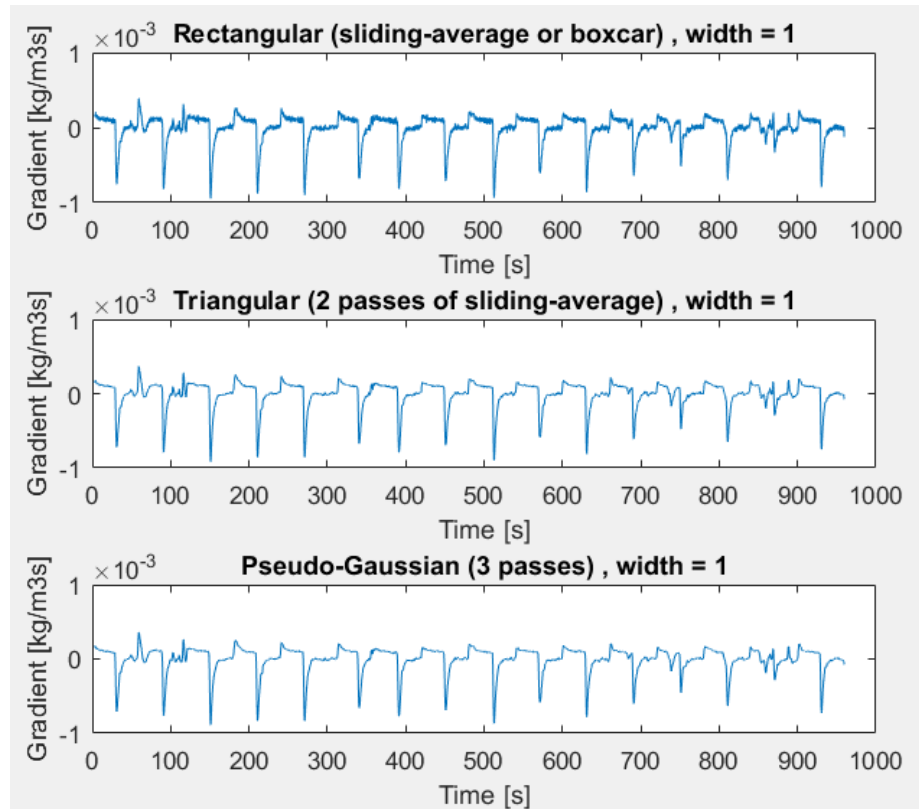


Figure 4.13: Sliding average methods applied to the gradient of humidity

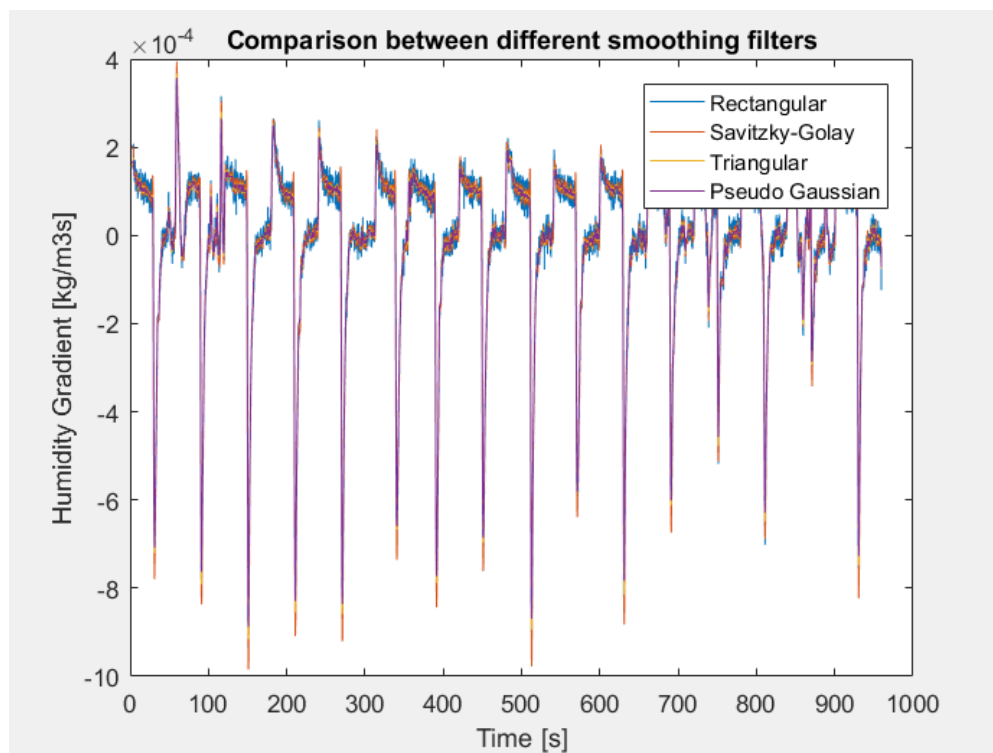


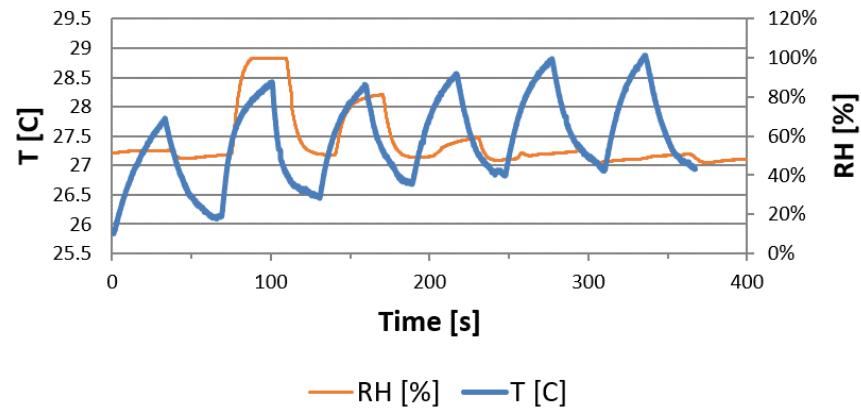
Figure 4.14: Comparison smoothing filters: rectangular, triangular, pseudo gaussian and Savitzky-Golay

**Improvements to gradient calculation method:** If the chamber was applied on the skin continuously, the gradient kept decreasing. This is because the difference of water concentration between the skin and the micro-climate decreases with time. In order to get a more stable flux measurement, the duration of the average was increased from 10 seconds to 25 seconds. By doing so, the error on the sixteen measurement sessions increased by an average of 22%. Therefore, gradient calculation is best performed on a longer duration. Another method to calculate the gradient was used on the same data set. During TEWL measurement, the gradient decreased in a way that suggests it is tending towards an asymptotic small value. This must be the TEWL at steady state. This time, the gradient was taken as the last flux value calculated before the flux became negative (or the last reading prior to the chamber being removed from the skin, whichever is sooner). This method could be called 'The limit positive flux'. In practice, the flux is usually read at regular times at the end of measurements: 30s, 90s, 150s, 210s, 270s, etc. With this method the coefficient of variation was reduced by 30% (n=5) compare to Average Smooth 10.

Another method used was as follows: The gradient can also be calculated as the difference of humidity of 2 points separated by 10 seconds. This method reduced the error by 74% from the Average Smooth 10 method, and 63% from the limit positive flux method.

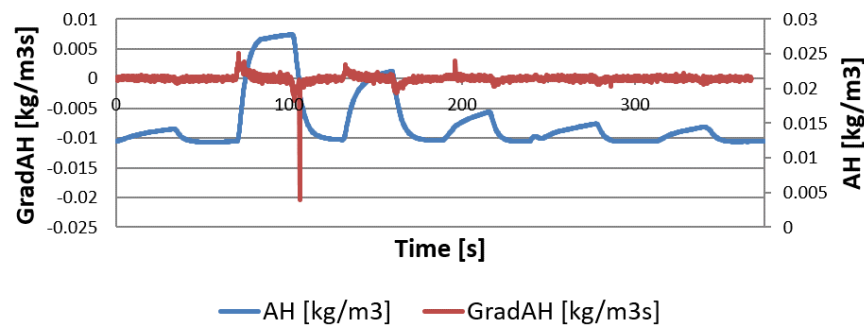
**Skin Surface Water Loss:** When observing the gradient, the first peak seen is suspected to be the SSWL. Chamber 3 equipped with two 12 mm fans running at full speed was used to measure moist skin during 6 applications of 30 seconds. The first application consist in measuring the normal measurements in terms of RH and temperature. The five next ones are the application of the chamber on moist skin, that slowly dried. Not surprisingly, the relative humidity saturated and the curve flattened at the top of the first application and slowly the size of the slope decreased on subsequent applications (Fig. 4.15a). Using the absolute humidity doesn't provide a better range as it's directly calculated from the relative humidity. The gradient was larger at the beginning of the measurement session than at the end (Fig. 4.15b). The coefficient of variation on the first three measurements after surface water application was 0.58 using the running average on 1 second.

### RH & T in Chamber #3-12mm on moist skin for 6x30s applications



(a) Temperature and RH

### AH & its gradient in Chamber #3-12mm on moist skin for 6x30s applications



(b) Humidity and gradient

Figure 4.15: Chamber 3 with a 12 mm blower measuring RH, AH, temperature and water flux on moist skin (six applications of 30 seconds on the VF)

#### 4.7.4.4 Calibration:

The measurement results were compared with the Aquaflex and a linear regression was performed on the results. Chamber 3 showed good correlation with the Aquaflex (see Fig. 4.16). The method used here is compared on Fig. 4.17 with the following alternative methods:

- Taking the limit positive flux, calculated as often as  $\Delta = 0.084s$  (orange);
- Taking a running average of one second (grey);
- Taking a large gradient over 10 seconds (yellow); and
- Taking an average of the running average over 10 seconds (blue).

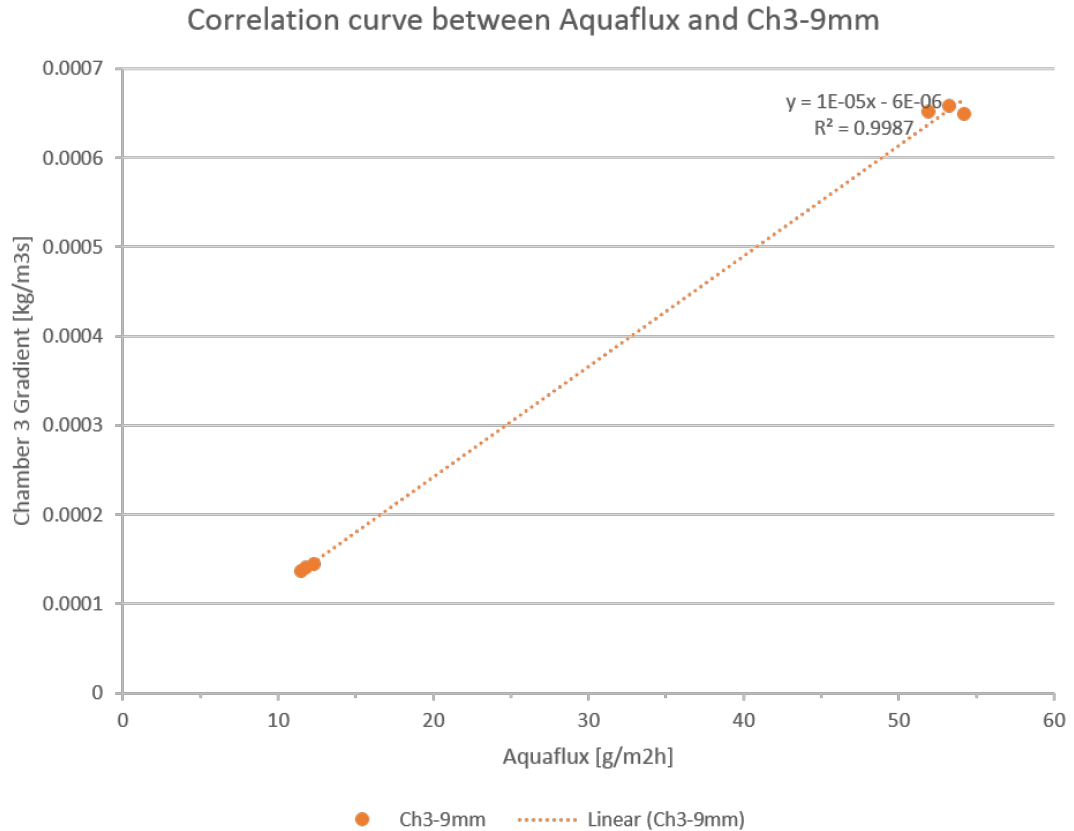


Figure 4.16: Correlation between Aquaflux and Chamber 3 using running average method: results presented here

Measuring repeatability of data of each of the instrument have assumed linear relationship between the two instruments.

As steeper slopes are better for calibration, so the method used here (Average Smooth 10) showed better sensitivity and accuracy with the Aquaflux than the other determination methods.

The curves with the shorter  $\Delta$  has high variability, especially for higher TEWL values: for 0.084 s, the points are more dispersed than for one second. Again the points are more dispersed for  $\Delta =$  one second than for 10 seconds. This is specially true for high TEWL see Fig. 4.17.

#### 4.7.4.5 Simulation:

**With and without a 9 mm fan:** A 2D model was set up for chamber 3 to compare the microclimate with a 9 mm fan on and off. A laminar flow is present in the chamber without the fan; the temperature and humidity profiles at  $t = 1, 15, 30$  seconds and at the steady state can be seen in Figs. 4.18a, 4.18b, 4.18c, 4.18d, and Figs. 4.19a, 4.19b, 4.19c, 4.19d. The temperature and humidity changes are slight and 5 digit precision was necessary to distinguish the time. According to the

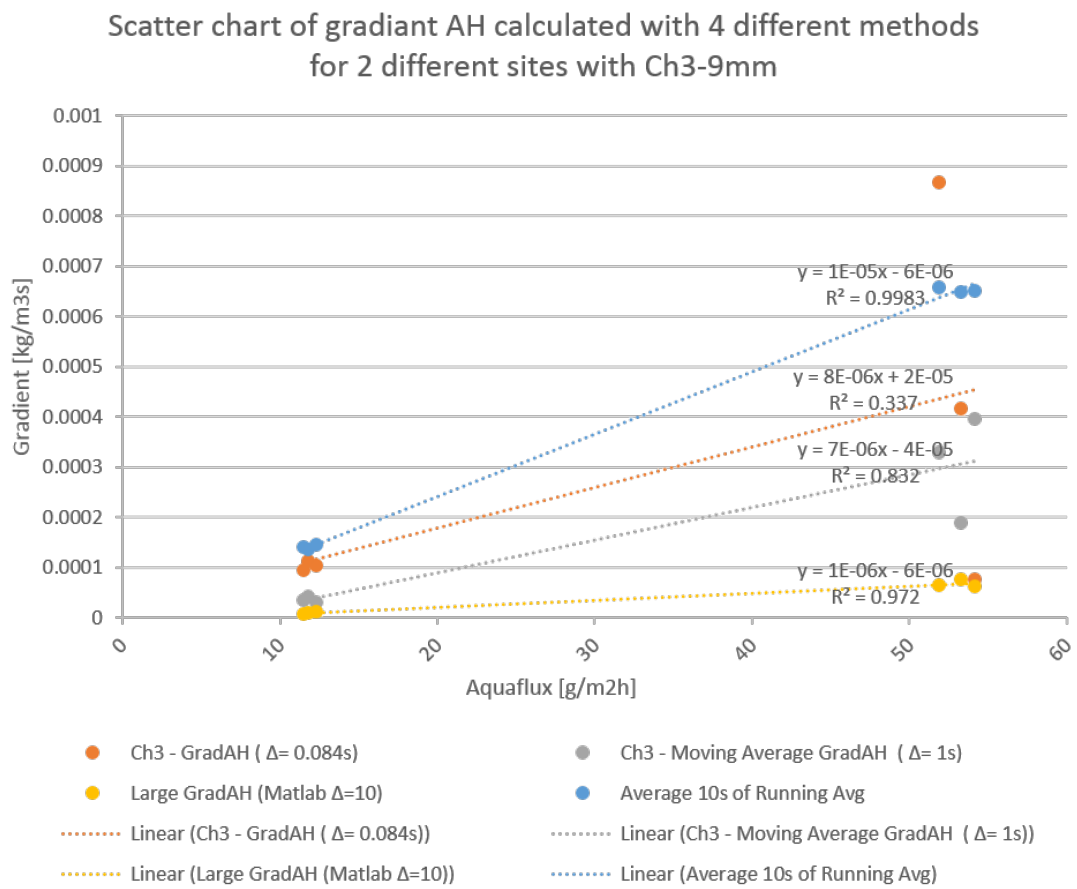


Figure 4.17: Correlation between Aquafux and Chamber 3 using different TEWL computations methods

literature, a gradient of 1 cm above the skin (Leveque 1989) exists (the boundary layer) but it doesn't appear clearly in the simulation.

With the 9 mm fan on, the temperature, humidity and velocity profiles for 4 times, ( $t = 1, 15, 30$  seconds and steady state) can be seen in Figs. 4.20a, 4.20b, 4.20c, 4.20d, and 4.21a, 4.21b, 4.21c, 4.21d, and 4.22a, 4.22b, 4.22c, 4.22d. The relative humidity distribution is interesting: the gradient is more important near the outlet of the blower because there is higher pressure and the temperature is lower than in the rest of the chamber. It is because the model in 2D describes the blower outlet at a fixed temperature always equal to the initial temperature, and therefore lower than the average temperature in the chamber. Although the relative humidity was not higher near the skin, the water vapour concentration was highest near the skin (Figs. 4.23a, 4.23b, 4.23c, 4.23d).

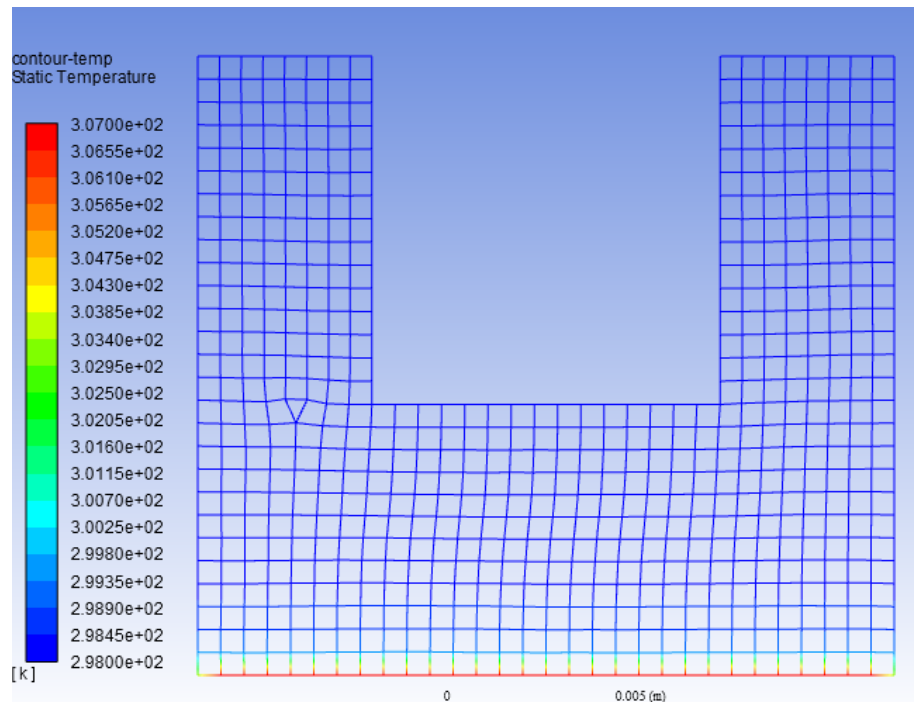
After 15 seconds, without a fan, the chamber has already reached its equilibrium for temperature (Fig. 4.18b). At 30 seconds, it had reached the equilibrium for humidity (see 4.19c). With the 9 mm fan (see Fig. 4.20d), the temperature gradient doesn't expand as much as without the fan (see Fig. 4.18d). Obviously, the temperature is higher near the heat sources: such as the skin. Interestingly, the temperature is higher in two oval regions on each side of the blower. In these two regions, the humidity is also lower (Fig. 4.21d). It's because of the inverse relationship of these two quantities: the relative humidity is lower when the temperature is higher. Noteworthy, the airflow magnitude is at its lowest in these two regions at the beginning, middle, end of the application time, as well as the steady state (see Fig. 4.22d). The most repeatable measurement configuration could be obtained by placing the sensors in these calm regions.

The water mass fraction has been plotted on Fig. 4.23 at 4 times: 1, 15, 30 seconds and steady state. They show the same figure, with the same contour, the same minimum and same maximum. Water Mass fraction is the ratio of mass between the weight of water and the sum of mass of two elements of the mixture air and  $H_2O$ .

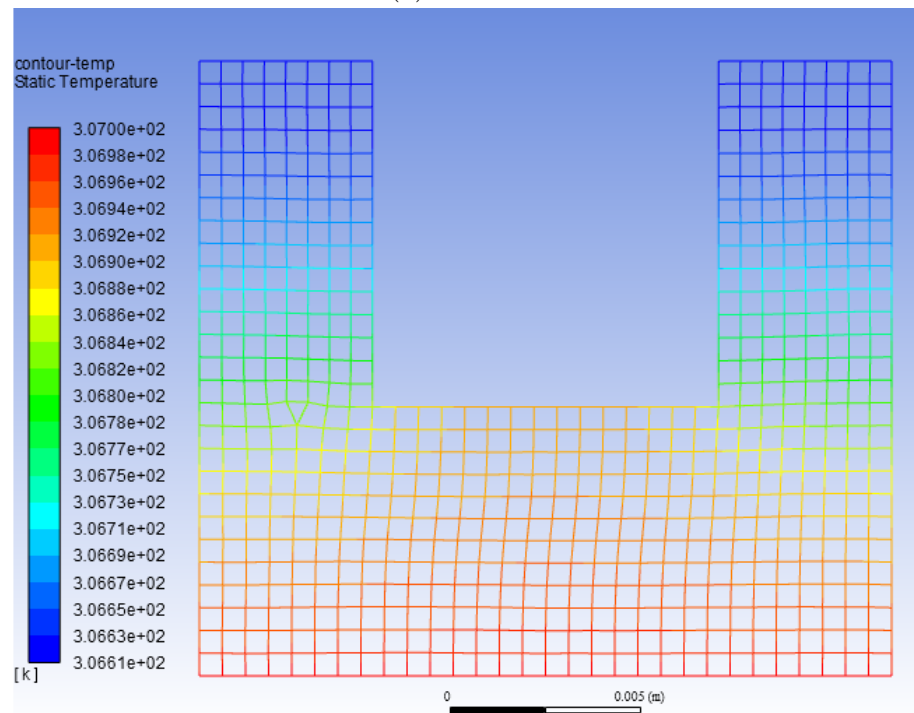
**Accounting for 9 mm fan dissipation:** The previous simulations did not account for the heat dissipation of blowers. A 9mm fan is run by a voltage of 3.3V and current of 20 mA so

$$P = U \cdot I = 6.6 \text{ mW} \quad (4.3)$$

On ANSYS it is not possible to set a velocity inlet in a Dirichlet condition. Thus, in the 2D model, the dissipation was only represented on the sides of the blower. The simulation showed that the blower produced much more heat than the human body (see Fig. 4.24).

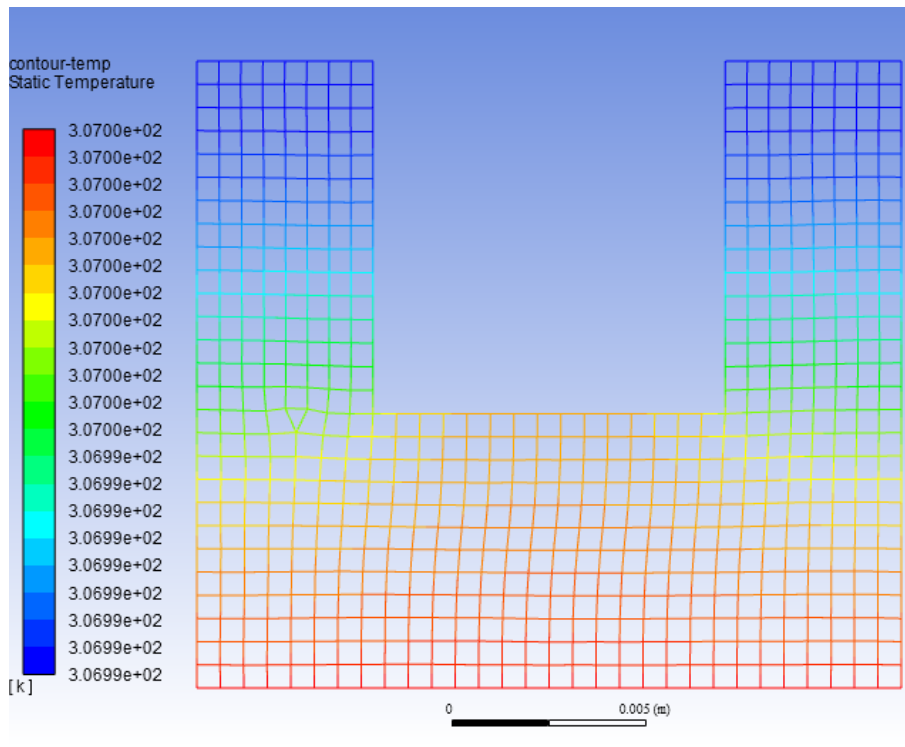


(a) 1 second

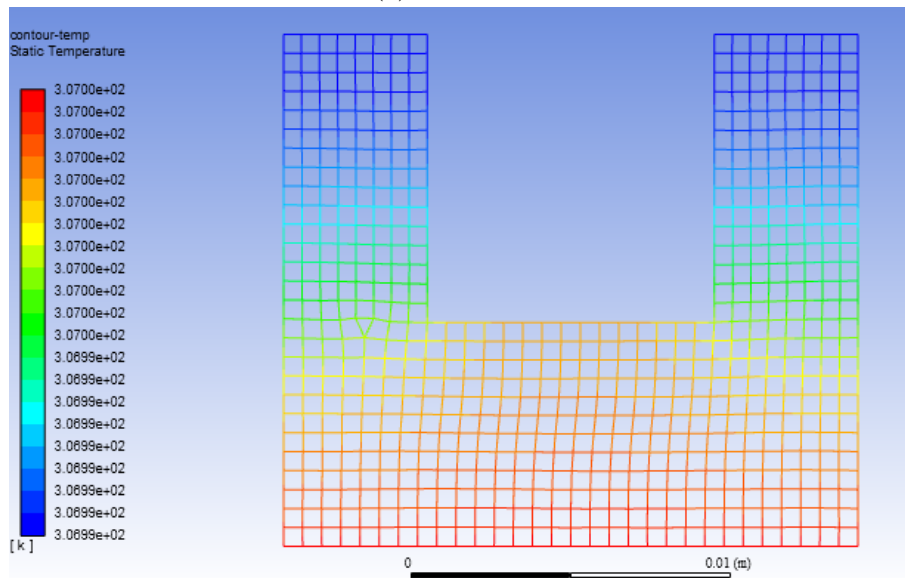


(b) 15 seconds

Figure 4.18: ANSYS simulations of temperature profile for a 2D model of Chamber 3 without the fan



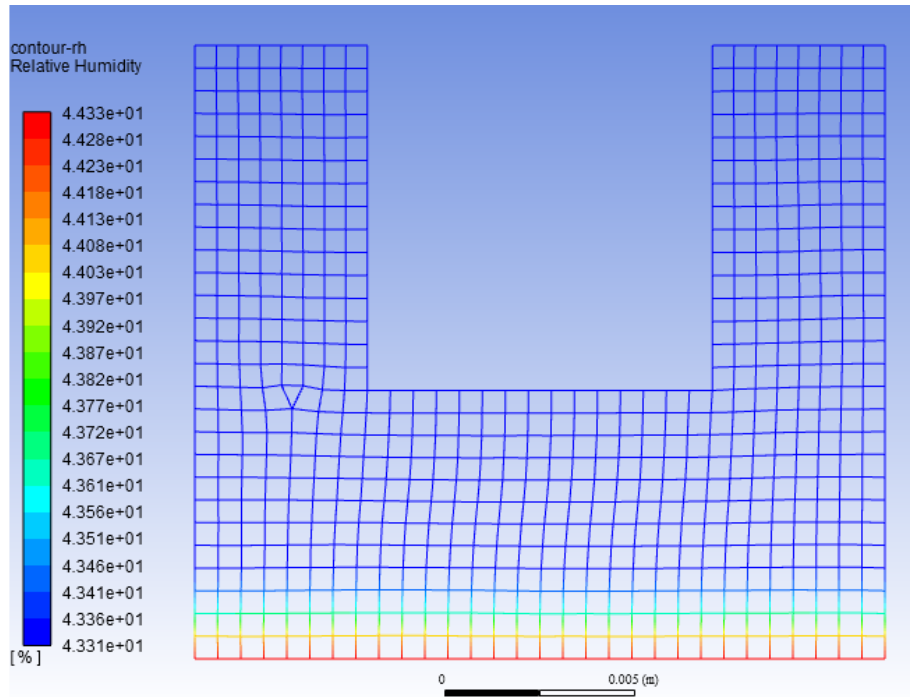
(c) 30 seconds



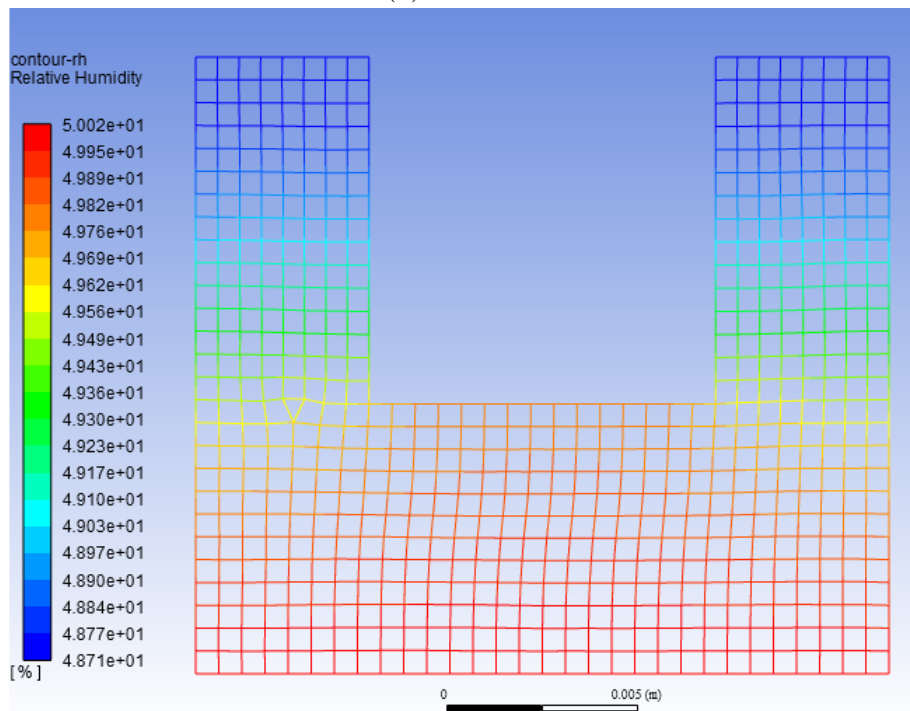
(d) Steady state

Figure 4.18: ANSYS simulations of temperature profile for a 2D model of Chamber 3 without the fan



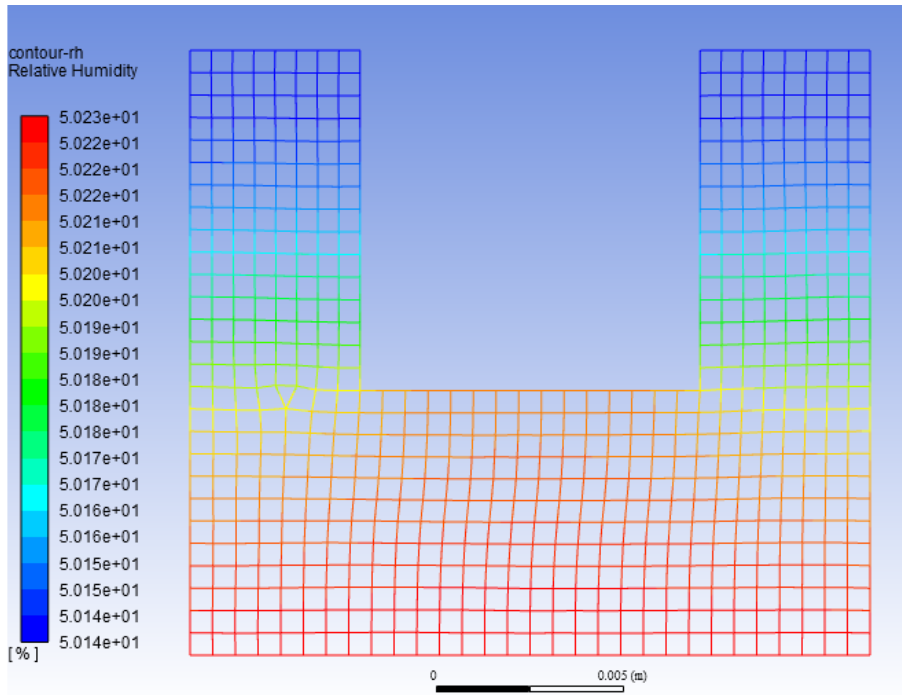


(a) 1 second

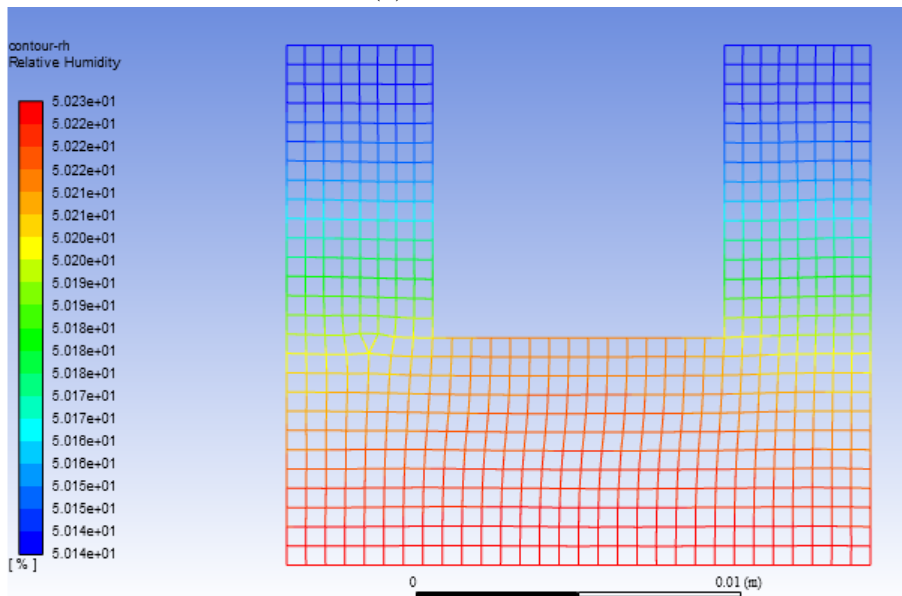


(b) 15 seconds

Figure 4.19: ANSYS simulations of humidity profile for a 2D model of Chamber 3 without the fan

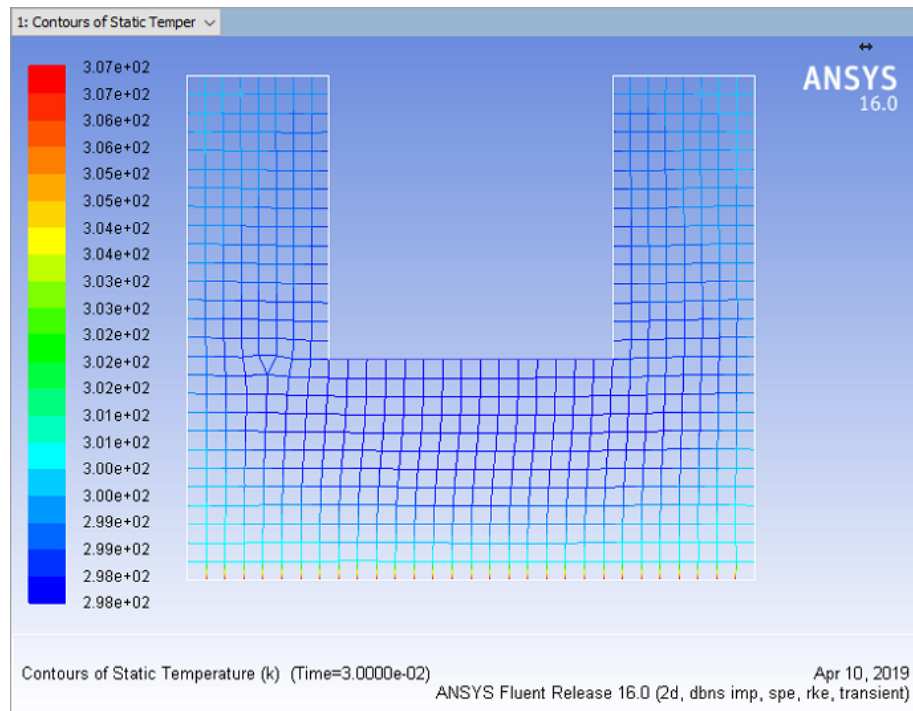


(c) 30 seconds

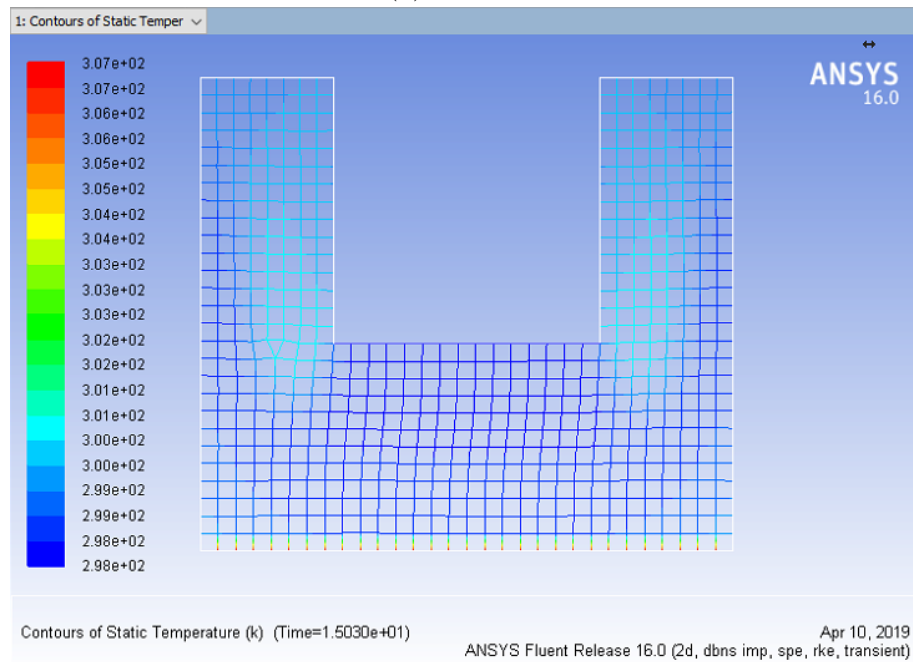


(d) Steady state

Figure 4.19: ANSYS simulations of humidity profile for a 2D model of Chamber 3 without the fan

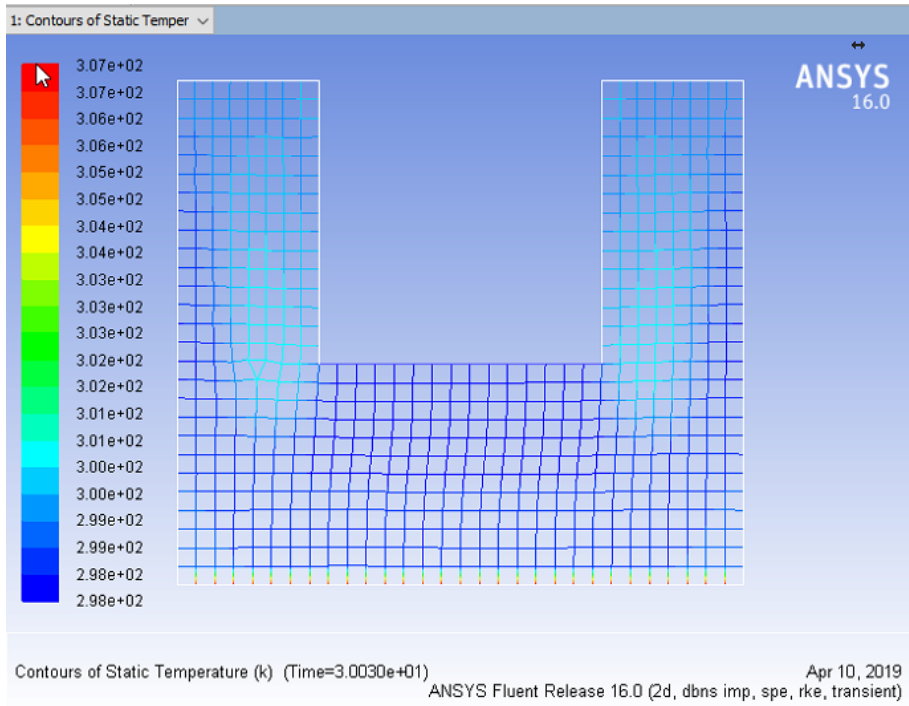


(a) 1 second

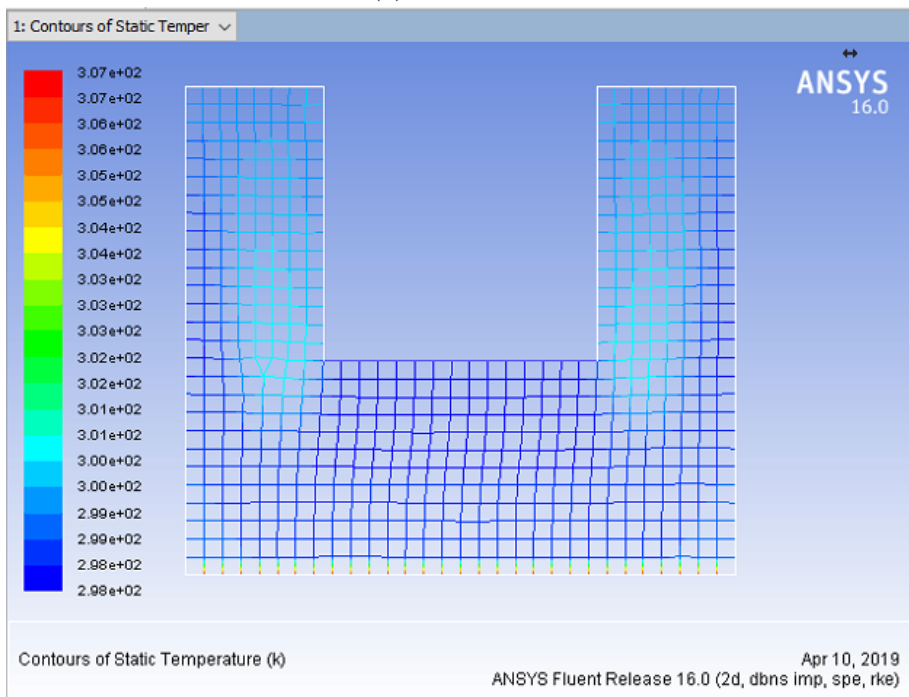


(b) 15 seconds

Figure 4.20: ANSYS simulations of temperature profile for a 2D model of Chamber 3 with 9 mm fan

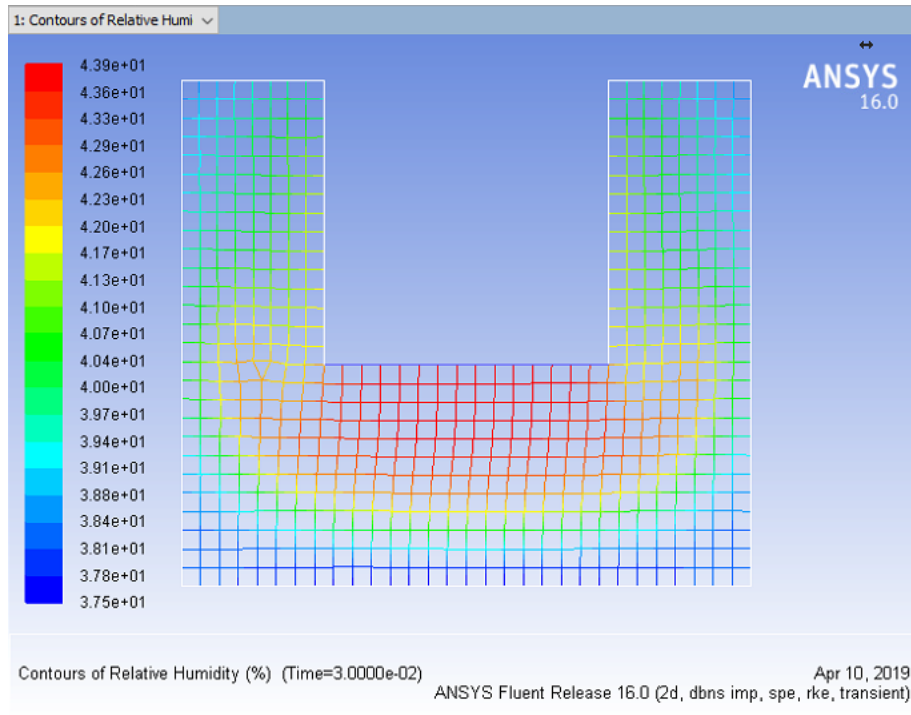


(c) 30 seconds

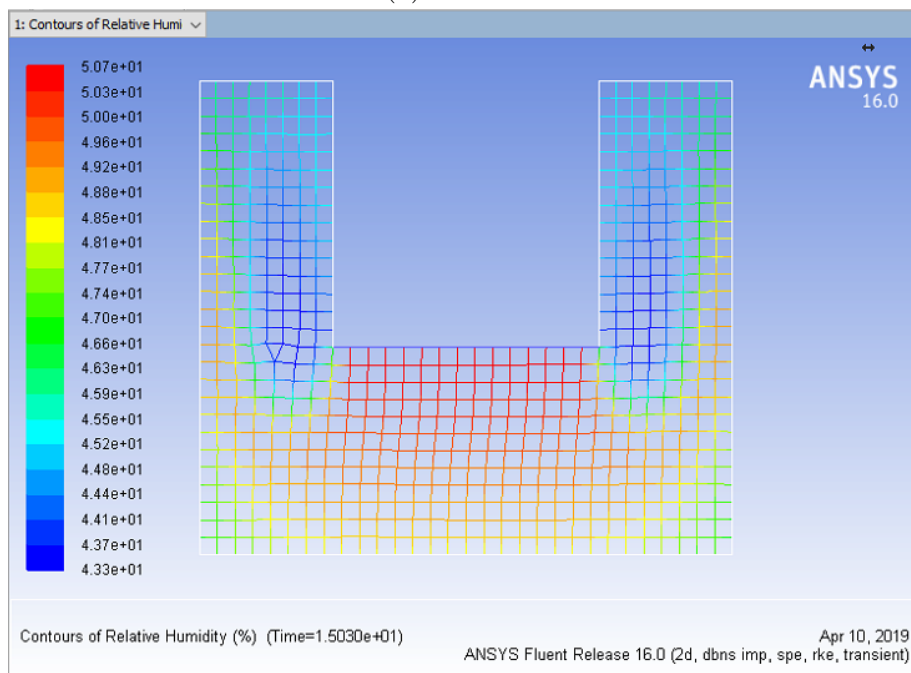


(d) Steady state

Figure 4.20: ANSYS simulations of temperature profile for a 2D model of Chamber 3 with 9 mm fan

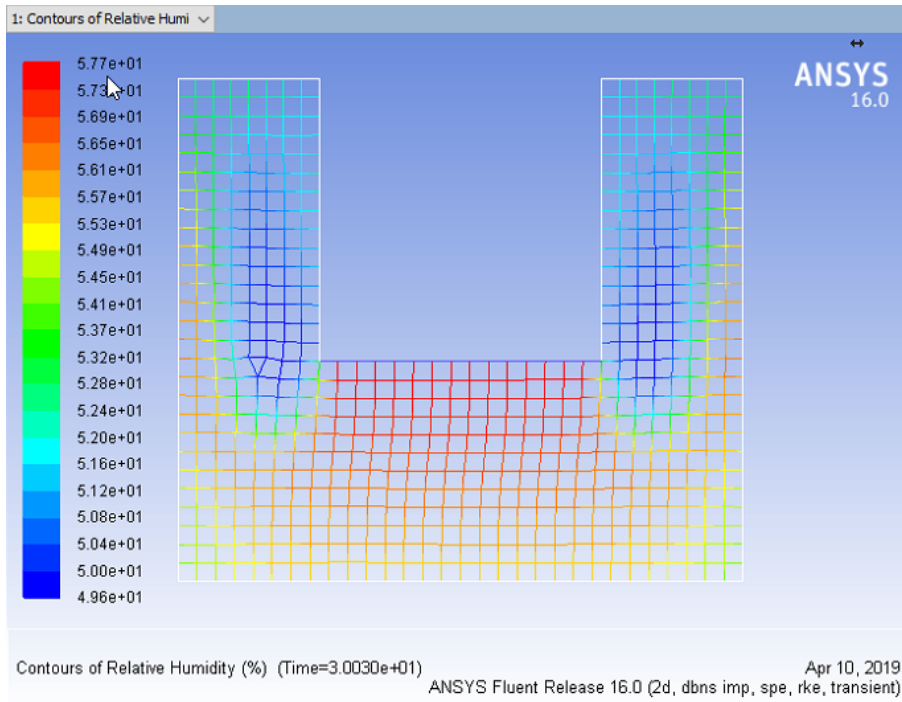


(a) 1 second

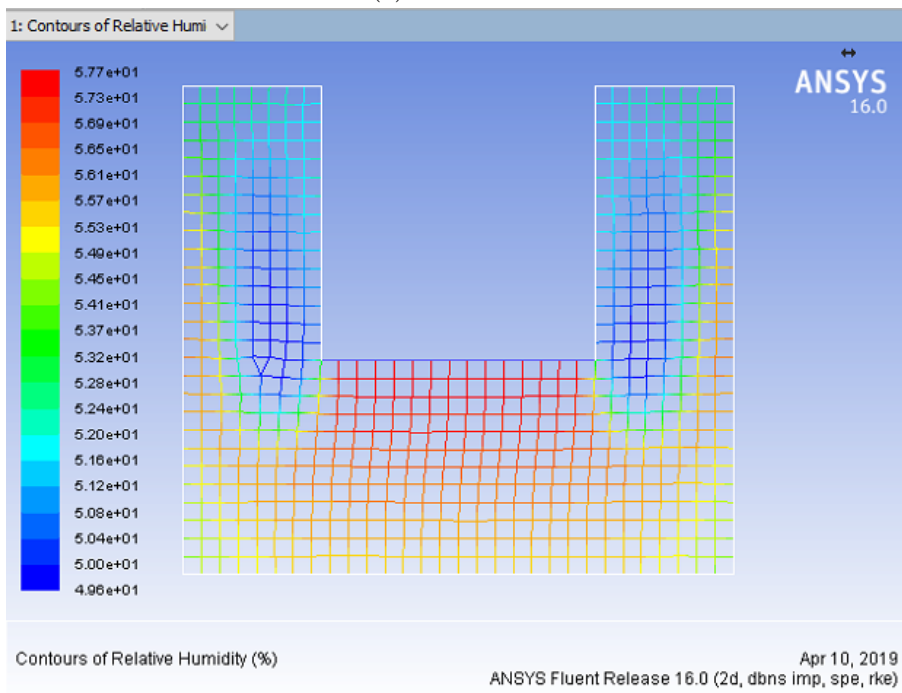


(b) 15 seconds

Figure 4.21: ANSYS simulations of humidity profile for a 2D model of Chamber 3 with 9 mm fan

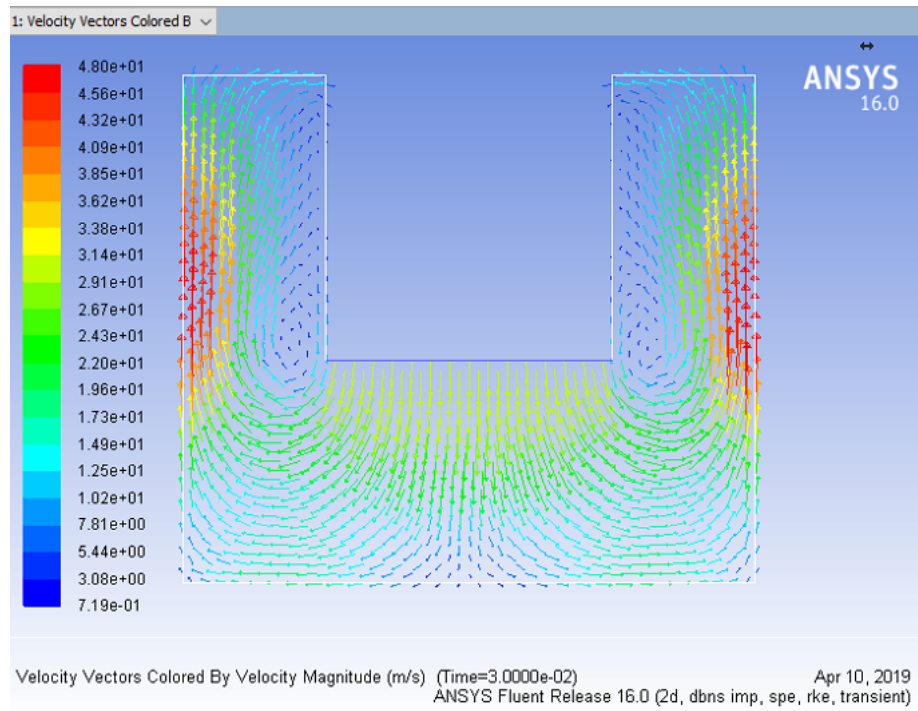


(c) 30 seconds

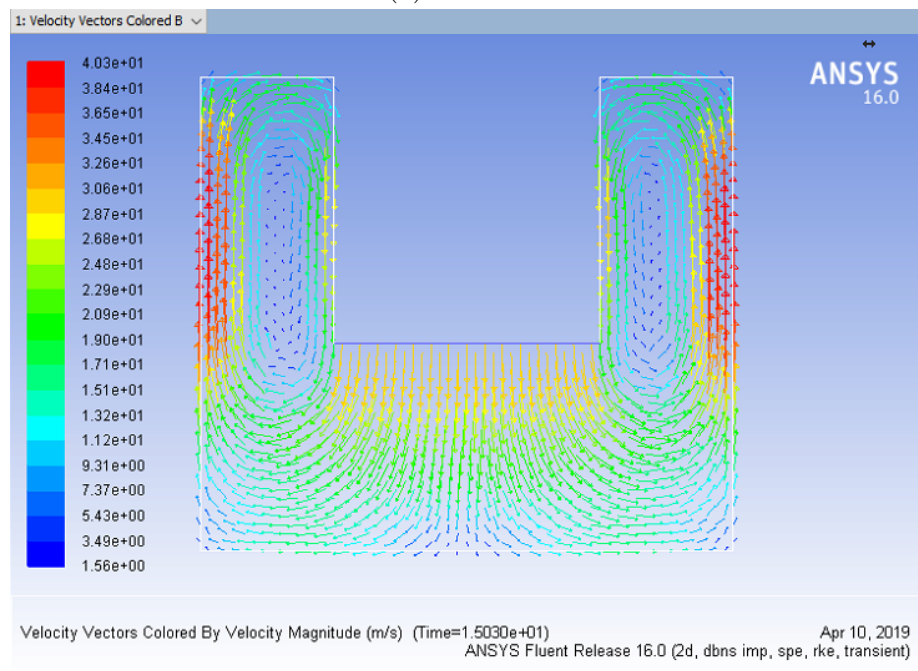


(d) Steady state

Figure 4.21: ANSYS simulations of humidity profile for a 2D model of Chamber 3 with 9 mm fan



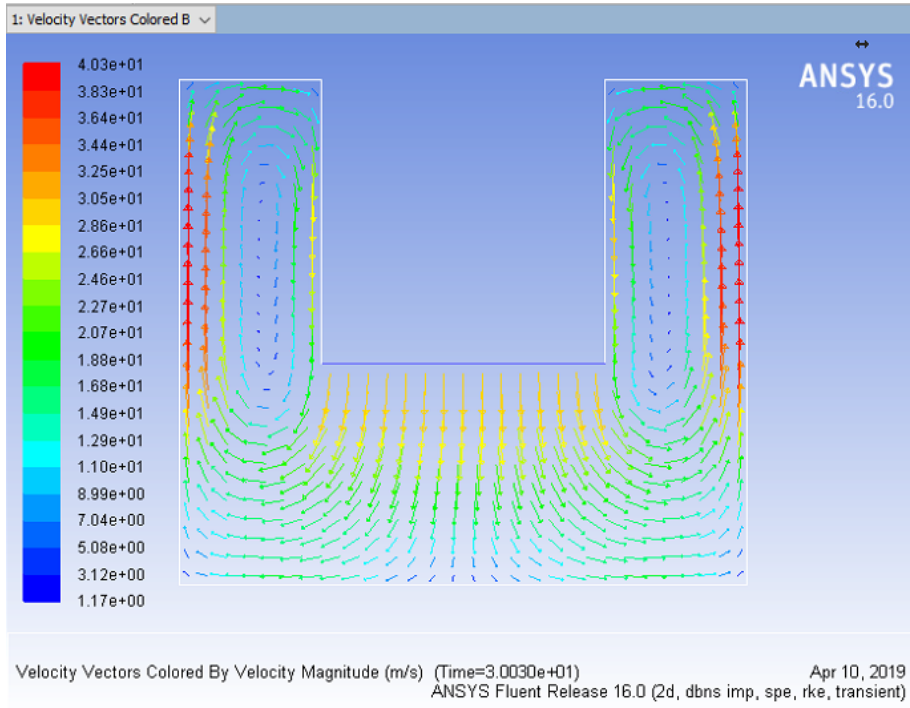
(a) 1 second



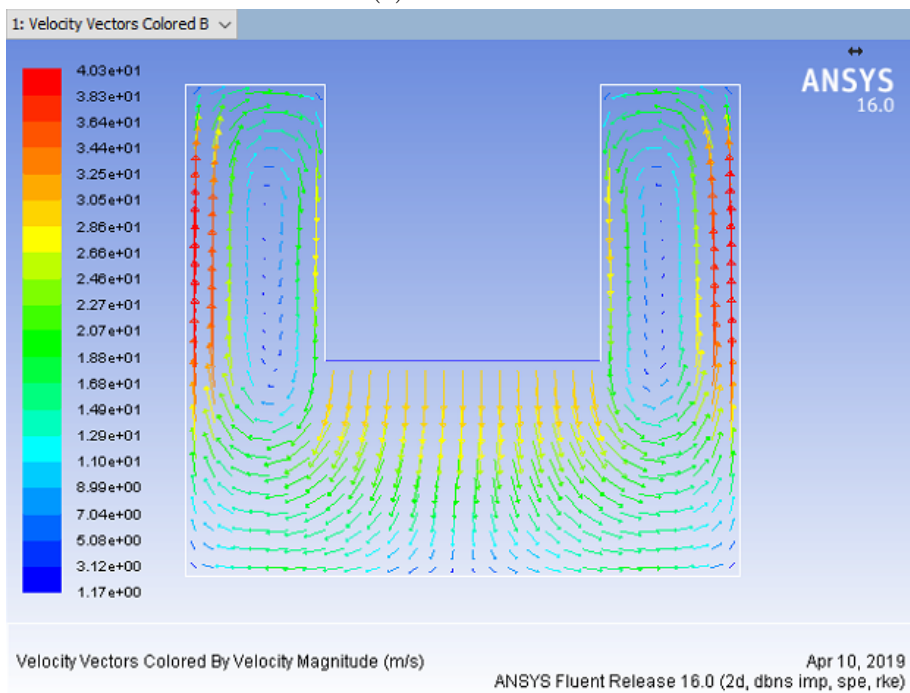
(b) 15 seconds

Figure 4.22: ANSYS Simulations of Velocity Vectors for a 2D model of Chamber 3 with 9 mm fan





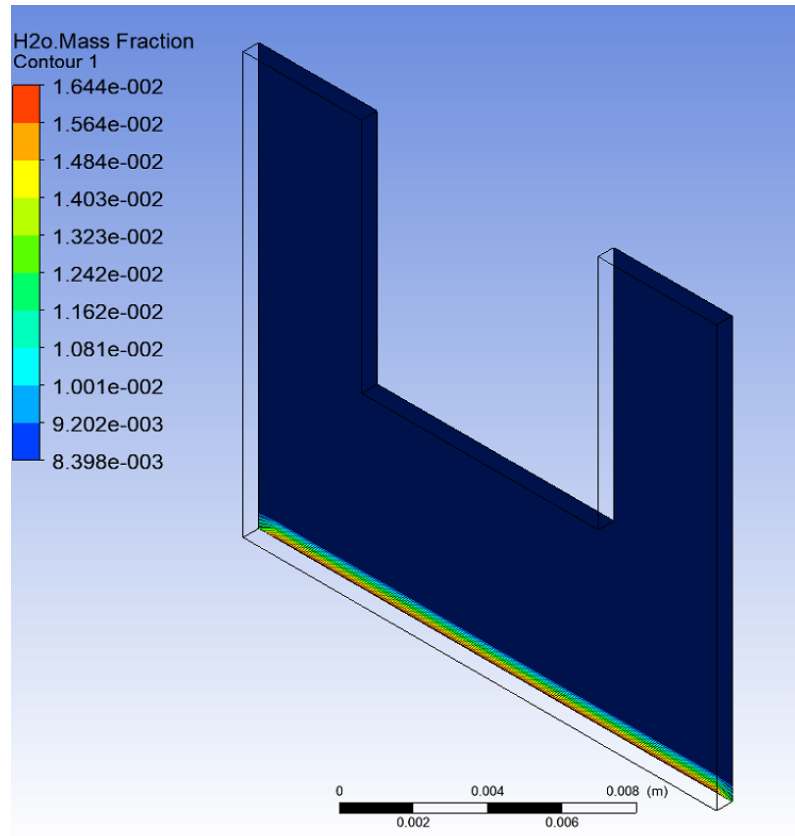
(c) 30 seconds



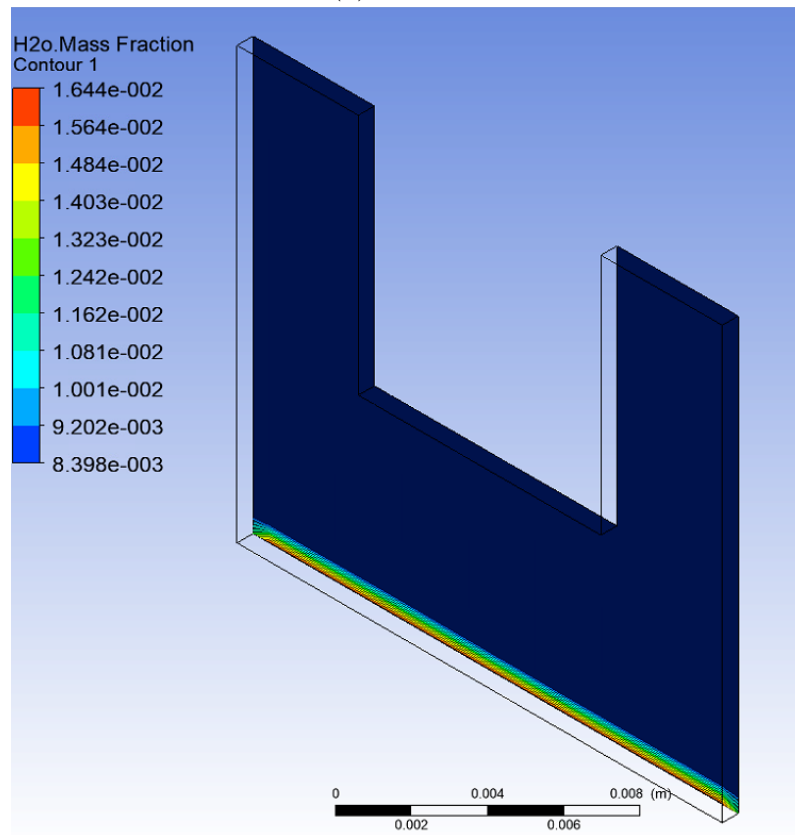
(d) Steady state

Figure 4.22: ANSYS Simulations of Velocity Vectors for a 2D model of Chamber 3 with 9 mm fan



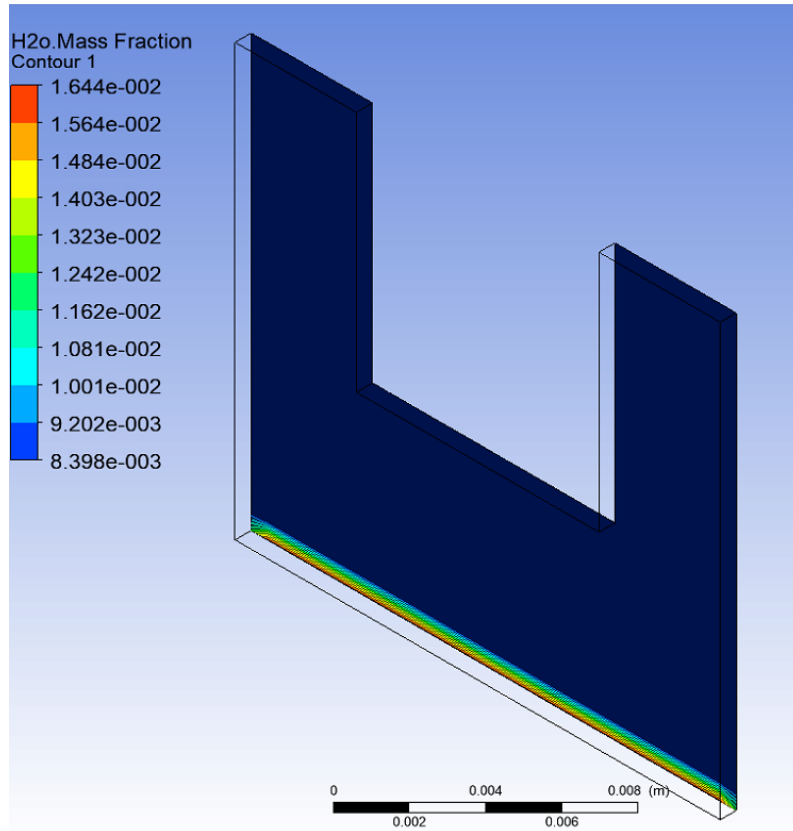


(a) 1 second

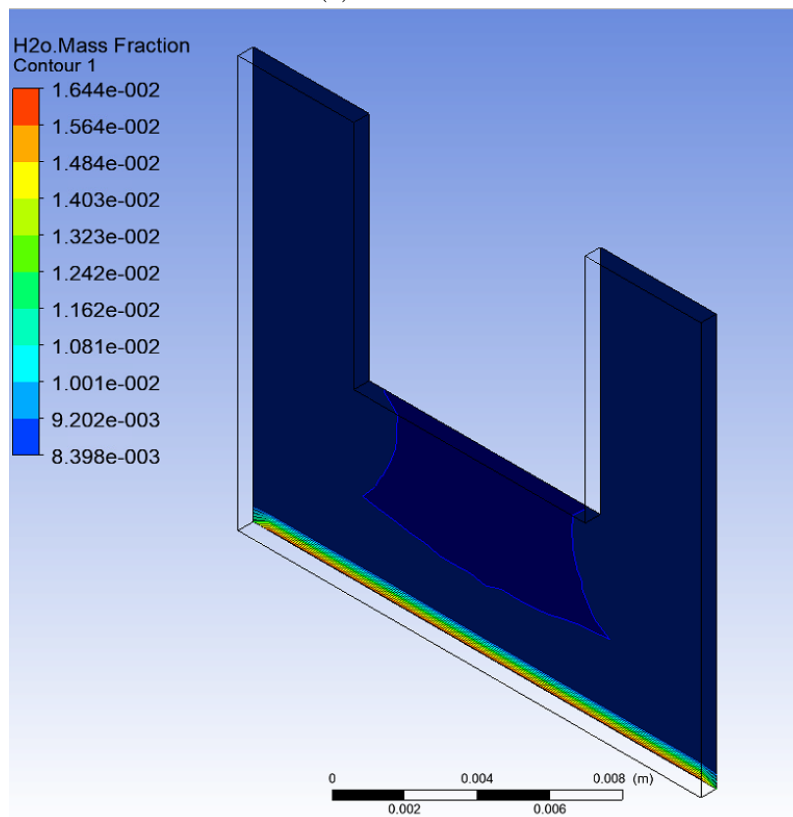


(b) 15 seconds

Figure 4.23: ANSYS simulations of water vapour concentration for a 2D model of Chamber 3 with 9 mm fan



(c) 30 seconds



(d) Steady state

Figure 4.23: ANSYS simulations of water vapour concentration for a 2D model of Chamber 3 with 9mm fan

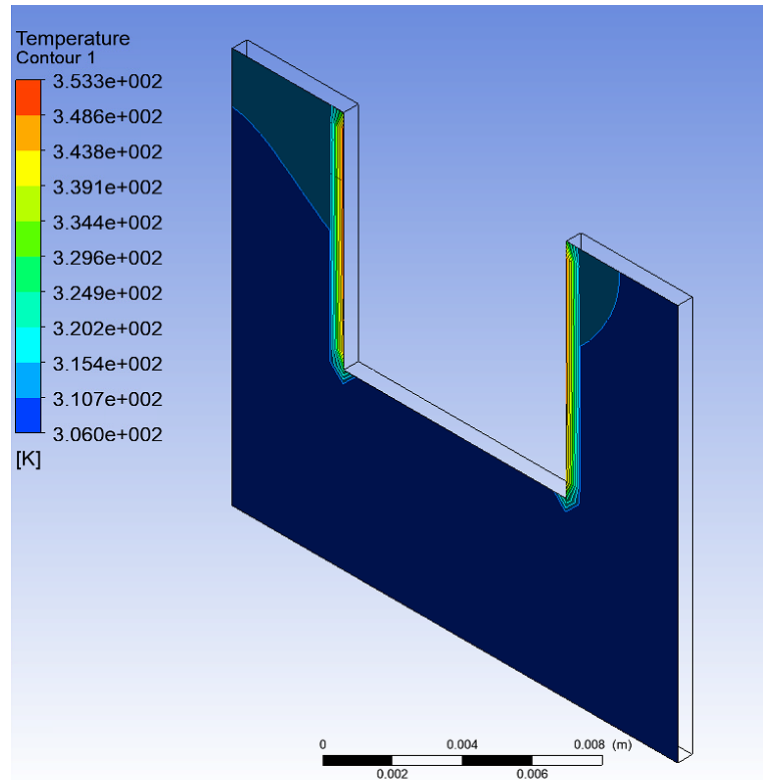


Figure 4.24: Heat profile of the dissipation

#### 4.7.5 Discussion

The aim of the project is to build an instrument with repeatable results in priority and able to work outside of a controlled environment. Ideally, the instrument would have sensitive and accurate results. For these metrics, the development prototype had been compared with the Aquaflex. An objective is to study the effect of the fan on the measurements. Increasing the number of fans from one to three 9 mm blower improved the variation coefficient and thus the repeatability. Same observation for the 12 mm blower: repeatability was better with two blowers rather than only one blower.

Regarding the duration of application, increasing the rest time from 30 s to one minute didn't improve considerably the repeatability, only a few percent for the two 9 mm blower case, and it wasn't observed for all cases (three 9 mm blowers and two 12 mm blowers).

Finally, the coefficient of variation was lower when not using a fan. It is possible to improve the repeatability by improving the gradient algorithm and signal processing. Regarding the gradient calculation method, there is a higher error with the method Average Smooth 10 and limit positive flux compared to a simple difference of  $\Delta$  between the two points. It's because the flux vary a lot between two time points. Even passing a few average windows on the signal do not improve the results as much as taking a simple difference for gradient.

For the same reason, the signal is more variable, the points are more dispersed for small  $\Delta$  4.12. Shortest delta gradient produce errors because the gradient vary quickly from positive to negative values. The  $\Delta$  value had needed to be parametrised to be studied more in detail in future sections. Regarding signal processing, pseudo-gaussian filtering permitted to reduce the variations of the signal as seen on Fig. 4.14. Savitzky-Golay provides a nice shape too, but the peaks have more important amplitudes, and it's something to avoid if there are calculations to do after.

Simulations have shown two regions on each side of the blower where the mixing is calmer. This is where the sensor was positioned, to the extent possible to fix it in the interior of the chamber. Because it is a 2D simplification of 3D model, where the walls of the blower are supposed to be infinite in the direction of the reader eye (depth), it may work better for two blowers back to back as their combined depth is larger than the depth of one blower.

One point worth mentioning is the heat from the blowers that was not accounted in the simulations. The simulations are inexact for a few reasons. First there are in 2D when the phenomena is in 3D. Moreover, the simulation doesn't allow the velocity outlet to be a heat source as well. It would have been possible in 3D because a flow would have been modelled rather than a black box model with inputs and outputs.

The aim of the project is to develop an instrument that work outside of a controlled environment. In other terms, it must be able to deal with the sweat and surface water. Some testing of the chamber 3 have been performed with a 12 mm blower (Fig. 4.15b). After five applications of the chamber with the 12 mm blower running at full speed, the curve of humidity was back at the initial level. There was saturation during the first application. One thing had to be improved for the next experiments: the quantity of water applied had to be smaller to not saturate the chamber. Another thing would be to increase the airflow, so it dries out quicker the skin. However, if there is still too much surface water, the micro-climate would still saturate. Finally measurements could be improved using a different calculation method.

#### 4.7.6 Conclusion

Chamber 3 permitted the testing of various calculation methods. The choice of gradient determination methods has a profound effect on the results, which will have an effect on repeatability and sensitivity.

For this chamber, three algorithms have been tested. And the best method was to take a difference between two time points, with a  $\Delta$  large like ten seconds. However, not all  $\Delta$  values have been tested. It is something to be explored in future prototypes. In addition, using filtering is an option to improve repeatability For this

chamber, pseudo Gaussian and Savitzky-Golay provided good results. Like gradient calculation methods, these results are specific to this chamber.

A few fans configurations have been tested: one, two, three 9 mm and one, two 12mm. It is difficult to draw any conclusions for the best configuration. A more detailed study needed to be performed, with a next prototype.

At this time of development, the least to be concluded about the effect of the fan is, without surprise, the turbulent flow decrease repeatability. Smaller coefficient of variation (or error rate) was found for measurements without the fan, compared to measurements with the fan.

Moreover, the simulations permitted to guide the placement of the sensor in the chamber. There are two regions that have calmer airflow: these are the ideal location for a repeatable results.

Besides, the measurement of TEWL was tested for the first time. A deeper analysis needed to be thought through to create a better experiment, data acquisition and analysis.

Overall it is good prototype (compare to chamber 2), worth mentioning in this thesis. However there is a helical ridge that could have an effect on the measurements. The future prototype interior would have to be smooth. In addition, it is just a chamber and not a full instrument. Therefore, it was needed to design another prototype, more complete: chamber 5 and here 5.1 are presented later in the thesis.

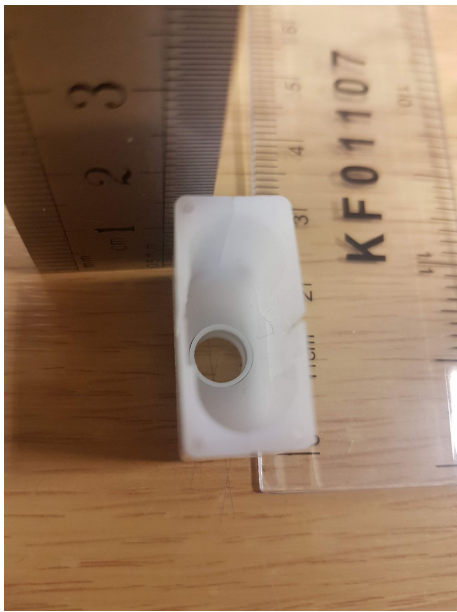
## 4.8 Prototype 4

### 4.8.1 Description

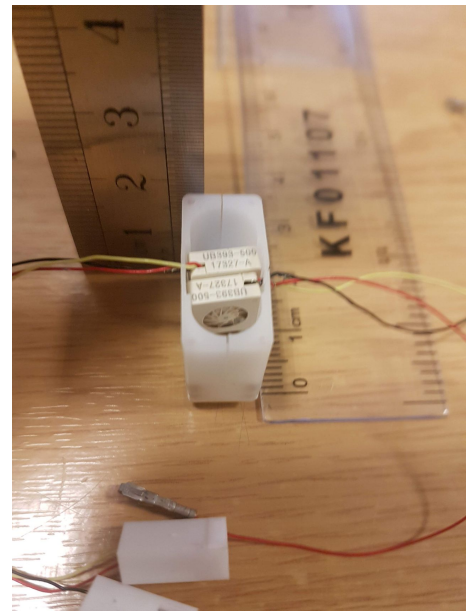
In parallel, Biox had developed chambers to test. These are Chamber 4 and 9. Biox's first prototype is a cylinder whose cross section is an ellipse longer than it is wide (Fig. 4.25). Its dimensions are for the ellipse long radius 18 mm, small radius 9 mm and the height of chamber is 18 mm. It has three sensors at different positions along the PCB, at the back of the chamber(see Fig. 4.26). The detail of the PCB can be seen on Fig. 4.27. It has two back-to-back 9 mm blowers.

### 4.8.2 Rationale

Chamber 4 aimed to test the smallest blowers possible. The smaller the component is, the easier it is to accommodate the design. Thus it gives more freedom for future design. Finally two blowers back to back have been included to test if only one suffice to provide enough mixing or if more airflow are necessary, thus the two blowers needed to be activated. Regarding the sensor positions, there are all located at the top of the chamber, because of there are surface mounted on a PCB. A total



(a) Inside chamber 4



(b) Chamber 4 with blowers

Figure 4.25: Chamber 4

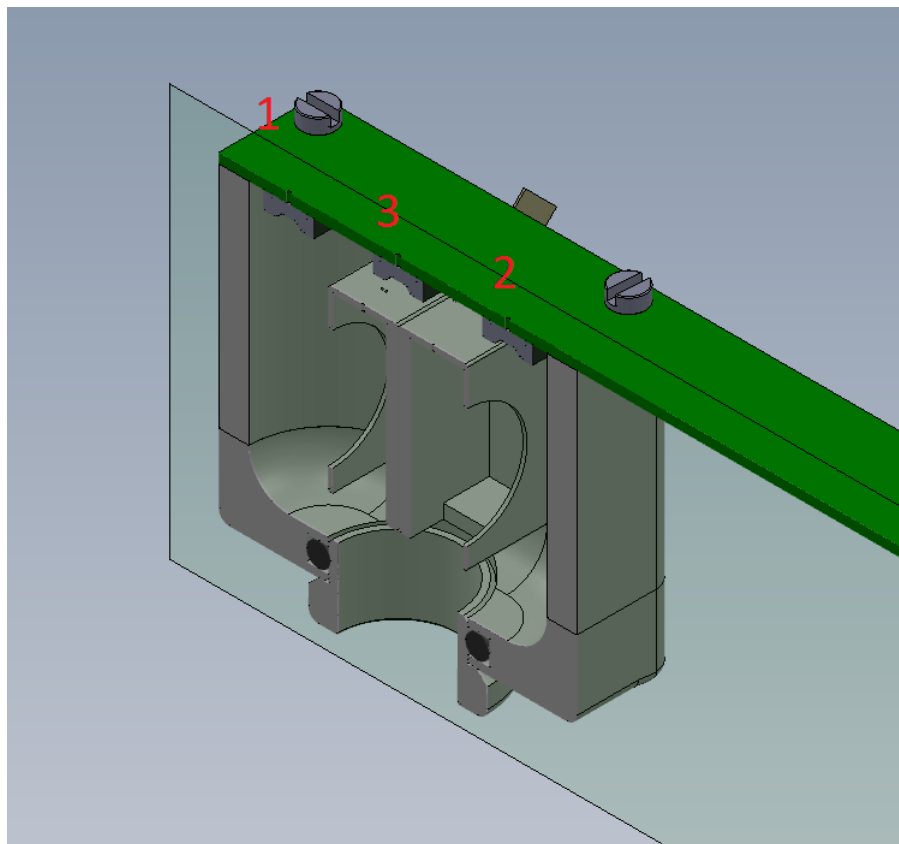


Figure 4.26: Chamber 4 cross section and identification of sensors

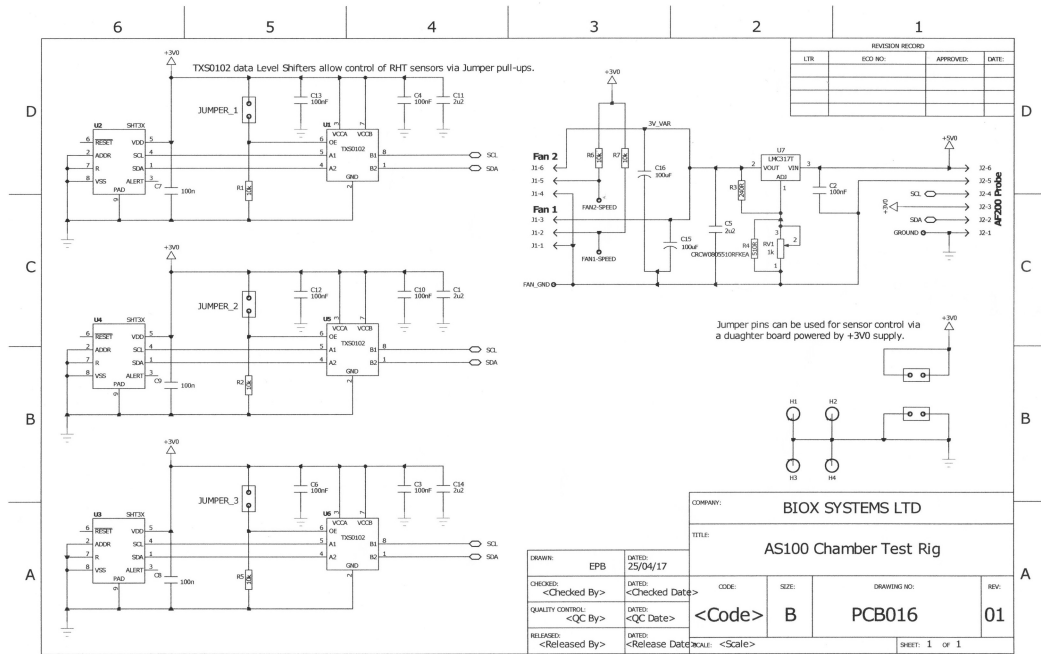


Figure 4.27: Probe 4 PCB

of three positions allows the comparison of readings between these locations, in order to check the turbulent mixing in these areas. The sensors are located behind the blowers on top of the chamber, where the air may be stagnant, and readings would yield repeatable TEWL measurements.

### 4.8.3 Testing

The general methodology can be found in section 4.2. With chamber 1 an operating protocol has been established: the measurements are performed by application of 30 seconds or longer and rest of 30 seconds. The location sites are the palm and volar forearm on one participant. All measurements are done in controlled environment and at least in triplicate. Measurements are done first on the prototype, then with the Aquaflex in order to have a reference for calibration.

With chamber 3, an application of 30 second and 60 seconds have been tested, and a longer application didn't provide better results. With chamber 3, the use of the fan and different fan configuration were tested as well. In addition, four gradient calculation algorithms were tested: the limit positive flux, a running average, a large gradient with  $\Delta$  a triangular gradient. However chamber 3 and 4 testing overlapped in time, so experiments conducted with one chamber could have been conducted with the other as well. This is the case for example for the application duration, as it is arbitrary. However, the majority of tests have been largely different. For this chamber 4, measurements have been done for different fan speeds: low, medium

and high speed. In addition, this chamber aims to try different sensor positions in the roof of the chamber. The testing will define the best speed and sensor position for this chamber design.

#### 4.8.4 Results

Chamber 4 is a really small chamber to get quicker results: the smaller is the chamber, the quicker an increase of water vapour concentration would be detected. Chamber 4 use therefore the smaller fans, that also provide a maximum design freedom for future designs. There is also 3 sensors on the PCB at the top of the chamber to compare the readings of each position. Comparing these three regions could help to evaluated where the mixing is not effective, in order to evaluate the turbulence effects from the fans.

##### 4.8.4.1 Gradient calculation method:

With this prototype, the method used was the limit positive flux. In practice the flux was read at regular time intervals (30s, 90s, 150s, 210s, 270s) during the measurement session at the end of each measurement (alternating between 30s application and 30s rest).

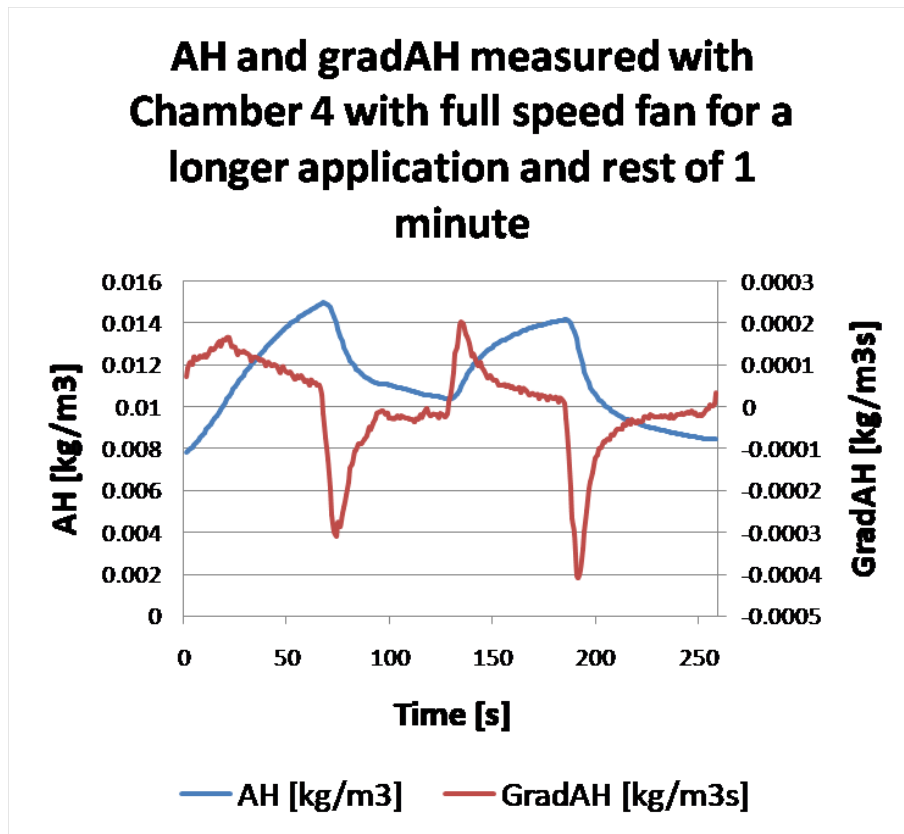
##### 4.8.4.2 Results:

**With and without the fan:** In order to compare the performances with and without the fan, the prototype was used following the standard methods found in methodology section: measurement on the volar forearm, in triplicate or more, with and without the fan. Between each measurement with the prototype, the same site was measurement with the Aquaflux, to have the reference to compare and calibrate with. The measurements with and without the fan were done during the same session lasting three hours. With the fan, the average error on the measurements was 60%. Without the fan it was 23%. For the same gradient calculation method, the fan had higher errors. Without the internal fan, the measurements were more repeatable. Furthermore, the gradient varied much less. However, a flat gradient was not observed. For the next section, the duration of the application on the skin was increased.

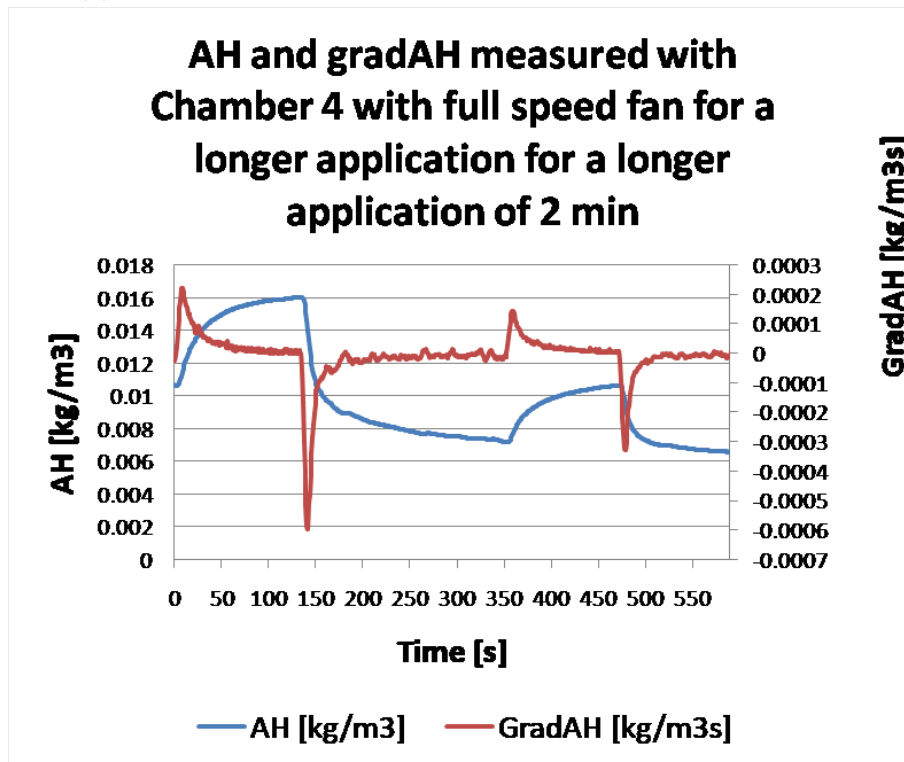
**With a longer application time:** A longer application of one minute increased the error to 80%. An application of two minutes increased the error to 134%. Doing an average on the last 10 seconds did not improve the error rate. Therefore, a longer application time does not improve the measurement errors. Despite providing flatter gradients (see Fig. 4.28), measurement times of 60 or 120 seconds are quite long.



In addition, long duration measurements with Chamber 4 are uncomfortable after 45 seconds because the blower produces a lot of heat.



(a) Application and rest of one minute instead of 30 seconds



(b) Application and rest of two minutes

Figure 4.28: Measurements of a long duration with Chamber 4

### Gradient measured with Chamber 4 at maximum speed with 3 sensors for 17 applications of 30s on the VF

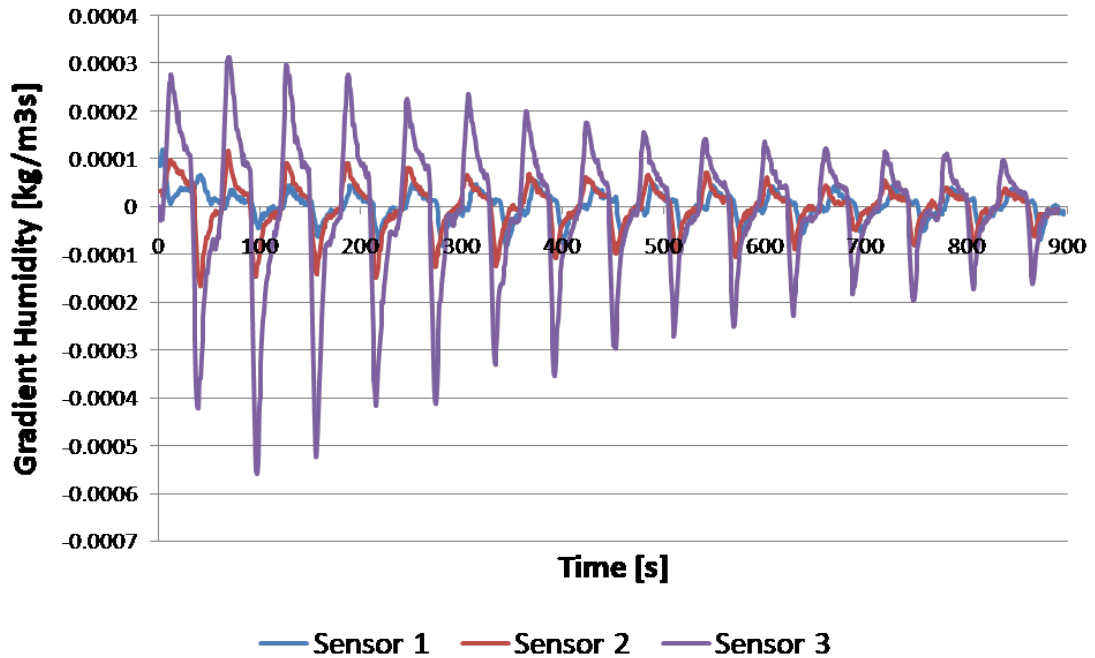


Figure 4.29: Comparison of gradient measured with 3 positions of sensor

**With different sensors:** Using the limit positive flux method, the rank of the less repeatable sensors were sensor 1 (81% error), sensor 3 (66% error) and then sensor 2 (61% error). The position of the sensor can be found on Fig. 4.26. The gradient provided by the sensors is compared on Fig. 4.29. For these measurements, sensor 1 and sensor 2 had very similar amplitudes, but sensor 3 had much bigger amplitudes.

**Effect of different fan speeds:** The error rate increased with increasing fan speed (Fig. 4.30).

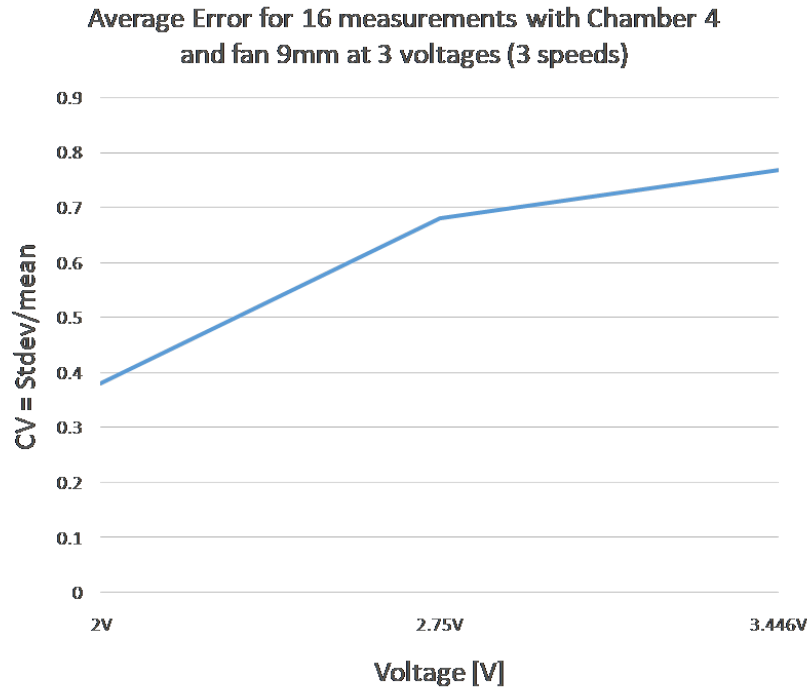


Figure 4.30: Evolution of error rate with the voltage (and therefore the fan speed) in chamber 4 with a 9mm blower

Two further studies have been conducted that were not planned in the methodology and testing planning. The first was the MagLev interference between two blowers. The second was the heat effect of the blowers.

**MagLev interference between blowers:** There was an uncomfortable grinding sound when start using this design. The blowers back to back were interfering with each other. It wasn't observed with chamber 3 where there was a slight space (1 mm). In order to measure interference between blowers, a aluminium plate was placed between two 9 mm blowers. Different plates were tested: 0.5 mm, 0.7 mm, 0.9 mm, 1mm and 2mm. They were also tested grounded or not (noted "GND" in Fig. 4.31). In addition a final test left a space of 10 mm between the two blowers, the blowers were "free" (noted "10+" in Fig. 4.31). Four measurements of speed for two blowers were taken. So this is a total of eight speed measurements.

The variation of speed was quite low with the various configuration (see Fig. 4.31). Obviously the higher speed was found when the blowers were free from each other, with 10 mm space in between. Grounding the plate didn't necessarily improved the error. The standard variation is pretty low, the points are not too dispersed and still within 30% of speed error from the manufacturer.

**Heat effect of the blowers:** To measure the effect of the blowers on the chamber, the microclimate was observed not in contact with skin but with the chamber sealed

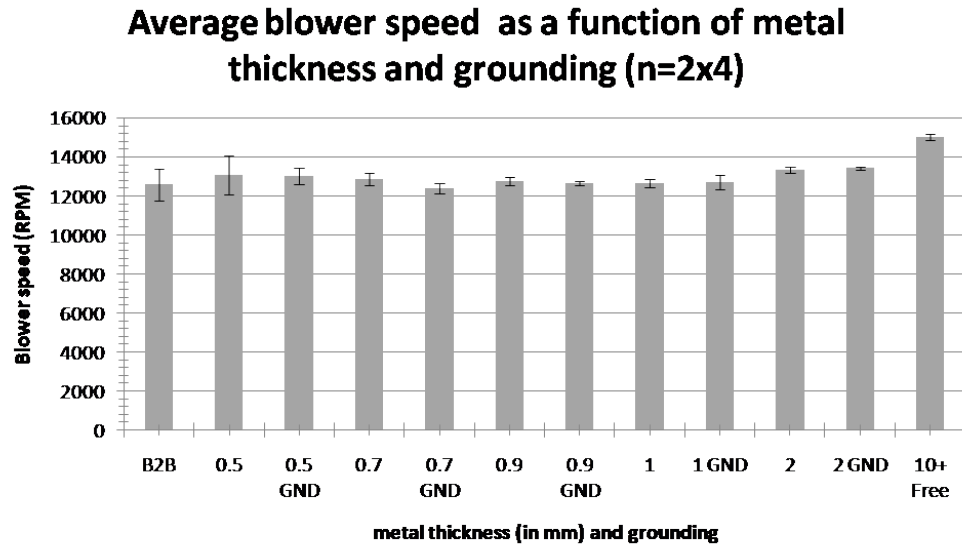


Figure 4.31: Back to back 9mm blowers speed varying with metal plate thickness and grounding

with Blu Tack. The internal fan created heat and circulated the humidity within the chamber. The Blu Tack (secret composition) may also dry and diffuse its humidity at this temperature. The same experiment was performed by sealing the chamber with paper: a notebook was applied and the relative humidity and temperature measured for 5 minutes (Fig. 4.32). The same curve was observed with both sealing materials, although RH rises slightly more with Blu Tack. By 311 seconds there was an increase in temperature of  $2.5^{\circ}\text{C}$  when sealed with Blu Tack and  $2^{\circ}\text{C}$  with paper. In other words, There was a temperature rise of  $0.48^{\circ}\text{C}$  per min with Blu Tack and  $0.4^{\circ}\text{C}$  per minute when sealed with paper.

The heat effect of the blowers is studied further in chamber 5.

#### 4.8.4.3 Impact of air conditioning:

The error rate was slightly less when air conditioning was used in the room (52% vs. 69%).

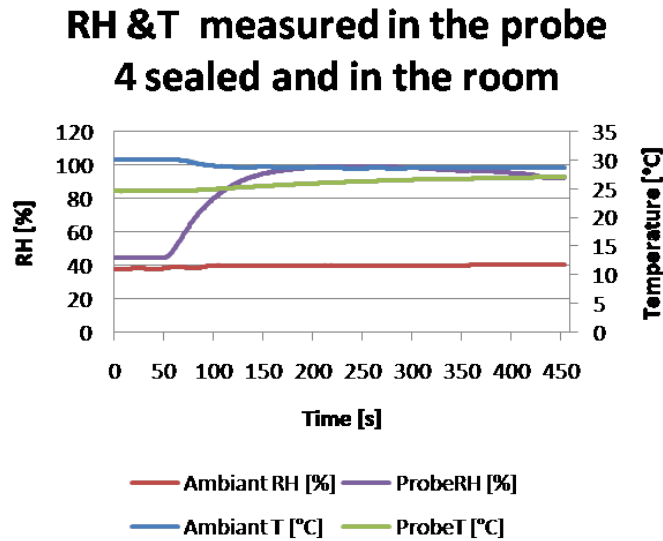


Figure 4.32: Observation of the effect of the blowers in the microclimate

#### 4.8.4.4 Calibration:

Chamber 4 was compared with the Aquaflux for the three sensor positions (Fig. 4.33). The measurements were taken at three different anatomical sites: the VF, the cheek and the palm of the same subject on which the PhD project experiments has been conducted, as presented in 4.5.2. The cheek TEWL was expected to be between the VF and palm (Mayrovitz et al. 2013). As expected based on the chamber geometry (see above), sensors 1 and 2 showed superior correlation to the Aquaflux than sensor 3.

#### 4.8.5 Discussion

The gradient calculation algorithm was chosen to be as simple as possible, signal processing have been avoided in order to get gross results.

The aim of the project is to build an instrument that provides repeatable measurements. There is a large difference of repeatability between the case where the fans are on and off. The coefficient of variation is much smaller without the fan. It is a bit different from chamber 3 where increasing the number of blowers actually increase repeatability, sometimes. Unfortunately, none of the experiments yielded a coefficient of variation smaller than 5%, the project objective. Further tests was needed with future prototypes.

A longer application of chamber 4 actually decrease the repeatability considerably. This is a different result from probe 1 and chamber 3 where the difference of coefficient of variation wasn't considerable.

For the first time, with this chamber 4 is tested the location of the sensors: with

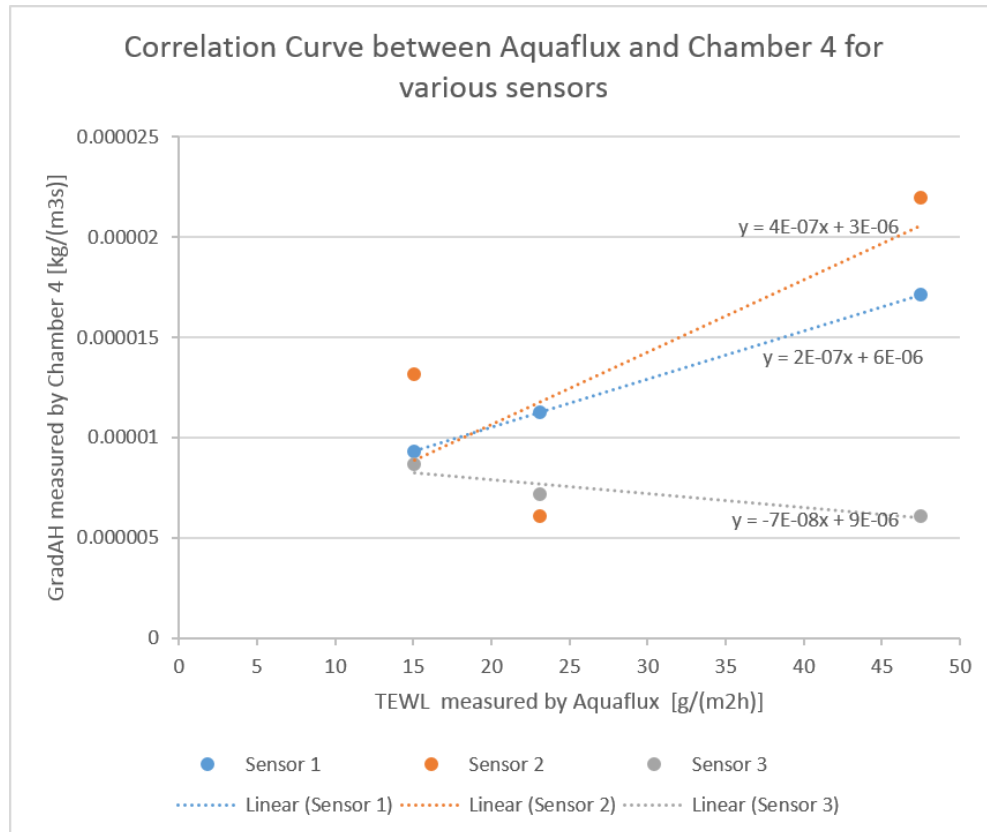


Figure 4.33: Correlation between the Aquaflux and the Chamber 4 with one 9mm blower, for 3 sensor positions

three different positions. The gradient measured by sensor three, in the middle and at the back of the blowers has more variation than sensor one and two. The curves of sensor one and two have similar amplitude because they are symmetric. However sensor three can measure much more water concentration variation. It doesn't mean it can measure more water concentration, but just more variation when the application of the chamber on the skin start and stop. This is positive to be able to measure higher variation, that means higher sensitivity and resolution. The aim of the project is also to develop a sensitive instrument. The calibration curve between the Aquaflux and Chamber 4 was created. However sensor three shown a negative correlation. And this negative correlation was confirmed by the fact that not only two sites (low and high TEWL value) were taken, but three sites in total (cheek as medium TEWL value) were taken into account. This highlight the fact the sensitivity cannot be interpreted only from the gradient curves such as 4.29 but more information is needed like in 4.33. Sensor two have higher amplitude in 4.29 but also higher slope coefficient in 4.33. Moreover, the coefficient of variation was the lowest for sensor two. Therefore sensor two is the best location of sensor for this chamber design. It is also the only position where the slope coefficient is higher or equal to the Aquaflux slope  $3 \cdot 10^{-7}$  that constitutes the project objective.

For the first time, with this chamber 4 is tested several speed. The speed vary with a potentiometer and the corresponding tension coming out can be measured. Chamber 4 has been tested with three different speed, low, medium and high, corresponding to low, medium and high voltage. The coefficient of variation increase with the voltage, thus with the fan speed. This correlates with the first observation that the error rate is higher with the fan on than the fan off. Repeatedly, the higher is the speed fan, the more turbulence there is, and the more variable the concentration is.

Finally, there were two effects unexpected before preparing the testing: it was the heat produced by the blowers and maglev interference. The maglev interference of the two blowers was more or less resolved after adding a thin plate between the two blowers. The problem wasn't found for chamber 3 with their chambers back to back because the flowers were glued together. The fixing agent layer was thick enough to not trigger the issue. However, the grinding noise was quite important and an instrument would not sound in full working order and therefore acceptable for customers. The chamber 4 felt hot for long applications. The design produced 0.4 °C per minute. The use of the air-con slightly improved the measurements repeatability.

#### **4.8.6 Conclusion**

This prototype tested three fan speeds and three sensors locations, by using the limit positive flux calculation method for gradient calculation. Better results in terms of precision and sensitivity were found with sensor 2, either with a fan at a lower speed or without the fan (like chamber 3). The use of the AC is also advised, because the two 9 mm blowers produce too much heat. This was the main problem with this prototype, that had to be rectify for the next iteration. The blowers produced too much heat that was uncomfortable for long applications. This is a critical concern. The amount of heat could have been evaluated but the pain or discomfort is something difficult to evaluate. There are no true measure of pain, it only relies on questionnaires with answers from 1 to 10 for example. In addition having the blowers back to back could have an influence because of the magnetism of their rotor and stator. It is not something that was anticipated with the simulations for example. However, the use of a plate between the blowers helped greatly to reduce the interference.





(a) Charging



(b) Detail chamber

Figure 4.34: Chamber 5.1

## 4.9 Prototype 5.1

### 4.9.1 Description

#### 4.9.1.1 Chamber

The chamber from probe 3 has a thread inside that allows it to be fastened to the Aquaflux. The original idea behind chamber 5.1 was to get rid of this ridge as a cylinder would facilitate better air flow. It is 20 mm in diameter and 20 mm deep (slightly bigger than chamber 3) to accommodate more fans flowing towards the skin (Fig. 4.34).

#### 4.9.1.2 PCB

The PCB was designed with Eagle and then printed in house (Fig. 4.35). The PCB follows the design rules from the university service, which allows a maximum of two layers. For the sake of keeping the size to a minimum, the bottom layer is not just a ground layer, but both layers have ground and signals. The university service doesn't do plated through-holes so vias had to be made. For the same reason, the connectors were difficult to solder because they had to be soldered on both side of the PCB. The edges had to be sanded to fit the PCB into the casing.

#### 4.9.1.3 Casing

The casing is a simple parallelepiped large enough to contain the PCB and the components. There are holes for the screen, the potentiometer and the two USB plugs to connect to the PC and recharge the battery (Fig. 4.36). On the side it has a hole for the wires of the blowers and the RHT sensor. The instrument can be



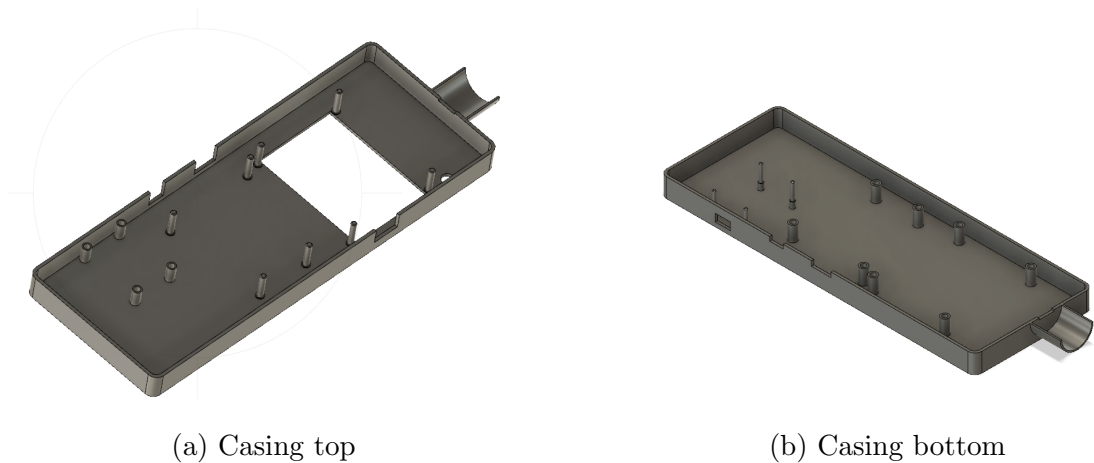


Figure 4.36: Chamber 5.1 casing design

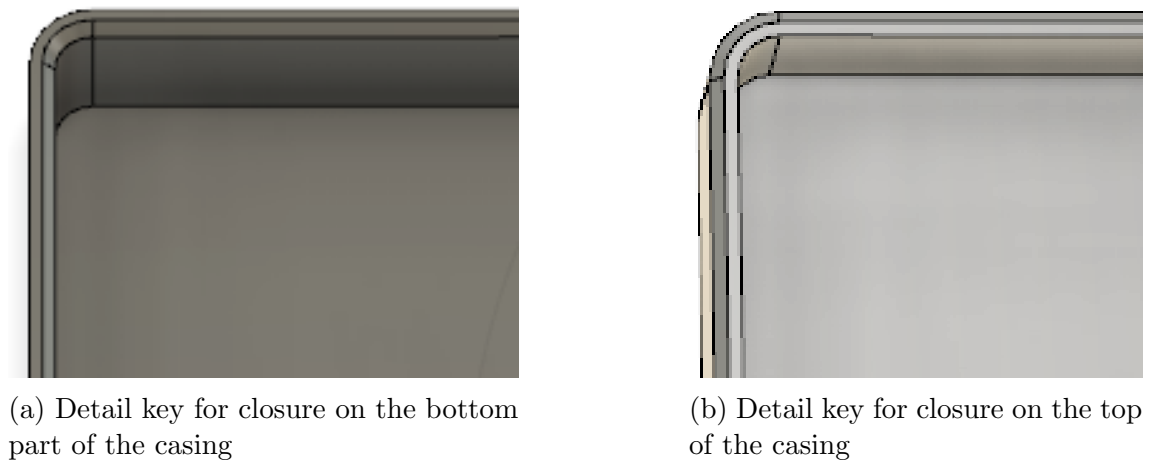


Figure 4.37: Casing closing design detail

opened along its length. We designed a long key between the top and the bottom of the box as a closure interface, see Fig. 4.37. We also designed cylindrical keys, mostly female on the bottom part (see Fig. 4.36b) and male on the top of the casing (see Fig. 4.36a).

## 4.9.2 Rationale

This probe is the first probe with hardware PCB and casing: all the previous prototypes were only measuring chambers. There is an integration of the chamber and the PCB into casing to be tested, as well as the performances of the chamber in terms of repeatability, accuracy and sensitivity.

In addition, Chamber 3 work had to be studied deeper: understand the air flow, the effect of blowers on the microclimate to find the best configuration of blowers: 9 mm, 12 mm, 15 mm. Chamber 5 is larger than chamber 3 and can accommodate two

15 mm blowers (and therefore, two 12 mm blowers or three 9mm blowers). Chamber 3 simulations shown quiet regions on the sides of the blowers: they would be better to avoid turbulences and increase repeatability. Finally, with this new prototype, threading from the interior of Chamber 3 is avoided.

Moreover, this prototype study built on top of Chamber 4 work: some issues were found with the space left between two blowers back to back. Similar fixating method from Chamber 3 was applied in order to avoid MagLev interference.

### 4.9.3 Testing

The general methodology can be found in section 4.2. With chamber 1 an operating protocol has been established. The duration of application has been lengthen with chamber 3 and 4 but no real benefits were found. Thus, the measurements were performed by application of 30 seconds on the skin and rest of the chamber during 30 seconds. Measurements are done first on the prototype, then with the Aquaflux in order to have a reference for calibration. The location sites are the palm, cheek and volar forearm on one participant. All measurements were done in a controlled environment. Measurements are done at least in triplicate.

For this probe, the testing goal is to gain some insight on the effect of a fan on TEWL measurements. Different fan speeds and airflows were tested by varying conglomerate of fan models (of different size and thus airflows).

Finally, the chamber was tested in ergonomic point of view: is is easy to handle and to use.

### 4.9.4 Results

#### 4.9.4.1 Gradient computation method:

With this prototype, the method used was the limit positive flux as used in all previous probes described here. The method can be found in section 4.7.4.3 . In practice the flux was read at regular time intervals (30s, 90s, 150s, 210s, 270s) during the measurement session at the end of each measurement (alternating between 30s application and 30s rest). A few other methods like sampling and running average were tested but they didn't yield improvements.

#### 4.9.4.2 Results:

The error on the measurements was between 120% and 150% while the error with the Aquaflux was 6% (14% for the palm). The repeatability was poor although the measurements look smooth (see Fig. 4.38).

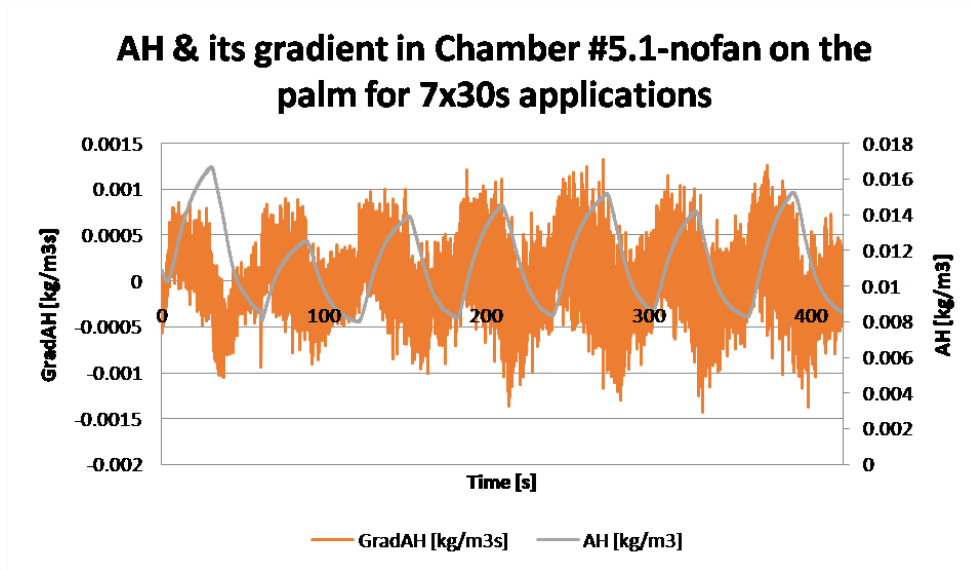


Figure 4.38: Humidity and gradient for Chamber 5.1 without blowers

**With and without the fan** In order to increase the repeatability of the measurement, some measurement were performed without the fan, on three skin location sites: the volar forearm, the cheek and the palm. Moreover, six measurements were taken for the palm, to reduce the coefficient of variation. However, all this tricks didn't yield better results, and measurements were even worse without the fan. Overall, taking triplicates on the volar forearm and the palm lead to 137.5% error (or coefficient of variation) with two 12 mm blowers back to back and 139.9% error without the fan.

#### 4.9.4.3 Calibration:

Chamber 5 with a 15mm blower was used to measure the TEWL on the VF and the palm and compare the results with the Aquaflex. The points of the correlation curve were poorly correlated (see Fig. 4.39), suggesting a low repeatability for the chamber 5. The more dispersed points are, the higher is the coefficient of variation. For complimentary information, readings are provided as follows: 122% CV for the volar forearm and 139.9% for the palm. Sensitivity was higher with a fan than without the fan. As explained in the general methodology, the sensitivity was measured as the slope of the calibration curve. The slope coefficient was  $7 \cdot 10^{-7}$  for the calibration curve without the fan and  $4 \cdot 10^{-7}$  with the two 15 mm blowers back to back (see full Sensitivity Ranking table A.2).

#### 4.9.4.4 Simulation:

Modelling results were very similar to those seen in chamber 3. Chamber 5.1 is just really slightly bigger than Chamber 3: 2 mm more to the radius and height.

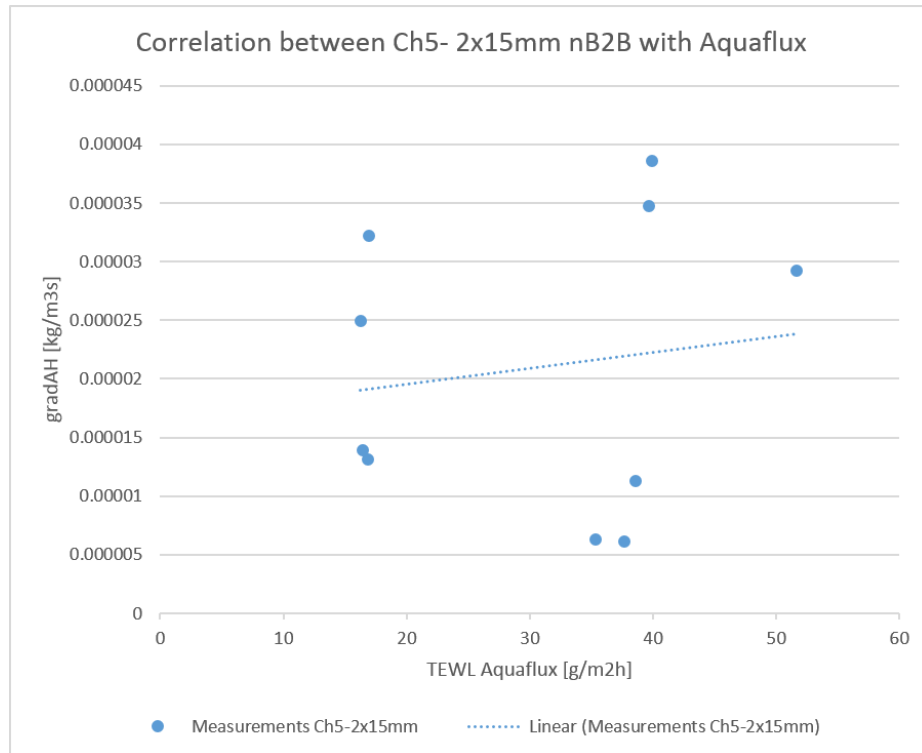


Figure 4.39: Calibration curve with Chamber 5.1 equipped with two 15mm blowers

The geometry is the same: it is a cylinder. The mixing due to the turbulences in the chamber is the same as for chamber 3. The less turbulent region allowing more repeatable results would be on the side of the blowers. Obviously it would depend on the size of the blowers: 9 mm, 12 mm or 15 mm. Repeatedly, the modelling had some assumptions and was only done in 2D although it is a 3D problem.

#### 4.9.5 Discussion

This probe was evaluated on two aspects. The first one is the instrument itself, in terms of hardware, PCB, casing. The second aspect were the performances in terms of repeatability and sensitivity. The instrument was calibrated with the Aquaflux. With regards to the performances, the repeatability was poor. The target in this project is 5%, but the result was 130% or more. Next instrument have to address this faux-pas and reach the 5% target. In terms of sensitivity though, the target is to have at least the same slope coefficient of the Aquaflux on the calibration curve, so the slope have to be higher than  $3 \cdot 10^{-7}$ . This was reached with two 12 mm fans on and off. Regarding the instrument itself, probe 5.1 is a bit too big to be convenient to use. The placement of the screen, the battery and board are such that either the probe would have been too large or too long. The latter case was chosen but future improvements were planned to reduce the size of the instrument.

### 4.9.6 Conclusion

Unfortunately, Chamber 5.1 didn't yield data with good repeatability on the few measurements taken. Some further improvements could be made to the gradient calculation, but this is unlikely to resolve the issue of repeatability. While the repeatability wasn't acceptable, the sensitivity, like the previous prototypes, reached the project target.

Finally, the casing is too cumbersome so a next step would be to reduce the size of the components to make a more compact instrument.

## 4.10 Prototype 7.1

### 4.10.1 Description

#### 4.10.1.1 Overview

Prototype 7.1 is also a fully functioning instrument, and can be considered as an update of probe 5.1 to make it smaller. It uses tinyTILE instead of Arduino 101, and has an integrated BLE and gyroscope. The code was updated because tinyTILE uses a 32 bits Intel Quark microcontroller with 384 kB flash memory (more than the Arduino 101).

#### 4.10.1.2 Geometry

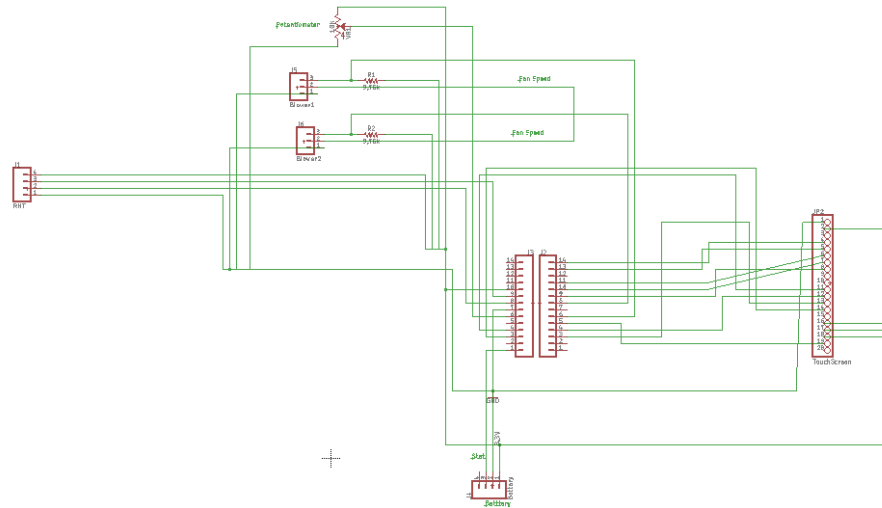
The chamber is a cylinder with diameter 15.5 mm and height 17 mm.

#### 4.10.1.3 PCB

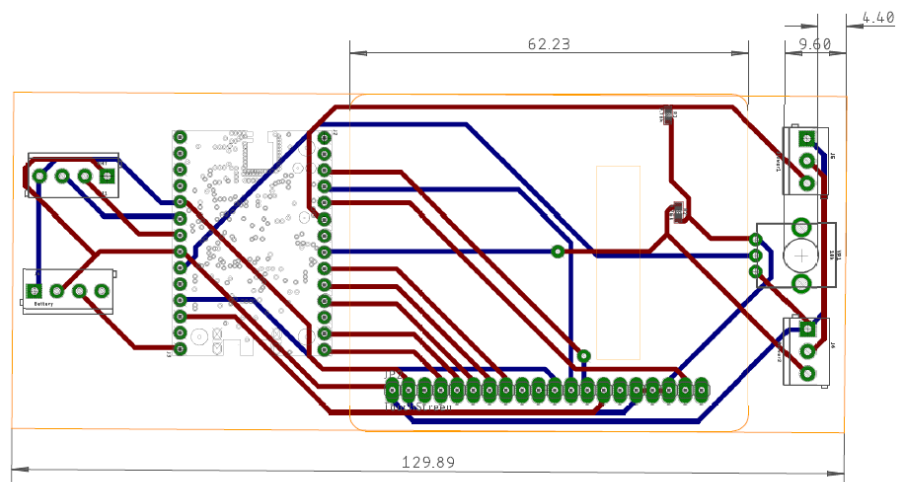
The design of PCB was updated from prototype 5.1 with the tinyTILE pins (Fig. 4.40). The blowers were updated to be controlled by a potentiometer instead of a PWM.

The board was first printed in house. Due to difficulty with soldering components on the two layer PCB despite senior technical assistance, a decision was made to order a manufactured PCB from a supplier. After studying the offers, the final choices were:

- Copper thickness of 1 oz. An ounce (or oz) is the unit of measure for copper thickness on a PCB. That corresponds to 1.37 mils (1.37 thousandths of an inch), equivalent 1 oz of copper being spread over a one square foot area. The currents in the PCB do not exceed 1A so a thickness of 1 oz is adequate
- No solder resist because the pitch is 3 mm so there is plenty of space between the pins



(a) Schematic



(b) board

Figure 4.40: Chamber 7.1 PCB and schematic

- The components were all plated through-hole
- Smaller thickness PCB base material of 1.6 mm (compared to 2.4 mm), which still allowed for fitting connector legs of up to 3 mm length
- Immersion silver finish as a cheaper alternative to Au/Ni finish
- A quick manufacture and delivery time at a reasonable price

The chamber designed was roughly the same size as the prototype 3 and 5.1 to allow for various tests with the blowers (Fig. 4.41).

To avoid any air leak, the instrument can be opened through its length without disrupting the chamber Fig.4.42. The cap has the chamber on one side, the closure design being detailed on Fig. 4.43.



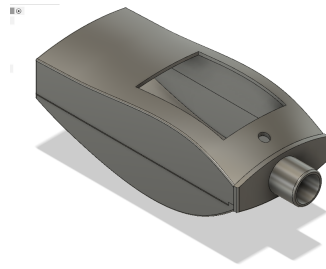
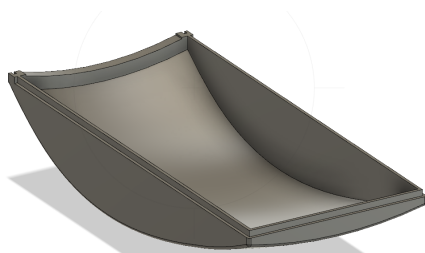
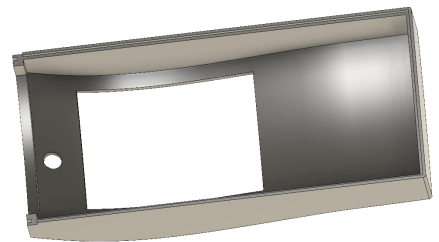


Figure 4.41: Chamber 7.1 casing design

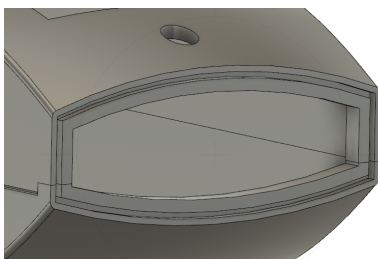


(a) bottom



(b) Top

Figure 4.42: Chamber 7.1 case closure



(a) Case closure

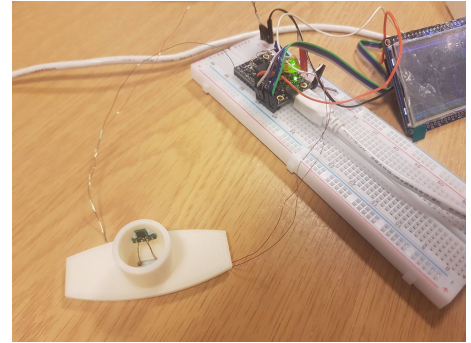


(b) Cap closure

Figure 4.43: Chamber 7.1 cap closure



(a) Probe 7.1 3D printed



(b) Debugging chamber 7.1

Figure 4.44: Chamber 7.1 casing and use

The 3D printer constraints were 1.5mm for Fused Deposition Modelling (FDM) and 1 mm for Polyjet. The result of the 3D printing can be seen on 4.44a. It was also used deconstructed to accurately repeat the probe position compared to the skin for all measurements 4.44b.

### 4.10.2 Gradient calculation

The microcontroller sends the data to a PC through serial COM at a rate of five times per second. A C# Windows program receives, saves and displays the data. It also performs a Least Square Fitting on the humidity. As it will be described further in 4.11.1.1, it provides the gradient of humidity. The software also performs a  $\chi^2$  test on the observed and expected humidity. The value it is compared to in the  $\chi^2$  test is an input of the Windows application. If the value calculated is below the target, then the value is displayed in green, otherwise it is displayed in red.

### 4.10.3 Rationale

This probe has been developed as a new version of probe 5.1, i.e. a probe with a casing, and chamber. In addition, a smaller development board was introduced, the tinyTILE, so the PCB and the casing could be smaller.

Moreover, this prototype study is built on top of Chamber 3 work: it aimed to understand the relationship between the airflow and the measurements, also primary objective for probe 5.1, that failed because of low repeatability of the results. Thus the design of the chamber is similar to probe 3 and 5.1. However it is a bit larger than chamber 3 to accommodate a 15 mm blower. But it is smaller than chamber 5.1 because the instrument itself is smaller (Probe 5.1 was too cumbersome to fit in the hand) while still being able to test the range of blowers available: 9 mm, 12 mm and 15 mm.

Another aim is to have good repeatability, so there is no helical ridge like Chamber 3.

#### 4.10.4 Testing

The general methodology can be found in section 4.2. With Chamber 1 an operating protocol was established: the measurements are performed by application of 30 seconds and rest of 30 seconds. The location sites were the palm and volar forearm on one participant. Measurements are done first on the prototype, then with the Aquaflux in order to have a reference for calibration. Measurements are done at least in triplicate. All measurements were done in controlled environment.

Moreover, this new probe aimed to build on Chamber 4 work: the comparison of more fan speeds. For this probe, measurements were planned to try different fan speeds and airflows varying with size or fan models. This probe was tested with a cap orifice but didn't yield good results and would not be presented here.

In addition, this prototype study was built on top of Chamber 3 work where the gradient calculation is being improved with different duration and timing: specific MATLAB scripts were used to calculate error rate in function of duration and timing. This constitutes the gradient computation study with  $\Delta$  and start time.

Furthermore, a portable instrument has to be convenient to use and have autonomy. These two factors lead to portability study.

Finally, this chamber aimed to test different types of calibrations.

#### 4.10.5 Results

##### 4.10.5.1 Gradient computation method:

The gradient was calculated using various values for  $\Delta$  and start time using a script on MATLAB. A script is list of procedures the computer would follow: it reads the humidity and temperature in input and performs a gradient calculation with the parameters  $\Delta$  and start time. On some experiments, it will be stated that the Least Square Fitting method was used.

##### 4.10.5.2 Results without the fan:

The gradient was calculated for different values of start time and  $\Delta$ . On Fig. 4.49 the points are more dispersed for the palm for  $\Delta = 1$  (orange), 2 (grey) and 3 (yellow). The value of  $R^2$  can also be used, the higher it is, the less dispersed are the points therefore, the more repeatable measurements the configuration would provide. Overall, the bigger the  $\Delta$ , the smaller the error (from  $\Delta = 4s$ ). On Fig. 4.46, the coefficient of variation or error rate at its smallest around 30% (for this set

of measurements). For a  $\Delta$  of one second, the best timing to start the measurement is 8, 9 or 10s. This will be discussed more in details later in this section.

#### 4.10.5.3 Comparison with and without the fan:

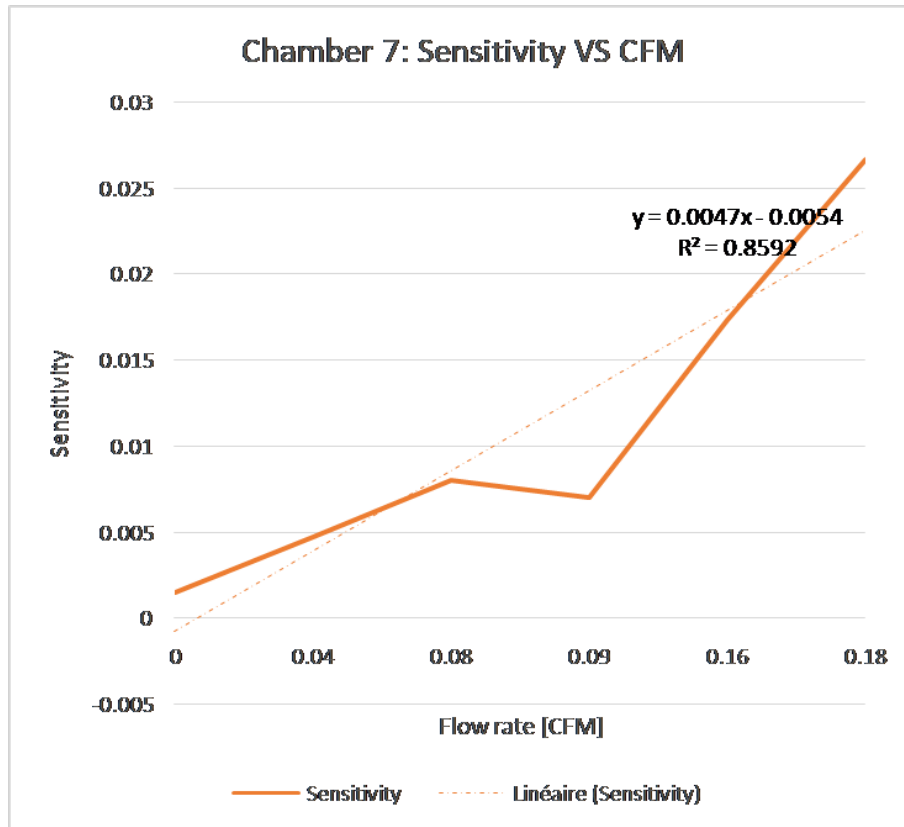
The chamber was applied for 30 seconds. The rest between measurements was the time to measure with the Aquaflux, usually 1 minute. The gradient was calculated using Least Square Fitting (described in section 4.11.1.1).  $\chi^2$  was calculated and tested against a threshold. In post-processing, the minimum  $\chi^2$  was found and the corresponding gradient retained. The average measurement values of Chamber 7 and the Aquaflux were calculated. The sensitivity compared to the Aquaflux is the slope coefficient of the linear regression plot. If we plot the sensitivity as a function of the flow rate and do a linear regression,  $R^2 = 0.8592$  (see Fig. 4.45a). If  $R^2 > 0.7$  then it is a good fit.

The larger the blower, the bigger the flow rate and the better the sensitivity was compared to the Aquaflux (Fig. 4.45a). However, increased flow rate was not associated with improved repeatability (Fig. 4.45b).

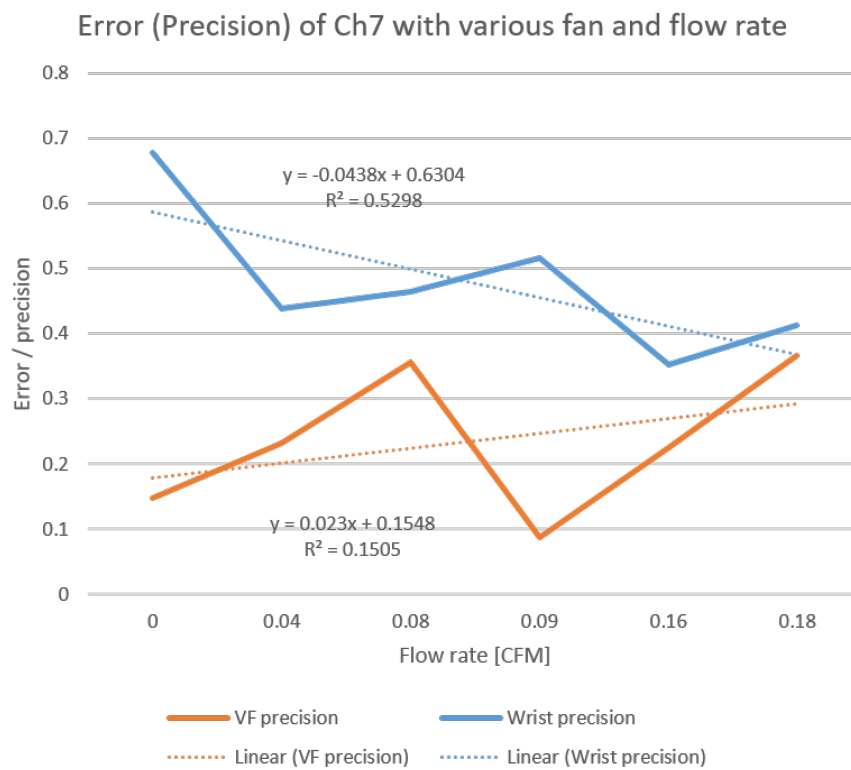
From the same figures 4.45 and the more general case of performances as function of air flow rates, the chamber with the fan can be compared to the case without the fan. Regarding the repeatability of the measurements on the volar forearm, the coefficient of variation is larger with the fan (one 9 mm produces 0.04 **CFM!**<sup>21</sup>) that without the fan (0 **CFM!**). So the measurements on the volar forearm are more repeatable without the fan. With regards to the repeatability of the measurement on the palm, the coefficient of variation is smaller with the fan (0.04 **CFM!**), than without the fan (0 **CFM!**). Thus, measurements on the palm are more repeatable with the fan.

---

<sup>21</sup>**CFM!**



(a) Sensitivity



(b) Repeatability

Figure 4.45: Performances of sensitivity and repeatability in function of the type of blowers (CFM=Cubic Feet per Minute)

#### 4.10.5.4 Results with different $\Delta$ and start time:

In this section, some adjustment to the gradient calculation is performed on a set of measurements on the volar forearm and the palm, with probe 7.1, without the fan on. Like for previous chamber, the humidity and temperature were measured and a gradient of humidity was calculated. The adjustments are performed at the time of calculating the gradient of humidity. The gradient computation can be delayed to start at a time called "start time" in order to wait for stabilisation of the microclimate in the chamber. The computation can last a duration delta ( $\Delta$ ). These two parameters were tested to obtain the best results defined as lowest error rate or highest precision. A script ran over a set of calibration results for all values of these parameters to a maximum total duration of 30 seconds. For one set of measurements the optimal couple was  $\{\text{start}, \Delta\}$  so  $\text{start} + \Delta = 15$  seconds (Fig. 4.46). The results were also valid for the palm calibration measurements as well. The error rate can be considerably diminished this way. The error rate was smallest for  $\Delta$  of 9 seconds and start time of 1 second.

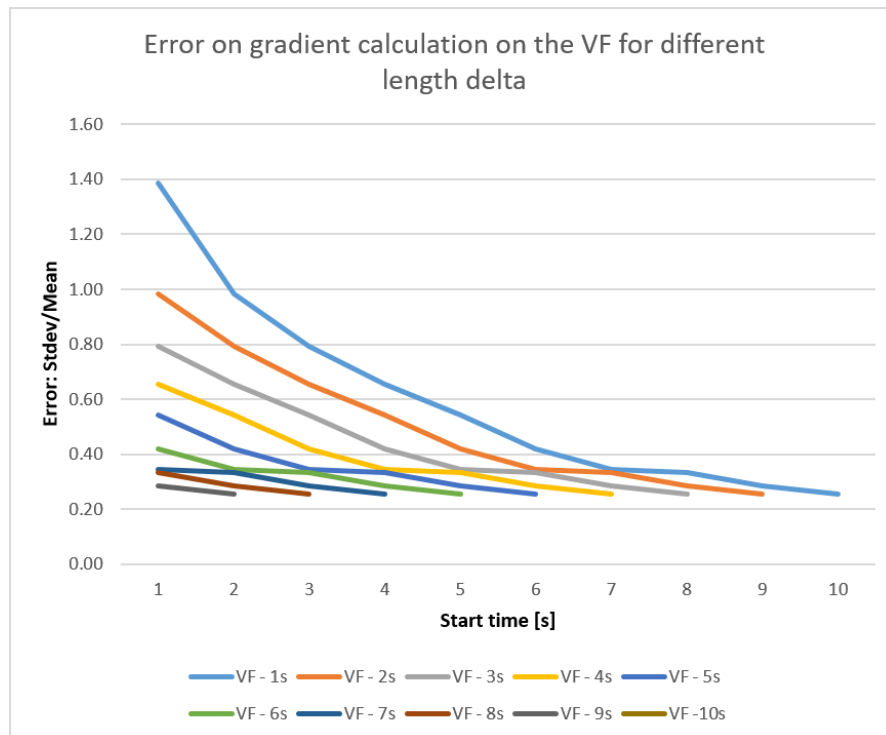


Figure 4.46: Variation of delta and start time on the error rate

#### 4.10.5.5 Calibration:

**With Aquaflux:** The correlation curve between the Aquaflux and Chamber 7.1 can be observed in Fig. 4.47. When using the chamber without the fan, the sensitivity was better with  $\Delta = 10$  seconds than  $\Delta = 3$  seconds. With the fan, the

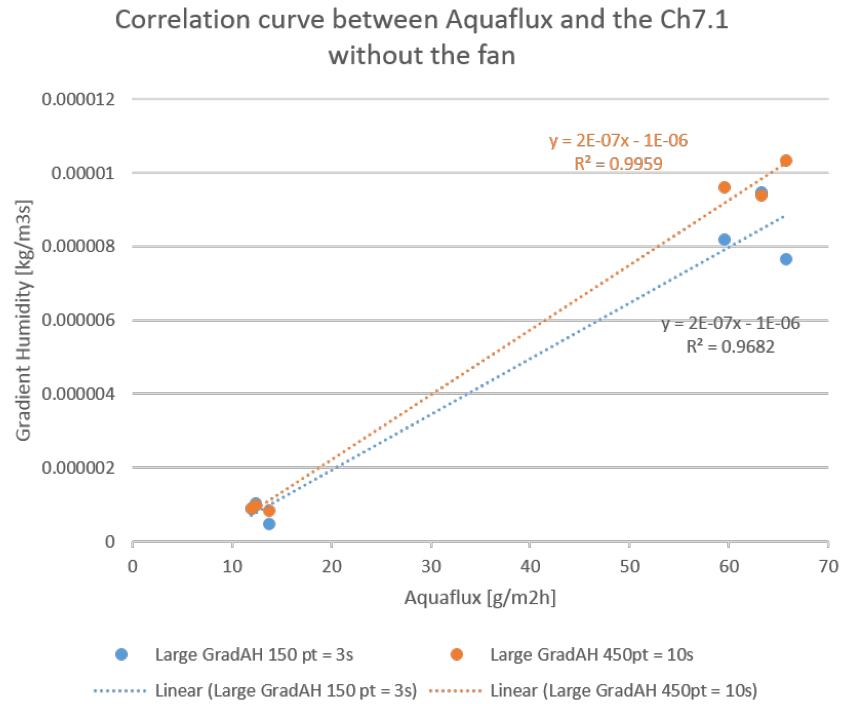


Figure 4.47: Correlation curve between Chamber 7.1 and the Aquaflux

correlation was slightly better with one fan rather than two fans (Fig. 4.48). In Fig. 4.49, the slope of the correlation curve was highest for  $\Delta = 4$  seconds (blue line) -  $R^2 = 0.9968$ . Therefore, the highest sensitivity was reached with delta at  $\Delta = 4$  seconds. During this calibration exercise, the repeatability for Chamber 7.1 was at its lowest while using the large gradient calculated as a difference between two humidity spaced by 10 seconds. The coefficient or error rate was 0.05.

The optimal parameters change with each measurement session, the instrument configuration and if there is fan or not. Finding the optimal parameters will be discussed for probe 9.

**Numerical Integration:** A formal calibration of probe 7.1 was attempted using precise measures of a quantity of water (2 mg) left to dry. The microclimate was measured during this process. The area under the curve of the humidity gradient was curve fitted with MATLAB. The mass is expected to be found as per Eq. 4.4:

$$m = A \int J dt \tag{4.4}$$

The area under the gradient curve is then integrated and should give a quantity proportional to the weight of water first measured. However, the results of these calibration attempts were not repeatable despite several attempts. The discrepancies could come from the precision of volume of water measured by the pipette, or the weight measured by the scale.

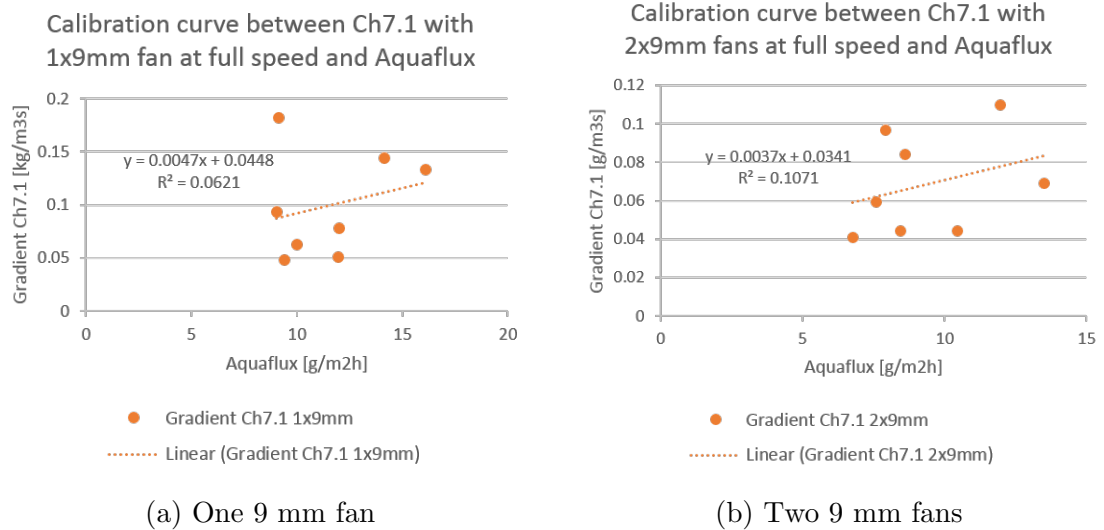


Figure 4.48: Calibration curve between probe 7.1 (with one or two fans) and the Aquaflux

**4.10.5.6 Simulation:**

Modelling results were very similar to those seen for chamber 3. Like Chamber 5 and 3, probe 7.1 is a cylinder where the fan is blowing towards the skin and the flow coming in the blower is parallel to the skin or the roof the chamber. There are no geometry changes, it is the same as chamber 5.

**4.10.5.7 Battery life:**

This prototype used a tinyTILE microprocessor. The battery is a 3.7V LiPo<sup>22</sup> battery. Autonomy tests were conducted with two LiPo batteries of the same model and the chamber lasted 21h10 and 20h30 respectively (Table 4.4):

Table 4.4: Autonomy comparison of two batteries

	Battery 1	Battery 2
	20h30	21h10
	19h50	21h10
	21h00	
	20h45	
Mean	20h30	20h10

**4.10.6 Discussion**

The aim of the project was to develop a TEWL instrument that works outside of a controlled environment. As a reminder, uncontrolled environment has for effect

<sup>22</sup>Lithium-ion Polymer



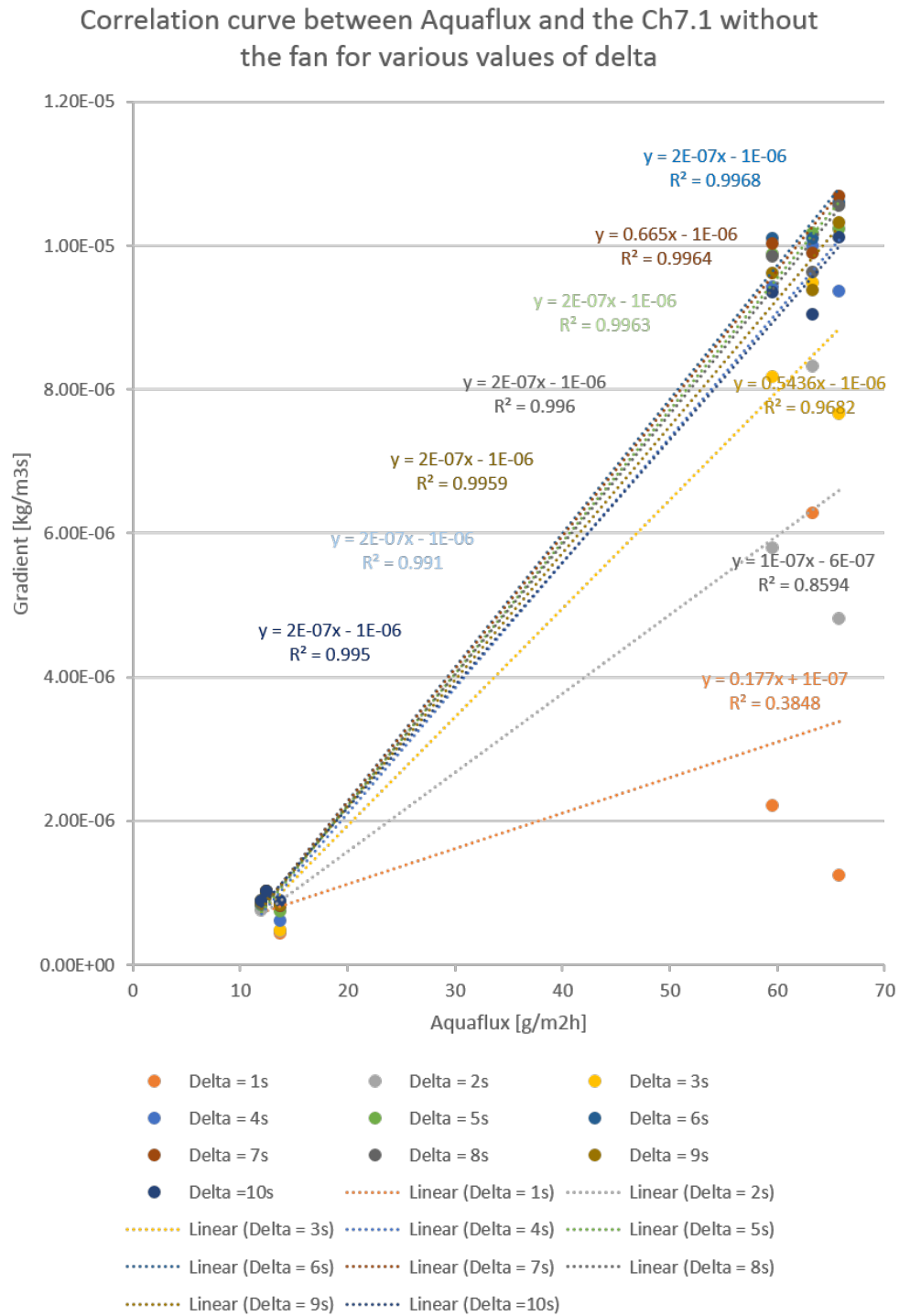


Figure 4.49: Correlation curve between Chamber 7.1 and the Aquafux for various values of  $\Delta$  time

sweating and the presence of surface water on the skin. The idea in this project is to remove water using a fan. Probe 7.1 aims to study the effect of the fan on the microclimate. The higher is the airflow, the higher is the sensitivity (see Fig. 4.45a).

However, regarding repeatability, there are two outcomes, either the flux measured is high (for the case of the palm) and the repeatability decreased with the airflow; or the flux measured is low (for the case of the volar forearm) and the the repeatability increased with the airflow (see Fig. 4.45b). In addition, the trends observed for the repeatability have their coefficient of determination  $R^2$  is below 0.6 so the correlation is moderate for the palm and very weak for the volar forearm where  $R^2$  is below 0.2. There is a lot of uncertainty for the repeatability trend because the x-axis is a flow rate in CFM. The flow rate has been increased by using different fans configurations: one or two blowers of different size: 9 mm, 12 mm, 15 mm. These different fan configurations changed the space available for the air the mix, as well as the airflow. With the overall space changing, the less turbulent regions are changing too. Again, the hypothesis is that the repeatability increases with quieter environment where the airflow is still. This is why on Fig. 4.45b, the trend is unclear. Following the same assumption there should be an inverse relationship between the repeatability and the sensitivity: the instrument can detect the slightest change of concentration due to turbulent flow. This is true for the trend of the repeatability on the wrist, that decrease with flow rate. This observation also confirms that simulations would need to be in 3D to identify quiet spots to optimally place the sensors. Finally, because repeatability and sensitivity looks inversely correlated, a trade-off has to be found between repeatability and sensitivity. By comparing the results with and without the fan, probe 7.1 yielded different results from the previous prototypes. Chamber 4 and probe 5.1 shown better repeatability without the fan for the volar forearm. Chamber 7.1 though had better repeatability with the fan. The discrepancy could be explained by the design of the chamber: the shape and size of the chamber have an impact on the regions where the sensor is located. In addition, linear regression on the repeatability results with probe 7.1 lead to a coefficient of determination really low. For high TEWL, probe 7.1 yielded better repeatability results without the fan. More generally, repeatability decrease with flow rate coming out from the blower. Although, it was only confirmed for high TEWL, this is the most likely trend, as it was confirmed by Chamber 4. Chamber yielded more repeatable result with the fan speed decreasing on Fig. 4.30. In addition, it would confirm the hypothesis on the use of the fan (the fan decreases the repeatability). However, it was too complicated to really understand what would be the best blowers configurations, as the change of geometry of the interior of the chamber has an impact on the mixing of the turbulent flow. Furthermore, a deeper study of the fans speed impact on the precision or error rate was necessary.

From chamber 3 work on gradient improvement, Chamber 7.1 was aiming to take into account the timing of the calculation of the gradient. Timing is important, as outlined for Chamber 3 in section 4.7.4.2 during the comparison with and without the fan. As a reminder, when taking measurements, repeatability was lower at the start of the application with the fan than without the fan. Precision was higher at 20 or 30 seconds after application of the chamber on the skin, with the fan than without the fan. The time to measure the gradient would depend on the fan speed. Moreover, when a probe is applied on the skin, it creates a turbulent flow caused by the movement of the instrument and the pressure applied on the skin. Logically, it would be best to wait a stabilisation time, for the microclimate to settle. At least, this would be true without the fan. For chamber 7.1, some measurements were taken on the volar forearm and the parameter "start" time was studied alongside with  $\Delta$ , the gradient calculation duration. The relation between the two parameters lead to an optimal repeatability (lowest coefficient of variation or error rate) with  $start + \Delta = 15$  seconds. In the previous prototypes, the parameter studied was only  $\Delta$ . The best repeatability was found for higher  $\Delta$ . With this prototype work, a relationship between  $start$  and  $\Delta$  has been identified. It will depends on the measurement set of course, because of the duration of application and the overall curve of the humidity increase. The aim of the project was to develop a TEWL instrument that had good repeatability. The target was 0.05. It was just reached for a set of measurement on the volar forearm, without the fan. For the next prototype, the repeatability with the fans needed to be improved.

Regarding the sensitivity, the target is to have slope higher than the Aquaflux ( $3 \cdot 10^{-7}$ ). For this prototype, three correlation curves can be found in this thesis: one with the fan off, one with a 9 mm fan, and the last one with two 9 mm fan.

On one hand, in the case of a laminar flow, i.e without a fan, the calibration curve slope was  $2 \cdot 10^{-7}$  for a gradient of 3 seconds (see Fig. 4.47). In order to improve the result, a gradient on a longer duration of 10 seconds was calculated. It did improve slightly the slope because the orange curve is higher than the blue curve. However the slope was  $2 \cdot 10^{-7}$  and that's still below the project objective.

On the other hand, in the case of turbulent flow, calibration curve slopes were higher than the project objective (see Fig. 4.48). This was tested for one 9 mm blower and two 9 mm blower at full speed. The slope was higher in the case of one 9 mm blower compared to the case with two 9 mm blowers.

Last but not least, the probe 7.1 is smaller than probe 5.1, while still having a touchscreen. It also have an autonomy of 21 hours in usage. These two aspects made this prototype mobile with regards to ergonomics and hardware.

### 4.10.7 Conclusion

Chamber 7.1 showed a better precision without the fan, compared to the case with the fan. The coefficient of variation reached the project objective of 0.05 in the case of the fan off and a large gradient calculation over 10 seconds. It was discussed that repeatability usually decrease with the blowers flow rate, even though it was only confirmed with the palm measurements. Precision was improved by finding an optimal couple of *start*,  $\Delta$ . The relationship between these two parameters depends on the set of measurements. Again, a trade-off has to be found between repeatability and sensitivity. A method was needed to make more automatic and optimal the parameters. A new method Least Square Fitting was used and presented in the next prototype section.

Moreover, probe 7.1 demonstrated better sensitivity than the Aquaflux, the project objective of having a slope higher than the Aquaflux in the calibration curves. This was true only for a turbulent flow: with one and two 9 mm blowers. However, in the case of the fan off, the sensitivity didn't meet the project objective. In addition, sensitivity improved when using a higher flow rate.

Finally, the new probe 7.1 was more portable than probe 5.1, and had an autonomy of 21 hours.

## 4.11 Prototype 9

### 4.11.1 Description

This chamber is a research prototype for the future product AquaSpeed from Biox Systems Limited. Prototype 9 comes with several caps sizes: small, medium and large with an orifice size of 4 mm, 7 mm and 10 mm diameter respectively. If a smaller cap is used, then a smaller flux is measured and better precision can be observed (Imhof & McFeat 2014). This prototype uses the same PCB as chamber 4 (see Fig 4.27) so there are three sensors, with one sensor outside of the chamber (Fig. 4.50).

A casing for chamber 9 has been designed with Fusion 360 (see Fig. 4.51 and 4.53a). It was 3D printed by extrusion with a RepRap Anet A8: see Fig. 4.52 and 4.53b.

#### 4.11.1.1 New gradient calculation method

The gradient calculation was enhanced compared to the previous prototypes, using Least Square Fitting for the humidity and the calculation of  $\chi^2$ . Least Square Fitting is a mathematical process to find the best fitting curve by minimizing the

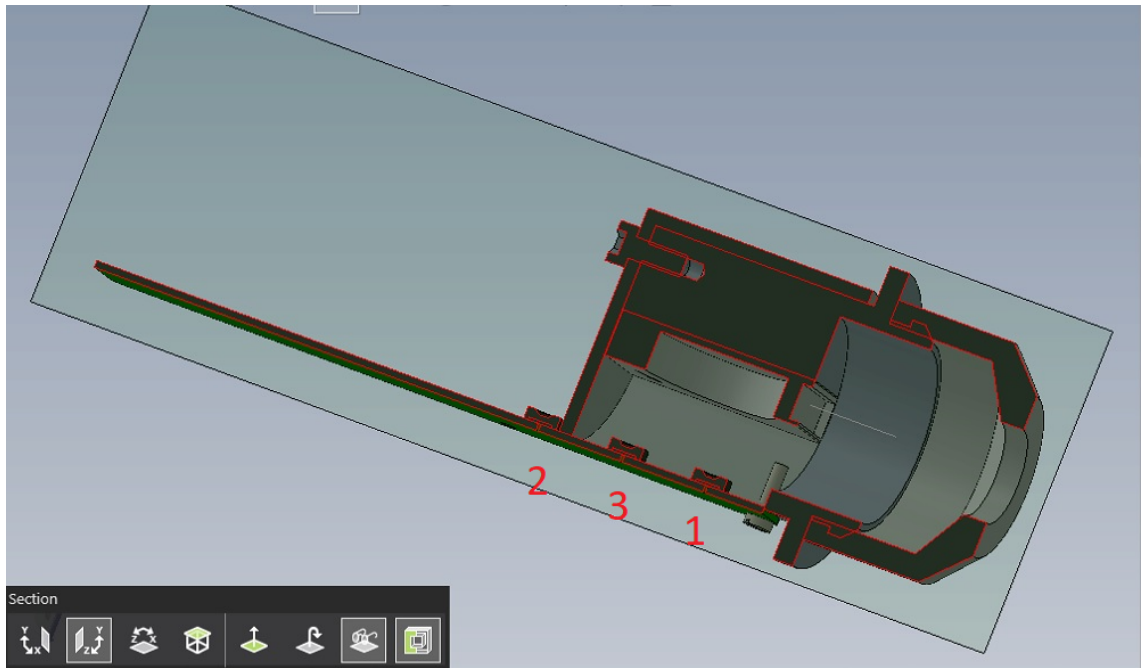


Figure 4.50: Chamber 9 cross section and sensor positions



(a) Casing

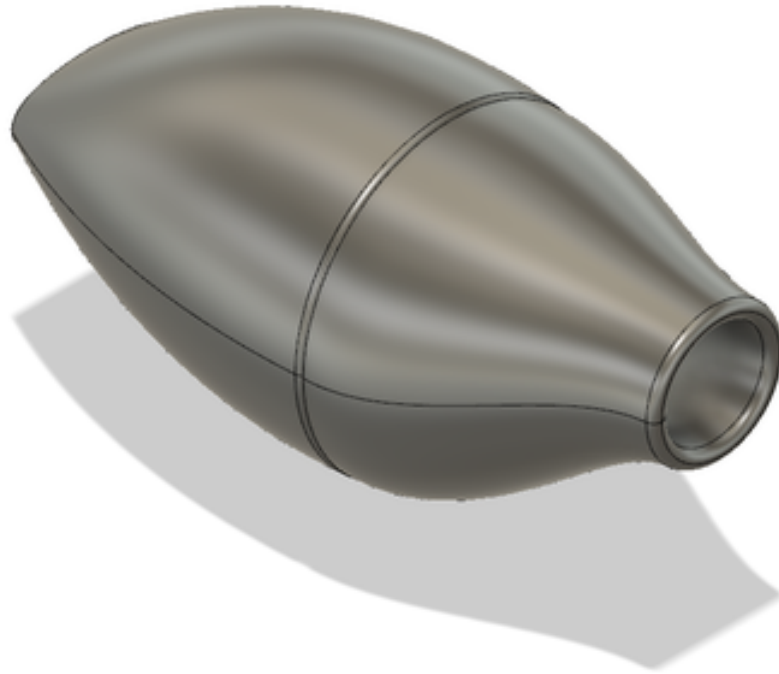
(b) Case opened

(c) Cap

Figure 4.51: Chamber 9 casing in CAD



Figure 4.52: First version of Chamber 9 casing 3D printed



(a) Casing CAD



(b) Casing 3D printed

Figure 4.53: Second version of the casing for Chamber 9

sum of the squares of the residuals. The algorithm calculates the expected humidity and compares it to the observed value. Then it computes the sum of the square of the previous values. The gradient and the offset of the curve are also determined. This is the gradient used for TEWL measurements in the experimental results. In addition, a  $\chi^2$  test is performed. The sum of the humidity squared is calculated; this represents the error that the algorithm aims to minimise. The lower the  $\chi^2$ , the closer the expected and observed humidity curves are. During measurement, it is interesting to monitor the value of  $\chi^2$  because when  $\chi^2$  is at its smallest, this means that the error is also at its smallest and therefore the TEWL measurement is most likely to be accurate to the true value of TEWL.

This new gradient computation requires not just a few scripts but the development of an application to be executed on a computer. This cannot be run on the Arduino 101 or tinyTILE because of computational power limitations. The computer used for application development used Windows 7, and the language used was C#.

#### 4.11.1.2 Implementation on C#

In this section the various aspects of the development of the C# application are discussed.

**Requirements:** The software needs the following components:

- The selection of the parameters:
  - The duration of the gradient of humidity measured,  $\Delta$
  - The time to start the measurement ( $t_{ini}$ ) waiting for stabilisation of the microclimate
  - The minimum error to reach  $\chi^2$  target
- Communication via COM port: the hardware interface for serial USB port
- Parsing the results with regular expression
- The gradient calculations
- Test if the error  $\chi^2$  is lower than the target and alert the user about the TEWL result
- The display of the measurements
- File writing to save the results

The flow of the application is described by the diagram Fig. 4.54. Least Square Fitting is used to calculate a linear fit of humidity against time. The implementation follows the formula of the linear fit described by Kenney & Keeping (1962). TEWL can be deduced from the gradient of the slope. The algorithm implemented follows the simplification provided in (Weisstein 2002) where the sums of squares are used to calculate the regression coefficient (see Eqs. 4.5 and 4.7):

$$flux = \frac{cov(t, H)}{\sigma_t} = \frac{SS_{tH}}{SS_{tt}} \quad (4.5)$$

Where flux is the TEWL, H the humidity, t the time and the sums of squares defined with t, H, their average,  $\bar{t}$  and  $\bar{H}$  respectively, and n the number of points (see Eq. 4.6):

$$SS_{tt} = \sum_{i=1}^n (t_i - \bar{t})^2 = \left( \sum_{i=1}^n t_i^2 \right) - n\bar{t}^2 \quad (4.6)$$

$$SS_{tH} = \sum_{i=1}^n (t_i - \bar{t})(H_i - \bar{H}) = \left( \sum_{i=1}^n t_i H_i \right) - n\bar{t}\bar{H} \quad (4.7)$$

**Graphs in Windows** In contrast to C++, windows graphics are easy to implement with Visual Basic or C#. They don't rely on OpenGL or libraries but Windows Forms, and it is easy to drag and drop the components needed into the window. In order to compare with previous gradient computations, the habitual gradient of humidity over a fixed period is also calculated and saved. The gradient isn't calculated before a period of stabilisation. In total there are three points with measurements and computations:

1. Relative humidity and temperature, with time, and absolute humidity
2. The gradient of the difference of humidity between the moment of computation and  $\Delta$  time
3. The least square fittings outputs: gradient, offset, observed and expected humidity with time

**USB connection** The System.IO.Ports and System.Linq have the ability to establish a USB connection. The baud rate sent by the Arduino was fixed to 115200. However by default, the Arduino establishes a serial link such as:

- No parity
- 8 bits
- With one stop bit



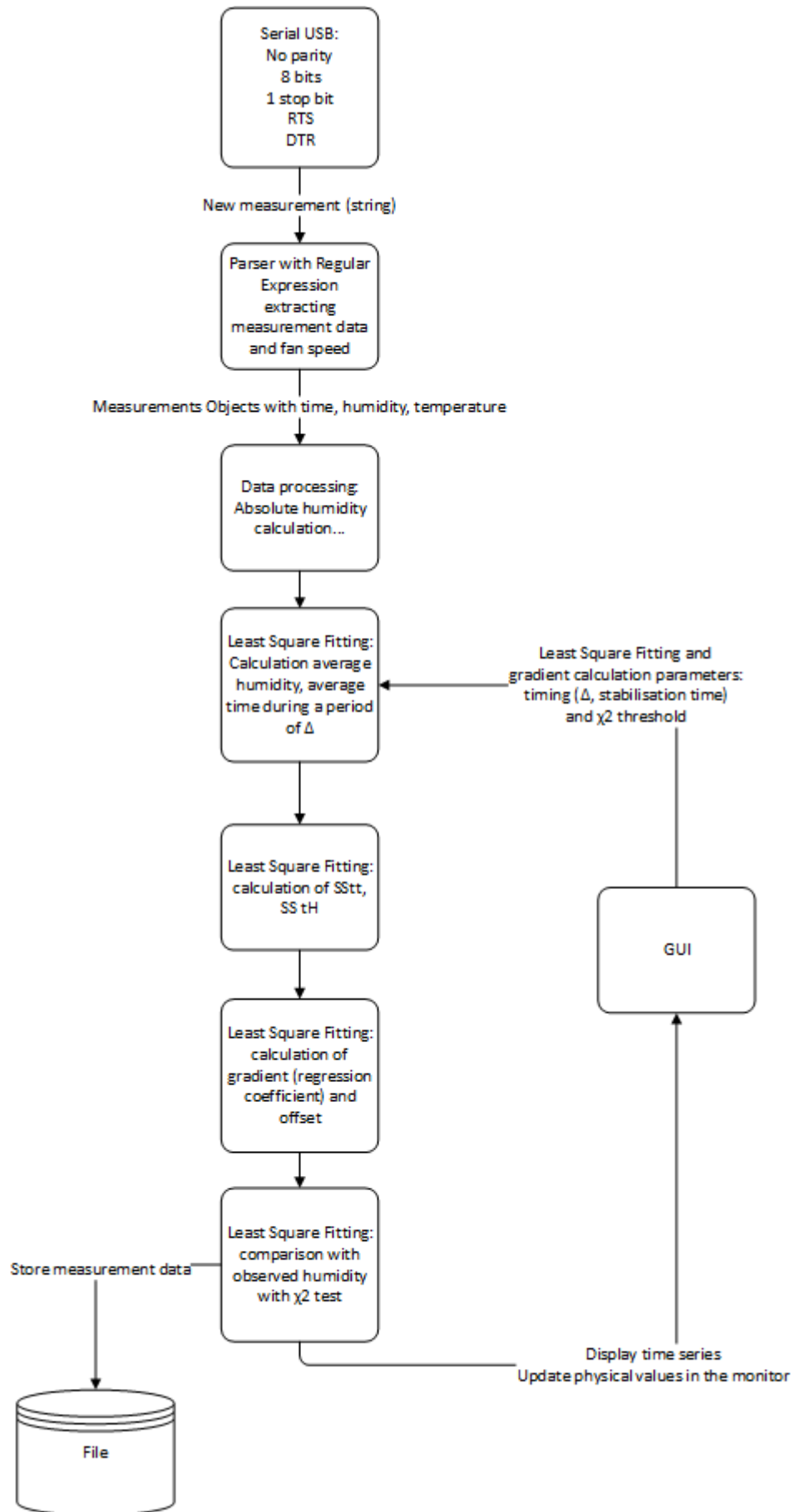


Figure 4.54: Least Square Fitting Software Flow Diagram

- Request To Send RTS enabled
- Data Terminal Ready DTR enabled

The C# software requires graphic user interface GUI through Windows Forms, USB connection management, data parsing and gradients computation. For accomplishing all these tasks, multi-threading is required.

**Threading:** Multithreading is quite straightforward in theory but can be quite complex in practice. It is fundamental to have thread safety, i.e. the shared data structures are modified in a logic that makes sure all threads behave appropriately. Threads behave appropriately if they respect the code specifications and there are no unforeseen interplays between them like deadlocks or race conditions. Deadlocks happen when thread 1 is waiting for thread 2 but thread 2 is waiting for thread 1. Race conditions are situations when two threads access a resource simultaneously. In this way, threads are different from processes because they are not fully isolated.

There are a few solutions to implement threads on C#:

- Using background threads and thread pools
- Using tasks
- Using low level threads

Simple threads have been chosen because tasks, although more powerful are also more complex and not required for this level of computation.

**Synchronisation** As in an operating system, the synchronisation can be done with a lock mutex or semaphore. A mutex provides mutual exclusion when concurrent threads access to a share resource. A semaphore ensures that no more than the specified number of threads can access the shared resources. In this software, a lock mutex was used on the data received from the USB port to the parser.

A screenshot of the software monitoring a good measurement can be observed in Fig. 4.55. The string of data is displayed before and after parsing. On the charts, the flux, the observed humidity and the expected humidity are displayed.

### 4.11.2 Rationale

For this prototype, the largest fan was tested. The largest fan can provide the larger range of flow rates. However, being the largest and more powerful, it would produce more heat. Heat was a problem identified during the literature review and requirements phase, as well during the testing of Chamber 4. In order to avoid the

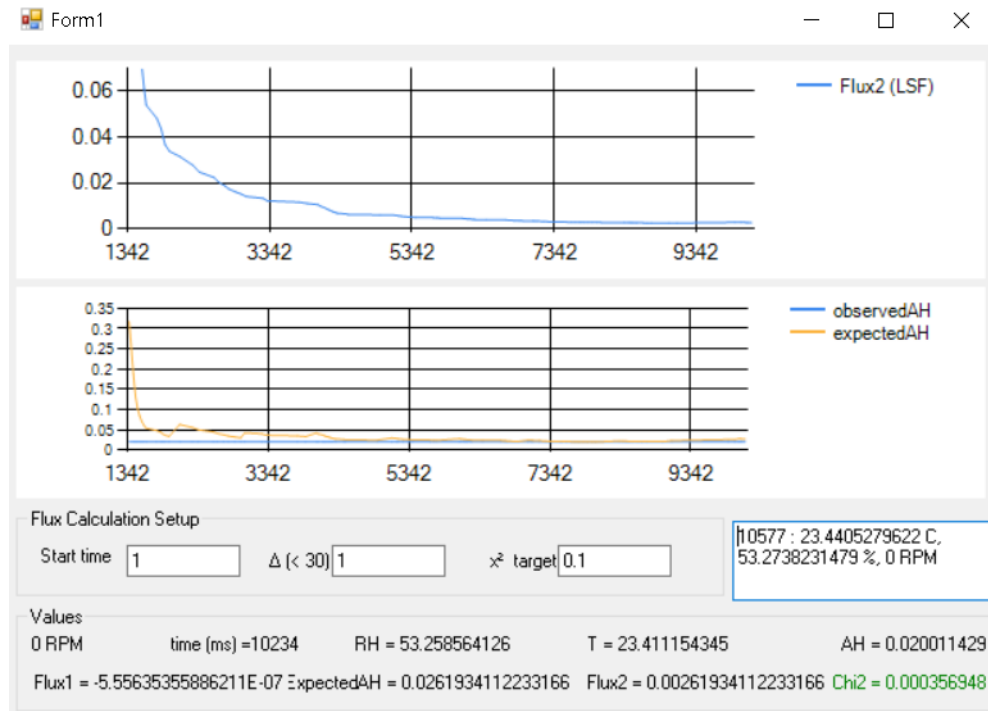


Figure 4.55: Screenshot of C# software to monitor the measurement data and perform least square fitting

air being warmed up, there was an aluminium plate at the back of the blower and the interior of chamber. This aluminium would conduct the heat away. This new L-shape design used the same PCB as Chamber 4. In order to keep the size of the chamber small, there are only two sensors placed inside the chamber: sensor 1 and 3. Moreover, like others TEWL instruments available on the market, accessories were designed for this probe: caps with different orifice size. They are used to allow more or less TEWL flux in input. For skin sites with high flux like the palm, instruments have higher error rates. Using a small orifice cap will improve repeatability on measurements on high flux skin location sites.

### 4.11.3 Testing

The general methodology can be found in section 4.2. With chamber 1 an operating protocol has been established: the measurements are performed by application of 30 seconds and rest of 30 seconds. The location sites are the palm and volar forearm on one participant. All measurements are done in controlled environment. Moreover, measurements are done first on the prototype, then with the Aquaflex in order to have a reference for calibration. In addition, measurements are done at least in triplicate. With Chamber 4 three speeds of blowers and three sensor positions were examined. Different flow rates with different blowers configurations were tested with probe 7.1. For this probe, measurements were planned to try a larger range of fan

speeds and two sensor positions. The goal was to study the effect of the fan on the skin and surface water. Chamber 3 and 7.1 showed the importance of gradient calculation. Another objective was to introduce another gradient computation method using Least Square Fitting. Finally, different caps to allow different skin TEWL in input were tested for the first time. There are three caps: small, medium and large orifice, corresponding to usage on high to low TEWL skin site.

#### 4.11.4 Results

For this probe, several methods, caps and sensor configurations were tested. Chamber 9 has a new design, with two sensors, and has three caps with different orifice size.

##### 4.11.4.1 Gradient calculation tentatives

Three methods of gradient calculation were compared; the positive limit method, the running average over 5 seconds and the difference of humidity over 10 seconds before the flux becomes negative.

##### 4.11.4.2 Results:

Conclusions are drawn on the measurements taken on the VF as the results were more likely to be consistent due to is being a low TEWL site. Data was gathered as text file in order to be analysed either with MATLAB, other scripts, or spreadsheets.

**Choice of gradient calculation method:** Using the probe without a cap with the fan at maximum speed the error rate (or coefficient of variation) was 0.323 for the limit positive flux and 0.146 with a running average on 5 seconds. For the palm the improvement was much less: 0.39 to 0.36 so only the volar forearm results are written here. A script calculated the gradient and the error rate for various values of  $\Delta$  : 1.033, 0.764, 0.565, 0.438, 0.344 for gradient taken as a simple difference between two points spaced by  $\Delta = 5, 10, 15, 20,$  and 25 seconds respectively. The longer is  $\Delta$ , the lower is the error rate. Another set of measurements yielded 0.116 for the running average 5 seconds, 0.353 for a  $\Delta$  of one second, and 0.127 for a  $\Delta$  of 10 seconds. Results between the running average over 5 seconds and the difference of humidity over 10 seconds provided similar results. The first was retained due to simplicity of execution compared to the latter. All results can be found in the repeatability ranking A.1

**Cap:** There is less error observed with a smaller cap compared to a larger cap. The smaller cap let less water vapour through and created less disturbance in the cham-

ber. Small caps are usually used in the industry to measure more precise quantities. A smaller error rate is sign of better repeatability. Only the gradient calculated with a  $\Delta$  of 1 second are presented here. For the volar forearm: coefficient of variation was 0.490, 0.546 and 0.664 for the small, medium and large cap respectively. For the palm, the error rate was 0.482, 0.852, 0.304 for the small, medium and large cap respectively. There is less error when using a large cap on the palm that has high flux. Using the running average method on 5 seconds (and the large cap on the palm), the coefficient of variation was 0.045, which is reaches the project objective of 0.05. Unsurprisingly, there is an improvement using a large cap to measure the high TEWL of the palm. Similarly, it's better to use a small cap to measure the low TEWL of the volar forearm.

**Fan Speed:** Only the gradient calculated with a running average of 5 seconds are presented here. For the volar forearm: coefficient of variation was 0.230, 0.329 and 0.225 for the low, medium and high speed respectively. For the palm, the error rate was 0.314, 0.183, 0.089 for the low, medium and high speed respectively. A low, medium and high speed were compared. The error rates did not vary drastically with the different speeds. In Fig. 4.56a, the Chamber 9 measurements on the VF are plotted against the Aquaflux measurements for three speeds (three voltages). The slope of medium and high speeds were closely correlated. Low speed provided the best sensitivity.

**Sensors:** Sensor 1 and sensor 3 provided similar repeatability. Sensor 1 showed a little bit less error than sensor 3 without a cap and for the wrist only (16% vs.24% with moving average 5s method).

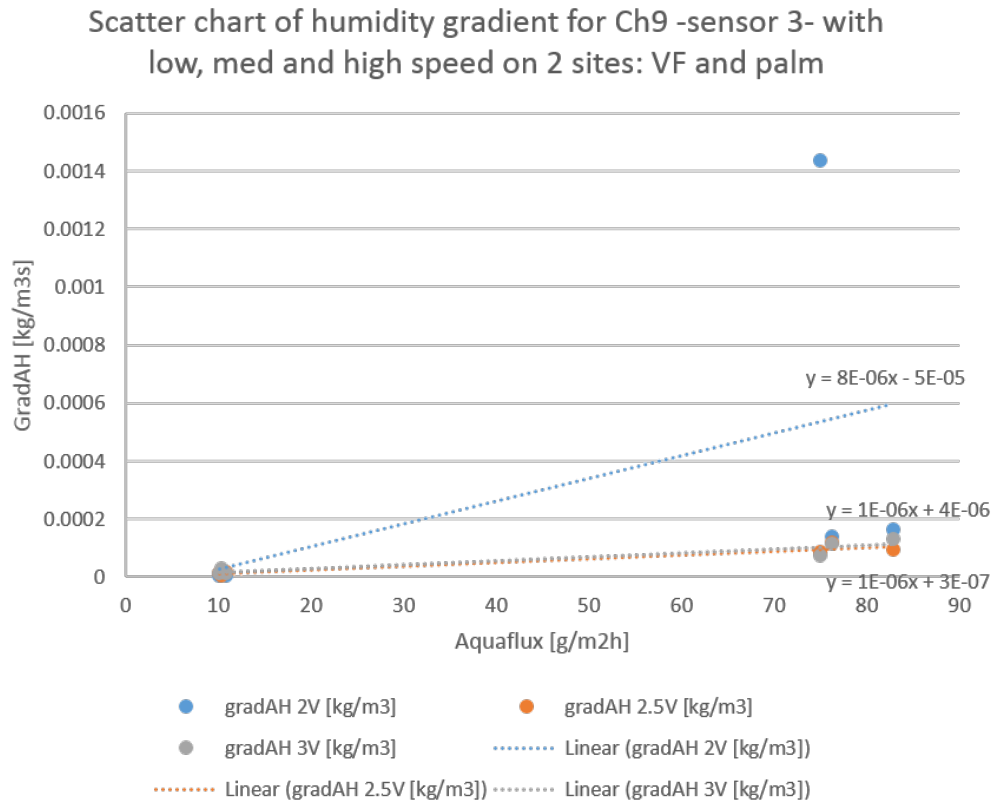
#### 4.11.4.3 Calibration:

Chamber 9 calibration curves showed better sensitivity with a larger cap than a medium or small cap (Fig. 4.56b) and with a low speed 4.56a.

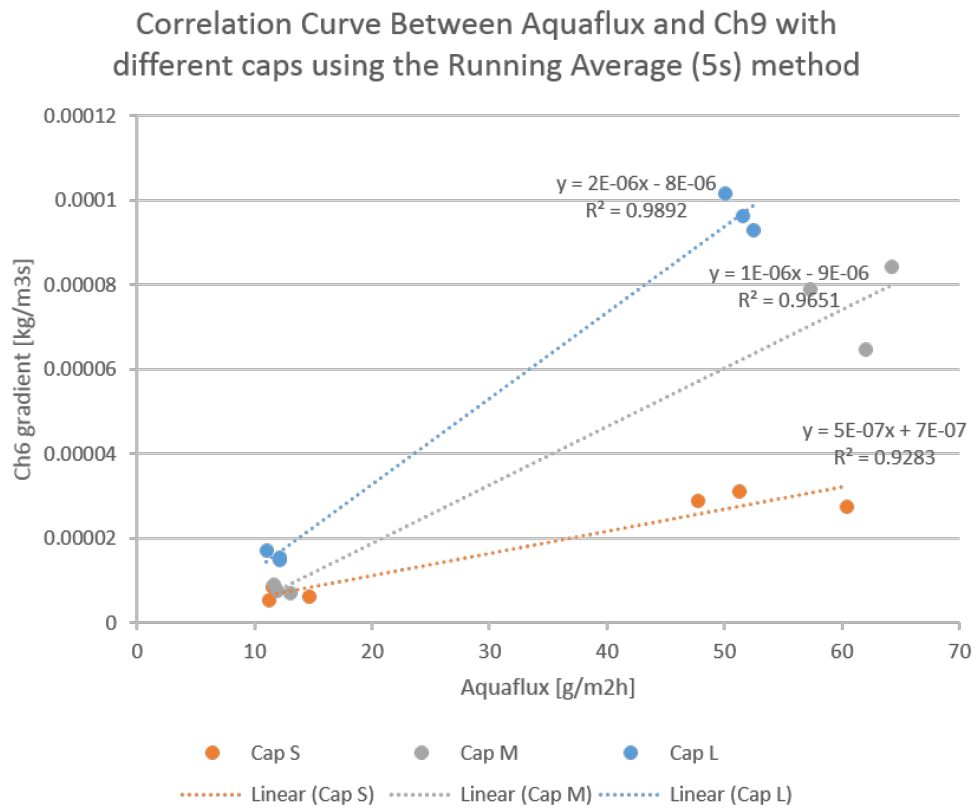
#### 4.11.4.4 Simulation:

The simulation was performed for the small cap only and with the blower working at maximum speed, with a TEWL value and initial conditions (relative humidity and temperature) specific to a measurement. The latter was then compared to the simulation results.

The simulation showed a slight gradient of humidity and temperature near the skin within the chamber (Fig. 4.57). As expected the blower homogenises the microclimate, by making the temperature and humidity uniform in the chamber. The velocity coming in and out of the blower is seen in Fig. 4.57c.

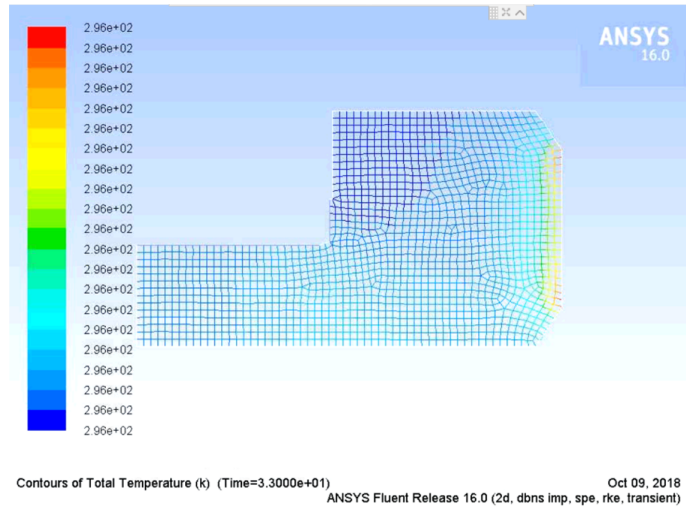


(a) Comparison of different voltages supplying the fan (i.e. speeds)

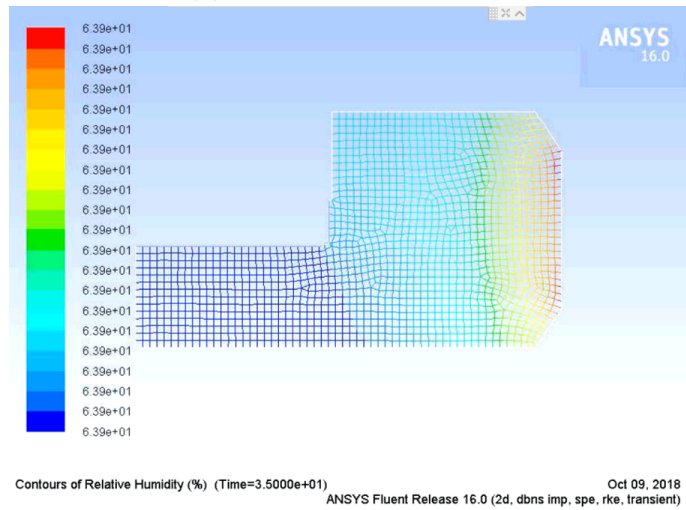


(b) Comparison of different caps: small, medium and large

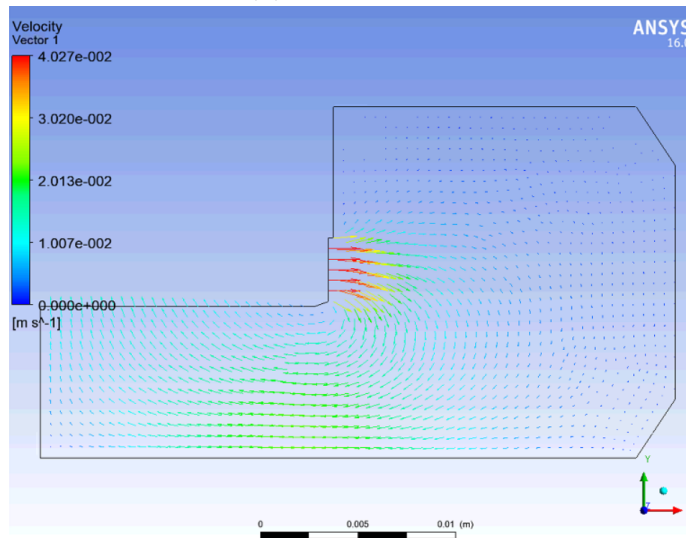
Figure 4.56: Correlation curves between chamber 9 and the Aquaflux



(a) Temperature gradient



(b) RH gradient



(c) Velocity

Figure 4.57: Chamber 9 Simulation results in Fluent at 30s: Temperature, RH distributions and velocity vectors at t = 30 seconds

Differences were observed between the video results and post-processing:

- RH gradient was bigger in the videos;
- RH was provided in Fluent, water mass fraction in post-processing; and
- Videos were not repeatable.

The causes of the videos not repeatable are likely to be because of a bug in the ANSYS software. Common software architecture design would programme videos generation to be originated from post processing results. Inconsistent titles and physical values were displayed in the videos. However, the author doesn't have access to proprietary code and cannot explain why there was a difference between videos and post processing results.

It is easier to work with relative humidity, so the results shown here come from Fluent. The videos were not repeatable, therefore surface and volume monitors were used.

The surface monitors were recorded at the same frequency as the measurements with Chamber 9. They are compared to the experimental values on Fig. 4.58. The average and maximum value of these surface monitors for temperature and RH are provided: T, Tmax and RH, RHmax. AH and its gradient are calculated according to section 2.7.3.

After excluding the first five seconds of simulation, the rest of the model closely resembles reality. The five seconds stabilisation time are the time needed by the model to pass the initialisation phase.

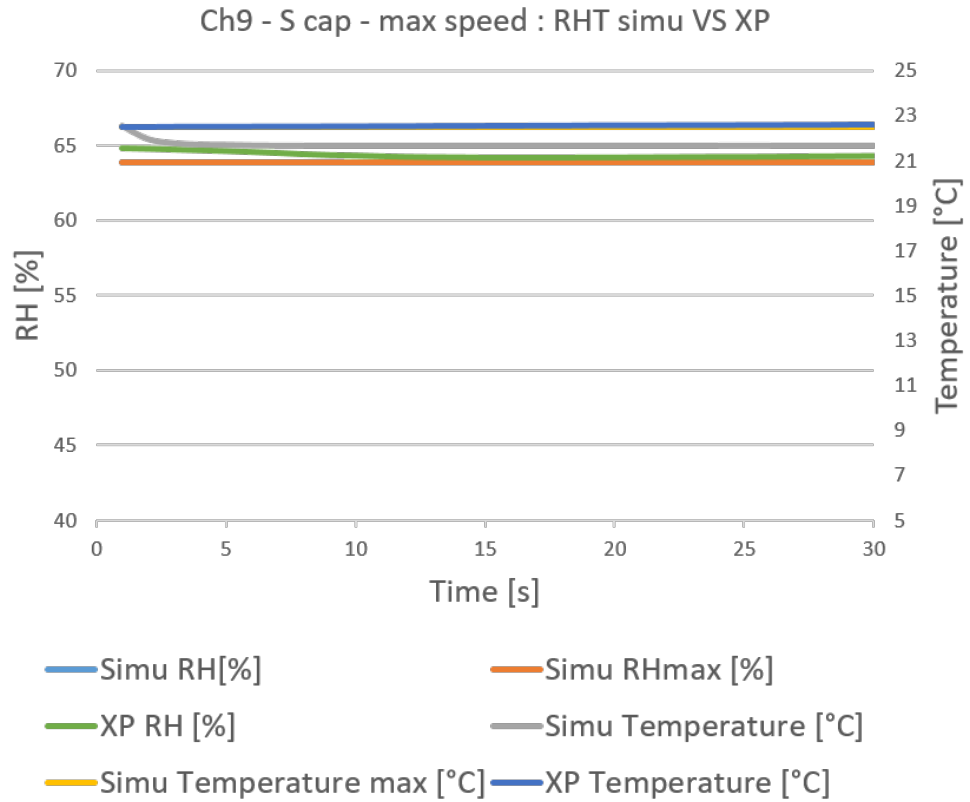
#### **4.11.5 Chamber 9 with the final method for gradient computation**

For this version (v9), least square fitting was used to calculate the expected humidity and the gradient.  $\chi^2$  is low when the distance between the observed and the expected curves are small. The gradient is taken when  $\chi^2$  is below a threshold to be determined. Two methods of gradient calculation were compared; one using the minimum  $\chi^2$  during the measurement period, and the other one using the last value before  $\chi^2$  is not below the threshold. The two points were usually close and the error rate was 18% less for the minimum.

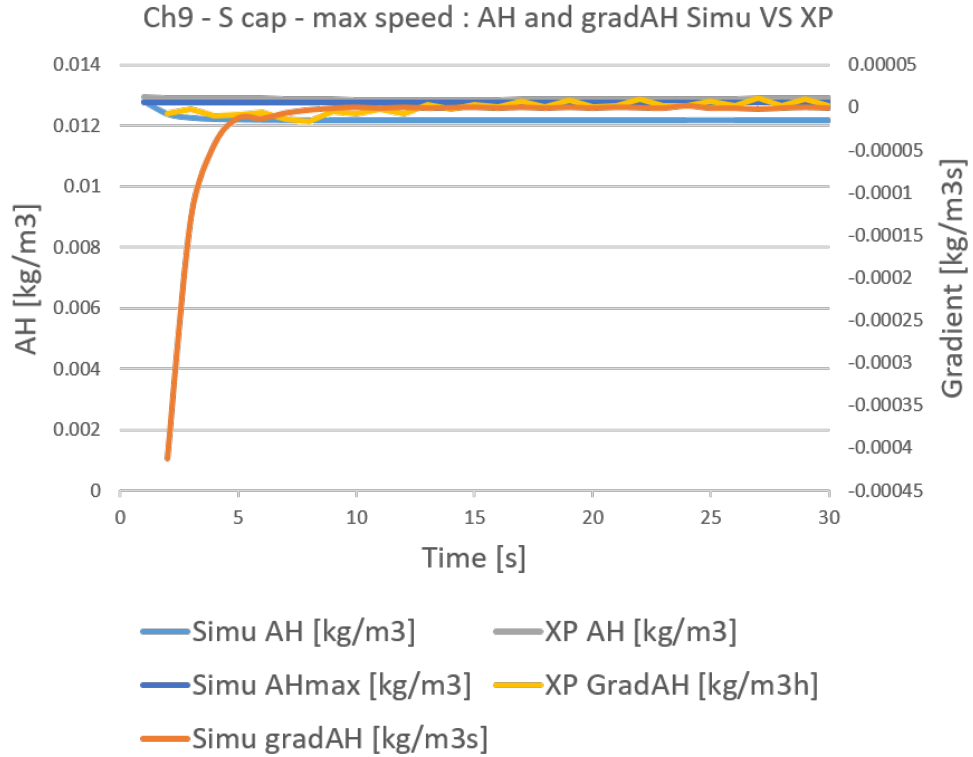
##### **4.11.5.1 Least squared fitting tuning:**

In order to tune the Least Square Fitting, measurements on the skin of one participant were taken according to the methodology stated in section 4.2 on page 91 and





(a) RH and Temperature measured and simulated



(b) AH and gradient measured and simulated

Figure 4.58: Real and simulated 30s measurement on the VF with fan at maximum speed

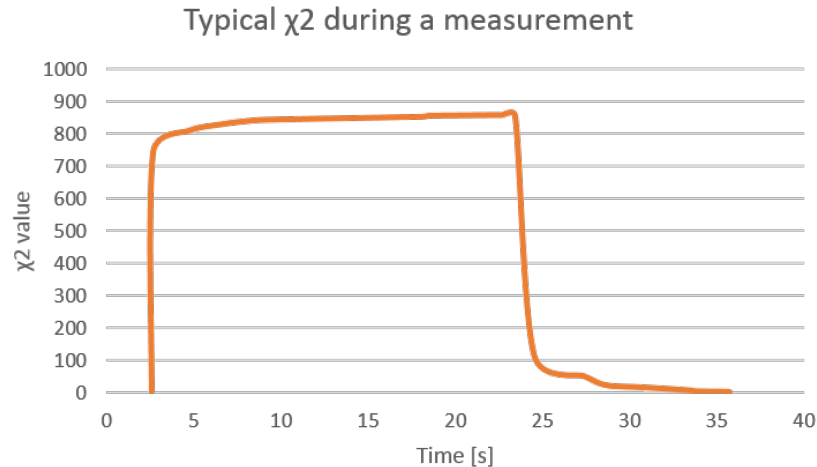


Figure 4.59: Typical curve of  $\chi^2$  variation with time during a measurement

the Testing part of this section. Measurements were taken on the volar forearm, for a duration of 30 seconds initially.

With Chamber 9 the  $\Delta$  and start time for the gradient computation are given as an input for the C# software.

In order to find the parameters for this chamber, the author based the first test on the results from the variation of  $\Delta$  experiments (duration of computation) and Start Time (stabilisation time) with Chamber 9. The same experiment was performed and presented for probe 7.1 in section 4.10.5.4. A script tried all variations of  $\Delta$  and start time to help identify an optimal couple  $\Delta$ , *start*. It was found that later start times and larger  $\Delta$ s reduced the error.

The error  $\chi^2$  was observed and it always followed the same behaviour; it increased rapidly and then decreased after a period of stability (see Fig. 4.59). After reaching a minimum it slowly increases. The minimum was usually below 1 and rarely below 0.01. A target threshold was set at 0.01: when the curve between the expected and the observed humidities are close together. The threshold was reached in 30 seconds on average with the small cap. However, a third of the measurements didn't reach the threshold within 40 seconds, the cut off for the measurement duration. The target threshold was smaller for sensor 1 (0.01) than sensor 3 (0.1). A script was run to find the duration of the peak across all measurements files. The peak width is on average 24 seconds for the different size of caps, sensor 1 and sensor 3.

The value of  $\chi^2$  was also observed at 40 seconds for different values of the parameters start time and  $\Delta$  (Please see Fig. 4.60 for data).  $\chi^2$  was smaller for smaller start times and  $\Delta$ s for sensor 1 and 3 when compared with the small, medium and large caps. For these reasons, when using the minimum  $\chi^2$  method it is not convenient to wait for a long time to calculate the gradient. In addition, slightly better results were observed with the couple  $(\Delta, \text{start time}) = (1,1)$  for sensor 1 and 3 when

compared with the small, medium and large cap (Please see Fig. 4.61a for data). For this couple (1,1), the minimum  $\chi^2$  was reached or the duration of stability state where  $\chi^2 < threshold$  was longer.

$\chi^2$  threshold had to be set up as an input for the program. It depends on the configuration of the chamber, the cap size, the fan speed and the sensor. A smaller  $\chi^2$  threshold means a smaller error between the expected and observed value, so a longer measurement for fitting is necessary. A smaller  $\chi^2$  leads to better repeatability. A few values for  $\chi^2$  were tested to determine the best configuration of the probe:  $10^{-2}$ ,  $10^{-3}$ ,  $10^{-4}$ ,  $10^{-5}$ ,  $10^{-6}$ . At low values,  $\chi^2$  decreases slowly, oscillates, and then finds a plateau until it increases again (see Fig. 4.59). An optimal value for  $\chi^2$  was found for  $10^{-4}$  to provide the lowest error rate (and therefore the best repeatability).

#### 4.11.5.2 Results:

The error rates were of the same order as chamber 5.1 i.e. really high therefore the precision was really low.

**With and without the fan:** The error rate was bigger with the fan at full speed than with the fan off. The slope of the calibration curve was 30% bigger with the fan at full speed than without the fan. Therefore, the sensitivity compared to the Aquaflux was better with the fan.

**With different speeds:** The fan speed did not influence the temperature in the chamber. Contrary to previous Chamber 4, it is nice to use and is not uncomfortable after a long measurement duration (2 minutes application on the skin). Measurements were taken with sensor 1 in quadruplicate for six speeds: 0 RPM, 6280 RPM, 8882 RPM, 10353 RPM, 12630 RPM and 13908 RPM. For the volar forearm, coefficient of variation were 0.904, 1.359, 0.208, 0.309, 0.419, 0.147 respectively. Sensitivity slope (taking into account VF and palm skin measurements) were  $6 \cdot 10^{-5}$ ,  $6 \cdot 10^{-6}$ ,  $3 \cdot 10^{-5}$ ,  $5 \cdot 10^{-5}$ ,  $3 \cdot 10^{-5}$ ,  $4 \cdot 10^{-5}$  respectively. The lowest speed at 6280 RPM didn't lead to good results. It is likely due to the difficulty to set a low speed with precision. Below a certain threshold (the lower speed), the fan doesn't run. Overall, repeatability is better at high speed. However sensitivity decreases with the fan speed.

Another experiment was conducted using sensor 3 on the volar forearm, the cheek and the palm. The coefficients of variation were 1.13 at minimum speed and 1.33 at maximum speed. Using sensor 3, the minimal speed yields better results.

**With different caps:** This chamber more often reached a  $\chi^2$  below the threshold with smaller cap, and rarely within 30 seconds with a larger cap. The quantity of

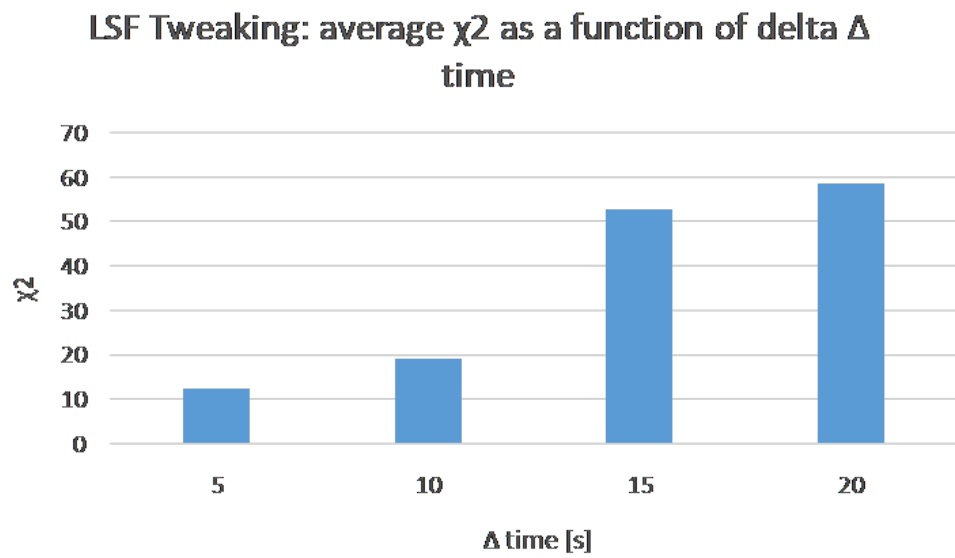
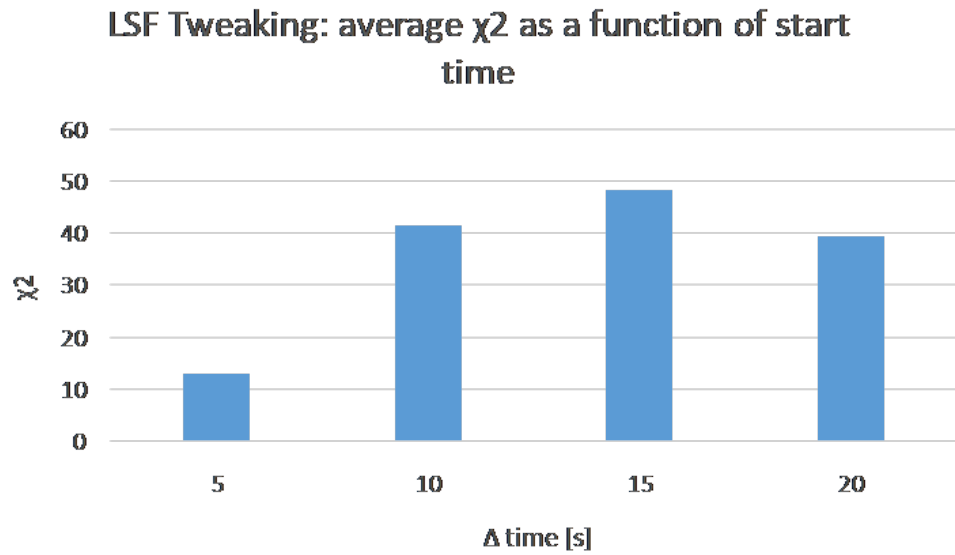
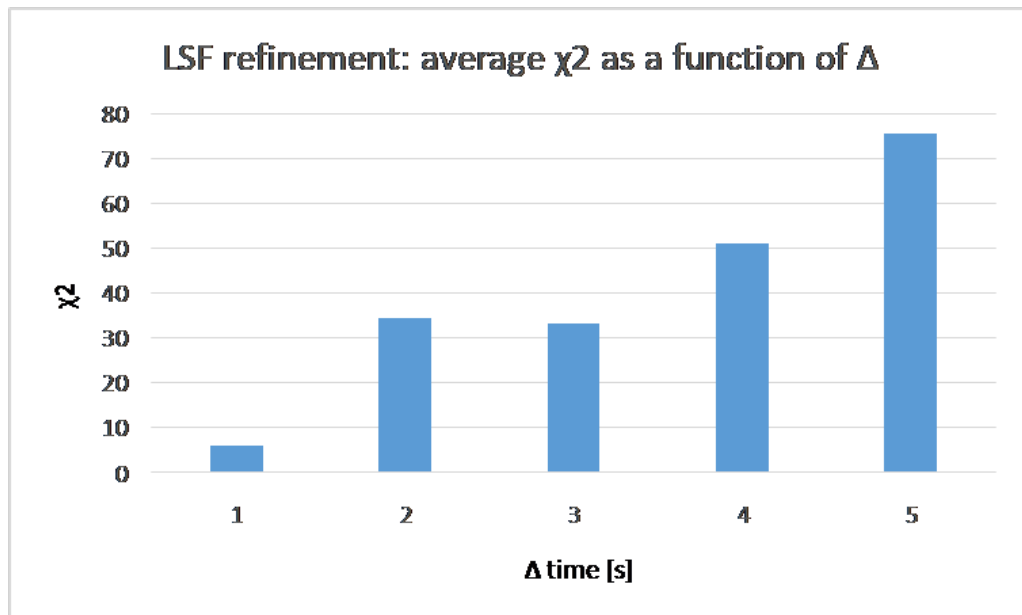
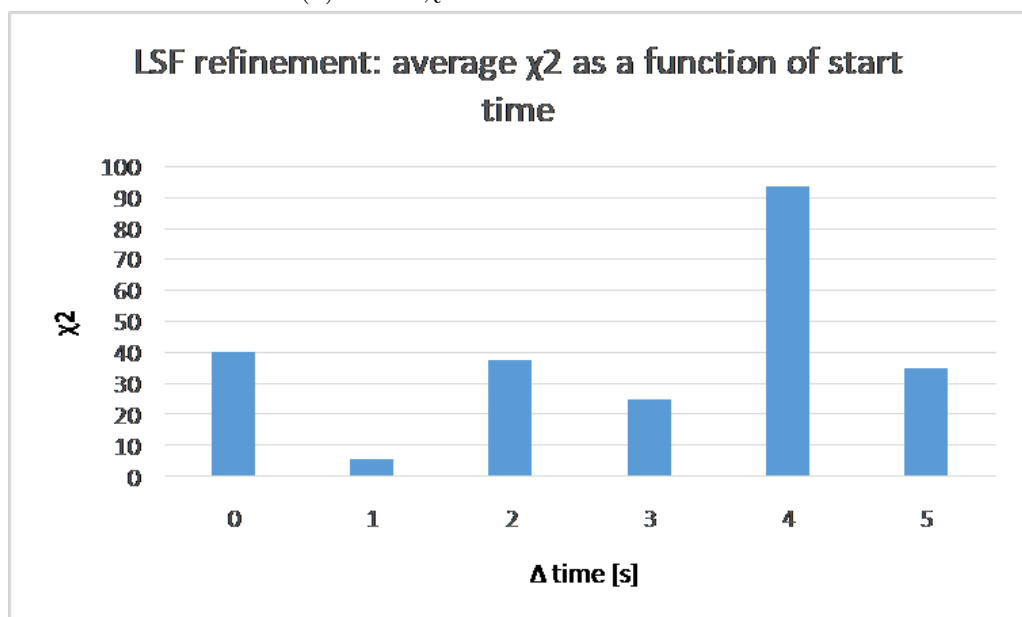
(a) Error  $\chi^2$  in function of  $\Delta$  time(b) Error  $\chi^2$  in function of start time

Figure 4.60: Coarse tweaking results



(a) Error  $\chi^2$  in function of  $\Delta$  time



(b) Error  $\chi^2$  in function of start time

Figure 4.61: Fine tweaking results

water coming through the opening of a larger cap or without a cap is greater and the LSF<sup>23</sup> usually need more time to stabilise. Measurements were taken on the volar forearm and the wrist in triplicate and quadruplicate for the following cases: without a cap, with a large cap, medium and finally a small cap. For the volar forearm, the error rates were 1.38, 1.43, 1.15, 1.33 respectively. The coefficient of variation decreased with the size of the orifice and therefore input of TEWL in the chamber. For the wrist, the errors rates were: 0.89, 1.32, 1.38, 1.47. The precision decreased when using a smaller cap, so the coefficient of variation increased with the inadequacy of the caps with a high TEWL.

**With sensor 1 and sensor 3:** This chamber showed less error and better repeatability with sensor 1 than sensor 3: the error rate was much higher with sensor 3 than sensor 1. The errors were higher using the Least Square Fitting method compared to the moving average method. The slope of the calibration curve with the Aquaflux was more important for sensor 3 than sensor 1. Thus, the sensitivity is higher with sensor 3 than sensor 1.

#### 4.11.5.3 Calibration:

Better results were obtained with the small cap rather than the large one (Fig. 4.62). Sensor 1 had a negative slope (Fig. 4.63), suggesting that in this set of measurements it was unable to differentiate between a small and a large TEWL. Sensor 3 had better results, with low speed providing better sensitivity than high speed (Fig. 4.64). These results were calculated used a running average over 5 seconds. The results were confirmed using LSF, although the points were more spread and therefore the measurements look less repeatable using this alternative calculation.

#### 4.11.5.4 Quick summary of the results to date

To summarise, this probe tested the previous gradient computation methods such as limit positive flux, gradient as a different between two time points, and running average.  $\Delta$  and start time were used as parameter to improve the results. Calculation of the gradient is a crucial part of a TEWL chamber design. A last method, Least Square Fitting was implemented, using the last two parameters as an input.

Using this method, a new value was introduced:  $\chi^2$ . It is used to measure the error on the measurement, in real time, at the moment when the measurement is taken. Using this method, the optimal  $\Delta$  and start time were  $\{ 1 ; 1 \}$ . Then the

---

<sup>23</sup>Least Square Fitting

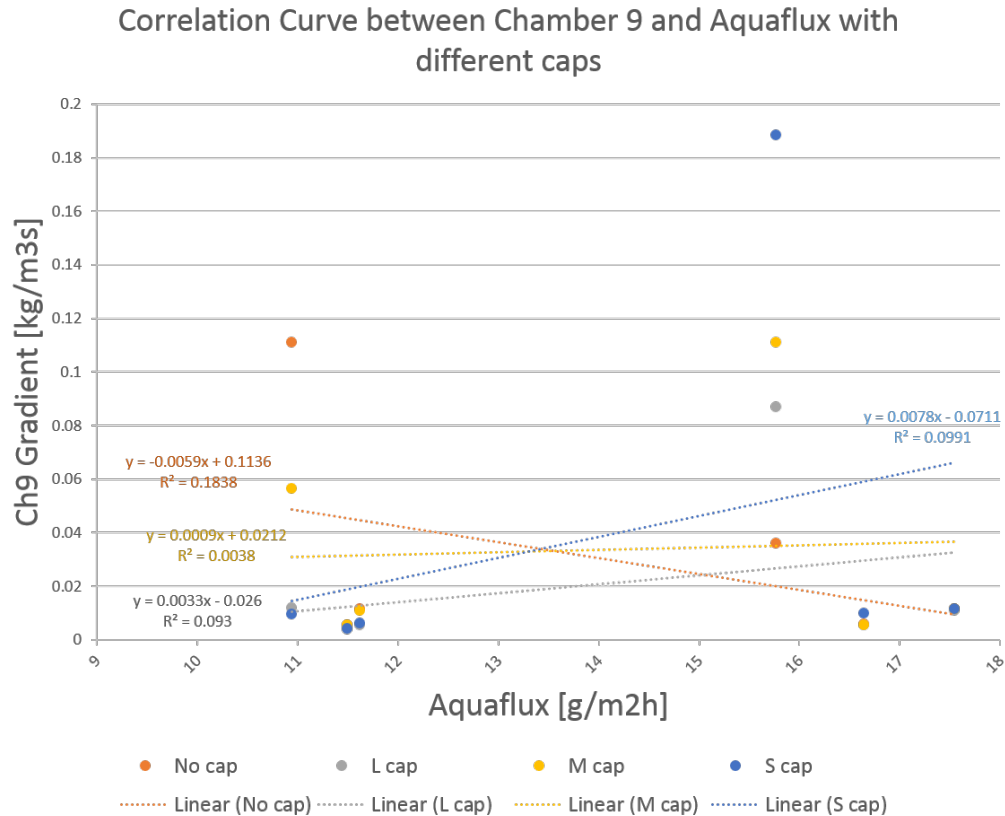


Figure 4.62: Correlation curve with different caps using Least Square Fitting

following battery of tests were performed: with and without the fan, with different sensors, fans speeds and caps.

Results shown better repeatability without the fan, but better sensitivity with the fan. This was confirmed with chamber 3, 4 and 7.1: coefficient of variation (or error rate) is higher without the fan. Sensitivity, deducted from the calibration curves shown a higher sensitivity with the fan, than without the fan. Similar results was found with probe 7.1.

Furthermore, higher speed of the fan yielded better precision. However sensitivity decreased with the fan speed. This were two surprising results, as it was contrary to previous observation with chamber 3, 4, and 7.1 where precision increased with lower fan speed and higher sensitivity was found with the fan. Again, a trade-off has to be found between repeatability and sensitivity.

In addition, probe 9 permitted the testing of caps:  $\chi^2$  reached its target quicker with a smaller cap than a larger cap. On one hand, the results confirmed that a smaller orifice is more adapted with smaller TEWL of the volar forearm, and using a larger orifice will decrease the precision. On the other hand, the results shown a larger orifice is more adapted to a high TEWL site and the repeatability of the measurement will decrease if a smaller cap is applied.

Moreover, results using LSF shown better repeatability using sensor 1, compared

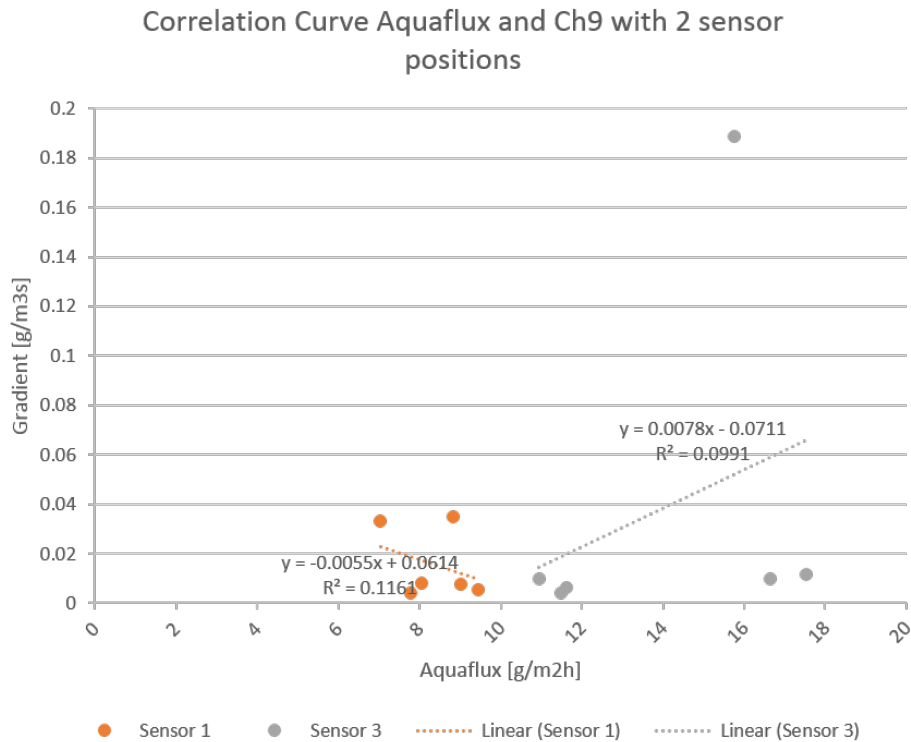


Figure 4.63: Correlation curve with sensor 1 and sensor 3

to sensor 3. However sensitivity was better for sensor 3 than sensor 1. Results with sensor 1 were actually unsatisfactory as the calibration curve had a negative slope.

The next section is an attempt to improve the results. More skin sites were studied. The volar forearm is chosen for its easiness to obtain repeatable results. Thus, a small cap was chosen because it yields better results on the volar forearm measurements. In addition, sensor 3 is retained because sensor 1 didn't provide acceptable results. Finally, a smaller fan speed was taken for better sensitivity. Using sensor 3, better precision was found with the minimal speed.

This constituted the optimal configuration for probe 9 and extended measurement session was conducted with it.



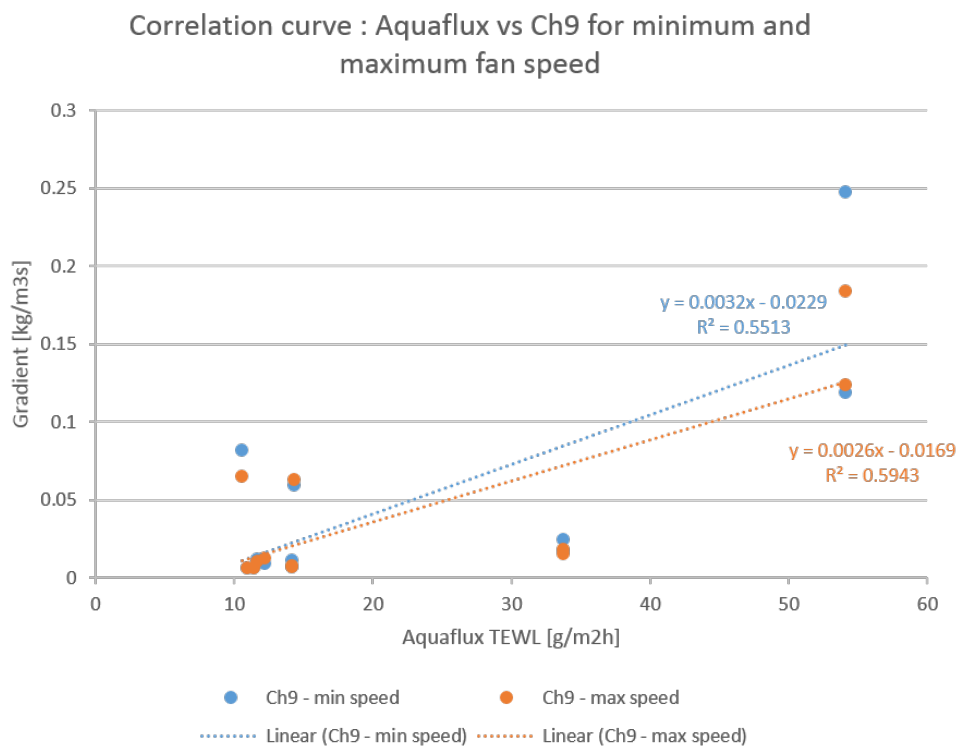


Figure 4.64: Correlation Curve with minimum and maximum speed, on the VF, cheek and palm



Figure 4.65: 7 skin sites of the arm

#### 4.11.5.5 Extended measurement session with the optimal configuration

An extended measurement session was conducted to increase the performance of the probe. It was performed all in one go, on the same subject, as per general methodology described before. However, to increase the performances, there were quintuplicate and more measurement sites. Measurements were taken on seven anatomical sites on the arm (see Fig. 4.65). The measurements were repeated five times per site with both chamber 9 and the Aquaflux. The optimal probe 9 configuration was: sensor 3, small cap, and low fan speed.  $\chi^2$  threshold was fixed at  $10^{-4}$  to reduce the error rate. The average error rate for chamber 9 was 46% (range 9-89%) (Fig. 4.66a and 4.66b). Decreasing the  $\chi^2$  threshold increased the measurement time. The calibration curve for  $\chi^2 = 10^{-2}$  can be seen in Fig. 4.66c. The amount of time taken for the  $\chi^2$  to converge would often take over 45 seconds; longer than the prototype objective for measurement time. The calibration with the Aquaflux is challenging because the Aquaflux had a large error rate for some skin sites. In the configuration settings of the Aquaflux, the target precision was set to  $0.075 \text{ g} \cdot \text{m}^2 \cdot \text{h}^{-1}$  but this was only reached on one of the seven anatomical sites

(middle of the VF). On site 6 (the wrist), the Aquaflux had 44 % error, common for the Aquaflux at this skin site that has high error variation : the contribution of sweating is sensitive to so many factors. The slope varies more for high flux values. Using the Aquaflux to calibrate an instrument is not as consistent as using a fixed quantity of water.

#### 4.11.5.6 Skin surface water loss:

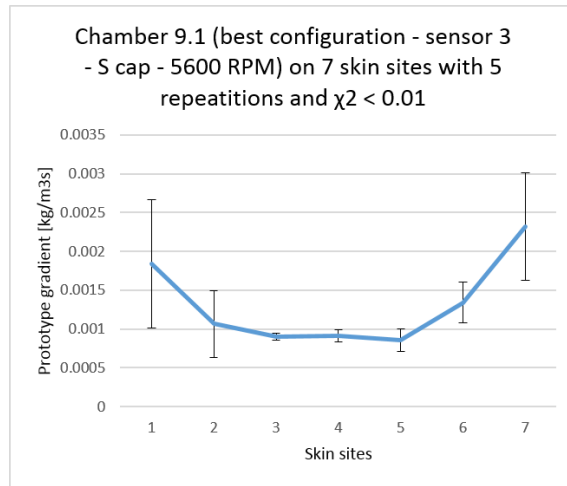
As explained in the methodology, in order to test the instrument outside of a controlled environment, SSWL was simulated with water on the skin and the measurement of TEWL and SSWL.

**Variation with time:** A series of tests were conducted measuring the TEWL of the VF after dropping a small amount of water on the measurement site and brushing it away immediately prior to measurement. Measurements were performed on the volar forearm, in triplicate at  $t = 0$  minute, 10 minutes and 20 minutes. They were also performed at minimum and maximum speed. The error rate was 1.13 at  $t = 0$  minute, and decreased at 0.0066 after 10 minutes and 0.0062 after 20 minutes with the fan at minimum speed. At maximum speed, the error rate was 1.33, 1.13 and 1.20 at  $t = 0$ , 10 and 20 minutes respectively. For the first measurements, Aquaflux would time out after 90 seconds or measure with 58% error. Chamber 9 would measure with 133 % and 113 % error at maximum and minimum speed respectively.

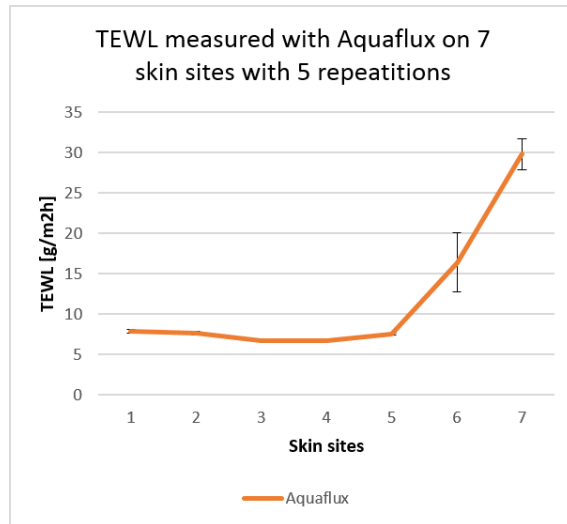
Results didn't show evident variations of water evaporation for the cases at 10 and 20 minutes. The same experiment was performed in a smaller time frame and data was collected before and twice after the application of water. Only the first measurement after application would show the surface water loss.

The humidity profile can be seen in Fig. 4.67. The humidity and the gradient measured was bigger at the beginning of the session. Before droplet application the error rate was 0.33, after it was 0.08, then a few minutes later 0.54. Repeatability of probe 9 was better after application of surface water, than before, or a few minutes after when measurements were conducted with the Aquaflux and had time to dry. The gradient measured was greater straight after the droplet, and 5 minutes after it was slightly lower than before the experiment. The same behaviour was confirmed with the Aquaflux.

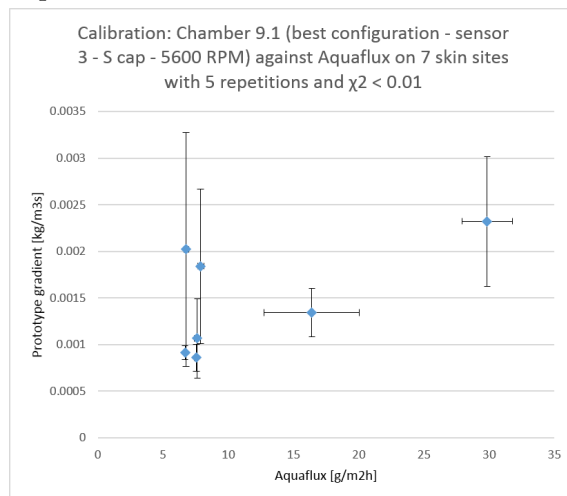
Similar experiments have been conducted by Tagami et al. (1980) with electrical measurement rather than TEWL. They found the water content of the SC wasn't influenced by the presence of water or other dielectric substances.



(a) 35 measurements on 7 skin sites with probe 9



(b) 35 measurements on 7 skin sites with the Aquaflux



(c) Correlation between probe 9 and the Aquaflux

Figure 4.66: Calibration of the last probe with the best configuration

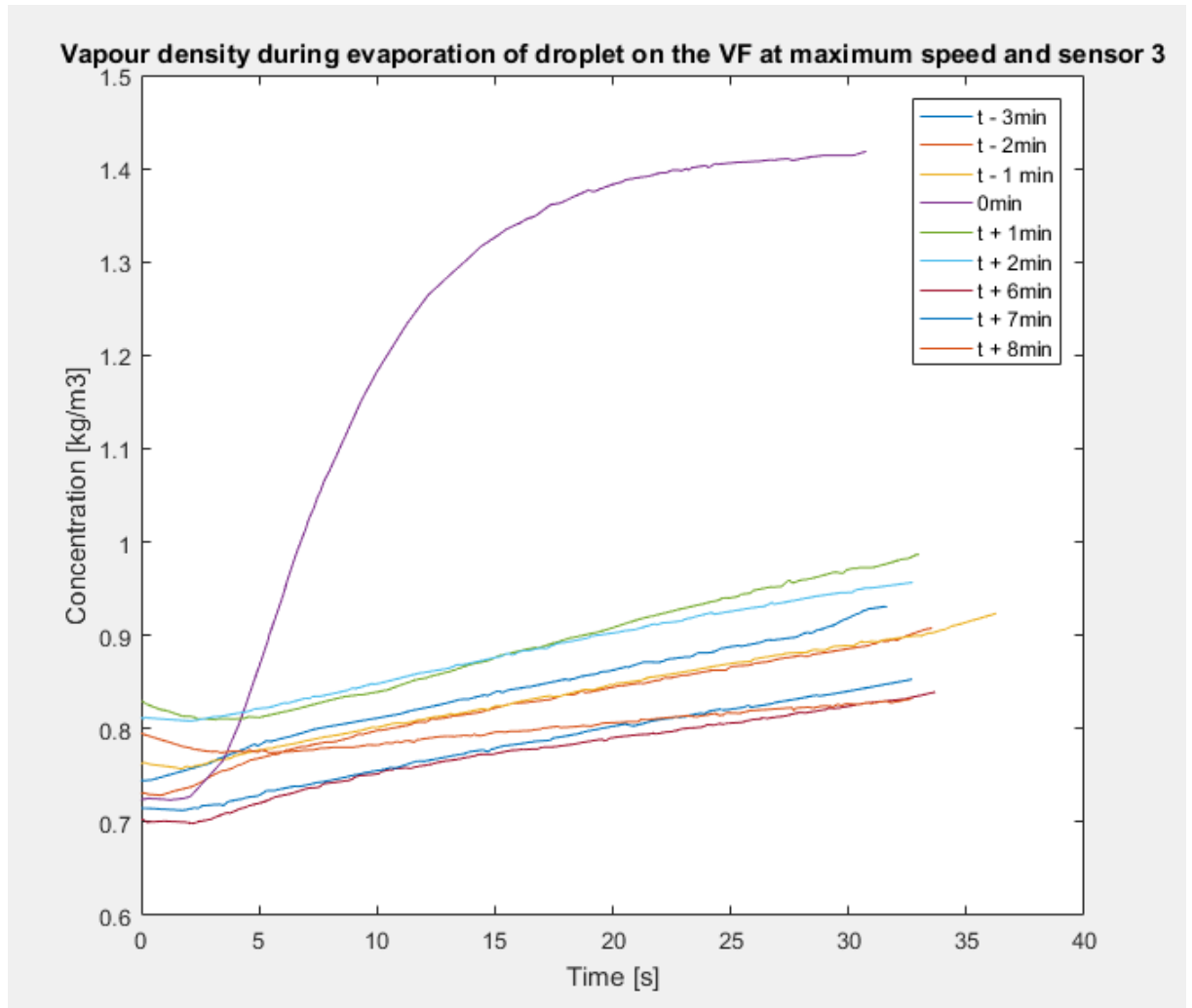


Figure 4.67: Droplet evaporation. Gradient measured at different times: 3 min, 2 min, 1 min before, immediately after, 1 min, 2 min, 6 min, 7 min and 8 min after the droplet application with chamber 9 at maximum speed with sensor 3 and the small cap.

**Variation with speed:** The speed increased the flux measured (Fig. 4.68). It is likely that the fan blows away more of the SSWL with increasing speeds.

In the other set of experiments mentioned above, on water on the skin surface, water was applied and brushed off as per the above experiment and then TEWL was measured at 0, 10 and 20 minutes afterwards with different fan speeds. In this experiment, the speed of the fan did not drastically change the error rate (a decrease of 6% from the maximum speed to the minimum speed) when measuring SSWL.

The flux measured increased with the fan speed, but the error rate was similar. Therefore, a lower speed is beneficial to measure the surface water in order to measure the smallest quantity possible. After the SSWL has evaporated, there is only the insensible perspiration to measure. At that time, the gradient measured varies and the slope of the humidity changes angle. Henceforth, a higher fan speed

to measure with better the TEWL with better sensitivity would be preferred.

The minimal speed the blower can achieve is 5000 RPM and that is sufficient to homogenise the microclimate in the chamber quickly. Regarding the optimal speed to measure TEWL, a trade off was found between repeatability and sensitivity. A speed around 11500 RPM constituted a good middle ground between lowest error rate and highest calibration slope.

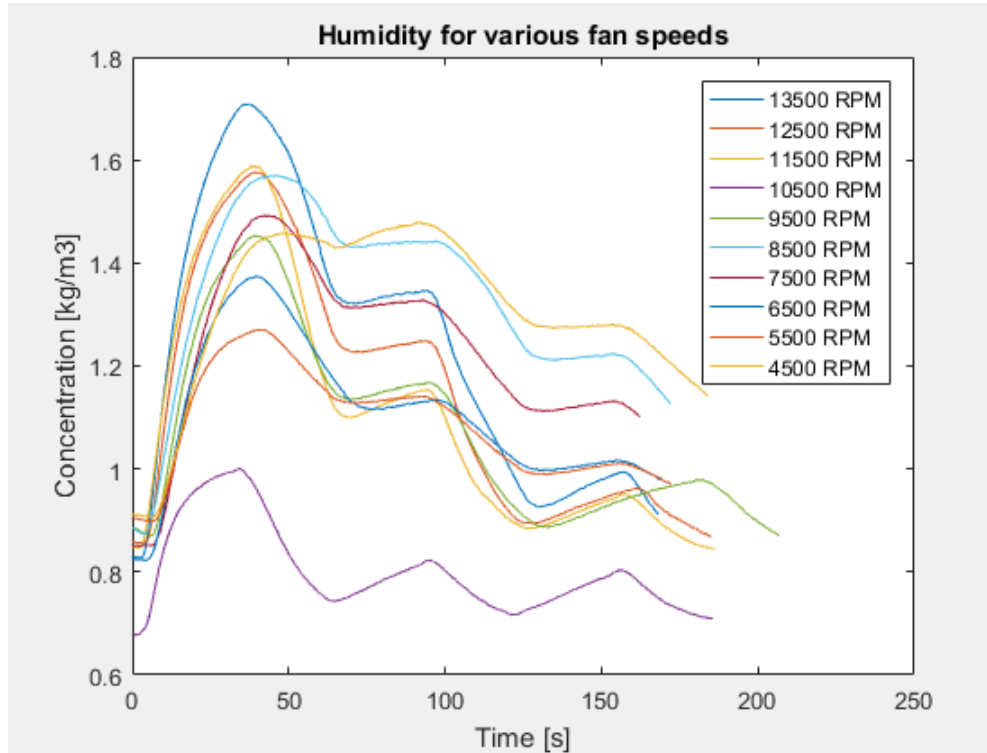


Figure 4.68: Evolution of the absolute humidity measured three times consecutively on the volar forearm with a droplet of water at different fan speeds.

**Data Limitations:** The results here have to be taken with precaution because the measurements were not very reproducible:

- The amount of water present within the chamber has to be small or the Aquaflux will time out before it gives a result.
- Small amounts of water are difficult to consistently measure; it is difficult to obtain error rates and sensitivities for small volumes because the water evaporates too quickly to perform triplicates (or even duplicates).
- The surface water evaporates quickly compared to the time of convergence of Least Square Fitting so it is not possible to take consecutive measurements (Fig. 4.68).

- The fan removes the surface water quickly and consecutive measurements show very little gradient change due to the lack of water in the chamber (Fig. 4.69).

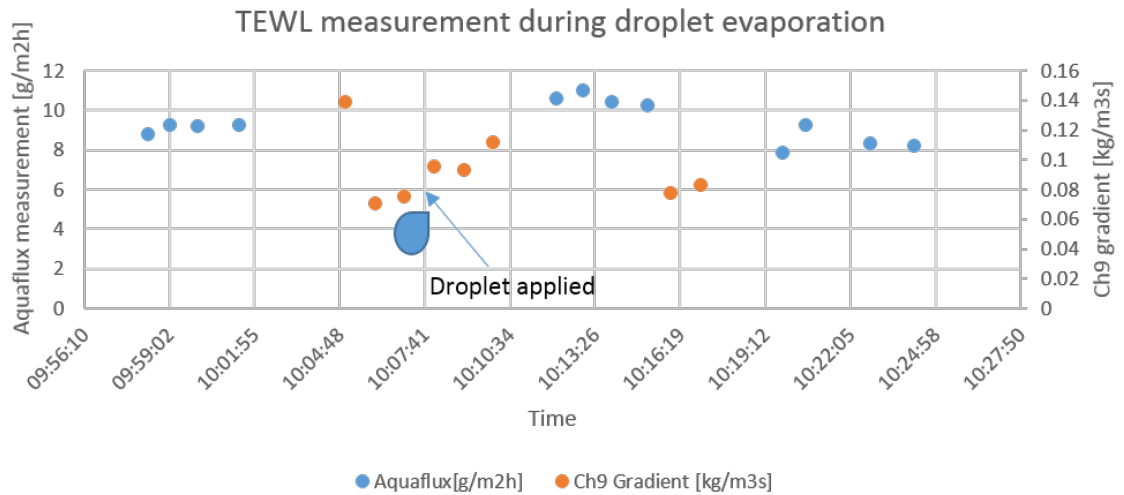


Figure 4.69: Evolution of TEWL with time on skin with forced surface water. This was measured at maximum fan speed with sensor 3 and the small cap.

## 4.11.6 Discussion

### 4.11.6.1 Basic gradient calculation method

With this probe were tested many gradient calculation methods, such as the positive limit method, the running average 5s and the large gradient of  $\Delta$  varying from 5 to 25 seconds. The favourite method was the running average on 5 seconds because of the overall good repeatability and the simplicity of implementation. Later in the project, Least Square Fitting was used. The discussion will first focus on the first part of the project.

Using a simple calculation method or adding a running average on top of it yielded the following results of repeatability: the coefficient of variation of volar forearm TEWL didn't vary much with the speed of the fan. However, the error rate of palm TEWL measurements decreased with the speed of the fan. Therefore the fan improve the repeatability of measurements of high flux.

With regards to sensors, 1 and 3 provided similar results, although sensor 1 was slightly better for higher flux. Sensor 1 is closer to the exit chamber. There may be more air mixing in this region, and it would be better for high TEWL to have a turbulent flow.

Moreover, the use of caps shown better results when they were used appropriately: the small cap on a low TEWL site such as the palm and the large cap on a

high TEWL site like the palm. In addition, the project objective of 0.05 was reached using the large cap on the palm (and a running average of 5 seconds).

Regarding sensitivity results, the calibration curves shown higher slope (and therefore better sensitivity) with low speed compared to high speed. However on the same graph 4.56a the points are more dispersed for a lower speed. Dispersed points are a sign of low repeatability. In addition, the sensitivity was higher using the large cap, rather than a medium cap, or even a smaller cap (see Fig. 4.56b). It is the case because the large cap don't have a problem to measure high TEWL. In addition, it shown good repeatability for low and high TEWL. The large cap is more versatile.

Chamber 9 using the running average over 5 seconds had better precision (i.e. repeatability) with a large cap, a low fan speed and using data from sensor 1 or 3.

The project objective was to develop an instrument that yield high repeatability, with a coefficient of variation or error rate below 0.05. This target was achieved using running average (5s) method with a large cap. For this case, the error rate was 4.5%.

In addition, another project objective was to develop an instrument that has good sensitivity. The slope of the calibration curves had to be higher than the Aquaflux which slope was  $3 \cdot 10^{-7}$ . This objective was attained with the probe 9, using sensor 3 and the running average method with a gradient of 5 seconds: using either low, medium and high speed, but also while varying the cap size: small, medium or large.

#### 4.11.6.2 Least Square Fitting gradient calculation method

Regarding probe 9 using the LSF method for gradient calculation, the results were quite different and provided higher coefficient of variation. The precision was lower, and didn't meet the project objective of 0.05, they are discussed hereafter.

The quick summary in 4.11.5.4 taught the optimal couple  $\{\Delta; start\}$  was  $\{1;1\}$ , while using a basic method to calculate the gradient (limit positive flux, with a running average or as a difference of humidity between two time points), results could be improved by tweaking  $\Delta$ , the time duration on which the gradient is calculated over. The longer was  $\Delta$ , the lower was the error rate. It is because the measurements had time to stabilise. Probe 7.1 introduced the optimisation of repeatability by changing the values of start time to wait for stabilisation and  $\Delta$  duration of computation. Similar experiment was conducted for probe 9. It was found that later start times and larger  $\Delta$ s reduced the error.

These were different results from the LSF gradient calculation method. The first computation methods evaluated the repeatability with the error rate or the coefficient of variation. With the Least Square Fitting Method coupled with a  $\chi^2$  test, the stability of the measurement is optimised.



Measurements are more repeatable on the volar forearm (or other low coefficient of variation sites ranked by Rogiers (Rogiers 2001) ). Probe 9 with LSF yielded better results with a small cap, sensor 3 and low speed. Using a more basic gradient calculation method, the optimal configuration was a large cap, a low speed with sensor 1 or 3.

The simulations shown turbulences to be more important in the region of the sensor near the skin, sensor 1, compared to the region near the back of the chamber, sensor 3. However, this is not the result found with probe 9 using LSF. The discrepancies could be explained by a few reasons. First, the difference of turbulences between the region of sensor 1 and region of sensor 3 are light. Although the simulations provided acceptable results in terms of accuracy for prediction of the overall RH, temperature and gradient (predicted values and experiments values are plotted on Fig. 4.58), the models are 2D. As such, they consider the L-shape of the blower to be infinite, and don't take into account it is a cylinder instead.

Regarding the sensitivity results, calibration curves were plotted for different caps, different sensors, and different fans speeds.

Using probe 9 with LSF, not using any cap didn't yield good results at all, the calibration curve shown a negative slope. This would have been caused by the uncertainty of high TEWL measurement. The best results were provided by the small cap, the large cap, then the medium cap (see Fig. 4.62), with a slope coefficient of 0.0078, 0.0033 and 0.0009 respectively. These three values are higher than the slope of the Aquaflux. Thus, these 3 configurations achieved the project objective. A small cap let less water coming in and the sensitivity is expected to be higher for instruments with smaller orifice and smaller chamber size.

The calibration curve with two sensors positions shown a negative slope for sensor 1 (see Fig. 4.63). The slope for sensor 3 is 0.0078 which is higher than the project target. Sensor 1 was expected to show better sensitivity. It was probably too sensitive, during the measurement of the low TEWL.

Using a low speed lead to higher slope than a higher speed, see Fig. 4.64, although the lines are close together: the slope for maximum and minimum speed are 0.0026 and 0.0032 respectively. These two slopes coefficients are higher than the project objective.

#### 4.11.6.3 Optimal configuration

The optimal configuration had for aim to improve the repeatability and for the coefficient of variation to reach the target of 0.05.

In addition, performing measurements in quintuplicates rather than triplicates can lower the coefficient of variation.

Moreover, another method to increase the repeatability was to lower the  $\chi^2$

target, and to maintain the application until the threshold is reached. This way, the instrument can trigger the measurement and calculation of the gradient when the readings are stable enough. The stabilisation time was quite long, and could take a minute or so. For probe 9, the measurement in the middle of the volar forearm were the more repeatable, where the error bar is quite small, especially for site 3, 4, 5 (see Fig. 4.66a). Using a  $\chi^2$  of 0.001, the repeatability was at the highest for skin site 5 where the coefficient of variation was 0.05 which meet the project objective. In addition, the calibration curve also had satisfying results. It lead to a slope coefficient of  $10^{-5}$  which is higher than the Aquaflux slope coefficient and met project objectives. On Fig. 4.66c, the horizontal bar are usually smaller than the vertical bar, except for skin site 6. The Aquaflux perform more repeatable measurements, except for this site. It's because the error on the measurement is quite high because it's near the wrist and sweating glands. Using a fan removed the surface water and could measure better area with high TEWL or surface water.

By choosing an optimal configuration, performing more measurements, waiting long enough to have a stable gradient helped to reach the project objectives.

#### 4.11.6.4 Surface Water

The aim of the project is to develop an instrument capable to work in an uncontrolled environment. The solution investigated in this thesis is to use a blower. In order to test this hypothesis, a few experiments on moist skin were conducted. First the variation of measurements with time, then with different fan speeds.

Two experiments were conducted when measuring TEWL and SSWL on the volar forearm at different time. The first experiment measured a low speed and full speed a skin site with some surface water applied at the start, and measured again after 10 minutes and 20 minutes. At low speed, the coefficient of the measurements at  $t = 0$  was much twice as much as  $t = 10$  or 20 minutes. However, at high speed, the coefficient of variation was quite high at all time. It is therefore better to measure SSWL and high flux in general at low speed.

At low speed, the difference between the case where the TEWL and SSWL are measured and the case where TEWL only is measure was clear while at full speed the evaporation process wasn't as clear. Another experiment was conducted to measure the evaporation of a droplet.

With a fan at full speed, the first measurement has an exponential growth and then a plateau (see Fig. 4.67.). This corresponds to a saturation of water vapour in the chamber. It comes from the droplet used to simulate surface water. From the second measurement onwards, the curves follow the same linear shape. The slope of these curves, is the gradient calculated along this thesis, TEWL. The droplet evaporated quickly with the fan at full speed. Interestingly, the results following the

evaporation of a droplet shown the prototype had better repeatability on moist skin than normal skin.

Regarding the project objectives, the aim was to have a coefficient of variation of 0.05, and it was reached twice. The minimum was 0.0062 after 20 minutes after the application of surface water. This is a really small coefficient of variation. However this waiting time is definitely out of acceptable range.

#### 4.11.7 Conclusion

The chamber 9 tried out a totally new design, to avoid the air of the interior of the chamber to heat. There were 2 sensor positions and a 15 mm fan. This probe 9 tested a few gradient calculation methods, and the configurations offered by various fan speeds, three caps with different orifice sizes and two sensors positions.

The gradient calculation method is important and yields different optimal configurations. Using the basic methods used for the previous prototypes, results were more repeatable using the large cap, with low fan speed. Using LSF, the optimal configuration was small cap, low fan speed and sensor 3. It is difficult to obtain repeatable results with LSF. The threshold is variable with the measurements. The minimum  $\chi^2$  (or  $\chi^2 < \text{threshold}$ ) doesn't always correspond with flux  $> 0$  (gradient  $\Delta = 1\text{s}$ ), corresponding to the time when the chamber is applied on the skin.  $\chi^2$  needs some time to stabilise and the minimum value is seen at the end of the application or during the rest period. Least Square Fitting is a slow calculation method and its momentum doesn't allow for quick measurements like the running average tested previously. The project objectives in terms of precision and sensitivity were met. First the coefficient of variation was below 0.05, during the droplet experiment, using the optimal configuration after 10 and 20 minutes. Then the sensitivity objective was reached. During the caps comparison experiment, the slope of the calibration curve was at the maximum 0.05 for the small cap.

The probe measure with more repeatability skin with surface water than normal skin. Whilst the results are encouraging, the reproducibility of the experiments with surface water could be improved. Moreover, the coefficient of variation were in general quite high in the cases without surface water and would need to be improved.

Having presented the design and the results of each chamber, the next section is going to compare the prototypes taken together.

### 4.12 Comparison of prototypes

A summary table ranking the most precise and most sensitive technique can be seen in appendices A.1 and A.2 respectively. According to industrial lean methodology,

the rule of thumb for error rate is:

- Less than 10% : Good measurement system.
- Between 10% and 30%: The measurement system is acceptable depending on the application and the cost to improve or repair the measurement system.
- Above 30%: The measurement system is unacceptable.

The Aquaflux target is a 5% error rate so the objective for chamber 9 is to have the same target of 5%.

#### **4.12.1 Error rate below 5% and ranking Top 4:**

Across the 155 configurations and use cases tested in this thesis, the most repeatable results were obtained with:

1. Chamber 9 using LSF with a 12 mm blower at minimum speed and small cap - error rate 0.6% (see page 214)
2. Chamber 2 with a 17 mm blower at full speed - error rate 3.2% (see page 234).
3. Chamber 9 using running average (5s) method with a large cap - error rate 4.5% (see page 200).
4. Chamber 7.1 without a fan and a gradient of 10s - error rate 5.0% (see page 186).

As mentioned in the previous paragraph, results can be found in: A.1 on page 234. The error rates above reach the target repeatability of 5% (i.e. the error rate of the Aquaflux).

#### **4.12.2 Accuracy**

No TEWL instrument provides the absolute TEWL value due to the nature of the measurements. However, in this thesis the Aquaflux is taken as the standard. The assumption made here is that the Aquaflux provides the 'true' value. When the prototype calibration curve is compared to the Aquaflux for a small and large value, the distance to the Aquaflux curve is the error compared to the true value, and therefore the accuracy. The closer to the Aquaflux curve, the more accurate the instrument is presumed to be.

### 4.12.3 Sensitivity

During linear regression, two items are provided,  $R^2$  and the equation of the regression with the form:  $y = ax + b$ . If  $R^2$  is above 0.7, it is considered to be a good fit. The higher the  $R^2$ , the better the repeatability. The slope of the calibration curve  $a$  represents the sensitivity of the test chamber compared to the Aquaflux.

All chambers, apart from chamber 1, reached the project objective to have a higher calibration slope than the Aquaflux. Higher slopes have been obtained with chamber 9 at the highest speed for various configurations (sensor 3, small cap, medium cap) followed by chamber 2 with the 17 mm blower. The higher the flow, the higher the slope of the correlation curve. Therefore the higher the velocity of the flow, the higher the sensitivity obtained.

### 4.12.4 Autonomy

Probe 7.1 was the only probe with which the autonomy was tested. The instrument measuring and communicating the results by BLE was working for 21 hours. The target was 12 hours, so the project objective was met. However, the development being modular, it would be trivial to adapt it for other chambers.

### 4.12.5 Mobility and portability

Probe 5, 7.1 and 9 were the only devices made with a casing. The other prototypes were just measurement chambers. Although they all had the same hardware and all have connectivity, they were not portable. Regarding the ergonomics, probe 5.1 was cumbersome whereas probe 9 didn't have a touchscreen. Only probe 7.1 had all the specified components. However, this hardware and casing would not be difficult to adapt for other chambers, although it may not look as good. Finally, connectivity is not mobility and a device management system would be a good feature to add.

### 4.12.6 Outside a laboratory

Only chamber 3 and 9 were tested with surface water. According to the rule described on page 223, chamber 3, with two 12 mm blowers, had unacceptable error rate, whereas chamber 9, using Least Square Fitting, sensor 3 and a fan at full speed, had the repeatability of a good instrument.

## 4.13 Summary of prototypes

The aim of the project was to develop a mobile instrument capable to work outside of a laboratory. All probes were mobile as they used WIFI or BLE. Probes were

also portable as they would fit in the hand. They had good autonomy. Having an instrument working well was translated as a requirement in terms of repeatability and sensitivity. The corresponding requirement was met for chamber 2 and probe 9. Probe 7.1 is not included because the good results were only without the fan, even though the repeatability was sufficient with a coefficient of variation below 0.05 (or 5%). However, the use of the fan is needed to remove surface water, caused by sweating in uncontrolled environment. Testing if the instrument work outside a laboratory was done by performing measurement on moist skin with a droplet. This was done with Chamber 3 and Chamber 9. Chamber 9 had good results (below 10 % as mentioned before), whereas chamber 3 had poor results (70%). Chamber 2 hasn't been mounted as a probe so it wasn't really portable. Therefore, the design specification was only really met by probe 9 (assuming autonomy, mobility and portability are easily transferred from probe 7.1).

Among all the tests results, probe 9 using sensor 3 was the most repeatable and sensitive instrument. It was the most repetitive at low speed and most sensitive at high speed. It doesn't mean that a 15 mm blower would provide good results and a 12 mm using the same design would not. Similarly, not all position along the PCB have been tested either. All this testing didn't established what is the best fan and sensor position because it wasn't fully crossed design ( $2^k$ ) with comparison among all parameters from which depends a good probe. However, all these experimentations permitted to draw some lessons on the effect of each parameters on TEWL measurement, as per the research question intended to (identification of factors that influence this performance). The parameters in question are: the sensor position, the fan speed, the cap, the calculation timing (or stabilisation time and duration of gradient computation), and the calculation method.

#### 4.13.1 Sensor position

The sensor position has an impact on chamber 4: Sensors 1 and 2 are symmetrical and have similar measurement amplitudes, whereas sensor 3 is more sensitive (see Figure 4.29). Despite this, repeatability was different between sensor 1 and 2.

The sensor position also has an impact in chamber 9. There are more errors for sensor 1 than sensor 3. Sensor 1 is closer to the skin and the flow of the blower so the environment is presumably more turbulent in this position.

#### 4.13.2 Fan Speed and SSWL

The fan speed has an impact on the measurement. The flux measured increases with the fan speed. It is better to measure large flows (e.g. the palm) with higher fan speeds or with a larger cap. Chamber 2 permits a large inflow. In chamber 9,

the fan could be used at the lowest speed to homogenise the microclimate. Then the fan can be set at a high speed to measure TEWL with a higher sensitivity. As the flux increases with higher fan speed, TEWL could be measured more quickly with higher precision at a higher speed.

### **4.13.3 Cap and anatomical site**

The accuracy is better with a smaller cap. The repeatability is higher with a larger cap and a higher flow because a smaller quantity of water is more difficult to measure.

### **4.13.4 Calculation timing**

Measurement timing (start time and  $\Delta$ ) is very important for TEWL calculation. However, optimal timing depends on the probe itself, the measurement site (lower or higher flux) and the measurement procedure. There are invariably differences between measurements: how quickly the probe is applied, the pressure with which it is applied, the microclimate around the skin just before measurement, etc. Therefore, it is preferable to have a dynamic gradient calculation method such as Least Square Fitting that doesn't depend on the time.

### **4.13.5 Calculation method**

Least Square Fitting is a slow method, but provides repeatable results. Good measurements have also been obtained with a 10 seconds length gradient calculation.

## **4.14 Conclusion**

In this chapter, the prototypes part of the development of a TEWL instrument have been discussed. First the methodology of development and scientific methods were defined. Subsequently the requirements of a TEWL measurement system were outlined from the literature review. Then the aspects related to the measurement as a physical phenomenon of TEWL were reviewed. These include:

- A quick measurement for precision;
- A controlled temperature as it should stay constant during measurement; and
- Adequate chamber geometry and optimal sensor position in this geometry.

The technical aspects were reviewed :

- Connectivity

- The blowers and their control with PID<sup>24</sup>
- The touch screen
- Non volatile memory

A final option was chosen for these components above. In addition, a solution for the battery and relative humidity and temperature sensor was proposed. Finally, the prototypes with their various implementations and results were presented.

Continuous development of the chambers led to multiple gradient determination methods. Every chamber was tested and compared with the Aquaflux AF200, and some of them were also compared with simulations when the physical design was unique.

TEWL measurement is a subtle art. A water gradient is not observable visually with a thermal camera. It requires strict measurement procedures because it can be affected by many confounding variables. The measurement of the gradient also demands a very precise mechanism. Use of the fan usually increases the sensitivity at the expense of the error rate. The higher the flow is, the higher the sensitivity achieved. The measurement result is also deeply linked to the measurement site and the flow coming into the chamber. Good results are obtained for appropriate caps on sites with low or high TEWL. Chamber 2, really wide, had remarkable results with palm measurements. The sensor position had a significant impact, especially on complex chamber geometry probes such as probe 4, and 9. These chambers have a non cylindrical shape that makes them unique compares to other TEWL measurement devices. The measurement of skin surface water is not possible with the Aquaflux (due to the device timing out before the result is provided) and the error with the other probes is large as well. The advantage of the fan solution is that it removes the water on the skin surface and homogenises the microclimate quickly. The design specifications were met with prototype 9. This probe reached and outmatched the project objectives in terms of repeatability and sensitivity. The hypothesis of the thesis were to improve the design the Aquaflux with portability and deal with the surface water. The prototype proposed is indeed portable and provide measurements with reasonable repeatability.

---

<sup>24</sup>Proportional Integral Derivative



# Chapter 5

## Conclusions and Future Work

### 5.1 Introduction

This thesis has shown the development of a mobile instrument for clinical diagnosis, from the theoretical studies to the design and testing. In this final chapter, the findings answering to the research questions will be wrapped up as well as the lessons learned and the resulting recommendations for future work explored.

### 5.2 Conclusions on research questions

The research question was: is it possible to develop an instrument working outside of a laboratory, and what factors influence this performance? To answer to this question, the project followed stages of problem definition and engineering activities of design, development and testing. First the skin assessment techniques were discussed in chapter 2 with the skin measurement guidelines. In addition the theoretical measurement processes were discussed for the main technologies of TEWL chambers: open, closed and condenser chambers. The light product design specification was derived from a requirement analysis with the study of existing systems, competitors and literature review. Afterwards, a detailed discussion of the mathematical modelling of a closed chamber was described as it is the base used in this project. The 3D modelling helped to identify quiet and more turbulent regions, in order to find optimal location of the sensors. However a 3D turbulent model was not possible during this thesis because of the geometrical complexity of the blower. This is future work for a mechanical engineer to consider.

Subsequently, this thesis presented the technical considerations for different designs and the theoretical and experimental results obtained for various assemblies of instruments. This project was an end-to-end development from conception to experimental evaluation, drawing, simulation and assembly.

The aim of the project was to develop a mobile instrument capable to work outside of a laboratory. Furthermore, instrument performances were evaluated with two methods: error rate (or coefficient of variation) for precision and calibration curve slopes for sensitivity. Thus the project objectives were: mobility firstly but also, a repeatability and sensitivity at least equal or higher than the Aquaflux. These three requirements were straightforward to test. The final prototype was mobile and could measure with 5% error, with a sensitivity as good as the Aquaflux. Finally, the last requirement was for the prototype to work well outside of a laboratory. Testing this last specification was done using the prototype on moist skin. Because no instrument on the market is able to do this, it was impossible to compare with the Aquaflux with a calibration curve. Only repeatability measurements have been provided. Probe 9 shown less than 10% of error rate. This level of repeatability is judged enough to be a good instrument system in many industries.

Furthermore, this project research question covered factors that influence the performance of such instrument. The testing to answer to this part of the question taught interesting lessons learnt. Lessons learnt are a vital part of any projects. They shall be used for future investigations.

Several prototypes have been tested and compared with the Aquaflux, the first instrument of Biox. The Aquaflux has shown good repeatability on small flux sites like the volar forearm. However, there were larger errors observed on high TEWL variability skin sites like the wrist and the palm and moist skin. It is more difficult to calibrate on skin sites with similar TEWL (like calibration Chamber 1). Therefore, it is preferable to take measurements from a small and large TEWL site for calibration. The calibration would ideally be performed with a fixed quantity of water rather than another instrument.

Before a measurement is performed, the gradient of humidity and temperature are stable within the chamber. During a measurement, the humidity increases rapidly, while the temperature increases slowly. The humidity increases even more quickly when it is measured on a high flux site. After a measurement, temperature and humidity slowly come back to room conditions.

The timing of a measurement depends on the calculation method. With the last Biox probe using Least Square Fitting for gradient computation, a quick and short gradient calculation was preferred. This thesis would constitute a good base for the future instrument as it tested a new method (LSF). Furthermore, this study tried a new method by getting rid of SSWL.

A large fan is preferable. Chamber 9 provided more repeatable results than the other prototypes. With Chamber 3 and 7.1, fan sizes and numbers were compared. One fan had better repeatability than two for Chamber 7.1. For Chamber 3 several fans had better repeatability than a single one. A larger single fan provided better

results for Chamber 2, 3, 5 and 7.1.

The performance of the Chamber 9 had good repeatability and sensitivity when compared to the Aquaflex. However, least square fitting is a slow computation technique in this setup.

The fan method increases the sensitivity because it increases the flux measured, but also increases the error rates. In addition, the fan can increase the temperature in the chamber and be a source of discomfort during measurements (e.g. Chamber 4). Finally, the fan chamber permits skin measurement in uncontrolled conditions as it removes the water on the surface of the skin and homogenises the microclimate in the chamber.

In this thesis, a few methods of gradient calculation have been tried for different probes and configurations. The gradient calculation (i.e. the determination of the slope humidity versus time) is the most challenging part of TEWL instrument development, as observed in other publications (Nuutinen et al. 2003).

The aim of the project was to build a mobile TEWL measurement system. This has been done with BLE and WiFi but other technologies are available.

## 5.3 Future work recommendations

Improvements and future work could be conducted in various areas; mathematical modelling, mechanical design of the casing and other specifics to skin measurements.

### 5.3.1 Technique development for the next version of prototype

#### 5.3.1.1 Device management

Complete integration in a device management system with the technologies described in 4.3.8.1 would be useful to follow up instrument history. It would be used to monitor, manage and secure instrument devices. If the instrument has access to a network it has to be secured. Moreover, it is patient data that is being sent. Although there was no name associated with TEWL measurement in this project, the data would not be kept anonymous if there are several subjects. Privacy is a hot topic in healthcare. As mentioned before, mobility is different from connectivity. The current prototype just sent readings to a broker that broadcasted the measurements. It was just a proof of concept of an IoT instrument for medical applications. This work will support the non functional requirements of management and security.

### 5.3.1.2 Full integration

A fully integrated instrument is a next step: the calculation of the gradient is currently done on a computer rather than the microcontroller. Another task should be created to manage this. Another integration aspect would consist of placing chamber 9 into probe 7.1 casing because probe 9 doesn't have a touchscreen. Autonomy tests were only performed with chamber 7.1. A full integration would allow to run more advanced computations like Least Square Fitting on the instrument itself. This work would support the mobility requirement: the prototype will be then truly portable.

### 5.3.1.3 Electronics

In order to manage more tasks, the project would need to be migrated from a development board to a more advanced microcontroller. Modules such as recognition of a good measurement, the MQTT connection, the end to end encryption and other features could not run at the same time in the current prototype. This will support the requirement above, to run advanced algorithms on the instrument itself. This will support the mobility requirement.

### 5.3.1.4 Computational fluid dynamics

The 3D modelling of a turbulent flow using ANSYS requires specialist input. Further work could be planned for better design. This would be useful to identify quiet and turbulent regions of the chamber, in order to find the optimal location of the sensor. It would also permit to test more configurations in terms of geometries and blower sizes easily. This way, the study would be closer to fully factorial design ( $2^k$ ) with a comparison with all parameters. This work would improve the repeatability of the instrument.

### 5.3.1.5 Mechanical design

The use of a more advanced 3D printer would be beneficial to get smaller parts and better printing results. Having smaller parts would make an instrument less cumbersome. This would improve the portability of the instrument.

## 5.3.2 Skin measurements

Further work related to skin measurements could be arranged for various aspects presented below.

### **5.3.2.1 The use of different caps**

There are other caps available with the Aquaflux. Future studies should include smaller or larger orifices, for sweat, hair, nails, etc. Different flux may need different blower speed. Tweaking of the Least Square Fitting settings may also lead to different results. This work would improve the range of usage of the instrument: it would reduce the errors while measuring on these specific sites.

### **5.3.2.2 Gravity study**

A gravity study with the orientation of the probe would be beneficial. For the Aquaflux, a complete assessment of the impact of the angle of handling the probe has shown a small impact (Imhof et al. 2009). This should be factored into any new chamber designs. This work would improve the general performances like repeatability and sensitivity of the instrument.

### **5.3.2.3 Contact pressure**

The contact pressure with which the device is pushed onto the skin influences TEWL (Barel & Clarys 2006). In this study, the measurement of the pressure of the probe on the skin could be measured by the deformation of the skin surface. This study would improve the repeatability and sensitivity of the instrument.

### **5.3.2.4 Calibration**

A calibration compared to the Aquaflux is not ideal because of the performance of the Aquaflux. The Aquaflux doesn't have good repeatability for high flux anatomical sites, e.g. near the palm or the wrist. A comparison with competitors instruments would be beneficial. A calibration with one of the methods presented in section 2.12.6 with a fixed quantity of water would be ideal. This work would improve the repeatability of the measurements and permit the evaluation of the accuracy of the instrument.

### **5.3.2.5 Observers and subjects**

A more formal experiment with more subjects and several observers is necessary to be recognised as a clinical study. This thesis is done within the field of telecommunications and technical considerations in prototype design, so these aspects were not prioritised. This would improve the quality assurance for evaluation of the performances of the prototypes. This would be needed for further publications.

## 5.4 Summary

The project aim to develop an mobile instrument measuring TEWL outside a laboratory. There were two quantified requirements, the repeatability and the sensitivity that were evaluated to meet Aquaflex performances. The target coefficient of variation and calibration slope were reached for a few devices. In addition, the last prototype was performant outside of a laboratory. The prototypes in this thesis are mobile with BLE and WiFi connectivity. A good autonomy was reached with 21 hours.

In addition, the research question covers what factors influence this performance. It was observed that instruments either have good repeatability or good sensitivity, but not both [because of the inverse relationship of the two](#). The fan method increases the sensitivity because it increases the flux measured, but also increase the error rates. The Least Square Fitting method provides good results that are both repeatable and sensitive, but this is a slow method compared to a running average. Gradient calculation is the most challenging aspect of instrument development as different instruments have different ideal calculation methods.

# Appendix A

## Probe Configuration Performances Comparison

### A.1 Repeatability Ranking

All measurement sessions repeatability compared with the error rate.  $n=3$ . Slope ranking is the same with any units (Linear transformation), the results are shown with SI units. S1-3 refers to the sensor 1, 2 ,3. Low and High refer to low speed and high speed of the fan respectively. SML cap refer to the size of the cap. Normal configuration is considered to be a measurement on the VF with one fan at full speed for 30 seconds and 30 seconds rest between the application, unless stated otherwise. "nFan" stands for no Fan.

Chamber	Config	Mean	Stdev	Error
Ch9	Sensor 3 - S cap Min Speed - 20 min	8.20E-2	1.19E-2	6.26E-3
Ch9	Sensor 3 - S cap Min Speed 10 min	5.96E-2	9.39E-3	6.64E-3
Ch2	Fan 17mm max speed	1.08E-2	3.40E-4	3.16E-2
Ch6	L cap	9.70E-5	4.36E-6	4.49E-2
Ch7.1	no fan	9.77E-6	4.90E-7	5.02E-2
Ch6	S cap	2.92E-5	1.88E-6	6.45E-2
Ch6	L cap	1.589E-5	1.19E-6	7.53E-2
Ch7.1	no fan	9.03E-7	7.29E-8	8.07E-2
Ch2	Fan 17mm max speed	9.79E-3	8.08E-4	8.25E-2
Ch6	High	7.90E-5	7.07E-6	8.95E-2
Ch7.1	no fan	8.44E-6	9.36E-7	0.11
Ch6	Ch6 – max speed – sensor 3	3.12E-5	3.61E-6	0.12
Ch6	M cap	7.59E-5	1.01E-5	0.13
Ch2	no fan	8.42E-3	1.12E-3	0.13

Ch6	M cap	7.80E-6	1.07E-6	0.14
Ch9	Sensor 1 - S cap no fan	2.00E-3	2.87E-4	0.14
Ch9	Sensor 1 - S cap 13908 RPM	8.99E-4	1.32E-4	0.15
Ch7.1	2x9OFF	4.48E-2	6.60E-3	0.15
Ch6	Ch6 – max speed - sensor 1	1.24E-5	2.08E-6	0.17
Ch6	Medium Speed Palm	1.11E-4	2.03E-5	0.18
Ch9	Sensor 1 - S cap 8882 RPM	9.27E-4	1.92E-4	0.21
Ch9	Sensor 1 - S cap 12630 RPM	2.00E-3	4.46E-4	0.22
Ch7.1	1x15mm	7.17E-2	1.619E-2	0.23
Ch6	High speed	1.42E-5	3.21E-6	0.223
Ch6	Low speed	8.13E-6	1.87E-6	0.23
Ch6	Ch6 – max speed – sensor 3	1.12E-4	2.58E-5	0.23
Ch7.1	1x9mm	8.94E-2	2.07E-2	0.23
Ch6	S cap	6.72E-6	1.62E-6	0.24
Ch7.1	2x9OFF	5.95E-2	1.79E-2	0.3
Ch1	app60 shake60 noAC	4.30E-5	1.3E-5	0.31
Ch9	Sensor 1 - S cap 10353 RPM	7.37E-4	2.28E-4	0.31
Ch6	Low	9.38E-5	2.94E-5	0.31
Ch3	Ch3-nFan	7.40E-5	2.54E-5	0.33
Ch6	Medium speed VF	1.56E-5	5.12E-6	0.33
Ch3	Ch3-3x9	1.28E-4	4.23E-5	0.33
Ch1	app60 rest360 noAC	4.27E-5	1.48E-5	0.34
Ch4	S3 - Low speed	2.84E-6	9.87E-7	0.35
Ch7.1	1x15mm	8.90E-2	3.14E-2	0.35
Ch1	Using a fan to drop temp	4.18E-5	1.50E-5	0.40
Ch7.1	no fan	8.07E-7	2.91E-7	0.36
Ch1	app30 rest30 (6 slopes)	2.65E-5	9.54E-6	0.36
Ch3	Ch3 -12 - SSWL	4.51E-4	2.15E-4	0.36
Ch7.1	2x12mm	4.95E-2	1.81E-2	0.37
Ch1	app30 rest240	3.80E-5	1.39E-5	0.37
Ch3	Ch3-2x12	9.16E-5	3.12E-5	0.37
Ch9	Sensor 1 - S cap 8882 RPM	1.93E-3	7.24E-4	0.37
Ch4	Ch4-LMHSpeed	2.07E-5	7.87E-6	0.38
Ch3	1x 9mm - app 60s	1.66E-4	6.66E-5	0.38
Ch1	app30 rest60	4.27E-5	1.64E-5	0.39
Ch1	app30 rest120	3.45E-5	1.34E-5	0.39
Ch9	Sensor 1 - S cap 10353 RPM	1.47E-3	5.80E-4	0.39



Ch3	1x 9mm - app 60s	3.31E-4	1.37E-4	0.40
Ch9	Sensor 3 - S cap	9.50E-2	3.81E-2	0.40
Ch7.1	1x9mm	5.93E-2	2.41E-2	0.41
Ch3	Ch3-2x9	1.80E-4	7.65E-5	0.41
Ch7.1	2x12mm	7.62E-2	3.15E-2	0.41
Ch4	S2 - Low	4.35E-6	1.80E-6	0.41
Ch9	Sensor 1 - S cap 12630 RPM	1.41E-3	5.93E-4	0.42
Ch4	S2 - High	5.33E-6	2.26E-6	0.42
Ch1	app30 rest240	4.42E-5	1.89E-5	0.43
Ch3	1x 9mm - app 60s	9.86E-5	3.68E-5	0.44
Ch7.1	1x9mm	0.10	4.44E-2	0.44
Ch6	Ch6 – max speed – sensor ?	7.36E-4	3.31E-4	0.45
Ch1	app15 fan30 1AC Insulated	3.54E-5	1.53E-5	0.46
Ch3	1MM	1.03E-4	5.03E-5	0.46
Ch7.1	2x9mm	5.87E-2	2.70E-2	0.46
Ch9	Sensor 1 - S cap 13908 RPM	1.53E-3	7.05E-4	0.46
Ch7.1	2x9mm	6.66E-2	3.09E-2	0.46
Ch4	Sensor 2	1.32E-5	6.13E-6	0.47
Ch3	Ch3-9-low speed	5.92E-5	3.04E-5	0.47
Ch1	app15 fan30 1AC	5.82E-5	2.78E-5	0.47
Ch4	S2 - VF	4.90E-6	2.32E-6	0.47
Ch9	Sensor 3 - S cap	3.27E-2	1.59E-2	0.49
Ch3	Ch3-9	1.97E-4	1.01E-4	0.50
Ch2	no fan	8.42E-3	4.20E-3	0.50
Ch7.1	12mm	2.99E-2	1.54E-2	0.51
Ch1	app30 rest360	2.04E-5	9.79E-6	0.52
Ch4	S3 - cheek	7.17E-6	3.79E-6	0.53
Ch1	app30 rest30 (7 slopes)	2.12E-5	7.52E-6	0.53
Ch7.1	12mm	3.13E-2	1.68E-2	0.54
Ch3	Ch3-9 high speed 1MM	8.30E-5	4.47E-5	0.54
Ch4	S2 - Cheek	6.11E-6	3.33E-6	0.55
Ch3	Ch3-12	5.12E-4	2.88E-4	0.56
Ch4	S2 - Med Speed	5.01E-6	2.80E-6	0.56
Ch4	S3 VF	8.66E-6	4.98E-6	0.57
Ch4	Sensor 3	7.42E-6	4.50E-6	0.61
Ch3	1MM	1.44E-4	8.78E-5	0.61
Ch7.1	1x9mm	9.65E-2	5.99E-2	0.62

Ch4	S3 - Med Speed	9.36E-6	6.10E-6	0.65
Ch4	S1 - Palm	1.71E-5	1.11E-5	0.65
Ch1	app30 rest360	2.18E-5	1.22E-5	0.66
Ch7.1	2x9OFF	2.72E-2	1.85E-2	0.68
Ch4	Ch4 – sensor 123	9.30E-6	6.39E-6	0.69
Ch1	Using a fan to drop temp	4.678E-5	3.42E-5	0.73
Ch4	Ch4-LMHSPEED	6.31E-6	4.84E-6	0.77
Ch4	S2 Palm	2.20E-5	1.78E-5	0.81
Ch4	Sensor 1	1.25E-5	1.02E-5	0.82
Ch4	Ch4-LMHSPEED	5.68E-6	4.72E-6	0.83
Ch4	S1 - Med Speed	4.75E-6	3.94E-6	0.83
Ch4	S3 - High Speed	5.33E-6	4.52E-6	0.85
Ch4	Ch4 – sensor 123	0.38	0.33	0.87
Ch4	Ch4 – sensor 123	0.55	0.48	0.87
Ch4	Sensor 3	5.85E-6	5.10E-6	0.87
Ch4	S3 Palm	6.10E-6	5.34E-6	0.88
Ch7.1	2x9OFF	4.33E-2	3.86E-2	0.89
Ch9	Sensor 3 - No cap	1.80E-2	1.61E-2	0.90
Ch4	Ch4 – sensor 123	0.42	0.38	0.90
Ch9	Sensor 1 - S cap no fan	9.77E-4	8.83E-4	0.90
Ch4	Sensor 1	1.05E-5	9.50E-6	0.91
Ch4	Sensor 2	1.38E-5	1.25E-5	0.91
Ch9	Sensor 1 - S cap 6280 RPM	1.71E-3	1.57E-3	0.92
Ch9	Sensor 1 - S cap 6280 RPM	1.17E-3	1.15E-3	0.98
Ch4	Ch4-LMHSPEED	9.30E-6	9.38E-6	1.01
Ch9	Sensor 1 - S cap	1.60E-2	1.64E-2	1.02
Ch4	S1 - High Speed	6.38E-6	6.60E-6	1.03
Ch9	Sensor 1 - S cap	1.52E-2	1.58E-2	1.04
Ch4	S1 - cheek	1.13E-5	1.25E-5	1.11
Ch9	Sensor 3 - S cap Max Speed	2.74E-2	3.09E-2	1.13
Ch9	Sensor 3 - S cap Min Speed	5.17E-2	5.84E-2	1.13
Ch1	Shake 30	4.18E-5	4.76E-5	1.13
Ch9	Sensor 3 - M cap	2.44E-2	2.81E-2	1.15
Ch5	no fan	3.27E-5	3.82E-5	1.17
Ch5	2x15mm	1.48E-5	1.74E-5	1.19
Ch9	Sensor 3 - S cap	3.46E-2	4.10E-2	1.18
Ch9	Sensor 3 - S cap	3.46E-2	4.10E-2	1.18

Ch9	Sensor 3 - S cap Max Speed	2.74E-2	3.28E-2	1.20
Ch5	2x15mm	7.52E-6	9.18E-6	1.22
Ch9	Sensor 3 - No cap	1.93E-2	2.45E-2	1.27
Ch9	Sensor 3 - L cap	3.45E-2	4.54E-2	1.32
Ch5	no fan	2.026E-4	2.66E-4	1.32
Ch9	Sensor 3 - S cap Max Speed	4.902E-2	6.50E-2	1.33
Ch9	Sensor 3 - S cap	2.00E-2	2.65E-2	1.33
Ch5	no fan	1.61E-5	2.15E-5	1.33
Ch9	Sensor 3 - M cap	4.29E-2	5.92E-2	1.38
Ch9	Sensor 3 - No cap	4.29E-2	5.92E-2	1.38
Ch5	no fan	7.18E-5	9.97E-5	1.39
Ch9	Sensor 3 - M cap	3.57E-2	5.02E-2	1.41
Ch5	no fan	1.75E-5	2.47E-5	1.41
Ch5	no fan	4.69E-6	6.63E-6	1.41
Ch5	no fan	7.12E-6	1.01E-5	1.41
Ch9	Sensor 3 - S cap Max Speed	6.99E-2	9.92E-2	1.42
Ch9	Sensor 3 - L cap	2.53E-2	3.63E-2	1.44
Ch9	Sensor 3 - M cap	4.83E-2	6.96E-2	1.44
Ch5	no fan	2.42E-6	3.55E-6	1.47
Ch9	Sensor 3 - S cap	7.00E-2	0.10	1.478
Ch9	Sensor 3 - S cap	5.50E-2	8.19E-2	1.49
Ch5	no fan	6.99E-5	1.05E-4	1.50
Ch9	Sensor 3 - S cap 0min	9.07E-2	0.14	1.50
Ch9	Sensor 3 - L cap	6.16E-2	9.47E-2	1.54
Ch9	Sensor 3 - S cap	6.40E-2	0.11	1.76
Ch9	Sensor 3 - L cap	8.003E-2	0.15	1.82
Ch1	app30 rest30 (5 slopes)	7.00E-6	2.65E-5	7.73

## A.2 Sensitivity with the Aquaflux

All measurement sessions sensitivities compared with their closeness to the Aquaflux. The higher the slope, the more sensitive the instrument and closer to the Aquaflux. The Aquaflux slope is  $3 \cdot 10^{-7}$ . Anything higher has higher sensitivity than the Aquaflux.

Chamber	Config	kg/m <sup>3</sup> s to g/m <sup>2</sup> h slope
Ch9 - sensor 3 - max speed	S cap	0.05
Ch9 - S cap - max speed	Sensor 3	0.05
Ch9 - sensor 3 - max speed	M cap	1.84E-2
Ch2	17mm fan	1.05E-2
Ch9 - sensor 3 - max speed	L cap	9.3E-3
Ch2	no fan	7.2E-3
Ch7.1	15mm	4.0E-3
Ch7.1	2x9mm	3.9E-3
Ch7.1	2x12mm	3.1E-3
Ch7.1	1x9mm	1.9E-3
Ch7.1	12mm	1.7E-3
Ch7.1	no fan	9.0E-4
Ch9 - S cap - max speed	Sensor 1	9.0E-4
Ch6	Sensor 3	8.0E-5
Ch6	Sensor 3	8.0E-5
Ch9 - Scap - sensor 1	no fan 0 RPM	6.0E-5
Ch9 - Scap - sensor 1	10353 RPM	5.0E-5
Ch6	Sensor 3	4.03E-5
Ch9 - Scap - sensor 1	13908 RPM	4.0E-5
Ch9 - Scap - sensor 1	8882 RPM	3.0E-5
Ch9 - Scap - sensor 1	12630 RPM	3.0E-5
Ch6	fan no cap 3v	1.0E-5
Ch6	fan no cap 3v	1.0E-5
Ch6	fan no cap 3v	1.0E-5
Ch7.1	no fan	9.02E-6
Ch6	fan no cap 3v	8.0E-6
Ch6	Low Speed	9.0E-6
Ch7.1	no fan	8.0E-6
Ch6	fan no cap 3v	7.0E-6
Ch1	Avg Drop Fan	6.0E-6
Ch9 - Scap - sensor 1	6280 RPM	6.0E-6
Ch3	9mm	4.0E-6
Ch3	9mm	3.0E-6
Ch6	Large Cap	2.0E-6
Ch6	Large Cap	2.0E-6
Ch3	9mm	1.0E-6

Ch6	Medium Cap	1.0E-6
Ch6	Large Cap	1.0E-6
Ch6	Medium Speed	1.0E-6
Ch6	High Speed	1.0E-6
Ch6	Medium Cap	9.0E-7
Ch5.1	no fan	7.0E-7
Ch6	Large Cap	7.0E-7
Ch6	Small Cap	5.0E-7
Ch6	Small Cap	5.0E-7
Ch4	Sensor 1	4.0E-7
Ch5.1	15mm	4.0E-7
Ch6	Small Cap	4.0E-7
Ch6	Medium Cap	4.0E-7
Ch5.1	no fan	3.0E-7
Ch4	Sensor 2	2.0E-7
Ch5.1	no fan	2.0E-7
Ch6	Small Cap	3.0E-8
Ch6	Medium Cap	-2E-8
Ch4	Sensor 3	-7.0E-8
Ch1	Avg Drop 240s	-7.0E-6
Ch7.1	no fan	-4.0E-3
Ch7.1	1x9mm	-7.0E-3
Ch9 - sensor 3 - max speed	No cap	-2.4E-2

# Bibliography

- 802 (2009), IEEE Standard for Information technology– Local and metropolitan area networks– Specific requirements– Part 11: Wireless LAN Medium Access Control (MAC)and Physical Layer (PHY) Specifications Amendment 5: Enhancements for Higher Throughput, Standard, Institute of Electrical and Electronics Engineers, New York, USA.
- 802 (2015), IEEE Standard for Low - Rate Wireless Networks, Standard, Institute of Electrical and Electronics Engineers, New York, USA.
- Adafruit (2016), ‘Adafruit MQTT Library’, [https://github.com/adafruit/Adafruit\\_MQTT\\_Library](https://github.com/adafruit/Adafruit_MQTT_Library). [Online; accessed 01-February-2020].
- Aguilar, R. & Meijer, G. (2002), Fast interface electronics for a resistive touch-screen, *in* ‘SENSORS, 2002 IEEE’, Vol. 2, IEEE, pp. 1360–1363.
- Aime, M. D., Calandriello, G. & Lioy, A. (2007), ‘Dependability in wireless networks: Can we rely on wifi?’, *IEEE Security & Privacy* **5**(1), 23–29.
- Alexander, H., Brown, S., Danby, S. & Flohr, C. (2018), ‘Research techniques made simple: transepidermal water loss measurement as a research tool’, *Journal of Investigative Dermatology* **138**(11), 2295–2300.
- Aly, A. A. (2011), ‘Pid parameters optimization using genetic algorithm technique for electrohydraulic servo control system’, *Intelligent Control and Automation* **2**(02), 69.
- Amrhein, W., Gruber, W., Bauer, W. & Reisinger, M. (2016), ‘Magnetic levitation systems for cost-sensitive applications—some design aspects’, *IEEE Transactions on Industry Applications* **52**(5), 3739–3752.
- Annisa, J., Darus, I. M., Tokhi, M. & Mohamaddan, S. (2018), Implementation of pid based controller tuned by evolutionary algorithm for double link flexible robotic manipulator, *in* ‘2018 International Conference on Computational Approach in Smart Systems Design and Applications (ICASSDA)’, IEEE, pp. 1–5.

Atmel (n.d.), ‘Mqtt quickstart’.

Bagsik, A., Schöppner, V. & Klemp, E. (2010), Fdm part quality manufactured with ultem\* 9085, *in* ‘14th international scientific conference on polymeric materials’, Vol. 15, pp. 307–315.

Barel, A. & Clarys, P. (1995), ‘Study of the stratum corneum barrier function by transepidermal water loss measurements: comparison between two commercial instruments: evaporimeter® and tewameter®’, *Skin pharmacology and physiology* **8**(4), 186–195.

Barel, A. & Clarys, P. (2006), Comparison of methods for measurement of transepidermal water loss., *in* J. Serup, B. E. Jemec & G. L. Grove, eds, ‘Handbook of non-invasive methods and the skin’, 2nd ed edn, CRC/Taylor & Francis, Boca Raton, pp. 179–184.

Barel, A., Clarys, P. & Gabard, B. (2017), Transepidermal Water Loss, *in* ‘Agache’s Measuring the Skin’, pp. pp 1–12.

**URL:** <http://link.springer.com/10.1007/978-3-319-32383-1>

Batisse, D., Giron, F. & Lévêque, J. L. (2006), ‘Capacitance imaging of the skin surface’, *Skin Research and Technology* **12**(2), 99–104.

Behmann, F. & Wu, K. (2015), *Collaborative internet of things (C-IoT): For future smart connected life and business*, John Wiley & Sons.

Berardesca, E., for Efficacy Measurements on Cosmetics, E. G. & (EEMCO), O. T. P. (1997), ‘Eemco guidance for the assessment of stratum corneum hydration: electrical methods’, *Skin Research and Technology* **3**(2), 126–132.

Berardesca, E., Loden, M., Serup, J., Masson, P. & Rodrigues, L. M. (2018), ‘The revised eemco guidance for the in vivo measurement of water in the skin’, *Skin Research and Technology* **24**(3), 351–358.

Bhalla, M. R. & Bhalla, A. V. (2010), ‘Comparative study of various touchscreen technologies’, *International Journal of Computer Applications* **6**(8), 12–18.

Biox (2019), ‘AquaFlux Model AF200’, <https://www.biox.biz/Products/AquaFlux/AF200Page01.php>. [Online; accessed 30-May-2019].

Biox Systems Ltd (2018), ‘Biox Epsilon Brochure 2018 Rev01a’, <https://www.biox.biz/Downloads/Brochures/Biox%20Epsilon%20Brochure%202018%20Rev01a.pdf>. [Online; accessed 13-January-2020].

- Blank, I. H., Moloney III, J., Emslie, A. G., Simon, I. & Apt, C. (1984), ‘The diffusion of water across the stratum corneum as a function of its water content’, *Journal of Investigative Dermatology* **82**(2), 188–194.
- Blank, I. H., Scheuplein, R. J. & MacFarlane, D. J. (1967), ‘Mechanism of percutaneous absorption. 3. the effect of temperature on the transport of non-electrolytes across the skin.’, *The Journal of investigative dermatology* **49**(6), 582–589.
- Blichmann, C. & Serup, J. (1987), ‘Reproducibility and variability of transepidermal water loss measurement. studies on the servo med evaporimeter.’, *Acta dermatovenereologica* **67**(3), 206–210.
- Bluetooth SIG (Bluetooth Special Interest Group): Kirkland Washington USA (2014), ‘Bluetooth core specification version 4.2’, *Specification of the Bluetooth System* p. 2302.
- Bluetooth SIG (Bluetooth Special Interest Group): Kirkland Washington USA (2016), ‘Bluetooth core specification v5. 0’, *Specification of the Bluetooth System* p. 2802.
- Brickell, E. & Li, J. (2007), Enhanced privacy id: A direct anonymous attestation scheme with enhanced revocation capabilities, *in* ‘Proceedings of the 2007 ACM workshop on Privacy in electronic society’, ACM, pp. 21–30.
- Brooks, H., Rennie, A., Abram, T., McGovern, J. & Caron, F. (2011), Variable fused deposition modelling: analysis of benefits, concept design and tool path generation, *in* ‘5th International Conference on Advanced Research in Virtual and Rapid Prototyping, Leiria, Portugal’, pp. 511–517.
- Buchberger, A., Coclite, A. & Bergmann, A. (2018), Fast humidity sensors for harsh environment, *in* ‘Multidisciplinary Digital Publishing Institute Proceedings’, Vol. 2, p. 988.
- Burnett, G., Large, D., Lawson, G., De-Kremer, S. & Skrypchuk, L. (2013), ‘A comparison of resistive and capacitive touchscreens for use within vehicles.’, *Advances in transportation studies* (31).
- Bush, N. E., Armstrong, C. M. & Hoyt, T. V. (2018), ‘Smartphone apps for psychological health: A brief state of the science review.’, *Psychological services* .
- Byrne, A. (2010), ‘Bioengineering and subjective approaches to the clinical evaluation of dry skin’, *International journal of cosmetic science* **32**(6), 410–421.



- Cain, P. (2019), 'Impact of the layer height', <https://www.3dhubs.com/knowledge-base/impact-layer-height-3d-print>. [Online; accessed 08-April-2019].
- Caspers, P. J., Bruining, H. A., Puppels, G. J., Lucassen, G. W. & Carter, E. A. (2001), 'In vivo confocal raman microspectroscopy of the skin: noninvasive determination of molecular concentration profiles', *Journal of investigative dermatology* **116**(3), 434–442.
- Chilcott, R. P. & Farrar, R. (2000), 'Biophysical measurements of human forearm skin in vivo: effects of site, gender, chirality and time', *Skin Research and Technology* **6**(2), 64–69.
- Chunxi, L., Ling, W. S. & Yakui, J. (2011), 'The performance of a centrifugal fan with enlarged impeller', *Energy Conversion and Management* **52**(8-9), 2902–2910.
- Clarys, P., Clijsen, R., Taeymans, J. & Barel, A. O. (2012), 'Hydration measurements of the stratum corneum: comparison between the capacitance method (digital version of the corneometer cm 825®) and the impedance method (skicon-200 ex®)', *Skin Research and Technology* **18**(3), 316–323.
- Cohen, J., Hartman, D., Garofalo, M., Basehoar, A., Raynor, B., Ashbrenner, E. & Akin, F. (2009), 'Comparison of closed chamber and open chamber evaporimetry', *Skin research and technology* **15**(1), 51–54.
- Cortex (2016), 'Dermalab Skin Lab', [http://www.cyberderm-inc.com/uploads/6/3/5/7/63578583/dermalab\\_combo\\_skinlab\\_spec\\_sheet\\_\\_2016\\_.pdf](http://www.cyberderm-inc.com/uploads/6/3/5/7/63578583/dermalab_combo_skinlab_spec_sheet__2016_.pdf). [Online; accessed 13-January-2020].
- Cortex (2020), 'Dermalab Single Parameter', <https://cortex.dk/single-parameter-dermalab/>. [Online; accessed 13-January-2020].
- Courage+Khazaka electronic GmbH (2019), 'Corneometer CM 825', [https://courage-khazaka.de/images/Downloads/Brochures/Wissenschaftlich/Brochure\\_Corneometer.pdf](https://courage-khazaka.de/images/Downloads/Brochures/Wissenschaftlich/Brochure_Corneometer.pdf). [Online; accessed 13-January-2020].
- Cravello, B. & Ferri, A. (2008), 'Relationships between skin properties and environmental parameters', *Skin research and technology* **14**(2), 180–186.
- Cruz, P., Shoemake, E., Adam, P. & Leachman, J. (2015), Tensile strengths of polyamide based 3d printed polymers in liquid nitrogen, in 'IOP Conference Series: Materials Science and Engineering', Vol. 102, IOP Publishing, p. 012020.

- Cui, Y., Xiao, P., Ciortea, L., De Jesus, M., Berg, E. & Imhof, R. (2007), 'Mathematical modelling for the condenser method of trans-epidermal water loss measurements', *Nondestructive Testing and Evaluation* **22**(4), 229–238.
- Cussler, E. L. (2009), *Diffusion: mass transfer in fluid systems*, Cambridge university press.
- Darlenski, R., Sassning, S., Tsankov, N. & Fluhr, J. (2009), 'Non-invasive in vivo methods for investigation of the skin barrier physical properties', *European Journal of Pharmaceutics and Biopharmaceutics* **72**(2), 295–303.
- de Dear, R. J., Arens, E., Hui, Z. & Oguro, M. (1997), 'Convective and radiative heat transfer coefficients for individual human body segments', *International Journal of Biometeorology* **40**(3), 141–156.
- De Paepe, K., Houben, E., Adam, R., Wiesemann, F. & Rogiers, V. (2005), 'Validation of the vapometer, a closed unventilated chamber system to assess transepidermal water loss vs. the open chamber tewameter®', *Skin research and technology* **11**(1), 61–69.
- Delphin (2020), 'Vapometer', [http://www.delfintech.com/en/vapometer\\_faq/](http://www.delfintech.com/en/vapometer_faq/). [Online; accessed 13-January-2020].
- Denda, M. & Tsuchiya, T. (2000), 'Barrier recovery rate varies time-dependently in human skin', *British Journal of Dermatology* **142**(5), 881–884.
- Dhiliwal, S. R. & Salins, N. (2015), 'Smartphone applications in palliative homecare', *Indian journal of palliative care* **21**(1), 88.
- Eckert, E. & Drake Jr, R. M. (1959), 'Heat and mass transfer mcgraw-hill', *New York* .
- Egawa, M., Hirao, T. & Takahashi, M. (2007), 'In vivo estimation of stratum corneum thickness from water concentration profiles obtained with raman spectroscopy', *Acta dermato-venereologica* **87**(1), 4–8.
- Elkeeb, R., Hui, X., Chan, H., Tian, L. & Maibach, H. I. (2010), 'Correlation of transepidermal water loss with skin barrier properties in vitro: comparison of three evaporimeters', *Skin Research and Technology* **16**(1), 9–15.
- Elsner, P., Maibach, H. I., Berardesca, E. & Fluhr, J. W. (2004), *Bioengineering of the skin: water and the stratum corneum*, CRC press.

- Engineering ToolBox (2003), ‘Water - Thermophysical Properties.’, [https://www.engineeringtoolbox.com/water-thermal-properties-d\\_162.html](https://www.engineeringtoolbox.com/water-thermal-properties-d_162.html). [Online; accessed 18-April-2019].
- Engineering ToolBox (2018a), ‘Air - Diffusion Coefficients of Gases in Excess of Air’, [https://www.engineeringtoolbox.com/air-diffusion-coefficient-gas-mixture-temperature-d\\_2010.html](https://www.engineeringtoolbox.com/air-diffusion-coefficient-gas-mixture-temperature-d_2010.html). [Online; accessed 18-April-2019].
- Engineering ToolBox (2018b), ‘Water - Thermal Diffusivity’, [https://www.engineeringtoolbox.com/water-steam-thermal-diffusivity-d\\_2058.html](https://www.engineeringtoolbox.com/water-steam-thermal-diffusivity-d_2058.html). [Online; accessed 18-April-2019].
- Fan, J., Zhang, C., Wang, Z., Dong, Y., Nino, C., Tariq, A. & Strangas, E. (2010), ‘Thermal analysis of permanent magnet motor for the electric vehicle application considering driving duty cycle’, *IEEE Transactions on Magnetics* **46**(6), 2493–2496.
- Farahmand, S., Tien, L., Hui, X. & Maibach, H. I. (2009), ‘Measuring transepidermal water loss: a comparative in vivo study of condenser-chamber, unventilated-chamber and open-chamber systems’, *Skin Research and Technology* **15**(4), 392–398.
- Farlex (2012), ‘Farlex partner medical dictionary’, *Splinting* .
- Firooz, A., Zartab, H., Sadr, B., Bagherpour, L. N., Masoudi, A., Fanian, F., Dowlati, Y., Ehsani, A. H. & Samadi, A. (2016), ‘Daytime changes of skin biophysical characteristics: A study of hydration, transepidermal water loss, ph, sebum, elasticity, erythema, and color index on middle eastern skin’, *Indian journal of dermatology* **61**(6), 700.
- Fluhr, J., ed. (2005), *Bioengineering of the skin: water and stratum corneum*, Dermatology, 2nd ed edn, CRC Press, Boca Raton.
- Fluhr, J. W. & Darlenski, R. (2014), Transepidermal water loss (tewl), in ‘Non invasive diagnostic techniques in clinical dermatology’, Springer, pp. 353–356.
- Fluhr, J. W., Feingold, K. R. & Elias, P. M. (2006), ‘Transepidermal water loss reflects permeability barrier status: validation in human and rodent in vivo and ex vivo models’, *Experimental dermatology* **15**(7), 483–492.
- Freire, B. & Lopes, P. S. (2019), ‘Catherine tolomei fabbron appas, ariane dalanda silva ladeira, thamires’, *Cosmetic Formulation: Principles and Practice* p. 175.

- Freitas, R., Wilcke, W., Kurdi, B. & Burr, G. (2008), Storage class memory, technology and use, *in* ‘Tutorial, 6th USENIX Conference on File and Storage Technologies’.
- Gilchrist, A. (2016), Middleware industrial internet of things platforms, *in* ‘Industry 4.0’, Springer, pp. 153–160.
- Gioia, F. & Celleno, L. (2002), ‘The dynamics of transepidermal water loss (tewl) from hydrated skin’, *Skin research and technology* **8**(3), 178–186.
- González-Jiménez, J., Galindo, C. & Ruiz-Sarmiento, J. (2012), Technical improvements of the giraff telepresence robot based on users’ evaluation, *in* ‘2012 IEEE RO-MAN: The 21st IEEE International Symposium on Robot and Human Interactive Communication’, IEEE, pp. 827–832.
- Goris, K., Saldien, J., Vanderniepen, I. & Lefeber, D. (2008), The huggable robot probot, a multi-disciplinary research platform, *in* ‘International Conference on Research and Education in Robotics’, Springer, pp. 29–41.
- Grice, K., Sattar, H., Sharratt, M. & Baker, H. (1971), ‘Skin temperature and transepidermal water loss’, *Journal of Investigative Dermatology* **57**(2), 108–110.
- Grove, G. L., Grove, M. J., Zerweck, C. & Pierce, E. (1999), ‘Computerized evaporimetry using the dermalab® tewl probe’, *Skin research and Technology* **5**(1), 9–13.
- Hassinen, T. (2006), Overview of wlan security, *in* ‘Seminar on Network Security’, Vol. 11, Citeseer.
- Holzinger, A. (2002), Finger instead of mouse: touch screens as a means of enhancing universal access, *in* ‘ERCIM Workshop on User Interfaces for all’, Springer, pp. 387–397.
- Horimukai, K., Morita, K., Narita, M., Kondo, M., Kabashima, S., Inoue, E., Sasaki, T., Niizeki, H., Saito, H., Matsumoto, K. et al. (2016), ‘Transepidermal water loss measurement during infancy can predict the subsequent development of atopic dermatitis regardless of filaggrin mutations’, *Allergology International* **65**(1), 103–108.
- Hua, W., Fan, L.-M., Dai, R., Luan, M., Xie, H., Li, A.-Q. & Li, L. (2017), ‘Comparison of two series of non-invasive instruments used for the skin physiological properties measurements: the dermalab® from cortex technology vs. the series of detectors from courage & khazaka’, *Skin Research and Technology* **23**(1), 70–78.

- HumanAnatomyLibrary (2018), ‘Diagram Skin Stratum Corneum’, <https://humananatomylibrary.co/s/skin-stratum-corneum-diagram-system.asp>. [Online; accessed 24-January-2019].
- Ibrahim, D. (2010), *SD card projects using the PIC microcontroller*, Newnes.
- Imhof, B. & McFeat, G. (2014), ‘11 evaluation of the barrier function of skin using transepidermal water loss (tewl)’, *Handbook of Cosmetic Science and Technology* p. 131.
- Imhof, B., Xiao, P. & Angelova-Fischer, I. (2014), Tewel, closed-chamber methods: Aquaflux and vapometer, in ‘Non Invasive Diagnostic Techniques in Clinical Dermatology’, Springer, pp. 345–352.
- Imhof, R. (2007), ‘In-vivo and in-vitro applications of closed-chamber tewl measurements’, *Lecture Notes: Intensive course in Dermato-cosmetic Sciences* .
- Imhof, R., Berg, E., Chilcott, R., Ciortea, L., Pascut, F. & Xiao, P. (2002), ‘New instrument for measuring water vapour flux density from arbitrary surfaces’, *IFSCC Mag* **5**(4), 297–301.
- Imhof, R. E., De Jesus, M. E. P., Xiao, P., Ciortea, L. I. & Berg, E. P. (2009), ‘Closed-chamber transepidermal water loss measurement: microclimate, calibration and performance’, *International Journal of Cosmetic Science* **31**(2), 97–118. **URL:** <http://doi.wiley.com/10.1111/j.1468-2494.2008.00476.x>
- Imhof, R., Xiao, P., Berg, E. & Ciortea, L. (2005), ‘Rapid measurement of tewl with a condenser chamber instrument’, *Skin Research and Technology* **11**(4).
- Jacques, S. (1979), ‘Linear measurement of the water content of the stratum corneum of human skin using a microwave probe.’, *Journal of Sound and Vibration* pp. 180–182.
- Jaen-Cuellar, A. Y., de J. Romero-Troncoso, R., Morales-Velazquez, L. & Osornio-Rios, R. A. (2013), ‘Pid-controller tuning optimization with genetic algorithms in servo systems’, *International Journal of Advanced Robotic Systems* **10**(9), 324.
- Ji, J.-C., Hansen, C. H. & Zander, A. C. (2008), ‘Nonlinear dynamics of magnetic bearing systems’, *Journal of Intelligent Material Systems and Structures* **19**(12), 1471–1491.
- Kenney, J. & Keeping, E. S. (1962), ‘Linear regression and correlation’, *mathematics of statistics* **1**, 221–223.

- Khalil, Z. (2017), ‘Iot foundations: Standards and ecosystems’, <https://www.lynda.com/Zahraa-Khalil/10236993-1.html>.
- Kikuchi, K., Asano, M., Tagami, H., Kato, M. & Aiba, S. (2017), ‘Comparison of the measuring efficacy of transepidermal water loss of a reasonably priced, portable closed-chamber system device h4500 with that of rather expensive, conventional devices such as tewameter® and vapometer®’, *Skin Research and Technology* **23**(4), 597–601.
- Kos, M. & Kramberger, I. (2017), ‘A wearable device and system for movement and biometric data acquisition for sports applications’, *IEEE Access* **5**, 6411–6420.
- Kottner, J., Lichterfeld, A. & Blume-Peytavi, U. (2013), ‘Transepidermal water loss in young and aged healthy humans: a systematic review and meta-analysis’, *Archives of dermatological research* **305**(4), 315–323.
- Kramer, M. & Gerald, A. (2006), ‘Energy measurements for micaz node’, *University of Kaiserslautern, Kaiserslautern, Germany, Technical Report KrGe06*.
- Kremer, G. M. (2011), The methods of chapman-ensskog and grad and applications, Technical report, UNIVERSIDADE FEDERAL DO PARANA CURITIBA (BRAZIL) DEPT DE FISICA.
- Krohling, R. A. & Rey, J. P. (2001), ‘Design of optimal disturbance rejection pid controllers using genetic algorithms’, *IEEE Transactions on Evolutionary computation* **5**(1), 78–82.
- Krohling, R., Jaschek, H. & Rey, J. (1997), Designing pi/pid controllers for a motion control system based on genetic algorithms, in ‘Proceedings of 12th IEEE International Symposium on Intelligent Control’, IEEE, pp. 125–130.
- Lanzotti, A., Del Giudice, D. M., Lepore, A., Staiano, G. & Martorelli, M. (2015), ‘On the geometric accuracy of rewrap open-source three-dimensional printer’, *Journal of Mechanical Design* **137**(10), 101703.
- Lanzotti, A., Martorelli, M. & Staiano, G. (2015), ‘Understanding process parameter effects of rewrap open-source three-dimensional printers through a design of experiments approach’, *Journal of Manufacturing Science and Engineering* **137**(1), 011017.
- Le Fur, I., Reinberg, A., Lopez, S., Morizot, F., Mechkouri, M. & Tschachler, E. (2001), ‘Analysis of circadian and ultradian rhythms of skin surface properties of face and forearm of healthy women’, *Journal of investigative dermatology* **117**(3), 718–724.

- Le, Y. & Wang, K. (2016), ‘Design and optimization method of magnetic bearing for high-speed motor considering eddy current effects’, *IEEE/ASME Transactions on Mechatronics* **21**(4), 2061–2072.
- Lee, C., Kim, S., Kim, H. & Ahn, S. (2007), ‘Measurement of anisotropic compressive strength of rapid prototyping parts’, *Journal of materials processing technology* **187**, 627–630.
- Leveque, J., Garson, J. & De, J. D. R. G. (1977), ‘Transepidermal water loss from dry and normal skin’.
- Leveque, J.-L., ed. (1989), *Cutaneous investigation in health and disease: noninvasive methods and instrumentation*, number #1 in ‘Clinical dermatology’, Dekker, New York.
- Leveque, J. L. & Querleux, B. (2003), ‘Skinchip®), a new tool for investigating the skin surface in vivo’, *Skin Research and Technology* **9**(4), 343–347.
- Li, M., Moll, E. & Chituc, C.-M. (2018), Iot for healthcare: An architecture and prototype implementation for the remote e-health device management using continua and lwm2m protocols, in ‘IECON 2018-44th Annual Conference of the IEEE Industrial Electronics Society’, IEEE, pp. 2920–2926.
- Li, X., Johnson, R. & Kasting, G. B. (2016), ‘On the variation of water diffusion coefficient in stratum corneum with water content’, *Journal of pharmaceutical sciences* **105**(3), 1141–1147.
- Li, X., Johnson, R., Weinstein, B., Wilder, E., Smith, E. & Kasting, G. B. (2015), ‘Dynamics of water transport and swelling in human stratum corneum’, *Chemical Engineering Science* **138**, 164–172.
- Lieberman, M. A. & Lichtenberg, A. J. (2005), *Appendix B: The Collision Integral*, John Wiley & Sons, Ltd, pp. 727–729.  
**URL:** <https://onlinelibrary.wiley.com/doi/abs/10.1002/0471724254.app2>
- Lowe, P. R. (1977), ‘An approximating polynomial for the computation of saturation vapor pressure’, *Journal of Applied Meteorology* **16**(1), 100–103.
- Luikov, A. (1968), ‘Analytical heat diffusion theory’.
- Mayrovitz, H. N., Bernal, M., Brilit, F. & Desfor, R. (2013), ‘Biophysical measures of skin tissue water: variations within and among anatomical sites and correlations between measures’, *Skin Research and Technology* **19**(1), 47–54.

- Mayrovitz, H. N., Davey, S. & Shapiro, E. (2009), 'Suitability of single tissue dielectric constant measurements to assess local tissue water in normal and lymphedematous skin', *Clinical physiology and functional imaging* **29**(2), 123–127.
- Miteva, M., Richter, S., Elsner, P. & Fluhr, J. W. (2006), 'Approaches for optimizing the calibration standard of tewameter tm 300', *Experimental dermatology* **15**(11), 904–912.
- Mole, R. H. (1948), 'The relative humidity of the skin', *The Journal of Physiology* **107**(4), 399–411.  
**URL:** <http://doi.wiley.com/10.1113/jphysiol.1948.sp004284>
- Montgomery, R. (1947), 'Viscosity and thermal conductivity of air and diffusivity of water vapor in air', *Journal of Meteorology* **4**(6), 193–196.
- Mündlein, M., Valentin, B., Chabicovsky, R., Nicolics, J., Weremczuk, J., Tarapata, G. & Jachowicz, R. (2008), 'Comparison of transepidermal water loss (tewl) measurements with two novel sensors based on different sensing principles', *Sensors and Actuators A: Physical* **142**(1), 67–72.
- Munir, A., Takada, S. & Matsushita, T. (2009), 'Re-evaluation of stolwijk's 25-node human thermal model under thermal-transient conditions: Prediction of skin temperature in low-activity conditions', *Building and Environment* **44**(9), 1777–1787.
- Nakatani, M., Fukuda, T., Arakawa, N., Kawasoe, T. & Omata, S. (2013), 'Softness sensor system for simultaneously measuring the mechanical properties of superficial skin layer and whole skin', *Skin Research and Technology* **19**(1), e332–e338.
- Nilsson, G. E. (1977), 'Measurement of water exchange through skin', *Medical & Biological Engineering & Computing* **15**(3), 209–218.  
**URL:** <http://link.springer.com/10.1007/BF02441040>
- Nonato, L. B. & Lund, C. H. (2001), 'Transepidermal water loss in the intensive care nursery: Measuring techniques and research recommendations', *Newborn and Infant Nursing Reviews* **1**(1), 11–20.
- Nuutinen, J., Alanen, E., Autio, P., Lahtinen, M.-R., Harvima, I. & Lahtinen, T. (2003), 'A closed unventilated chamber for the measurement of transepidermal water loss', *Skin Research and Technology* **9**(2), 85–89.  
**URL:** <http://doi.wiley.com/10.1034/j.1600-0846.2003.00025.x>
- Olivo, J., Carrara, S. & De Micheli, G. (2012), Ironic patch: A wearable device for the remote powering and connectivity of implantable systems, in '2012 IEEE



- International Instrumentation and Measurement Technology Conference Proceedings', Ieee, pp. 286–289.
- Olsen, J., Holmes, J. & Jemec, G. B. (2018), 'Advances in optical coherence tomography in dermatology—a review', *Journal of Biomedical Optics* **23**(4), 040901.
- Ou, X., Pan, W. & Xiao, P. (2014), 'In vivo skin capacitive imaging analysis by using grey level co-occurrence matrix (glcm)', *International journal of pharmaceutics* **460**(1-2), 28–32.
- Paglialonga, A., Pincioli, F., Tognola, G., Barbieri, R., Caiani, E. G. & Riboldi, M. (2017), e-health solutions for better care: Characterization of health apps to extract meaningful information and support users' choices, in '2017 IEEE 3rd International Forum on Research and Technologies for Society and Industry (RTSI)', IEEE, pp. 1–6.
- Pereir, C., Guimarães, D., Mesquita, J., Santos, F., Almeida, L. & Aguiar, A. (2018), Feasibility of gateway-less iot e-health applications, in '2018 European Conference on Networks and Communications (EuCNC)', IEEE, pp. 324–328.
- Pesch, A. H., Smirnov, A., Pyrhönen, O. & Sawicki, J. T. (2015), 'Magnetic bearing spindle tool tracking through  $\mu$ -synthesis robust control', *IEEE/ASME Transactions on Mechatronics* **20**(3), 1448–1457.
- Pham, Q. D., Björklund, S., Engblom, J., Topgaard, D. & Sparr, E. (2016), 'Chemical penetration enhancers in stratum corneum—relation between molecular effects and barrier function', *Journal of Controlled Release* **232**, 175–187.
- Pinnagoda, J., Tupkek, R. A., Agner, T. & Serup, J. (1990), 'Guidelines for transepidermal water loss (TEWL) measurement: A Report from the Standardization Group of the European Society of Contact Dermatitis', *Contact Dermatitis* **22**(3), 164–178.  
**URL:** <http://doi.wiley.com/10.1111/j.1600-0536.1990.tb01553.x>
- Plessis, J. d., Stefaniak, A., Eloff, F., John, S., Agner, T., Chou, T.-C., Nixon, R., Steiner, M., Franken, A., Kudla, I. et al. (2013), 'International guidelines for the in vivo assessment of skin properties in non-clinical settings: Part 2. transepidermal water loss and skin hydration', *Skin research and technology* **19**(3), 265–278.
- Portugal-Cohen, M., Oron, M., Boaz, M., Shtendik, L., Biro, A., Cernes, R., Barnea, Z., Kazir, Z., Kohen, R. et al. (2011), 'Noninvasive skin measurements to monitor chronic renal failure pathogenesis', *Biomedicine & Pharmacotherapy* **65**(4), 280–285.

- Qassem, M. & Kyriacou, P. (2019), 'Review of modern techniques for the assessment of skin hydration', *Cosmetics* **6**(1), 19.
- Rambaud, N. (2016), 'What is the best layer height for your printer', <http://doc.3dmodularsystems.com/what-is-the-best-layer-height-for-your-printer/>. [Online; accessed 08-April-2019].
- Raynor, B., Ashbrenner, E., Garofalo, M., Cohen, J. & Akin, F. (2004), 'The practical dynamics of transepidermal water loss (tewl): pharmacokinetic modeling and the limitations of closed-chamber evaporimetry', *Skin Research and Technology* **10**(4), 3.
- Redwood, B. (2019), 'How does part orientation affect a 3D Print?', <https://www.3dhubs.com/knowledge-base/how-does-part-orientation-affect-3d-print>. [Online; accessed 08-April-2019].
- Reinberg, A., Le, I. F. & Tschachler, E. (1998), 'Problems related to circadian rhythms in human skin and their validation.', *The Journal of investigative dermatology* **111**(4), 708–709.
- Rianjanu, A., Julian, T., Hidayat, S., Suyono, E., Kusumaatmaja, A. & Triyana, K. (2018), Polyacrylonitrile nanofiber as polar solvent n, n-dimethyl formamide sensor based on quartz crystal microbalance technique, in 'Journal of Physics: Conference Series', Vol. 1011, IOP Publishing, p. 012067.
- Rivas-Echeverria, F., Rios-Bolivar, A. & Casales-Echeverria, J. (2001), 'Neural network-based auto-tuning for pid controllers', *Neural Network World* **11**(3), 277–284.
- Rogiers, V. (1995), Transepidermal Water Loss Measurements in Patch Test Assessment: The Need for Standardisation, in P. Elsner & H. Maibach, eds, 'Current Problems in Dermatology', Vol. 23, S. Karger AG, pp. 152–158.  
**URL:** <http://www.karger.com/?doi=10.1159/000424310>
- Rogiers, V. (2001), 'EEMCO Guidance for the Assessment of Transepidermal Water Loss in Cosmetic Sciences', *Skin Pharmacology and Physiology* **14**(2), 117–128.  
**URL:** <http://www.karger.com/?doi=10.1159/000056341>
- Rohsenow, W. M., Hartnett, J. P. & Cho, Y. I., eds (1998), *Handbook of heat transfer*, McGraw-Hill handbooks, 3rd ed edn, McGraw-Hill, New York.
- Salinas, R. (2014), *3D printing with RepRap cookbook*, Packt Publishing Ltd.

- Saltin, B., Gagge, A. P., Bergh, U. & Stolwijk, J. (1972), 'Body temperatures and sweating during exhaustive exercise.', *Journal of applied physiology* **32**(5), 635–643.
- Salvo, P., Melai, B., Calisi, N. & Di Francesco, F. (2014), Current technology and advances in transepidermal water loss sensors, *in* 'Mobile point-of-care monitors and diagnostic device design', CRC Press Boca Raton, pp. 63–78.
- Sandhya, S. & Devi, K. S. (2012), Analysis of bluetooth threats and v4. 0 security features, *in* '2012 International Conference on Computing, Communication and Applications', IEEE, pp. 1–4.
- Schofield, J., Grindlay, D. & Williams, H. (2009), 'Centre of evidence based dermatology, university of nottingham,'skin conditions in the uk: A health care needs assessment''.
- Scott, R., Oliver, G., Dugard, P. & Singh, H. (1982), 'A comparison of techniques for the measurement of transepidermal water loss', *Archives of dermatological research* **274**(1-2), 57–64.
- Shah, J. H., Zhai, H. & Maibach, H. I. (2005), 'Comparative evaporimetry in man', *Skin Res Technol* **11**(3), 205–208.
- Sotoodian, B. & Maibach, H. I. (2012), 'Noninvasive test methods for epidermal barrier function', *Clinics in dermatology* **30**(3), 301–310.
- Spruit, D. (1971), 'The diurnal variation of water vapour loss from the skin in relation to temperature', *British Journal of Dermatology* **84**(1), 66–70.
- Stamatas, G. N., de Sterke, J., Hauser, M., von Stetten, O. & van der Pol, A. (2008), 'Lipid uptake and skin occlusion following topical application of oils on adult and infant skin', *Journal of dermatological science* **50**(2), 135–142.
- Tagami, H., Kobayashi, H. & Kikuchi, K. (2002), 'A portable device using a closed chamber system for measuring transepidermal water loss: comparison with the conventional method', *Skin Res Technol* **8**(1), 7–12.
- Tagami, H., Ohi, M., Iwatsuki, K., Kanamaru, Y., Yamada, M. & Ichijo, B. (1980), 'Evaluation of the skin surface hydration in vivo by electrical measurement', *Journal of Investigative Dermatology* **75**(6), 500–507.
- van Erp, P. E., Peppelman, M. & Falcone, D. (2018), 'Noninvasive analysis and minimally invasive in vivo experimental challenges of the skin barrier', *Experimental dermatology* **27**(8), 867–875.

- van Logtestijn, M. D., Domínguez-Hüttinger, E., Stamatas, G. N. & Tanaka, R. J. (2015), 'Resistance to water diffusion in the stratum corneum is depth-dependent', *PloS one* **10**(2), e0117292.
- Wang, T.-F., Kasting, G. B. & Nitsche, J. M. (2006), 'A Multiphase Microscopic Diffusion Model for Stratum Corneum permeability. I. Formulation, Solution, and Illustrative Results for Representative Compounds', *Journal of Pharmaceutical Sciences* **95**(3), 620–648.  
**URL:** <http://linkinghub.elsevier.com/retrieve/pii/S0022354916319633>
- Weisstein, E. W. (2002), 'Least squares fitting'.
- Wheldon, A. E. & Monteith, J. L. (1980), 'Performance of a skin evaporimeter', *Medical & Biological Engineering & Computing* **18**(2), 201–205.  
**URL:** <http://link.springer.com/10.1007/BF02443295>
- Wu, M.-S. (1983), 'Water diffusivity and water concentration profile in human stratum corneum from transepidermal water loss measurements', *J Soc Cosmet Chem* **34**, 191–196.
- Xue, C. J., Sun, G., Zhang, Y., Yang, J. J., Chen, Y. & Li, H. (2011), Emerging non-volatile memories: opportunities and challenges, in '2011 Proceedings of the Ninth IEEE/ACM/IFIP International Conference on Hardware/Software Codesign and System Synthesis (CODES+ ISSS)', IEEE, pp. 325–334.
- Ya-Xian, Z., Suetake, T. & Tagami, H. (1999), 'Number of cell layers of the stratum corneum in normal skin—relationship to the anatomical location on the body, age, sex and physical parameters', *Archives of dermatological research* **291**(10), 555–559.
- Yosipovitch, G., Xiong, G. L., Haus, E., Sackett-Lundeen, L., Ashkenazi, I. & Maibach, H. I. (1998), 'Time-dependent variations of the skin barrier function in humans: transepidermal water loss, stratum corneum hydration, skin surface ph, and skin temperature', *Journal of investigative dermatology* **110**(1), 20–23.
- Youngson, R. M. (2005), *Collins dictionary of Medicine fourth edition*, Harper Collins.
- Zribi, A., Chtourou, M. & Djemel, M. (2018), 'A new pid neural network controller design for nonlinear processes', *Journal of Circuits, Systems and Computers* **27**(04), 1850065.
- Zuza, M. (2018), 'Everything about nozzles with a different diameter', <https://www.prusaprinters.org/>

[everything-about-nozzles-with-a-different-diameter/](#). [Online; accessed 08-April-2019].